Evidence-Based Complementary and Alternative Medicine

Pharmacology, Toxicology, and Therapeutics of Minerals in Traditional Medicine 2021

Lead Guest Editor: Jie Liu
Guest Editors: Uma Maheswari Krishnan and Lixin Wei

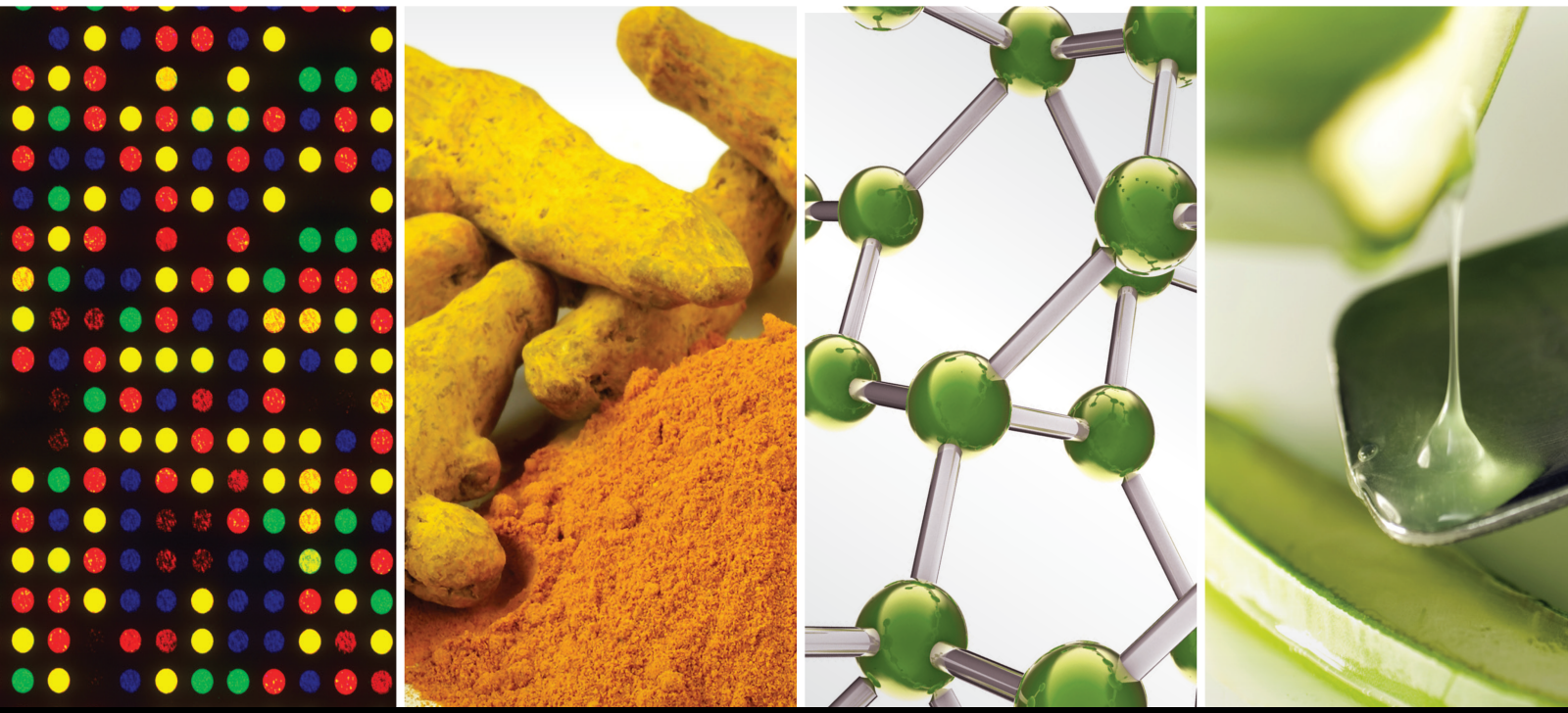

Pharmacology, Toxicology, and Therapeutics of Minerals in Traditional Medicine 2021

Evidence-Based Complementary and Alternative Medicine

Pharmacology, Toxicology, and Therapeutics of Minerals in Traditional Medicine 2021

Lead Guest Editor: Jie Liu
Guest Editors: Uma Maheswari Krishnan and Lixin Wei

Copyright © 2022 Hindawi Limited. All rights reserved.

This is a special issue published in “Evidence-Based Complementary and Alternative Medicine.” All articles are open access articles distributed under the Creative Commons Attribution License, which permits unrestricted use, distribution, and reproduction in any medium, provided the original work is properly cited.

Chief Editor

Jian-Li Gao, China

Associate Editors

Hyunsu Bae, Republic of Korea
Raffaele Capasso, Italy
Jae Youl Cho, Republic of Korea
Caigan Du, Canada
Yuewen Gong, Canada
Hai-dong Guo, China
Kuzhuvelil B. Harikumar, India
Ching-Liang Hsieh, Taiwan
Cheorl-Ho Kim, Republic of Korea
Victor Kuete, Cameroon
Hajime Nakae, Japan
Yoshiji Ohta, Japan
Olumayokun A. Olajide, United Kingdom
Chang G. Son, Republic of Korea
Shan-Yu Su, Taiwan
Michał Tomczyk, Poland
Jenny M. Wilkinson, Australia

Academic Editors

Eman A. Mahmoud, Egypt
Ammar AL-Farga, Saudi Arabia
Smail Aazza, Morocco
Nahla S. Abdel-Azim, Egypt
Ana Lúcia Abreu-Silva, Brazil
Gustavo J. Acevedo-Hernández, Mexico
Mohd Adnan, Saudi Arabia
Jose C Adsuar, Spain
Sayeed Ahmad, India
Touqeer Ahmed, Pakistan
Basiru Ajiboye, Nigeria
Bushra Akhtar, Pakistan
Fahmida Alam, Malaysia
Mohammad Jahoor Alam, Saudi Arabia
Clara Albani, Argentina
Ulysses Paulino Albuquerque, Brazil
Mohammed S. Ali-Shtayeh, Palestinian Authority
Ekram Alias, Malaysia
Terje Alraek, Norway
Adolfo Andrade-Cetto, Mexico
Letizia Angiolella, Italy
Makoto Arai, Japan
Daniel Dias Rufino Arcanjo, Brazil
Duygu AĞAGÜNDÜZ, Turkey
Neda Baghban, Iran
Samra Bashir, Pakistan
Rusliza Basir, Malaysia
Jairo Kenupp Bastos, Brazil
Arpita Basu, USA
Mateus R. Beguelini, Brazil
Juana Benedí, Spain
Samira Boulbaroud, Morocco
Mohammed Bourhia, Morocco
Abdelhakim Bouyahya, Morocco
Nunzio Antonio Cacciola, Italy
Francesco Cardini, Italy
María C. Carpinella, Argentina
Harish Chandra, India
Guang Chen, China
Jianping Chen, China
Kevin Chen, USA
Mei-Chih Chen, Taiwan
Xiaojia Chen, Macau
Evan P. Cherniack, USA
Giuseppina Chianese, Italy
Kok-Yong Chin, Malaysia
Lin China, China
Salvatore Chirumbolo, Italy
Hwi-Young Cho, Republic of Korea
Jeong June Choi, Republic of Korea
Jun-Yong Choi, Republic of Korea
Kathrine Bisgaard Christensen, Denmark
Shuang-En Chuang, Taiwan
Ying-Chien Chung, Taiwan
Francisco José Cidral-Filho, Brazil
Daniel Collado-Mateo, Spain
Lisa A. Conboy, USA
Kieran Cooley, Canada
Edwin L. Cooper, USA
José Otávio do Amaral Corrêa, Brazil
Maria T. Cruz, Portugal
Huantian Cui, China
Giuseppe D'Antona, Italy
Ademar A. Da Silva Filho, Brazil
Chongshan Dai, China
Laura De Martino, Italy
Josué De Moraes, Brazil

Arthur De Sá Ferreira, Brazil
Nunziatina De Tommasi, Italy
Marinella De leo, Italy
Gourav Dey, India
Dinesh Dhamecha, USA
Claudia Di Giacomo, Italy
Antonella Di Sotto, Italy
Mario Dioguardi, Italy
Jeng-Ren Duann, USA
Thomas Efferth, Germany
Abir El-Alfy, USA
Mohamed Ahmed El-Esawi, Egypt
Mohd Ramli Elvy Suhana, Malaysia
Talha Bin Emran, Japan
Roger Engel, Australia
Karim Ennouri, Tunisia
Giuseppe Esposito, Italy
Tahereh Eteraf-Oskouei, Iran
Robson Xavier Faria, Brazil
Mohammad Fattahi, Iran
Keturah R. Faurot, USA
Piergiorgio Fedeli, Italy
Laura Ferraro, Italy
Antonella Fioravanti, Italy
Carmen Formisano, Italy
Hua-Lin Fu, China
Liz G Müller, Brazil
Gabino Garrido, Chile
Safoora Gharibzadeh, Iran
Muhammad N. Ghayur, USA
Angelica Gomes, Brazil
Elena González-Burgos, Spain
Susana Gorzalczany, Argentina
Jiangyong Gu, China
Maruti Ram Gudavalli, USA
Jian-You Guo, China
Shanshan Guo, China
Narcís Gusi, Spain
Svein Haavik, Norway
Fernando Hallwass, Brazil
Gajin Han, Republic of Korea
Ihsan Ul Haq, Pakistan
Hicham Harhar, Morocco
Mohammad Hashem Hashempur, Iran
Muhammad Ali Hashmi, Pakistan
Waseem Hassan, Pakistan
Sandrina A. Heleno, Portugal
Pablo Herrero, Spain
Soon S. Hong, Republic of Korea
Md. Akil Hossain, Republic of Korea
Muhammad Jahangir Hossen, Bangladesh
Shih-Min Hsia, Taiwan
Changmin Hu, China
Tao Hu, China
Weicheng Hu, China
Wen-Long Hu, Taiwan
Xiao-Yang (Mio) Hu, United Kingdom
Sheng-Teng Huang, Taiwan
Ciara Hughes, Ireland
Attila Hunyadi, Hungary
Liaqat Hussain, Pakistan
Maria-Carmen Iglesias-Osma, Spain
Amjad Iqbal, Pakistan
Chie Ishikawa, Japan
Angelo A. Izzo, Italy
Satveer Jagwani, USA
Rana Jamous, Palestinian Authority
Muhammad Saeed Jan, Pakistan
G. K. Jayaprakasha, USA
Kyu Shik Jeong, Republic of Korea
Leopold Jirovetz, Austria
Jeeyoun Jung, Republic of Korea
Nurkhalida Kamal, Saint Vincent and the Grenadines
Atsushi Kameyama, Japan
Kyungsu Kang, Republic of Korea
Wenyi Kang, China
Shao-Hsuan Kao, Taiwan
Nasiara Karim, Pakistan
Morimasa Kato, Japan
Kumar Katragunta, USA
Deborah A. Kennedy, Canada
Washim Khan, USA
Bonglee Kim, Republic of Korea
Dong Hyun Kim, Republic of Korea
Junghyun Kim, Republic of Korea
Kyungho Kim, Republic of Korea
Yun Jin Kim, Malaysia
Yoshiyuki Kimura, Japan

Nebojša Kladar, Serbia
Mi Mi Ko, Republic of Korea
Toshiaki Kogure, Japan
Malcolm Koo, Taiwan
Yu-Hsiang Kuan, Taiwan
Robert Kubina, Poland
Chan-Yen Kuo, Taiwan
Kuang C. Lai, Taiwan
King Hei Stanley Lam, Hong Kong
Fanuel Lampiao, Malawi
Ilaria Lampronti, Italy
Mario Ledda, Italy
Harry Lee, China
Jeong-Sang Lee, Republic of Korea
Ju Ah Lee, Republic of Korea
Kyu Pil Lee, Republic of Korea
Namhun Lee, Republic of Korea
Sang Yeoup Lee, Republic of Korea
Ankita Leekha, USA
Christian Lehmann, Canada
George B. Lenon, Australia
Marco Leonti, Italy
Hua Li, China
Min Li, China
Xing Li, China
Xuqi Li, China
Yi-Rong Li, Taiwan
Vuanghao Lim, Malaysia
Bi-Fong Lin, Taiwan
Ho Lin, Taiwan
Shuibin Lin, China
Kuo-Tong Liou, Taiwan
I-Min Liu, Taiwan
Suhuan Liu, China
Xiaosong Liu, Australia
Yujun Liu, China
Emilio Lizarraga, Argentina
Monica Loizzo, Italy
Nguyen Phuoc Long, Republic of Korea
Zaira López , Mexico
Chunhua Lu, China
Ângelo Luís, Portugal
Anderson Luiz-Ferreira, Brazil
Ivan Luzardo Luzardo-Ocampo, Mexico
Michel Mansur Machado, Brazil
Filippo Maggi, Italy
Juraj Majtan, Slovakia
Toshiaki Makino, Japan
Nicola Malafronte, Italy
Giuseppe Malfa, Italy
Francesca Mancianti, Italy
Carmen Mannucci, Italy
Juan M. Manzaneque, Spain
Fatima Martel, Portugal
Carlos H. G. Martins, Brazil
Maulidiani Maulidiani, Malaysia
Andrea Maxia, Italy
Avijit Mazumder, India
Isac Medeiros, Brazil
Ahmed Mediani, Malaysia
Lewis Mehl-Madrona, USA
Ayikoé Guy Mensah-Nyagan, France
Oliver Micke, Germany
Maria G. Miguel, Portugal
Luigi Milella, Italy
Roberto Miniero, Italy
Letteria Minutoli, Italy
Prashant Modi, India
Daniel Kam-Wah Mok, Hong Kong
Changjong Moon, Republic of Korea
Albert Moraska, USA
Mark Moss, United Kingdom
Yoshiharu Motoo, Japan
Yoshiki Mukudai, Japan
Sakthivel Muniyan, USA
Saima Muzammil, Pakistan
Benoit Banga N'guessan, Ghana
Massimo Nabissi, Italy
Siddavaram Nagini, India
Takao Namiki, Japan
Srinivas Nammi, Australia
Krishnadas Nandakumar, India
Vitaly Napadow, USA
Edoardo Napoli, Italy
Jorddy Neves Cruz, Brazil
Marcello Nicoletti, Italy
Eliud Nyaga Mwaniki Njagi, Kenya
Cristina Nogueira, Brazil

Sakineh Kazemi Noureini, Iran
Rômulo Dias Novaes, Brazil
Martin Offenbaecher, Germany
Oluwafemi Adeleke Ojo, Nigeria
Olufunmiso Olusola Olajuyigbe, Nigeria
Luís Flávio Oliveira, Brazil
Mozaniel Oliveira, Brazil
Atolani Olubunmi, Nigeria
Abimbola Peter Oluyori, Nigeria
Timothy Omara, Austria
Chiagoziem Anariochi Otuechere, Nigeria
Sokcheon Pak, Australia
Antônio Palumbo Jr, Brazil
Zongfu Pan, China
Siyaram Pandey, Canada
Niranjan Parajuli, Nepal
Gunhyuk Park, Republic of Korea
Wansu Park, Republic of Korea
Rodolfo Parreira, Brazil
Mohammad Mahdi Parvizi, Iran
Luiz Felipe Passero, Brazil
Mitesh Patel, India
Claudia Helena Pellizzon, Brazil
Cheng Peng, Australia
Weijun Peng, China
Sonia Piacente, Italy
Andrea Pieroni, Italy
Haifa Qiao, USA
Cláudia Quintino Rocha, Brazil
DANIELA RUSSO, Italy
Muralidharan Arumugam Ramachandran, Singapore
Manzoor Rather, India
Miguel Rebollo-Hernanz, Spain
Gauhar Rehman, Pakistan
Daniela Rigano, Italy
José L. Rios, Spain
Francisca Rius Diaz, Spain
Eliana Rodrigues, Brazil
Maan Bahadur Rokaya, Czech Republic
Mariangela Rondanelli, Italy
Antonietta Rossi, Italy
Mi Heon Ryu, Republic of Korea
Bashar Saad, Palestinian Authority
Sabiu Saheed, South Africa
Mohamed Z.M. Salem, Egypt
Avni Sali, Australia
Andreas Sandner-Kiesling, Austria
Manel Santafe, Spain
José Roberto Santin, Brazil
Tadaaki Satou, Japan
Roland Schoop, Switzerland
Sindy Seara-Paz, Spain
Veronique Seidel, United Kingdom
Vijayakumar Sekar, China
Terry Selfe, USA
Arham Shabbir, Pakistan
Suzana Shahar, Malaysia
Wen-Bin Shang, China
Xiaofei Shang, China
Ali Sharif, Pakistan
Karen J. Sherman, USA
San-Jun Shi, China
Insop Shim, Republic of Korea
Maria Im Hee Shin, China
Yukihiro Shoyama, Japan
Morry Silberstein, Australia
Samuel Martins Silvestre, Portugal
Preet Amol Singh, India
Rajeev K Singla, China
Kuttulebbai N. S. Sirajudeen, Malaysia
Slim Smaoui, Tunisia
Eun Jung Sohn, Republic of Korea
Maxim A. Solovchuk, Taiwan
Young-Jin Son, Republic of Korea
Chengwu Song, China
Vanessa Steenkamp, South Africa
Annarita Stringaro, Italy
Keiichiro Sugimoto, Japan
Valeria Sulsen, Argentina
Zewei Sun, China
Sharifah S. Syed Alwi, United Kingdom
Orazio Taglialatela-Scafati, Italy
Takashi Takeda, Japan
Gianluca Tamagno, Ireland
Hongxun Tao, China
Jun-Yan Tao, China
Lay Kek Teh, Malaysia
Norman Temple, Canada

Kamani H. Tennekoon, Sri Lanka
Seong Lin Teoh, Malaysia
Menaka Thounaojam, USA
Jinhui Tian, China
Zipora Tietel, Israel
Loren Toussaint, USA
Riaz Ullah, Saudi Arabia
Philip F. Uzor, Nigeria
Luca Vanella, Italy
Antonio Vassallo, Italy
Cristian Vergallo, Italy
Miguel Vilas-Boas, Portugal
Aristo Vojdani, USA
Yun WANG, China
QIBIAO WU, Macau
Abraham Wall-Medrano, Mexico
Chong-Zhi Wang, USA
Guang-Jun Wang, China
Jinan Wang, China
Qi-Rui Wang, China
Ru-Feng Wang, China
Shu-Ming Wang, USA
Ting-Yu Wang, China
Xue-Rui Wang, China
Youhua Wang, China
Kenji Watanabe, Japan
Jintanaporn Wattanathorn, Thailand
Silvia Wein, Germany
Katarzyna Winska, Poland
Sok Kuan Wong, Malaysia
Christopher Worsnop, Australia
Jih-Huah Wu, Taiwan
Sijin Wu, China
Xian Wu, USA
Zuoqi Xiao, China
Rafael M. Ximenes, Brazil
Guoqiang Xing, USA
JiaTuo Xu, China
Mei Xue, China
Yong-Bo Xue, China
Haruki Yamada, Japan
Nobuo Yamaguchi, Japan
Junqing Yang, China
Longfei Yang, China
Mingxiao Yang, Hong Kong
Qin Yang, China
Wei-Hsiung Yang, USA
Swee Keong Yeap, Malaysia
Albert S. Yeung, USA
Ebrahim M. Yimer, Ethiopia
Yoke Keong Yong, Malaysia
Fadia S. Youssef, Egypt
Zhilong Yu, Canada
RONGJIE ZHAO, China
Sultan Zahiruddin, USA
Armando Zarrelli, Italy
Xiaobin Zeng, China
Y Zeng, China
Fangbo Zhang, China
Jianliang Zhang, China
Jiu-Liang Zhang, China
Mingbo Zhang, China
Jing Zhao, China
Zhangfeng Zhong, Macau
Guoqi Zhu, China
Yan Zhu, USA
Suzanna M. Zick, USA
Stephane Zingue, Cameroon

Contents

Hindawi
Evidence-Based Complementary and Alternative Medicine
Volume 2022, Article ID 4831261, 13 pages
https://doi.org/10.1155/2022/4831261

Research Article

Botanical from the Fruits Mesocarp of *Raphia vinifera* Displays Antiproliferative Activity and Is Harmless as Evidenced by Toxicological Assessments

Gaëlle S. Nguenang,[1] Armelle T. Mbaveng,[1] Idrios N. Bonsou,[1] Godloves F. Chi,[2] and Victor Kuete[1]

[1]*Department of Biochemistry, Faculty of Science, University of Dschang, Dschang, Cameroon*
[2]*Department of Chemistry, Faculty of Science, University of Buea, Buea, Cameroon*

Correspondence should be addressed to Victor Kuete; kuetevictor@yahoo.fr

Received 27 December 2021; Revised 1 March 2022; Accepted 11 March 2022; Published 29 March 2022

Academic Editor: Jie Liu

Copyright © 2022 Gaëlle S. Nguenang et al. This is an open access article distributed under the Creative Commons Attribution License, which permits unrestricted use, distribution, and reproduction in any medium, provided the original work is properly cited.

Raphia vinifera is widely used to treat several diseases including digestive disorders, dysentery, and genitourinary infections. In this study, the mineral contents, the cytotoxicity, and the toxicological effect of the crude $CHCl_3$/MeOH extract (RVM) from the mesocarp of *Raphia vinifera* were evaluated. The mineral contents were evaluated using the method described by the Association of Official Analytical Chemists (AOAC). The cytotoxicity of both extract and chemical compounds from the plants was determined by a resazurin reduction assay (RRA). The toxicological studies were carried out using the experimental procedure of the Organization for Economic Cooperation and Development (OECD). After killing the rats, biochemical, histopathological, and hematological studies were performed. The result indicated that RVM is rich in zinc (6.52 mg/100 g of DM) and sodium (194.5 mg/100 g of DM). RVM had a cytotoxicity effect with IC_{50} values lower than 30 μg/mL in 18/18 cancer cell lines tested. These recorded IC_{50} values were between 12.35 μg/mL (toward CCRF-CEM leukemia cells) and 26.66 μg/mL (toward SKMel-505 BRAF wild-type melanoma cells). Raphvinin 4 displayed good cytotoxicity against MaMel-80aBRAF-V600E homozygous mutant with the IC_{50} of 10.42 μM. RVM was relatively nontoxic to rats, the median lethal dose (DL_{50}) being above 5000 mg/kg body weight. However, during the oral administration period extending for 28 days, precautions should be taken due to the increase in urinary creatinine level and decrease in spleen weight in the male rats given the highest dose (1000 mg/kg) of extract. Conclusively, the extract of *Raphia vinifera* is weakly toxic in rats and could be further used in the development of anticancer phytomedicines.

1. Introduction

Despite the numerous means to fight against cancer, the number of deaths caused by this disease is increasing significantly in many countries [1]. In 2018, WHO (World Health Organization) recorded 9.6 million deaths and 18.1 million new cases because of cancer [2]. Due to morbidity and mortality that it generates, cancer represents a major health problem both nationally and globally. This pathology becomes increasingly difficult to diagnose and to treat when cancer cells develop resistance mechanisms against the usual chemotherapeutic agents [3]. Regarding the increasing resistance developed by these cells, research for alternative treatments should be performed. The varieties of secondary metabolites contained in medicinal plants are responsible for the pharmacological effects including cytotoxic activity [4].

Raphia vinifera (Arecaceae) is a plant from the genus *Raphia*; medicinal properties of different parts of the plants have been demonstrated. Raffia wine from *Raphia vinifera* is rich in lactic acid bacteria [5], which prevents the incidence of diarrhea and promotes the course of the immune response in rats; these probiotic isolates could strengthen the immune system in children [6]. Also, many medicinal plants used in Africa have shown interesting antiproliferative properties against the sensitive and multi-drug-resistant (MDR) cancer cells linked to their secondary metabolites [4, 7]. The boiled

solution of apical bud of *Raphia* vinifera is used to treat some diseases like genitourinary infections and gonorrhea in West Cameroon. The leaf is used to fight against poison and for various sexually transmitted diseases and witchcraft [8]. To solve liver problems, the young leaves of this plant are used, and the crushed fruits are poured into water to capture fish easily [9, 10].

Palm has been proven to have minerals like calcium [11]. The *Raphia vinifera* fruit pulp and pericarps were found to contain a high concentration of saponins, alkaloids, and oxalate; a moderate concentration of tannin, flavonoid, and steroid; and a low concentration of phytate, phenol, and glycoside, which are responsible for its therapeutic activity [12]. This plant has provided steroidal saponins [13], which are beneficial in preventing tumors and treating many cancers with high efficiency associated with weak toxicological effect [13]. In addition, saponins are also cytotoxic and act by blocking the cell cycle and could significantly disrupt the mitochondrial membrane potential and selectively upregulate the protein levels of Bax, cytochrome C, and cleaved caspase 3/9 and downregulate the levels of Bcl-2 [14]. The pulp of *Raphia* vinifera contains oil that was extracted and characterized physically and chemically by Igwenyi et al. [15].

Many investigations have demonstrated the ability of medicinal plants in the prevention and treatment of many diseases [4, 16]. However, little information is provided on the toxicological effect of plants on consumers. The research on toxicological effects of medicinal plants and their extract is crucial in the development of drugs and to rise human safety [17]. Many toxicological studies have been carried out using *Raphia vinifera* on fish [11], but studies hardly describe the biochemical toxicity of this plant on rats. This investigation was therefore carried out to evaluate antiproliferative potential of *Raphia vinifera* extract and its constituents, as well as the toxicity of the crude extract.

2. Material and Methods

2.1. Chemicals and Preparation of the Extract. The phytochemicals used were (25*R*)-spirost-5-ene-3β, 22β-3-O-β-D-glucopyranosyl(1 ⟶ 2)-O-α-L-rhamnopyranoside (1); (25 S)-26-O-(β-D-galactopyranosyl)-furost-5-ene-3β, 22α, 26-trihydroxy-3-O-β-D-glucopyranosyl-(1 ⟶ 2)-α-L-rhamnopyranoside or raphvinin 1 (2); (25*R*)-26-O-(β-D-galactopyranosyl)-furost-5-ene-3β, 22α, 26-trihydroxy-3-O-β-D-glucopyranosyl-(1 ⟶ 2)-[α-L-rhamnopyranosyl-(1 ⟶ 3)]-β-D-glucopyranoside or raphvinin 2 (**3**); (25*R*)-26-O-[β-D-glucopyranosyl-(1 ⟶ 4)]-β-D-galactopyranosyl)-furost-5-ene-3β, 26-dihydroxy-22α-methoxy-3-O-β-D-glucopyranosyl -(1 ⟶ 2) -[α-L-rhamnopyranosyl-(1 ⟶ 2)] -β-D-lucopyranosyl-(1 ⟶ 4)-β-D-glucopyranoside or raphvinin 3 (4); diosgenin (5); diosgenin-3-O-β-D-glucopyranoside or (22*R*, 25*R*)-3β-spirost-5-ene-3-O-β-D-glucopyranoside or trillin (6); deltonin (7); 26-O-β-D-glucopyranosyl-(22*R*,25*R*)-3β, 22, 26-trihydroxyfurost-5-ene-3-O-β-D-glucopyranoside (**8**); and sitosterol (**9**). The NMR spectra and the chemical shifts of compounds 1–9 are provided in the Supplementary file (S1 to S18). They are isolated from *Raphia vinifera* fruits collected in Bambili, Northwest Region of Cameroon on April 2016, and identified at the Cameroon National Herbarium (voucher number: 38374/HNC) as previously reported [18]. Doxorubicin 98.0% (Sigma-Aldrich) (Munich, Germany) comes from the Medical Center of the Johannes Gutenberg University (Mainz, Germany) and is dissolved in phosphate buffer saline (PBS; Invitrogen, Eggenstein, Germany) at 10 mM. The fruits of *Raphia vinifera* were dried and powdered. This powder (1 kg) was thereafter macerated in $CHCl_3$/MeOH (5 L) in the proportions 1 : 1 at room temperature. After 2 days, the extract obtained was filtered with Whatman filter paper (No. 1) and rotary evaporator (Buchi R-200) was used to concentrate the filtrate at 40°C. The crude extract was assembled in sterile flask and dried by oven (40°C) until the solvent completely evaporated.

2.2. Cell Cultures and Origins. 18 cancer cell lines and normal hepatocyte AML12 were used in the present study. *Cancer* cell lines such as drug-sensitive leukemia CCRF-CEM and multidrug-resistant P-glycoprotein-over-expressing subline CEM/ADR5000 cells [19–21], breast cancer MDA-MB-231-*pcDNA* cells and its resistant subline MDA-MB-231-*BCRP* clone 23 cells [22], colon cancer HCT116 $p53^{+/+}$ cells and its knockout clone HCT116 $p53^{-/-}$, glioblastoma U87MG cells, and its resistant subline U87MG.Δ*EGFR* [7, 23, 24]. The maintenance of HepG2 cells and AML12 hepatocytes was also published [25]. The CC531 rat colon carcinoma cells, B16-F1, B16-F10, A2058, SK-Mel505, MaMel-80a, MV3, SkMel-28, and Mel-2A, were previously reported [26–30].

2.3. Experimental Animals. For the toxicological studies, adult *Wistar* rats (8 to 9 weeks old) of the 2 sexes were selected. To ensure their growth, the animals engaged in the animal house received food daily and tap water. They were maintained at standard laboratory conditions of regular 12 h light/12 h dark cycle. This work was carried out with respect to the well-being of rats like the Institutional Ethical Review Committee of the University of Dschang Cameroon recommended.

2.4. Determination of the Mineral Contents. Mineral contents (Ca, P, Mg, Fe, Na, Zn, and K) were determined by the extract using the AOAC method [31]. *Raphia* vinifera fruit extract was introduced into a porcelain crucible and calcinated at 450°C for 2 hrs. The contents of potassium (K), magnesium (Mg), calcium (Ca), sodium (Na), iron (Fe), zinc (Zn), and phosphorus (P) were determined colorimetrically by UV-visible spectrophotometer (Technel 752 P), according to AOAC procedure. Mineral contents of the sample were determined from calibration curves of standard minerals. All minerals were analyzed in duplicate.

2.5. Cytotoxicity Assay. Different types of human cancer cell lines were used in this study. The resazurin reduction assay

(RRA) as previously described [24, 32] with similar experimental conditions to those reported earlier [26–30] was used to measure the cell cytotoxicity. Fluorescence was measured on an Infinite M2000 Pro™ plate reader (Tecan, Germany) using an excitation wavelength of 544 nm and an emission wavelength of 590 nm. The viability was determined based on a comparison with untreated cells. The values representing the sample's concentrations required to inhibit 50% of cell proliferation (IC_{50}) were calculated from a calibration curve by linear regression using Microsoft Excel 2013 [33, 34].

2.6. Acute Toxicity Study in Rats. This test was realized under the OECD guidelines [35]. We followed the methods described by Nguenang [36]. Three adult female rats (8–9 weeks) were treated orally with one dose of extract (5000 mg/kg), after 12 hrs of fasting. These rats were individually and frequently observed to check any signs of toxicity during the first day; observation was continued daily for a total of 14 days of the experiment. The body weight of animals on the 15th day was measured. Subsequently, they were anesthetized through intraperitoneal injection with a solution containing diazepam and ketamine (0.2/0.1 ml per 100 grams of the animal), the vital organs such as lung, spleen, heart, kidneys, and liver were removed and weighed, and the macroscopic examinations were performed on those organs. The relative organ weight was determined.

2.7. Subchronic Toxicological Study

2.7.1. Treatments. This study was performed under the protocol of the OECD Guidelines [37]. We followed the methods described by Nguenang [36]. Thirty-two *Wistar* rats (16 males and 16 females) aged from 08 to 09 weeks were distributed in 4 groups of 4 rats per group. The groups treated received the doses of 250, 500, and 1000 mg/kg b.w. of extract, while the control group received only distilled water during 28 days of treatment. These rats were individually and frequently observed to check any signs of toxicity. The body weights of all animals were measured after every four days during the experimental period. All animals were weighed on the 29th day, and subsequently, they were anesthetized with solution containing diazepam and ketamine (0.2/0.1 ml per 100 grams of the animal). Blood samples were collected into EDTA and nonheparinized tubes for the measurement of hematological and biochemical parameters, respectively. The organs such as heart, lung, liver, kidneys, and spleen were weighed, and one part of each organ was conserved in the solution of formalin (10%) for histopathological examination. The relative organ weight was determined.

2.7.2. Evaluation of Hematological Parameters. To determine these parameters, the blood sample of rats was collected in the EDTA tubes after the kill. The hematological analysis was performed using an automated analyzer hematology (QBC Autoread plus, United Kingdom). The hematological parameters analyzed included white blood cells (WBCs), hemoglobin (Hb), red blood cells (RBCs), hematocrit (HCT), mean corpuscular volume (MCV), lymphocytes (LYMs), mean corpuscular hemoglobin concentration (MCHC), platelets (PLTs), monocytes, granulocytes, mean corpuscular hemoglobin (MCH), and mean platelet volume (MPV).

Table 1: Mineral composition of RVM.

Mineral (mg/100 g)	RVM
Calcium	536.5 ± 0.5
Iron	5.28 ± 0.02
Potassium	575.4 ± 0.4
Magnesium	133.67 ± 0.02
Sodium	194.5 ± 0.5
Phosphorus	277.49 ± 0.52
Zinc	6.52 ± 0.02

The table values are presented as mean ± standard deviation.

2.7.3. Evaluation of Biochemical Parameters. The blood collected in dry tubes was centrifuged at 3000 rpm for 15 min to obtain the serum. The biochemical parameters measured were as follows: total serum protein (TP), alanine aminotransferase (ALT), aspartate aminotransferase (AST), serum creatinine (CREA), alkaline phosphatase (ALP), high-density lipoprotein-cholesterol (HDL-C), total cholesterol (TC), serum urea (UREA), low-density lipoprotein-cholesterol (LDL-C), and triglycerides (TG).

2.7.4. Histopathological Examination. After killing the rats, kidneys and liver were removed and cleaned in saline solution. The parts of these organs were collected for histological studies. These tissues were fixed in formalin (10%) during at least 24 h, dehydrated in a graded series of ethanol (80–100°), and enclosed (embedded) in paraffin. Thereafter, 5-μm sections were prepared using a microtome and stained with hematoxylin-eosin before the microscopic examination. The microscopic features of the animal's (male and female) organs-treated groups were compared with the control group [36, 38].

2.8. Statistical Analysis. The data are expressed as mean ± standard deviation (SD). These results have been submitted to the analysis of variance (ANOVA) at one factor according to the general linear model. Statistical analysis was done using version 21 of the IBM-SPSS statistical program, and statistical comparisons were made using the test of Waller Duncan for the subchronic toxicity at the 5% probability level.

3. Results

3.1. Mineral Content in Extract. The mineral composition of RVM is presented in Table 1. The data obtained from the mineral levels showed that RVM contains more zinc (6.52 mg/100 g of DM) and sodium (194.5 mg/100 g of DM) and less potassium (575.4 mg/100 g of DM), calcium

Table 2: Cytotoxicity of RVM and doxorubicin against drug-sensitive cell lines, their resistant counterparts, and normal hepatocytes as determined by RRA.

Cell lines	IC_{50} values (μg/mL) and degrees of resistance * or selectivity index**	
	RVM	Doxorubicin
CCRF-CEM	12.35 ± 1.03	0.02 ± 0.00
CEM/ADR5000	14.22 ± 0.98	—
*Degree of resistance**	(1.15)	Nd
MDA-MB-231-*pcDNA*	17.67 ± 2.01	0.13 ± 0.01
MDA-MB-231-*BCRP*	16.92 ± 0.86	0.79 ± 0.08
*Degree of resistance**	(0.96)	
HCT116 ($p53^{+/+}$)	14.56 ± 1.65	0.48 ± 0.06
HCT116 ($p53^{-/-}$)	15.28 ± 0.67	1.78 ± 0.08
*Degree of resistance**	(1.05)	
U87MG	13.93 ± 1.16	0.26 ± 0.03
U87MG.Δ*EGFR*	18.76 ± 1.64	0.98 ± 0.07
*Degree of resistance**	(1.35)	
HepG2	20.13 ± 1.78	4.56 ± 0.48
AML12	56.12 ± 3.77	52.90 ± 4.09
*Selectivity index***	(2.79)	

(*): The degree of resistance was determined as the ratio of IC_{50} value in the resistant divided by the IC_{50} in the sensitive cell line; CEM/ADR5000, MDA-MB-231-*BCRP*, HCT116 p53−/−, and U87MG.Δ*EGFR* were used as the corresponding resistant counterpart for CCRF-CEM, MDA-MB-231-pc DNA, HCT116 p53+/+, and U87MG cell lines, respectively; (**): The selectivity index was determined as the ratio of IC_{50} value in the normal AML12 hepatocytes divided by the IC_{50} in HepG2 hepatocarcinoma cells; nd: not determined.

Table 3: Cytotoxicity of RVM, compounds, and doxorubicin against animal cancer cell lines as determined by RRA.

Features and cell lines		Samples, IC_{50} values in μg/mL (extract) or μM (compounds) ± SD						
		RVM	1	2	4	5	6	Doxorubicin
BRAF-V600E homozygous mutant	MaMel-80a	18.92 ± 1.23	33.47 ± 2.06	65.45 ± 7.66	10.42 ± 1.26	—	—	8.66 ± 0.56
	SKMel-28	20.04 ± 0.85	54.28 ± 5.71		14.27 ± 1.10	—	—	2.14 ± 0.12
BRAF-V600E heterozygous mutant	A2058	18.56 ± 2.43	19, 46	56.12 ± 4.29	48.18 ± 5.18	27.06 ± 1.18	38.91 ± 2.78	0.29 ± 0.04
	Mel-2a	23.87 ± 3.19	42.10 ± 3.27	—	45.23 ± 3.29	—	—	6.63 ± 0.41
BRAF wild type	MV3	23.18 ± 1.74	—	—	35.26 ± 2.80	—	—	7.09 ± 0.59
	SKMel-505	26.66 ± 2.19	—	—	43.19 ± 3.72	—	—	9.39 ± 1.01
Rat colon adenocarcinoma	CC531	16.39 ± 0.96	—	58.90 ± 5.25	17.35 ± 3. 1	—	—	0.44 ± 0.23
Murine melanoma	B16-F1	14.98 ± 0.76	—	84.29 ± 6.63	23.19 ± 2.81	—	79.18 ± 5.39	0.22 ± 0.01
	B16-F10	16.55 ± 2.05	—	—	19.89 ± 1.06	—	—	0.24 ± 0.03

(−): IC_{50} values above 100 μM; the IC_{50} values were above 100 μM on all cell lines tested with compounds 3, 7, 8, and 9; *the selectivity index was determined as the ratio of IC_{50} value in the normal AML12 hepatocytes divided by the IC_{50} in other cell lines; (25*R*)-spirost-5-ene-3β, 22β-3-O-β-D-glucopyranosyl(1 ⟶ 2)-O-α-L-rhamnopyranoside (1), raphvinin (2), raphvinin 2 (3), raphvinin 3 (4), diosgenin (5), trillin (6), deltonin (7), 26-O-β-D-glucopyranosyl-(22*R*,25*R*)-3β, 22, 26-trihydroxyfurost-5-ene-3-O-β-D-glucopyranoside (8), and sitosterol (9).

(536.5 mg/100 g of dry matter), phosphorus (277.49 mg/100 g of DM), iron (5.28 mg/100 g of DM), and magnesium (133.67 mg/100 g of DM).

3.2. Cytotoxicity of Extract. The RRA was used to evaluate the effects of RVM, compounds 1–9, and doxorubicin on the proliferation of 18 cancer cell lines and normal AML12 hepatocytes (Tables 2 and 3; Figure 1). The degree of resistance (D. R.) was calculated as the ratio of the IC_{50} value of the resistant cell line divided by that of the corresponding parental sensitive cell line. The D. R. lower than 0.9 was defined as hypersensitivity or collateral sensitivity; D. R. around 1 was interpreted as normal sensitivity, while D. R. greater than 1.2 was signified as cross-resistance. The botanical RVM and doxorubicin revealed antiproliferative effects against the 18 cancer cell lines (Tables 2 and 3). The IC_{50} values obtained were from 12.35 μg/mL (towards CCRF-CEM leukemia cells) to 26.66 μg/mL (against SKMel-505 melanoma cells) for RVM and from 0.02 μM (against CCRF-CEM cells) to 9.39 μM (against SKMel-505 melanoma cells) for doxorubicin. Normal sensitivity was achieved with MDA-MB-231-*BCRP* cells (D.R. of 0.96), with HCT116 (*p53*−/−) (D.R. of 1.05) and CEM/ ADR5000 (D.R. of 1.15), respectively, compared with their sensitive congeners MDA-MB-231-pc DNA cells, HCT116 (p53+/+) cells, and CCRF-CEM cells (Table 2). U87MG.Δ*EGFR* cells (D.R. of 1.35) were cross-resistant to extract compared with their respective sensitive counterpart U87MG cells. RVM (selectivity index (S.I.): 2.76) displayed acceptable selectivity to HepG2 cells as compared to normal AML12 hepatocytes (Table 2). In addition to the fact that RVM had recordable

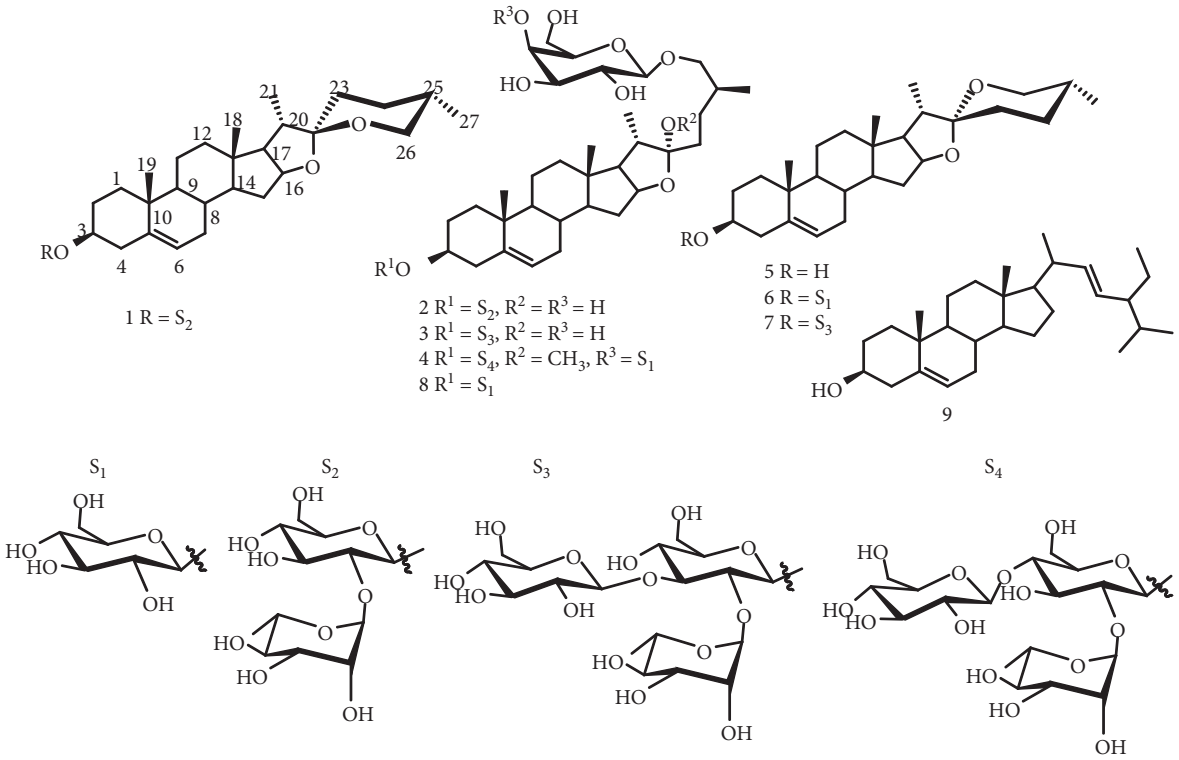

Figure 1: Chemical structures of the tested compounds. (25*R*)-spirost-5-ene-3β, 22β-3-O-β-D-glucopyranosyl(1 $\longrightarrow$ 2)-O-α-L-rhamnopyranoside (1); raphvinin 1 (2); raphvinin 2 (3); raphvinin 3 (4); diosgenin (5); diosgenin-3-O-β-D-glucopyranoside or (22*R*, 25*R*)-3β-spirost-5-ene-3-O-β-D-glucopyranoside or trillin (6); deltonin (7); 26-O-β-D-glucopyranosyl-(22*R*,25*R*)-3β, 22, 26-trihydroxyfurost-5-ene-3-O-β-D-glucopyranoside (8); and sitosterol (9).

values, extract displayed good antiproliferative activity with IC_{50} values below 20 μg/ mL and 30 μg/ mL in 15/18 and 18/18 cancer cell lines, respectively. Compound 4 (IC_{50}: 10.42 μM) displayed good cytotoxicity against MaMel-80aBRAF-V600E homozygous mutant; compounds 4 and 1 displayed moderate antiproliferative activity against 8/9 and 3/9 cell lines, respectively. Compounds 3, 7, 8, and 9 were not active ($IC_{50} > 100$ μM) towards the tested cell lines.

3.3. Acute Toxicity of RVM. During this experiment, no animals died among the female rats receiving 5000 mg/kg of RVM. The signs of toxicities were not detected based on the behavior of rats during the observation period (14 days). Therefore, lethal dose (LD_{50}) of this extract was estimated greater than 5000 mg/kg in female rats. Tables 4 and 5 represent the body weights (g) and relative organ weights in the female rats during acute toxicity, respectively.

Table 4: Evolution of body weights (g) of rats treated with RVM during acute toxicity study.

Period (days)	Body weights of female rats (g)		
	Female 1	Female 2	Female 3
1st day	133	128	124
15th day	183	168	166

Table 5: Relative organ weights (g) of the female rats treated with RVM during acute toxicity.

Organs	Organ weight of female rats (g)		
	Female 1	Female 2	Female 3
Liver	2.92	2.98	2.80
Kidneys	0.74	0.72	0.66
Lung	0.89	0.73	0.71
Heart	0.32	0.32	0.30
Spleen	0.32	0.33	0.30

3.4. Subchronic Toxicity of RVM

3.4.1. Food Consumption. The food consumption changes in both female and male rats treated with different doses (250, 500, and 1000 mg/kg b.w.) of extract are presented in Figures 2(a) and 2(b). During the treatment period, both sexes of rats showed reduction in the food intake compared with the control group. However, the reduction of food consumption was significant from the 16th day of treatment in male rats treated at highest with respect to controls.

3.4.2. Body Weight. The body weight gain changes in both female and male rats treated with different doses (250, 500, and 1000 mg/kg b.w.) of extract are represented in Figures 3(a) and 3(b). At all doses during the treatment period, the female and male rats showed a decrease in their

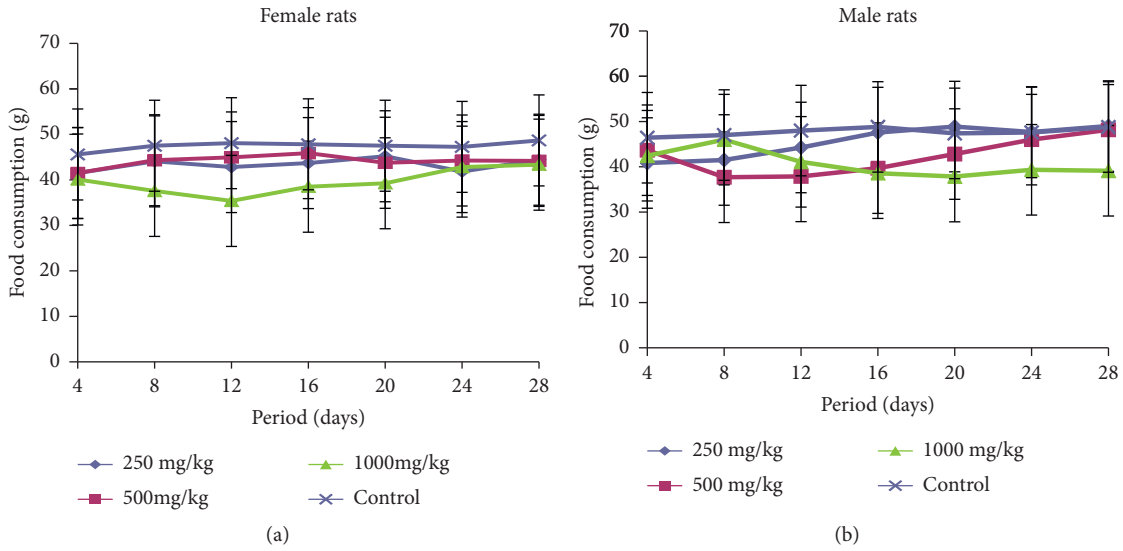

Figure 2: (a). Food consumption changes of female rats treated with RVM during subchronic toxicity study. (b). Food consumption changes of male rats treated with RVM during subchronic toxicity study.

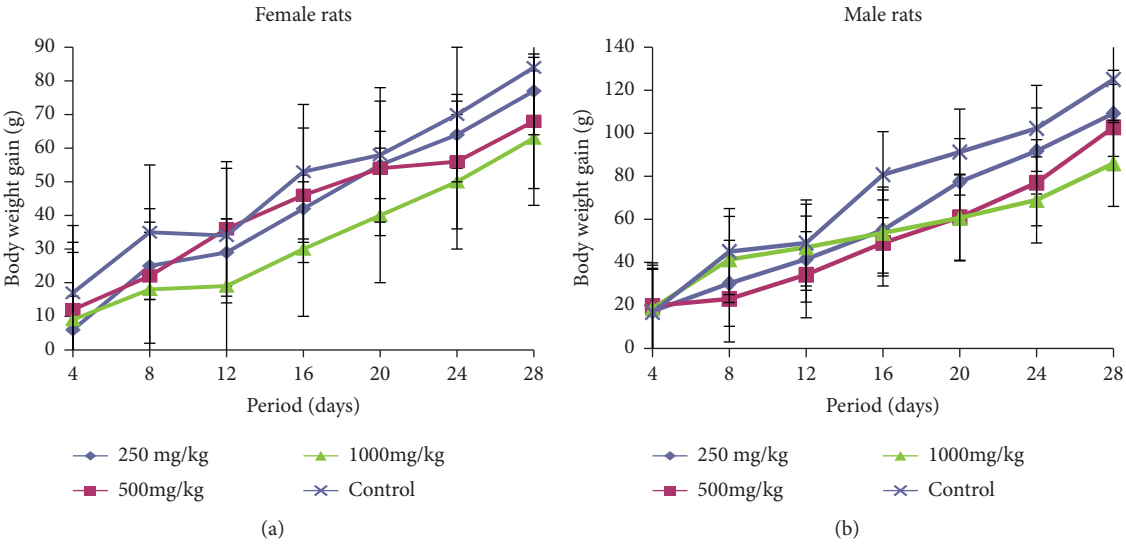

Figure 3: (a). Body weight changes of female rats treated with RVM during subchronic toxicity study. (b) Body weight changes of male rats treated with RVM during subchronic toxicity study.

body weight compared with the control group. This body weight of treated groups reduced inversely proportional to doses administered with respect to the control group. However, the decrease of body weight in male rats treated at highest dose (1000 mg/ kg) with respect to the control group was significant from the 16th day of treatment.

3.4.3. Organ Weights. Table 6 represents the effect of RVM on organ weights (g) of both female and male rats during subchronic toxicity. The results show that no significant difference ($p < 0.05$) was remarked in organ weights of treated rats with respect to those of the controls. Nevertheless, the spleen weight of male rat was significantly decreased at the dose 1000 mg/kg compared with the control group.

3.4.4. Biochemical Parameters

(1) Effect of Extract on ALT, AST, ALP Activity, and Total Serum Protein Levels. The effect of different doses of extract on the activity of transaminases (ALT and AST), total serum protein levels, and alkaline phosphatase levels is shown in Table 7. After repeated administration doses of extract, the results showed that, in female and male rats, the activity of serum total proteins and alkaline phosphatase was significantly reduced at doses 250 and

Table 6: Effect of RVM on organ weights (g) of the rats during subchronic toxicity study.

Sexes	Organs (g)	Control	Extract doses (mg/kg)		
			250	500	1000
Female	Liver	3.12 ± 0.16^{a}	2.91 ± 0.17^{a}	2.93 ± 0.16^{a}	3.06 ± 0.28^{a}
	Kidneys	$0.65 \pm 0.02^{a,b}$	0.68 ± 0.04^{a}	0.61 ± 0.05^{b}	0.69 ± 0.03^{a}
	Lung	0.57 ± 0.04^{a}	0.54 ± 0.04^{a}	0.54 ± 0.03^{a}	0.66 ± 0.26^{a}
	Heart	$0.30 \pm 0.01^{a,b}$	$0.29 \pm 0.01^{a;b}$	0.27 ± 0.01^{a}	0.32 ± 0.01^{a}
	Spleen	0.20 ± 0.02^{a}	0.36 ± 0.15^{a}	0.26 ± 0.12^{a}	0.30 ± 0.08^{a}
Male	Liver	3.39 ± 0.44^{a}	3.16 ± 0.57^{a}	3.23 ± 0.31^{a}	3.06 ± 0.15^{a}
	Kidneys	0.65 ± 0.05^{a}	0.65 ± 0.05^{a}	0.65 ± 0.10^{a}	0.58 ± 0.04^{a}
	Lung	0.59 ± 0.12^{a}	0.65 ± 0.05^{a}	0.52 ± 0.04^{a}	0.53 ± 0.06^{a}
	Heart	0.32 ± 0.04^{a}	0.31 ± 0.01^{a}	0.30 ± 0.01^{a}	0.31 ± 0.01^{a}
	Spleen	0.35 ± 0.09^{b}	0.40 ± 0.09^{b}	$0.30 \pm 0.10^{a,b}$	0.20 ± 0.01^{a}

The table values are presented as mean ± standard deviation of 4 repetitions. In the same line and by sex, the values bearing the different letters are significantly different according to Waller Duncan's multiple comparison test ($p < 0.05$).

Table 7: Effect of RVM on biochemical parameters (ALT, AST, total proteins, and alkaline phosphatase) of the rats during subchronic toxicity study.

Sexes	Parameters	Control	Extract doses (mg/kg)		
			250	500	1000
Female	ALT	69.69 ± 1.13^{c}	57.88 ± 0.71^{a}	66.63 ± 1.43^{b}	65.53 ± 0.84^{b}
	AST	98.88 ± 2.14^{c}	85.31 ± 3.39^{b}	74.38 ± 3.27^{a}	86.63 ± 1.89^{b}
	T. proteins	11.14 ± 0.31^{c}	8.80 ± 0.29^{a}	$9.29 \pm 0.46^{a,b}$	9.90 ± 0.36^{b}
	PAL	358.42 ± 7.52^{d}	342.46 ± 2.30^{c}	324.67 ± 3.94^{b}	281.35 ± 4.80^{a}
Male	ALT	67.72 ± 1.31^{b}	62.47 ± 1.31^{a}	69.03 ± 1.80^{b}	69.25 ± 2.47^{b}
	AST	$103.69 \pm 5.37^{b,c}$	87.94 ± 1.52^{a}	101.50 ± 5.72^{b}	109.38 ± 1.24^{c}
	T. proteins	11.31 ± 1.07^{b}	9.31 ± 0.82^{a}	9.59 ± 1.09^{a}	$9.95 \pm 0.52^{a,b}$
	PAL	438.22 ± 5.65^{d}	417.70 ± 2.98^{c}	396.26 ± 4.80^{b}	317.83 ± 5.65^{a}

The table values are presented as mean ± standard deviation of 4 repetitions. In the same line and by sex, the values bearing the different letters are significantly different according to Waller Duncan's multiple comparison test ($p < 0.05$). Indicators: ALT: alanine aminotransferase, AST: aspartate aminotransaminase; T. proteins: total proteins, ALP: alkaline phosphatase.

Table 8: Effect of RVM on the level of serum creatinine, serum urea, and urinary protein.

Sexes	Parameters (mg/dL)	Control	Extract doses (mg/kg)		
			250	500	1000
Females	Serum urea	$30.55 \pm 1,\ 15^{b}$	27.38 ± 1.10^{a}	27.15 ± 0.84^{a}	25.33 ± 1.78^{a}
	Urinary urea	1522.85 ± 12.30^{c}	1280.32 ± 8.08^{b}	1259.83 ± 5.57^{a}	$1268.66 \pm 6.12^{a,b}$
	Serum creatinine	$0.83 \pm 0.05^{a,b}$	$0.83 \pm 0.02^{a,b}$	0.88 ± 0.05^{b}	0.80 ± 0.01^{a}
	Urinary creatinine	94.51 ± 5.40^{c}	55.49 ± 1.22^{a}	79.27 ± 1.41^{b}	82.93 ± 3.98^{b}
	Urinary protein	12.73 ± 1.84^{a}	10.74 ± 1.52^{a}	12.33 ± 2.72^{a}	10.34 ± 0.92^{a}
Males	Serum urea	26.07 ± 1.82^{a}	24.67 ± 1.40^{a}	23.65 ± 1.15^{a}	24.58 ± 1.04^{a}
	Urinary urea	1318.40 ± 9.24^{c}	1235.84 ± 6.10^{b}	1184.87 ± 4.80^{a}	1231.34 ± 4.45^{b}
	Serum creatinine	1.07 ± 0.07^{c}	0.83 ± 0.04^{b}	$0.81 \pm 0.02^{a,b}$	0.73 ± 0.04^{a}
	Urinary creatinine	112.20 ± 3.45^{b}	95.12 ± 1.99^{a}	96.95 ± 4.17^{a}	119.51 ± 1.99^{c}
	Urinary protein	15.51 ± 1.52^{a}	14.72 ± 1.52^{a}	14.32 ± 1.84^{a}	15.51 ± 0.80^{a}

The table values are presented as mean ± standard deviation of 4 repetitions. In the same line and by sex, the values bearing the different letters are significantly different according to Waller Duncan's multiple comparison test ($p < 0.05$).

500 mg/kg compared with the control group. In female rats, the activity of ALT and AST was significantly decreased ($p < 0.05$) at all doses compared with controls. No significant difference was observed in the activity of transaminases at doses 500 and 1000 mg/kg in the male rats. However, in male rats, the significant reduction of these parameters was observed at dose 250 mg/kg compared with the control group.

(2) Effect of RVM on Level of Urea, Creatinine, and Urinary Protein. The effects of RVM on the level of serum creatinine, serum urea, and urinary protein are represented in Table 8. Serum and urinary urea level and urinary creatinine level showed a significant reduction in female rats compared with their control group. Urinary urea and serum creatinine levels were significantly reduced in male rats treated at all doses with respect to control groups. However, urinary

Table 9: Effect of RVM on lipid profile in both sexes of rats during subchronic toxicity study.

Sexes	Parameters (mg/dL)	Control	Extract doses (mg/kg)		
			250	500	1000
Females	TC	80.41 ± 2.31^{a}	82.44 ± 3.81^{a}	84.73 ± 3.54^{a}	84.22 ± 1.47^{a}
	HDL	50.95 ± 0.41^{a}	52.08 ± 1.67^{a}	53.22 ± 1.86^{a}	52.46 ± 1.09^{a}
	TG	52.00 ± 5.80^{a}	50.71 ± 3.83^{a}	55.51 ± 6.28^{a}	50.26 ± 2.90^{a}
	LDL	19.46 ± 1.14^{a}	20.62 ± 3.73^{a}	20.41 ± 1.90^{a}	21.71 ± 2.45^{a}
Males	TC	103.82 ± 4.16^{a}	104.33 ± 3.30^{a}	106.30 ± 3.13^{a}	101.78 ± 4.28^{a}
	HDL	59.52 ± 1.48^{b}	54.60 ± 2.12^{a}	54.10 ± 1.99^{a}	54.60 ± 4.33^{a}
	TG	62.87 ± 4.59^{a}	91.18 ± 4.20^{c}	92.83 ± 3.67^{c}	72.24 ± 3.31^{b}
	LDL	31.72 ± 2.43^{a}	31.49 ± 1.54^{a}	33.63 ± 1.30^{a}	32.73 ± 4.65^{a}

The table values are presented as mean ± standard deviation of 4 repetitions. In the same line and by sex, the values bearing the different letters are significantly different according to Waller Duncan's multiple comparison test ($p < 0.05$). Indicators: TG: triglyceride; TC: total cholesterol; HDL: high-density lipoproteins; LDL: Low-density lipoproteins.

Table 10: Effect of RVM on hematological parameters of the rats treated with RVM during subchronic toxicity study.

Sexes	Parameters	Control	Extract doses (mg/kg)		
			250	500	1000
Females	WBCs ($\times 10^3$ /μl)	4.60 ± 0.36^{a}	5.03 ± 0.72^{a}	4.25 ± 0.65^{a}	7.30 ± 0.87^{b}
	Lymph (%)	64.00 ± 4.90^{a}	65.93 ± 5.66^{a}	63.88 ± 3.63^{a}	63.87 ± 3.62^{a}
	MONO (%)	6.27 ± 0.40^{b}	6.23 ± 0.18^{b}	5.75 ± 0.15^{b}	4.27 ± 0.97^{a}
	GR (%)	29.73 ± 4.51^{a}	28.20 ± 1.23^{a}	30.45 ± 3.55^{a}	31.87 ± 2.26^{a}
	PLT ($\times 10^3$/μl)	847.00 ± 7.94^{a}	855.00 ± 6.00^{a}	850.00 ± 2.00^{a}	871.50 ± 5.50^{b}
	MPV (fL)	6.77 ± 0.12^{a}	6.97 ± 0.31^{a}	6.87 ± 0.40^{a}	6.90 ± 0.20^{a}
	RBCs ($\times 10^6$/μl)	8.88 ± 0.01^{a}	8.55 ± 0.15^{a}	8.48 ± 0.31^{a}	8.62 ± 0.16^{a}
	Hb (g/dL)	18.30 ± 0.66^{b}	$17.47 \pm 0.95^{a,b}$	$16.70 \pm 0.82^{a,b}$	16.50 ± 0.79^{a}
	HCT (%)	54.43 ± 1.66^{b}	$51.20 \pm 2.07^{a,b}$	$51.17 \pm 0.55^{a,b}$	47.90 ± 3.81^{a}
	MCV (fL)	60.10 ± 0.78^{a}	59.90 ± 1.56^{a}	60.37 ± 2.15^{a}	60.83 ± 1.12^{a}
	MCH (pg)	20.23 ± 0.93^{a}	20.40 ± 0.82^{a}	19.70 ± 0.20^{a}	21.00 ± 1.04^{a}
	MCHC (g/dL)	33.63 ± 1.14^{a}	34.33 ± 0.55^{a}	32.70 ± 1.55^{a}	34.50 ± 1.08^{a}
Males	WBCs ($\times 10^3$/μl)	6.20 ± 1.00^{a}	6.40 ± 0.26^{a}	5.55 ± 1.05^{a}	6.35 ± 0.35^{a}
	Lymph (%)	69.80 ± 1.91^{b}	68.57 ± 3.42^{b}	62.30 ± 3.90^{b}	51.57 ± 2.43^{a}
	MONO (%)	4.40 ± 0.66^{a}	4.53 ± 0.55^{a}	5.10 ± 0.90^{a}	5.47 ± 0.32^{a}
	GR (%)	26.80 ± 0.30^{a}	26.90 ± 3.60^{a}	31.10 ± 1.50^{a}	47.97 ± 4.44^{b}
	PLT ($\times 10^3$/μl)	666.33 ± 10.97^{a}	662.33 ± 4.51^{a}	664.00 ± 5.29^{a}	860.33 ± 17.04^{b}
	MPV (fL)	6.90 ± 0.00^{a}	7.43 ± 0.23^{a}	7.10 ± 0.20^{a}	6.90 ± 1.00^{a}
	RBCs ($\times 10^6$/μl)	9.11 ± 0.67^{a}	8.67 ± 0.44^{a}	9.21 ± 0.65^{a}	9.55 ± 0.50^{a}
	Hb (g/dL)	17.53 ± 0.12^{a}	17.20 ± 0.85^{a}	18.05 ± 1.05^{a}	17.83 ± 1.47^{a}
	HCT (%)	54.57 ± 2.94^{a}	53.50 ± 1.00^{a}	56.67 ± 1.14^{a}	56.63 ± 4.29^{a}
	MCV (fL)	59.97 ± 2.03^{a}	60.53 ± 0.76^{a}	61.70 ± 3.75^{a}	59.27 ± 2.57^{a}
	MCH (pg)	19.30 ± 1.56^{a}	19.87 ± 0.06^{a}	20.03 ± 0.76^{a}	18.67 ± 0.85^{a}
	MCHC (g/dL)	32.17 ± 1.91^{a}	32.80 ± 0.35^{a}	32.50 ± 0.82^{a}	31.50 ± 0.30^{a}

The table values are presented as mean ± standard deviation of 4 repetitions. In the same line and by sex, the values bearing the different letters are significantly different according to Waller Duncan's multiple comparison test ($p < 0.05$). Indication: WBCs: white blood cells, Lymph: lymphocytes, Mono: monocytes, GR: granulocytes, PLT: platelets, MPV: mean platelet volume, RBCs: red blood cells, Hb: hemoglobin, HCT: hematocrit, MCV: mean corpuscular volume, MCH: mean corpuscular hemoglobin, MCHC: mean corpuscular hemoglobin concentration.

creatinine level was significantly decreased in rats treated at doses 250 and 500 mg/kg but significantly increased in male rats treated at dose 1000 mg/kg with respect to the control group.

(3) Effect of RVM on Serum Lipid Profile. The effect of administration of extract on lipid profile in both female and male rats is represented in Table 9. The HDL cholesterol levels reduced in males treated at three doses compared with the control group. An increment in triglyceride levels (TG) was observed in male rats treated at three doses of extract compared with controls. As compared to the control groups, other parameters measured did not show significant differences.

3.4.5. Hematological Parameters. Table 10 presents the effect of RVM on hematological parameters of the rats treated with RVM. A significant decrease was observed in the level of monocytes, hemoglobin, and hematocrit in the female rats treated with extract at the highest dose compared with controls, while lymphocyte levels significantly reduced in the same group of rats with respect to controls. A significant increase was remarked in the level of platelets in both sexes

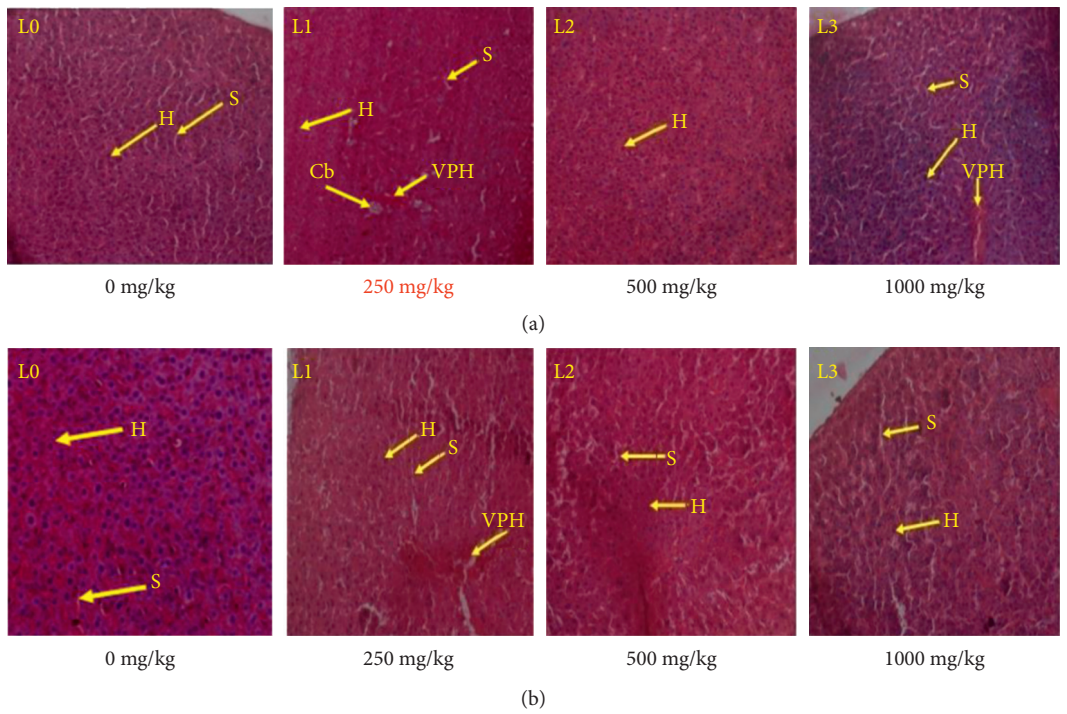

Figure 4: (a). Effect of RVM on liver histopathology in female rats during subchronic toxicity study: (L_0): control group; (L_1): 250 mg/kg; (L_2): 500 mg/kg; and (L_3): 1000 mg/kg. Indicators: (Cb): bile duct; (VPH): hepatic portal vein; (H): hepatocytes; (S): sinusoid. (b) Effect of RVM on liver histopathology in male rats during subchronic toxicity study: (L_0): control group; (L_1): 250 mg/kg; (L_2): 500 mg/kg; and (L_3): 1000 mg/kg. Indicators: (VPH): hepatic portal vein; (H): hepatocytes; and (S): sinusoid. The liver photomicrographs presented in the document represent the general appearance observed in at least three of four animals in each group.

treated with extract at dose 1000 mg/kg compared with control groups. In male rats, granulocytes were significantly higher in treated animals who received highest dose of extract; the lymphocyte level indicated significant reduction in same group of rats compared with the control group. The significant differences did not show in the rest of hematological parameters measured compared with the control group.

3.4.6. Histopathological Examination. Histopathological examinations were performed on the liver and kidneys to verify whether these organs or tissues had been damaged. No remarkable pathological change was shown on all organs after the microscopic observation compared with the control group. The effect of RVM on liver and kidneys histology in female and male rats during subchronic toxicity study is presented in (Figures 4(a) and 4(b)) and (Figures 5(a) and 5(b)).

4. Discussion

Several mineral elements and metabolic products of plant cells are capable to influence the metabolism. These minerals are very important as they have several biological functions, and their deficiency generally leads to nutritional disorders [39]. In this study, zinc (Zn) and sodium (Na) were detected. Zinc plays a vital role in human growth and development. High zinc content was observed in RVM (6.52 mg/100 g DM). The recommended daily dose is between 0.3 and 1 mg/kg in adults [40]. This result is not the same as that of Doungue [41] who obtained 0.88 mg/100 g of DM in *Raphia* (*Raphia hookeri*). This variation of values might be due to the difference in *Raphia* species used.

Medicinal plants are good cytotoxic agents if their IC_{50} value is below 20 μg/mL; phytochemicals are significantly cytotoxic if their $IC_{50} < 10$ μM and moderately cytotoxic if $10\ \mu M < IC_{50} < 50\ \mu M$ [42]. Also, according to Suffness and Pezzuto, if the IC_{50} values of plant extracts are lower than or around 30 μg/mL, they deserve to be purified in order to find active components [43]. Hence, plant extract with IC_{50} values lower than 20 μg/mL and 30 μg/mL as obtained in this assay against 15/18 and 18/18 cancer cell lines, respectively. Compound 4 showed IC_{50} equal to 10.42 against MaMel-80aBRAF-V600E homozygous mutant; compounds 4 and 1 showed $10\ \mu M < IC_{50} < 50\ \mu M$ against 8/9 and 3/9 cell lines, respectively. Regarding criterion of anticancer activities, the plant extracts (RVM), compound 4 (Raphvinin), could therefore be considered as potential cytotoxic drug towards sensitive and resistant phenotypes. Those activities are due to different chemical compounds present in the plant extract. This result is in agreement with those of some authors [18, 26], which have shown that the *Raphia vinifera* compounds have cytotoxicity activity against cancer cell lines. Previous research showed that saponins from *Raphia vinifera* (Progenin III) induced necroptosis, autophagy, and apoptosis in leukemia cells [26]. Zhao et al. have shown that steroidal saponins

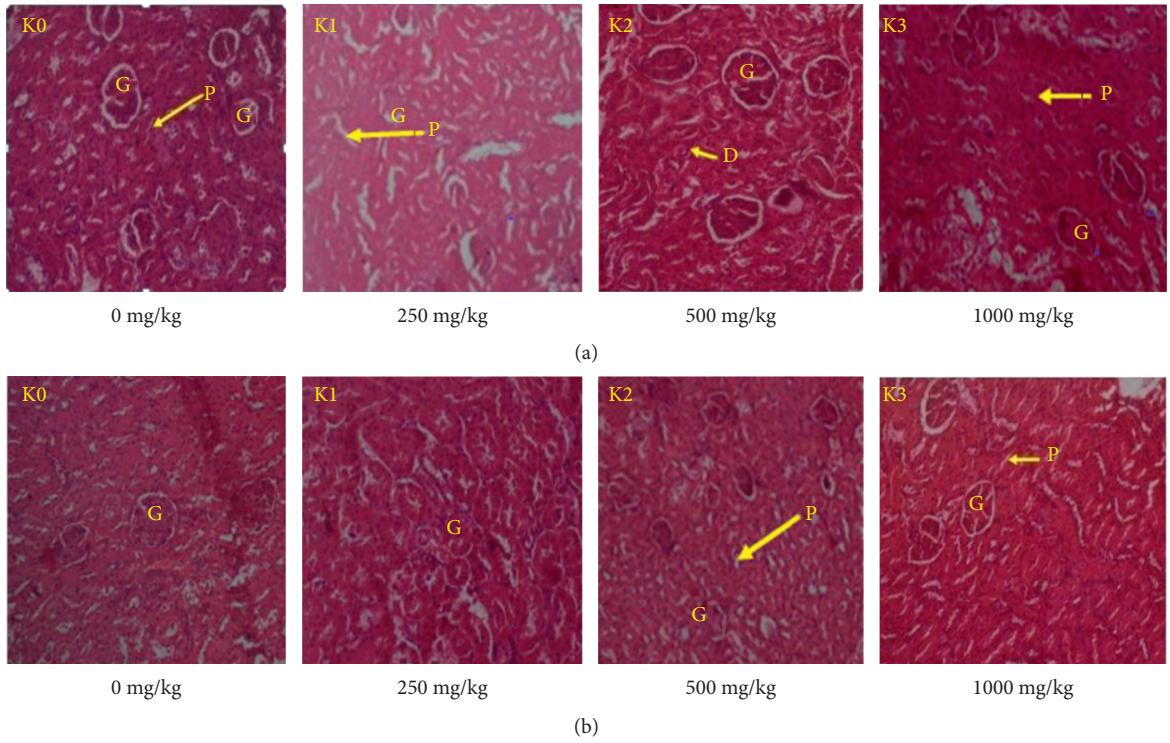

Figure 5: (a) Effect of RVM on kidney histopathology in female rats during subchronic toxicity study: (k_0): control group; (k_1): 250 mg/kg; (k_2): 500 mg/kg; and (k_3): 1000 mg/kg. Indicators: (G): glomerulus; (P): proximal tubule; (D): distal tubule. (b) Effect of RVM on kidney histopathology in male rats during subchronic toxicity study: (k_0): control group; (k_1): 250 mg/kg; (k_2): 500 mg/kg; and (k_3): 1000 mg/kg. Indicators: (G): glomerulus; (P): proximal tubule. The kidney photomicrographs presented in the document represent the general appearance observed in at least three of four animals in each group.

previously exhibited cytotoxic effects by blocking the *S* phase of interphase [14].

The undesirable effects observed in animals after substance intake predict the toxic effects in humans after its administration [44]. The dosage of markers that ensures the correct functioning of the organism in rats can provide information on the toxicological effect of a substance. For the acute toxicity, the single dose (5000 mg/kg b.w.) of extract administered in rats did not cause animal deaths. Therefore, LD50 was estimated to be greater than 5000 mg/kg since no acute toxicity was detected. The extract has low toxicity when their LD_{50} is between 2000 mg/kg and 5000 mg/kg after oral administration [35]. Some authors had obtained LD_{50} higher than 4000 mg/kg b.w. after administration of the root extract of *Raphia spp.* (*Raphia hookeri*) in same experience [45]. The high safety margin presented by this genus proof its safety for consumers [45].

For the subchronic toxicity study, the rats received 3 doses (250, 500, and 1000 mg/kg) of extract. The results showed that the amount of food intake had a direct effect on animal growth. The significant reductions of food consumption and animal growth were observed in male rats treated at highest dose (1000 mg/kg) from the 16^{th} day of treatment with respect to the control group. The weight loss of animals during this work can be explained by the presence of tannins and saponins (antinutritional substances) in this plant extract. These substances that have the ability to reduce absorption of nutrients in the body [46] would be responsible for the reduction of food consumption, and thus, the reduction in body weight of rats treated at the highest dose of extract. This is agreed with that of Felix and Mello [47] who have reported that tannins showed inhibitory activities on digestive enzymes and decrease the protein quality of foods.

The levels of transaminases and ALP are generally used as biomarkers associated with liver damage [48, 49]. The decrease in serum transaminase, total proteins, and alkaline phosphatase levels at all doses observed in the female rats with respect to control groups could reflect the hepatoprotective activity of secondary metabolite contents in RVM. This result is in agreement with those obtained by Kamga and Russell [9, 12] who have shown that the young leaves of *Raphia vinifera* are used against liver problems. Also, many types of research showed that many flavonoids and saponins present in root, leaf, and epicarp of *Raphia ssp* (*R. hookeri*) have hepatoprotective, antioxidative, anti-inflammatory, and anticancer activities [50–52]. This hepatoprotective activity is proven by histopathological analysis of the liver that revealed no damage in both sexes in rats treated at all doses.

The significant increase of triglyceride levels (TG) was remarked in male rats treated at all doses of extract with respect to their control groups. These could be due to the fact that the extract contains oil, which is rich in triglyceride. This is in accordance with the idea of Igwenyi et al. [15] who have

extracted oil from the dried pulp of *Raphia vinifera*. Noubangue et al. [39] have extracted oil from the dried pulp of *Raphia spp* using the maceration method.

Kidney is an organ, which excrete waste product of metabolism outside organism. However, prolonged exposure of the kidney to toxic substances may be altered the renal tubules [53]. The significant reduction of urea and creatinine levels in rats treated with lower doses (250 mg/kg and 500 mg/kg) of extract compared with the control group would be due to the fact that the extract contains secondary metabolism responsible for nephroprotective effect. Some studies have shown that the phenolic compound contents in the extract have nephroprotective activities [52]. However, the apical bud is taken to treat gonorrhea and other genitourinary infections [8]. These results are reinforced by the kidney sections of rats, which present no alteration. The possible kidney malfunction is suspected when the serum levels of creatinine and urea are abnormally high [54]. The increase in urinary creatinine levels in rat treated at dose 1000 mg/kg is due to antinutrient (oxalate) contained in the extract. In fact, the oxalic acid is nocive to the kidney and heart [55] and the symptoms of mild oxalate poisoning include kidney diseases [56].

Hematological components are useful for assessing food's toxicity [57]. The significant increase of lymphocyte levels in female rats treated at highest dose (1000 mg/kg) of extract with respect to their control group was observed since extract contains lactic acid responsible for immunoprotection effect. The investigations performed by some authors showed that raffia wine of *Raphia vinifera* contains lactic acid bacteria [5] that stimulate the immune system of rats [6]. These results agree with those of some authors [58] who have shown that lymphocyte and monocyte levels increase at dose 1000 mg/kg in rat treated with ethanol extracts. The significant increase in blood platelets in both sexes treated at highest dose would indicate thrombocytosis. Moreover, the investigation carried out showed that extracts of *Raphia vinifera* fruit showed an increase in platelet indices counts [58]. The significant reduction of hemoglobin and hematocrit level in female rats treated at highest dose of extract could be because these rats had anemia. Several types of research demonstrate that, when the hemoglobin level is decrease, the patient has anemia [59]. However, investigations carried out by Ogidi et al. [58] showed that methanol and ethanol extracts of RVM showed an increase in red blood cell with respect to control groups. These contradictory results could be explained by the difference in the qualitative or quantitative composition of those two extracts of *Raphia*.

5. Conclusion

The aim of this investigation was to evaluate the antiproliferative potential of *Raphia vinifera* extract and its constituents on cancer cells, as well as the toxicity of the crude extract. It also showed that this extract is relatively nontoxic. However, caution should be taken when consuming the extract of the fruit mesocarp of *Raphia vinifera* during 28 days of treatment at highest dose, as it may induce some liver and kidney injuries. In general, *Raphia vinifera* is a safe medicinal plant that deserves further investigation to afford an anticancer phytomedicine.

Data Availability

All data obtained or generated during this work are incorporated in this published article.

Conflicts of Interest

The authors declare that they have no conflicts of interest.

Authors' Contributions

GSN and INB carried out the study; GFC, VK, and ATM designed the experiments; GSN wrote the manuscript; VK supervised the work; and all authors read and approved the final manuscript.

Acknowledgments

The authors thank gratefully to the Cameroon National Herbarium for the identification of plants. No funding was declared by the authors.

Supplementary Materials

S1: ^{1}H NMR (400 MHz DMSO) Spectrum of Compound **1**; **S2**: ^{13}C NMR (100 MHz DMSO) Spectrum of Compound **1**; **S3**: ^{1}H NMR (600 MHz, CD_3OD) Spectrum of Compound **2**; **S4**: ^{13}C NMR (150 MHz, CD_3OD) Spectrum of Compound **2**; **S5**: ^{1}H NMR (400 MHz CD_3OD) Spectrum of Compound **3; S6**: ^{13}C NMR (100 MHz CD_3OD) Spectrum of Compound **3**; **S7**: ^{1}H NMR (400 MHz CD_3OD) Spectrum of Compound **4**; **S8**: ^{13}C NMR (100 MHz CD_3OD) Spectrum of Compound **4**; **S9**: ^{1}H NMR (400 MHz $CDCl_3$) Spectrum of Compound **5; S10**: ^{13}C NMR (100 MHz $CDCl_3$) Spectrum of Compound **5; S11**: ^{1}H NMR (300 MHz DMSO) Spectrum of Compound **6**; **S12**: ^{13}C NMR (75 MHz DMSO) Spectrum of Compound **6**; **S13**: ^{1}H NMR (400 MHz DMSO) Spectrum of Compound **7**; **S14**: ^{13}C NMR (100 MHz DMSO) Spectrum of Compound **7**; **S15**: ^{1}H NMR (400 MHz CD_3OD) Spectrum of Compound **8; S16**: ^{13}C NMR (100 MHz CD_3OD) Spectrum of Compound **8; S17**: ^{1}H NMR (400 MHz, $CDCl_3$) Spectrum of Compound **9; S18**: ^{13}C NMR (100 MHz, $CDCl_3$) Spectrum of Compound **9**. (*Supplementary Materials*)

References

[1] T. P. Kingham, O. I. Alatise, V. Vanderpuye et al., "Treatment of cancer in sub-Saharan Africa," *The Lancet Oncology*, vol. 14, no. 4, pp. e158–e167, 2013.

[2] International Agency for Research on Cancer (IARC), *Latest Global Cancer Data: Cancer Burden Rises to 18.1 Million New Cases and 9.6 Million Cancer Deaths in 2018*, Press Release, London, UK, 2020.

[3] M. Feve, "Utilisation d'une approche de chimie biologie intégrative dans la recherche de nouvelles molécules actives sur la prolifération et la différenciation des cellules souches cancéreuses," *Sciences du Vivant, Aspects moléculaires et*

cellulaires de la biologie, Université de Strasbourg, Strasbourg, France, 2012.

[4] A. T. Mbaveng, H. T. Manekeng, G. S. Nguenang et al., "Cytotoxicity of 18 Cameroonian medicinal plants against drug sensitive and multi-factorial drug resistant cancer cells," *Journal of Ethnopharmacology*, vol. 222, pp. 21–33, 2018.

[5] O. Obire, "Activity of Zymonas species in palm–sap obtained from three areasin Edo State, Nigeria," *Journal of Applied Sciences & Environmental Management*, vol. 9, no. 1, pp. 25–30, 2005.

[6] T. N. Flore, Z. N. François, and T. M. Félicité, "Immune system stimulation in rats by *Lactobacillus sp*. isolates from Raffia wine (*Raphia vinifera*)," *Cellular Immunology*, vol. 260, no. 2, pp. 63–65, 2010.

[7] V. Kuete, L. P. Sandjo, B. Wiench, and T. Efferth, "Cytotoxicity and modes of action of four Cameroonian dietary spices ethno-medically used to treat Cancers: *Echinops giganteus, Xylopia aethiopica, Imperata cylindrica* and *Piper capense*," *Journal of Ethnopharmacology*, vol. 149, no. 1, pp. 245–253, 2013.

[8] M. Gruca, T. R. van Andel, and H. Balslev, "Ritual uses of palms in traditional medicine in sub-Saharan Africa: a review," *Journal of Ethnobiology and Ethnomedicine*, vol. 10, no. 60, 2014.

[9] M. S. Kamga, B. Sonké, and T. Couvreur, "Raphia vinifera (Arecaceae; Calamoideae): misidentified for far too long," *Biodiversity Data Journal*, vol. 7, Article ID e37757, 2019.

[10] T. A. Russell, "The Raphia palms of west Africa," *Royal Botanic Gardens*, Kew Bulletin, vol. 19, pp. 173–196, , Kew, London", 1965.

[11] N. R. SikameTagne, T. E. Mbou, O. Harzallah et al., M. Fogue and J-Y. Drean, Physicochemical and mechanical characterization of raffia vinifera pith," *Advances in Materials Science and Engineering*, vol. 2020, Article ID 8895913, 10 pages, 2020.

[12] A. A. Idowu, S. O. Ayoola, V. E. Nwekoyo, F. I. Adeosun, and G. E. Adesiyan, "Toxicity effect of varying concentations of Raphia vinifera fruit extract on african cat fish (Clarias giriepinus Burchell, 1922) fingerlings," *Dutse journal of agriculture and food security*, vol. 6, no. 1, pp. 1–18, 2019.

[13] S. Ma, J. Kou, and B. Yu, "Safety evaluation of steroidal saponin DT-13 isolated from the tuber of *Liriope muscari* (Decne.) Baily," *Journal of Food Chemical Toxicology*, vol. 49, no. 9, pp. 2243–2251, 2011.

[14] Y. Z. Zhao, Y. Y. Zhang, H. Han et al., "Advances in the antitumor activities and mechanisms of action of steroidal saponins," *Chinese Journal of Natural Medicines*, vol. 16, no. 10, pp. 732–748, 2018.

[15] I. O. Igwenyi, O. U. Njoku, O. E. Ikwuagwu, and C. P. Nwuke, "Extraction, characterization and potentials of raphia mesocarp oil for the production of biodiesel," *Journal of Agriculture, Biotechnology and Ecology*, vol. 1, no. 1, pp. 53–61, 2008.

[16] S. G. Nguenang, T. A. Mbaveng, G. A. Fankam et al., "*Tristemma hirtum* and five other cameroonian edible plants with weak or no antibacterial effects modulate the activities of antibiotics against Gram-negative multidrug-resistant phenotypes," *Scientific World Journal*, vol. 2018, Article ID 7651482, 12 pages, 2018.

[17] L. D. F. Dias and S. C. Takahashi, "Cytogenetic evaluation of aqueous extracts of the medicinal plants Alpinia mutans rose (Zingerberaceae) and Pogostemum hyneanus benth (Labitae) on Wistar rats and Allium cepa (Liliaceae) root tip cells," *Brazilian Journal of Genetics*, vol. 17, no. 2, pp. 175–180, 1994.

[18] G. F. Chi, R. V. T. Sop, A. T. Mbaveng et al., "Steroidal saponins from *Raphia vinifera* and their cytotoxic activity," *Steroids*, vol. 163, Article ID 108724, 2020.

[19] A. Kimmig, V. Gekeler, M. Neumann et al., "Susceptibility of multidrug-resistant human leukemia cell lines to human interleukin 2-activated killer cells," *Cancer Research*, vol. 50, no. 21, pp. 6793–6799, 1990.

[20] J. Gillet, T. Efferth, D. Steinbach et al., "Microarray-based detection of multidrug resistance in human tumor cells by expression profiling of ATP-binding cassette transporter genes," *Cancer Research*, vol. 64, no. 24, pp. 8987–8993, 2004.

[21] O. Kadioglu, J. Cao, N. Kosyakova, K. Mrasek, T. Liehr, and T. Efferth, "Genomic and transcriptomic profiling of resistant CEM/ADR-5000 and sensitive CCRF-CEM leukaemia cells for unravelling the full complexity of multi-factorial multidrug resistance," *Scientific Reports*, vol. 636754 pages, 2016.

[22] L. A. Doyle, W. Yang, L. V Abruzzo et al., "A multidrug resistance transporter from human MCF-7 breast cancer cells," *Proceedings of the National Academy of Sciences of the United*, vol. 95, no. 26, pp. 15665–15670, 1998.

[23] V. Kuete, L. Sandjo, O. J. Nantchouang, H. Fouotsa, B. Wiench, and T. Efferth, "Cytotoxicity and modes of action of three naturally occurring xanthones (8-hydroxycudraxanthone G, morusignin I and cudraxanthone I) against sensitive and multidrug-resistant cancer cell lines," *Phytomedicine*, vol. 21, no. 3, pp. 315–322, 2013.

[24] V. Kuete, P. D. Tchakam, B. Wiench et al., "Cytotoxicity and modes of action of four naturally occurring benzophenones: 2,2′,5,6′-tetrahydroxybenzophenone, guttiferone E, isogarcinol and isoxanthochymol," *Phytomedicine*, vol. 20, no. 6, pp. 528–536, 2013.

[25] V. Kuete, L. P. Sandjo, D. E. Djeussi et al., "Cytotoxic flavonoids and isoflavonoids from Erythrina sigmoidea towards multifactorial drug resistant cancer cells," *Investigational New Drugs*, vol. 32, no. 6, pp. 1053–1062, 2014.

[26] A. T. Mbaveng, G. F. Chi, G. S. Nguenang et al., "Cytotoxicity of a naturally occurring spirostanol saponin, progenin III, towards a broad range of cancer cell lines by induction of apoptosis, autophagy and necroptosis," *Chemico-Biological Interactions*, vol. 326, pp. 1–8, Article ID 109141, 2020.

[27] A. T. Mbaveng, C. G. T. Noulala, A. R. M. Samba et al., "The alkaloid, soyauxinium chloride, displays remarkable cytotoxic effects towards a panel of cancer cells, inducing apoptosis, ferroptosis and necroptosis," *Chemico-Biological Interactions*, vol. 333, Article ID 109334, 2021.

[28] A. T. Mbaveng, G. F. Chi, I. N. Bonsou et al., "N-acetylglycoside of oleanolic acid (aridanin) displays promising cytotoxicity towards human and animal cancer cells, inducing apoptotic, ferroptotic and necroptotic cell death," *Phytomedicine*, vol. 76, Article ID 153261, 2020.

[29] A. T. Mbaveng, F. Damen, M. F. Guefack et al., "8, 8-bis-(Dihydroconiferyl)-diferulate displayed impressive cytotoxicity towards a panel of human and animal cancer cells," *Phytomedicine*, vol. 70, Article ID 153215, 2020.

[30] B. E. N. Wamba, P. Ghosh, A. T. Mbaveng et al., "Botanical from *Piper capense* fruit can help to combat the melanoma as demonstrated by *in vitro* and *in vivo* studies," *Evidence-Based Complementary and Alternative Medicine*, vol. 2021, Article ID 8810368, 15 pages, 2021.

[31] AOAC, *Official Methods of Analysis*, Association of Official Analytical Chemists, Washington, DC, USA, 15th edition, 1990.

[32] J. O'Brien, I. Wilson, T. Orton, and F. Pognan, "Investigation of the Alamar Blue (resazurin) fluorescent dye for the

assessment of mammalian cell cytotoxicity," *European Journal of Biochemistry*, vol. 267, no. 17, pp. 5421–5426, 2000.

[33] V. Kuete, A. T. Mbaveng, L. P. Sandjo, M. Zeino, and T. Efferth, "Cytotoxicity and mode of action of a naturally occurring naphthoquinone, 2-acetyl-7-methoxynaphtho[2,3-b]furan-4,9-quinone towards multi-factorial drug-resistant cancer cells," *Phytomedicine*, vol. 33, pp. 62–68, 2017.

[34] A. T. Mbaveng, B. L. Ndontsa, V. Kuete et al., "A naturally occurring triterpene saponin ardisiacrispin B displayed cytotoxic effects in multi-factorial drug resistant cancer cells via ferroptotic and apoptotic cell death," *Phytomedicine*, vol. 43, pp. 78–85, 2018.

[35] OCDE, *Lignes Directrices de l' OCDE Pour Les Essais de Produits Chimiques № 425 Toxicité Orale Aiguë Méthode de l' Ajustement des Doses*, OCDE, Paris, France, 2008.

[36] G. S. Nguenang, A. S. M. Ntyam, and V. Kuete, "Acute and subacute toxicity profiles of the methanol extract of *Lycopersicon esculentum* L. Leaves (tomato), a botanical with promising *in vitro* anticancer potential," *Evidence-based Complementary and Alternative Medicine*, vol. 2020, Article ID 8935897, 10 pages, 2020.

[37] OCDE, *Lignes Directrices de l'OCDE Pour Les Essais de Produits Chimiques № 407, Étude de Toxicité Orale à Dose répétée Pendant 28 Jours Sur Les Rongeurs*, OCDE, Paris, France, 2008.

[38] H. S. M. Di Fiore, *Atlas of Human Histology*, Lea & Febiger, Philadelphia, PA, USA, 2nd edition, 1963.

[39] N. R. V. Noubangue, S. E. Ngangoum, T. F. Djikeng, T. H. Doungue, and M. H. Womeni, "Physico-chemical properties of Raphia fruit (*Raphia hookeri*) pulp from Cameroon," *Journal of Food Stability*, vol. 3, no. 2, pp. 59–69, 2020.

[40] Fao/Who, "Codex alimentarius commission," 2014, http://www.Codexalimentarius.net/download/standards/34/CXG_002e.pd.

[41] T. H. Doungue, A. P. N. Kengne, F. T. Djikeng, G. B. Teboukeu, and H. M. Womeni, "Nutritional value of Raphia hookeri fruit, hematological properties of its powder and aqueous extract in a model of aluminum chloride inducing neurotoxicity by using rats," *Journal of Food Research*, vol. 9, no. 5, pp. 113–124, 2020.

[42] V. Kuete and T. Efferth, "African flora has the potential to fight multidrug resistance of cancer," *BioMed Research International*, vol. 2015, Article ID 914813, 25 pages, 2015.

[43] M. Suffness and J. Pezzuto, "Assays related to cancer drug discovery," in *Methods in Plant Biochemistry: Assays for Bioactivity*, pp. 71–133, Academic Press, Cambridge, MA, USA, 1990.

[44] R. Heywood, "Target organ toxicity," *Toxicology Letters*, vol. 8, no. 6, pp. 349–358, 1981.

[45] O. G. Mbaka, O. S. Ogbonnia, O. T. Olubamido, I. P. Awopetu, and A. D. Ota, "Evaluation of acute and subchronic toxicities of aqueous ethanol root extract of *Raphia hookeri* (palmaceae) on Swiss albino rats," *British Journal of Pharmacology and Toxicology*, vol. 5, no. 4, pp. 129–135, 2014.

[46] K. Deivanai, "In vivo studies on evaluation of potential toxicity of unspent tannins using albino rats (Rattus novergicus)," *Food and Chemical Toxicology*, vol. 46, no. 6, pp. 2288–2295, 2008.

[47] J. P. Felix and D. Mello, *Farm Animal Metabolism and Nutrition*, CABI, Oxford, England, 2000.

[48] N. Bencheikh, M. Bouhrim, L. Kharchoufa, M. Choukri, M. Bnouham, and M. Elachouri, "Protective effect of *Zizyphus lotus* L. (Desf.) fruit against CCl_4-induced acute liver injury in rat," *Evidence-based Complementary and Alternative Medicine*, vol. 9, 2019.

[49] M. Bouhrim, H. Ouassou, M. Choukri et al., "Hepatoprotective effect of Opuntia dillenii seed oil on CCl4 induced acute liver damage in rat," *Asian Pacific Journal of Tropical Biomedicine*, vol. 8, no. 5, pp. 254–260, 2018.

[50] M. A. Lacaille-Dubois and H. Wagner, "A review of the biological and pharmacological activities of saponins," *Phytomedicine*, vol. 2, no. 4, pp. 363–386, 1996.

[51] A. A. Ajao, N. A. Moteeteea, and S. Sabiu, "From traditional wine to medicine: phytochemistry, pharmacological properties and biotechnological applications of *Raphia hookeri* G. Mann & H. Wendl (Arecaceae)," *South African Journal of Botany*, vol. 138, no. 3, pp. 184–192, 2021.

[52] S. Kumar and A. K. Pandey, "Chemistry and biological activities of flavonoids: an overview," *The Scientific World Journal*, vol. 2013, Article ID 162750, 16 pages, 2013.

[53] A. N. Bayomy, R. H. Elbakary, M. A. A. Ibrahim, and Z. E. Abdelaziz, "Effect of lycopene and rosmarinic acid on gentamycin induced renal cortical oxidative stress, apoptosis, and autophagy in adult male albino rat," *The Anatomical Record*, vol. 300, no. 6, pp. 1137–1149, 2017.

[54] M. Palm and A. Lundblad, "Creatinine concentration in plasma from dog, rat, and mouse: a comparison of 3 different methods," *Veterinary Clinical Pathology*, vol. 34, no. 3, pp. 232–236, 2005.

[55] Who, *Trace Element in Human Nutrition*, WHO, Geneva, Switzerland, 1996.

[56] U. D. Akpabio, A. E. Akpakpan, U. E. Udo, and U. C. Essien, "Physicochemical characterization of exudates from raffia palm (*Raphia hookeri*)," *Advances in Applied Science Research*, vol. 3, no. 2, pp. 838–884, 2012.

[57] B. M. Oyawoye and H. N. Ogunkunle, *Biochemical and Haematological Reference Values in Normal Experimental Animals"*, Masson, New York, NY, USA, 2004.

[58] O. I. Ogidi, A. C. Ibe, U. M. Akpa, and K. O. Okpomu, "Effect of methanol and ethanol extracts of *Raphia vinifera* fruit mesocarp on the hematological parameters of wistar albino rats," *Elixir Pharmacy*, vol. 143, pp. 54412–54416, 2020.

[59] H. K. Walker, W. D. Hall, and J. W. Hurst, *Clinical Methods: The History, Physical, and Laboratory Examinations*, Butterworths, London, UK, 3rd edition, 1990.

Hindawi
Evidence-Based Complementary and Alternative Medicine
Volume 2022, Article ID 2626645, 11 pages
https://doi.org/10.1155/2022/2626645

Research Article

Neurodoron® for Stress Impairments: A Prospective, Multicenter Non-Interventional Trial

Juliane Hellhammer,[1] **Katja Schmidt**,[1] **Cristina Semaca**,[2] **and Rebecca Hufnagel**[2]

[1]*Contract Research Institute, Daacro, Trier 54296, Germany*
[2]*Clinical Research, Weleda AG, Schwäbisch Gmünd 73525, Germany*

Correspondence should be addressed to Rebecca Hufnagel; rhufnagel@weleda.de

Received 10 December 2021; Accepted 26 January 2022; Published 25 February 2022

Academic Editor: Jie Liu

Copyright © 2022 Juliane Hellhammer et al. This is an open access article distributed under the Creative Commons Attribution License, which permits unrestricted use, distribution, and reproduction in any medium, provided the original work is properly cited.

Introduction. Stress is associated with a multitude of physical and psychological health impairments. To tackle these health disorders, over-the-counter (OTC) products like Neurodoron® are popular since they are considered safe and tolerable. Experience reports and first studies indicate that Neurodoron® is efficient in the treatment of stress-associated health symptoms. To confirm this, a non-interventional study (NIS) with pharmacies was conducted. *Methods*. The NIS was planned to enroll female and male patients who suffered from nervous exhaustion with symptoms caused by acute and/or chronic stress. The main outcome measures were characteristic stress symptoms, stress burden, and perceived stress. Further outcome measures included perceived efficacy and tolerability of the product as assessed by the patients and collection of adverse drug reactions (ADRs). A study duration of about 21 days with a recommended daily dose of 3–4 tablets was set. *Results*. 279 patients were enrolled at 74 German pharmacies. The analyzed set (AS) included 272 patients (mean age 44.8 ± 14.4 years, 73.9% female). 175 patients of the AS completed the NIS. During the study, all stress symptoms declined significantly (total score 18.1 vs. 12.1 (of max. 39 points), $p < 0.0001$). Furthermore, a reduction of stress burden (relative difference in stress burden, VAS = −29.1%, $p < 0.0001$) was observed. For most patients, perceived stress was reduced at the study end (PSQ total score decreased in 70.9% of the patients). 75.9% of the study population rated the product efficacy as "good" or "very good" and 96.6% rated its tolerability as "good" or "very good." One uncritical ADR was reported. *Discussion/Conclusion*. This study adds information on the beneficial effects of Neurodoron® in self-medication. The results from this NIS showed a marked reduction in stress burden and perceived stress, along with an excellent safety profile of the medicinal product (MP) Neurodoron®. Further trials are required to confirm these results.

1. Introduction

The link between stress and a variety of physical and mental health disorders has been sufficiently proven by scientific evidence [1–6]. Thus, the WHO declares stress as one of the greatest health threats of the 21st century. Modern lifestyle, social media, and technologies such as digitalization, including the associated overstimulation, have made stress virtually omnipresent, regardless of culture and living environment [7, 8]. The numbers of stress-related costs regularly published by authorities and insurances speak for themselves and call for action [9–11]. In 2016, the German Opinion Research Institute forsa carried out a representative study on behalf of Techniker Krankenkasse, a statutory health insurance fund, according to which 60% of respondents in Germany perceive an increased stress burden within the past three years [12]. In the age group of 18 to 29-year-olds, this proportion was even as high as 75%. The same study confirms a particularly high correlation between stress and mental health.

In fact, stress is a physiologically sensible adaptation process to stimuli and impacts, helping the organism to respond as effectively and appropriately as possible. A psychological stress situation is usually characterized by novelty, uncontrollability, unpredictability, and the expectation of negative consequences that are personally relevant

[13, 14]. Facing such a situation, the two central stress systems, the sympathetic nervous system, and the hypothalamic-pituitary-adrenal axis, are activated and orchestrate the organism accordingly while other systems, especially serotonergic and parasympathetic systems, are downregulated. While short-term stressors upregulate both stress systems followed by a normalization after the stressful situation comes to an end, chronic or extreme stress, as well as a certain stress vulnerability, can lead to a more permanent dysregulation of stress systems [1, 15] which in turn promotes diseases. While stress by itself is not a disease according to the criteria of the Diagnostic and Statistical Manual of Mental Disorders, Fifth Edition (DSM-5) [16], chronic stress favors a large number of diseases such as cardiovascular disease, diabetes, and skin and mental disorders. The first signs of stress-related health problems are typically nervousness, irritability, sleep disorders, headaches, and digestive problems, as well as anxiety disorders and depression [17–19]. Mental disorders, especially depression, anxiety, and adjustment disorders, are widespread [20] and often associated with particularly long downtime at work (in 2016 an average of 43 days [21]). A survey of students in the German federal state North Rhine-Westphalia has shown that stress often leads to the use of medication: one in two respondents said to be often or always stressed, complained of nervousness, fatigue, headaches, and sleep disorders. Here, every 10th student stated to fight stress with psychotropic drugs. A comparison of the prescribed daily doses showed a 55% increase between 2006 and 2010 [22]. Simultaneously, however, the proportion of people relying on complementary and alternative medicine (CAM) or dietary supplements increased when facing stress [23]. There are many different effective CAM options for the treatment of stress and other psychiatric disorders, ranging from music therapy to tai chi to phytotherapy [24–27], to mention some of the main ones. Herbal, homeopathic, and anthroposophic medicines are also very popular, as they are generally considered safe and are widely used in various indications [28–33].

Anthroposophic medicine commonly uses mineral substances for therapeutic use. Beyond naturally occurring minerals (e.g., quartz), the category also includes purified substances such as metals possibly having undergone specific treatment (e.g., gold prepared as "metallic mirror" by distillation under vacuum), inorganic compounds (e.g., potassium diphosphate), and "compositions" (e.g., Ferrum-Quarz), which are the result of complex preparation processes involving several mostly mineral-inorganic starting materials, not unlike preparations used in ayurvedic and Siddha medicine or in homeopathy (e.g., Causticum). These "mineral" substances are described in anthroposophic medicine and pharmacy textbooks and the Anthroposophic Pharmaceutical Codex. Once prepared as starting material, they are usually potentized according to processes described in anthroposophic and official homeopathic pharmacopoeias [34, 35].

In anthroposophic therapy, mineral remedies are of particular significance because they are the farthest removed from the living processes of the human organism. The MP of this NIS, Neurodoron®, is one of them. The integration of the mineral remedies in the organism requires the involvement of stronger organic forces than are needed for the integration of vegetal or animal substances, whose composition and structure are closer to that of the human organism. These forces originate in the I-organization, the hierarchically uppermost organizational level of the human organism, of spiritual nature, that works in all metabolic processes and enables the human being to harbor individual reflective consciousness. As a result, mineral remedies are considered to have a deeper and more durable action than vegetal or animal-based remedies [36–39].

For Neurodoron®, two clinical studies were performed between 2008 and 2012, indicating that the anthroposophic drug can be an efficient treatment for stress-related health problems [40, 41]. A first multicenter NIS conducted by practicing physicians in Germany from 2008 to 2009 [40] investigated the effect of the MP in participants reporting stress-related nervous fatigue. After an average of 46 days of Neurodoron® therapy, a significant reduction of all 39 recorded symptoms was observed. In the period between 2011 and 2012, a double-blind, placebo-controlled RCT with Neurodoron® [41] followed to demonstrate the efficacy in participants with nervous fatigue following diagnostic criteria defined in ICD-10 [42]. Significant improvements were observed for the symptoms of nervousness and irritability. Furthermore, the majority of the symptoms tested showed favourable trends in the Neurodoron® group when compared with the placebo group.

The following NIS should complement the data based on research with Neurodoron® gathered from both the previous RCT and NIS. Since the drug is predominantly used in self-medication, this prospective, pharmacy-based NIS should add information about the real-life use of the product.

2. Methods

2.1. Design. This prospective, pharmacy-based, multicenter NIS was conducted to collect data on the use of Neurodoron® regarding efficacy and safety in the approved indication. The NIS was notified to the German Federal Institute for Drugs and Medical Devices in September 2014 and was coordinated by the contract research organization (CRO) Winicker Norimed GmbH Medizinische Forschung/ Germany. Two study visits were scheduled, a baseline visit and a final assessment on day 21:

(1) At baseline/day 1/beginning: when purchasing Neurodoron®, customers were asked whether they would like to take part in a NIS. If interested, the pharmaceutical staff checked the inclusion and exclusion criteria, explained the course of the study, and carried out the baseline survey after the patient had signed the consent form. The following data were collected:

   (a) Demographic, anthropometric, socioeconomic, and general data
   (b) Reason for the use of Neurodoron®

(c) Previous therapy for neurasthenia
(b) Intake of Neurodoron®
(e) Stress symptoms
(f) Stress burden (visual analog scale, VAS)
(g) Perceived stress questionnaire (PSQ)

(2) Second assessment/day 21/end: towards the end of the 21 days study period, the patients received the end-of-study documentation by mail with the request to fill it out and return it directly to the CRO. The end-of-study documentation included the recording of the following parameters:

(a) Intake of Neurodoron®
(b) Subjective evaluation of Neurodoron®
(c) Further therapeutic measures
(d) Stress symptoms
(e) Stress burden (VAS)
(f) PSQ
(g) Subjective assessment of efficacy and tolerability

Throughout the course, (suspected cases of) ADRs were recorded.

2.2. Patients. To be included in the study, patients had to have self-reported symptoms of nervous fatigue due to acute and/or chronic stress. No strict age limits were set. The preferred age range was 25 to 49 (due to the expected peak of cases in the study indication). Patients with known hypersensitivity to wheat starch, lactose intolerance, present pregnancy, or lactation were excluded from participation unless their doctor had explicitly recommended the use of Neurodoron®. All study patients were informed orally and in writing about the NIS and gave their written informed consent to participate. The NIS was notified to the German Federal Institute for Drugs and Medical Devices (BfArM) in accordance with § 67 para. 6, Sentence 1 AMG (German Arzneimittelgesetz (German Drug Law)).

2.3. Medicinal Product. The MP has been on the market for about 60 years. It has been authorized under the name Neurodoron® as an anthroposophic medicine (AM) with the indication of nervous exhaustion and metabolic dysfunction (Commission C monograph [43], registration number 6646311.00.00). One tablet contains the following active ingredients: 83.3 mg *Aurum metallicum praeparatum trituration* (*trit.)* D10, 83.3 mg *Kalium phosphoricicum trit*. D6, 8.3 mg *Ferrum-Quarz trit.* D2 (excipients: wheat starch and lactose). According to the market authorization, the daily intake of 3–4 tablets over the course of the day is recommended. The tablet can either be left to dissolve in the mouth or can be taken with liquid. Neurodoron® is taken for the duration of the NIS, which is 21 days.

2.4. Measurement of Study Parameters

2.4.1. Demographic, Anthropometric, Socioeconomic, and General Data. Age, gender, height, weight, smoking status, marital status, and professional situation, including sector, were recorded.

2.4.2. Reason for the Use of Neurodoron®. Patients were asked if they were suffering from acute or chronic stress or a combination of both. They could mark several reasons such as professional situation, exam, family situation, multiple burden/time deficit, and others as the origin of their perceived stress.

2.4.3. Previous Therapy for Neurasthenia and Further Therapeutic Measures during the Study. Drugs that had already been used as a treatment for stress-related symptoms should be indicated and assessed regarding their efficacy and tolerability. Furthermore, questions related to a previous Neurodoron® therapy were asked, e.g., efficacy and safety were assessed on a rating scale ("1 = very good" to "4 = unsatisfactory" or "5 = I do not know"). At the end of the study, patients were asked whether they took other drugs besides the MP or whether they pursued other non-therapeutic measures as, e.g., psychotherapy, stress improvements techniques, sports, and/or yoga/pilates.

2.4.4. Intake of Neurodoron®. If patients were using Neurodoron® for the first time, the start of use during the study was documented (i.e., at the earliest on the date of patient consent). If Neurodoron® was already taken before the start of the study, the respective start of intake was noted. In addition, the patients were asked about the dosage.

2.4.5. Stress Symptoms and Symptom Sum Score. The patients rated the following 13 characteristic stress symptoms on a four-level Likert scale from "0 = absent" over "1 = mild," "2 = moderate" to "3 = severe": irritability, restlessness, nervousness, listlessness, depressive mood, mood swings, anxiety states, troubles to concentrate/lack of concentration, headache, sleep disorders, digestive disorders, muscular pain/tensions, fatigue. From the symptom scores, an additional sum score was calculated, which could reach a maximum value of 39 points.

2.4.6. Stress Burden (VAS). The patients assessed their stress burden on a 100 mm VAS [44]. The VAS is a widely accepted procedure with a bipolar scale ranging from "0 = not stressed at all" to "100 = maximally stressed."

2.4.7. Perceived Stress (PSQ). In the present study, the revised German version of the PSQ consisting of 20 items was used [45]. The PSQ is a validated tool for assessing the individual perception, assessment, and processing of stressors. Respondents indicate on a scale from "1 = almost never" over "2 = sometimes," "3 = often" to "4 = usually" how frequently they experience certain stress-related feelings such as feeling frustrated or tense. The PSQ provides results for the four subscales "worries," "tension," "joy," and "demands," in addition to a total score. For calculation of the total score, the values for "joy" are inverted. Thus, higher total scores indicate greater levels of stress. In order to assess scale values and a PSQ index representing the overall perceived stress, mean

values are calculated from the raw item scores and linearly transformed to values between 0 and 100.

2.4.8. Subjective Evaluation of Neurodoron®. As a final evaluation of the MP, patients were asked whether they would continue with the MP treatment and whether they would recommend the product ("yes," "no," "I do not know," respectively). In addition, patients indicated their satisfaction with the treatment on a scale from "very satisfied" over "satisfied," "unsatisfied" to "very unsatisfied" or "not specified." Impact of the MP on the development of the disease was also rated ("great," "small," "not specified").

2.4.9. Subjective Assessment of Efficacy and Tolerability. Patients rated on a scale from "very good" over "good," "satisfactory" to "unsatisfactory" or "I do not know" how they assessed the efficacy and tolerability of the MP.

2.4.10. Safety/ADRs. Pharmacies informed patients at baseline that suspected cases of ADRs shall be reported separately by the patient to the pharmacy. These ADRs were documented by the pharmacies and redirected immediately (i.e., within 24 hours) to the sponsor for further action. Rating options regarding relatedness of the ADR to the MP were "certain," "likely," "possible," "unlikely," "unknown," "not assessable."

2.5. Statistical Calculations. Details of this descriptive evaluation were specified within a statistical analysis plan before database lock. All outcome measures were analyzed based on the AS. The AS includes all patients who met all inclusion and no exclusion criteria and had at least one intake of Neurodoron®. Missing values were not replaced. For the exploratory statistical analyses, only complete records were used. Statistical outliers were not excluded. Stress symptoms were tested with Wilcoxon signed-rank tests, while stress burden and perceived stress according to PSQ were analyzed using a paired t-test. Two-sided tests with an alpha level of 0.05 were performed. Statistical analyses were performed using SAS Version 9.2. Means of variables were reported as mean values ± standard deviation (SD) or standard error (SE) and were calculated using the AS.

3. Results

This multicenter NIS was conducted at a total of 74 pharmacies in Germany. The baseline documentation of the first patient was done on September 29, 2014, and the final documentation of the last patient was done on May 9, 2016. Out of 279 recruited patients, 272 (97.5%) patients were assigned to the AS (6 patients violated at least 1 exclusion criterion, 1 patient had not signed the consent form). 175 patients (64.3%) of the AS completed the NIS.

3.1. Demographic, Anthropometric, and Socioeconomic Data. The mean age was 44.8 years. More female (73.9%) than male persons (25.4%) participated in this study. The demographic, anthropometric, and socioeconomic data of the 272 patients are summarized in Table 1. 61.4% of the patients were married or in a relationship, 24.3% were single, and 14.0% were separated, divorced, or widowed. The majority of patients indicated that they were working (71.7%). Most worked in the social sector (39.3%).

3.2. Reason for the Use of Neurodoron®. When asked about the reasons for the use of Neurodoron®, the patients mainly reported a combination of acute and chronic stress (82.7%). As the most common causes of acute stress, patients ($N = 258$) reported the professional (58.1%) or familial (35.3%) situation. Chronic stress ($N = 239$) was also mostly based on the professional situation (56.1%), followed by multiple burden/time deficit (38.5%), the family situation (37.7%), and persistent psychological/emotional distress (33.9%).

3.3. Previous Therapy for Neurasthenia and Further Therapeutic Measures during the Study. When asked about concomitant therapies, 23.5% of patients said they were taking other medications (most frequent: 6.3% cardiovascular drugs, 5.9% systemic hormone preparations) and 49.3% used at least one non-drug therapy (28.7% sport, 20.6% stress management techniques, 10.7% yoga or pilates).

144 patients (52.9%) had previous treatment with other drugs against stress-related disorders. Efficacy of the best previous treatment was rated as "good" or "very good" by 60.4% of the patients, while 78.5% of the patients rated the tolerability of the previous treatment as "good" or "very good."

3.4. Intake of Neurodoron®. Most patients followed the recommended dosage of 3–4 tablets per day ($N = 220$ in the beginning and $N = 135$ in the end of the NIS). 33.5% ($N = 91$) of the patients already used Neurodoron® before participating in the NIS. The study duration and correspondingly the intake duration of Neurodoron® varied widely between patients. The mean individual study duration was 37 ± 31 days (median: 29 days, range: 9–290 days, $N = 153$), the mean Neurodoron® intake duration during the NIS was 36 ± 34 days (median: 28 days, range: 8–289, $N = 121$). The overall mean Neurodoron® intake, including the intake before the NIS, was 100 ± 214 days (median: 32 days, range: 14–1751, $N = 109$).

3.5. Efficacy/Safety

3.5.1. Stress Symptoms and Symptom Sum Score. All symptoms showed a significant improvement during the study (all $p < 0.0001$), with the most noticeable symptoms being fatigue ($\Delta = -0.7 \pm 1.0$), irritability ($\Delta = -0.6 \pm 0.9$), and sleep disorders ($\Delta = -0.5 \pm 1.0$). The results for all 13 stress symptoms are shown in Figure 1. The mean total score of stress symptoms for patients with values for both study visits was 18.1 ± 5.9 at baseline and 12.1 ± 6.4 at study end

Table 1: Demographic, anthropometric, socioeconomic, and general data of the patients.

Variable		All patients ($N = 272$)
Age, years	Mean ± SD	44.8 ± 14.4
	Range	16.0–88.0
	Missing data	3
Gender, N (%)	Male	69 (25.4)
	Female	201 (73.9)
	Missing data	2 (0.7)
Height (cm)	Mean ± SD	170.1 ± 8.9
	Range	150.0–202.0
	Missing data	4
Weight (kg)	Mean ± SD	71.9 ± 15.7
	Range	42.0–125.0
	Missing data	4
Smoking status, N (%)	Nonsmokers	212 (77.9)
	Smokers	55 (20.2)
	Missing data	5 (1.8)
Marital status, N (%)	Single	66 (24.3)
	Married	136 (50.0)
	In a relationship	31 (11.4)
	Separated	13 (4.8)
	Divorced	13 (4.8)
	Widowed	12 (4.4)
	Missing data	1 (0.4)
Professional situation	Working	195 (71.7)
	Unemployed	8 (2.9)
	Pupils/students/trainees	20 (7.4)
	Retired	35 (12.9)
	Housewife/househusband	11 (4.0)
	Missing data	3 (1.1)
Sector	Social sector	107 (39.3)
	Service	30 (11.0)
	Trade	17 (6.3)
	Industry/digital economy	15 (5.5)
	Craft sector/trade	10 (3.7)
	Administration/commercial area	25 (9.2)
	Other	13 (4.8)
	Missing data	55 (20.2)

(max. total score: 39). Thus, there was a significant improvement of −6 ± 6.5 points ($p < 0.0001$, $N = 170$).

3.5.2. Stress Burden (VAS). For stress burden VAS data of 166 patients were available at both study visits. These patients showed mean values of 68.3 ± 15.7 at the beginning and 43.5 ± 21.6 at the end of the study (shown in Figure 2). This corresponds to a significant improvement of the stress burden by -29.1% ± 86.3% ($p < 0.0001$).

3.5.3. Perceived Stress (PSQ). In the majority of patients, perceived stress decreased during the study, as reflected in the total score. For the three subscales, "worries," "tension," and "demands," the values decreased in most patients. For the subscale "joy," the values predominantly increased compared to study start, i.e., the patients experienced more joy compared to baseline. The total score for perceived stress decreased in 70.9% of the patients. In 3.5%, there was no change and in 25.6%, the total score increased (shown in Figure 3).

3.5.4. Subjective Evaluation of Neurodoron®. 61.7% of patients who reached the end of the study ($N = 175$) reported they would continue with the therapy, and 82.9% of patients would recommend the Neurodoron® therapy. 86.9% of the patients were "satisfied" or "very satisfied" with the treatment, and 45.7% rated its influence on the disease as "great" (29.1% answered with "not specified" or data was missing).

3.5.5. Subjective Assessment of Efficacy and Tolerability. Based on the data of 174 patients, efficacy was rated as "good" or "very good" by 75.9% of patients at the end of the NIS, while 96.6% of patients rated the tolerability of Neurodoron® as "good" or "very good" (shown in Figure 4).

3.5.6. Safety/ADRs. One ADR was reported, which was abdominal pain and nausea. As a potential reason, intolerance to lactose, an excipient of Neurodoron®, was considered. As other reasons (e.g., diet) could not be excluded, the relatedness with the MP was classified as "possible."

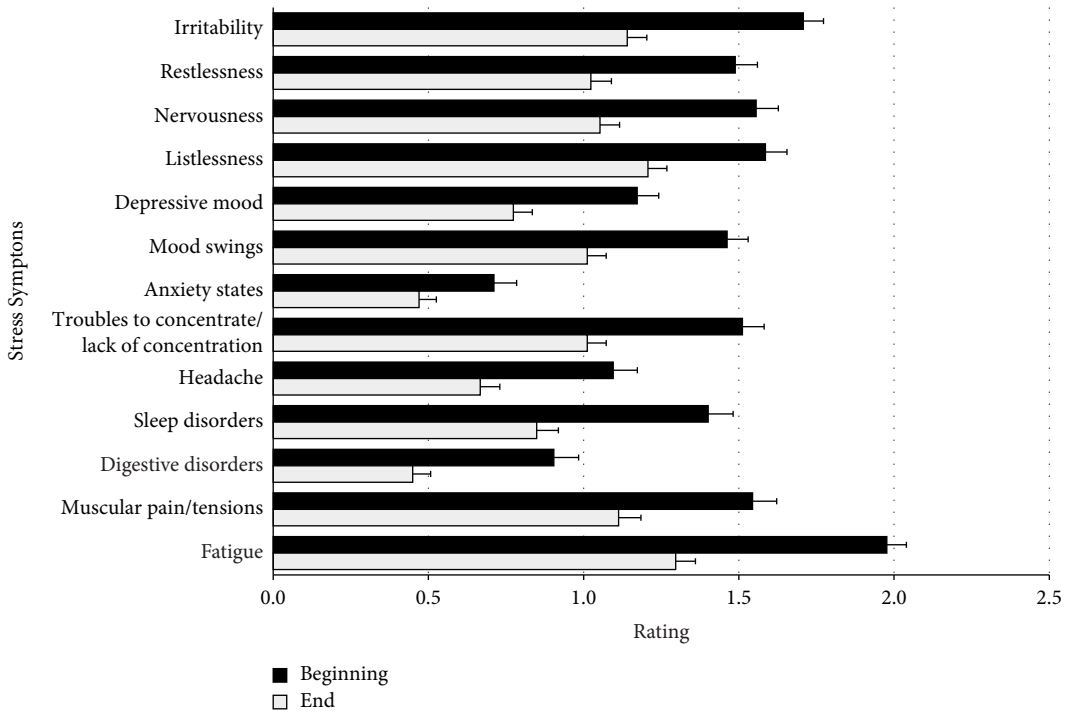

Figure 1: Changes in the 13 stress symptoms shown as mean and SE (N between 166 and 172, respectively) after a median study time of 29 days; "0 = absent," "1 = mild," "2 = moderate," "3 = severe."

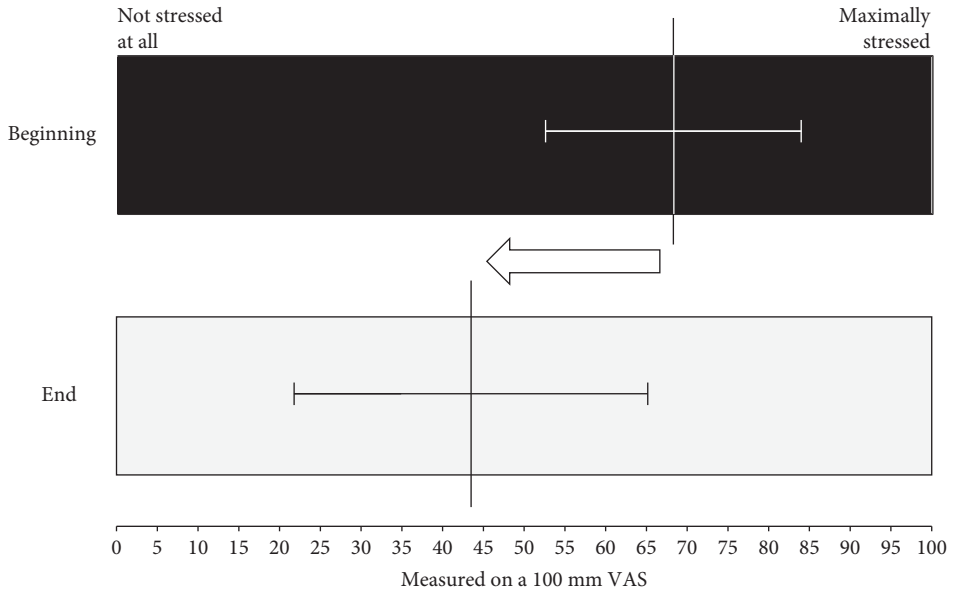

Figure 2: Changes in stress burden measured on a 100 mm VAS shown as mean ± SD ($N = 166$) after a median study time of 29 days; "0 = not stressed at all," "100 = maximally stressed."

4. Discussion

While stress and its associated symptoms are increasingly prevalent in today's society [7], the importance of an efficient treatment is increasing. Aside from, psychotropic drugs, herbal, homeopathic, and AM are very popular in fighting stress-related health impairment.

AM sees itself as integrative medicine, which extends the so-called university medicine to holistic aspects of the concept of disease and complementary medical approaches in the fields of drugs and various forms of art therapy and external applications [46]. In the physician-based multicenter NIS from 2008/2009 [40], 300 patients with stress-related nervous fatigue were analyzed, a good third of whom

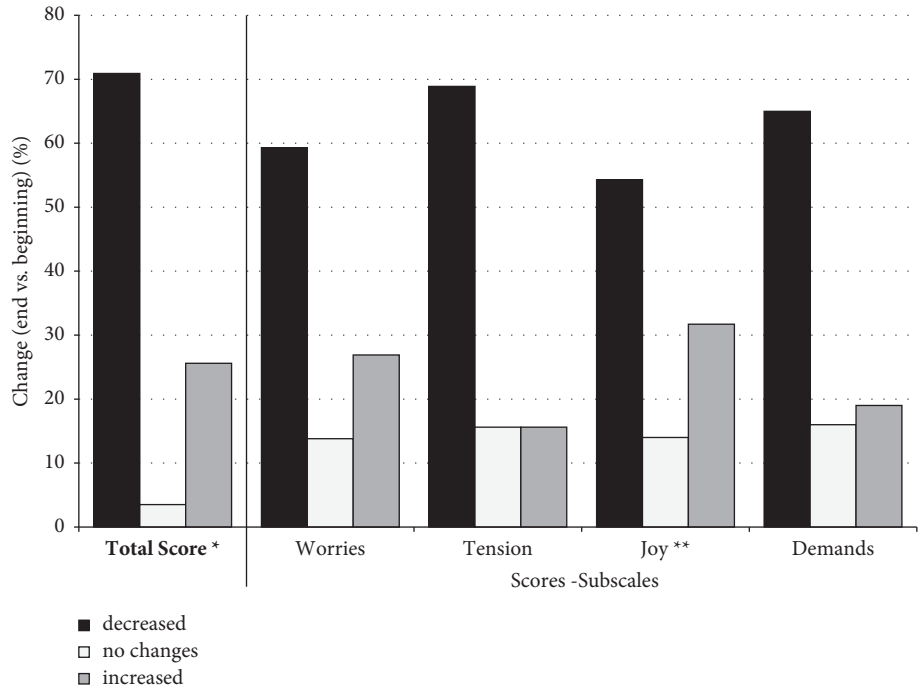

Figure 3: Changes in perceived stress according to PSQ in percent (N between 163 and 172, respectively) after a median study time of 29 days. ** "Joy" values were inverted for calculation of total score. ** "Joy" values are shown inverted for better understanding.*

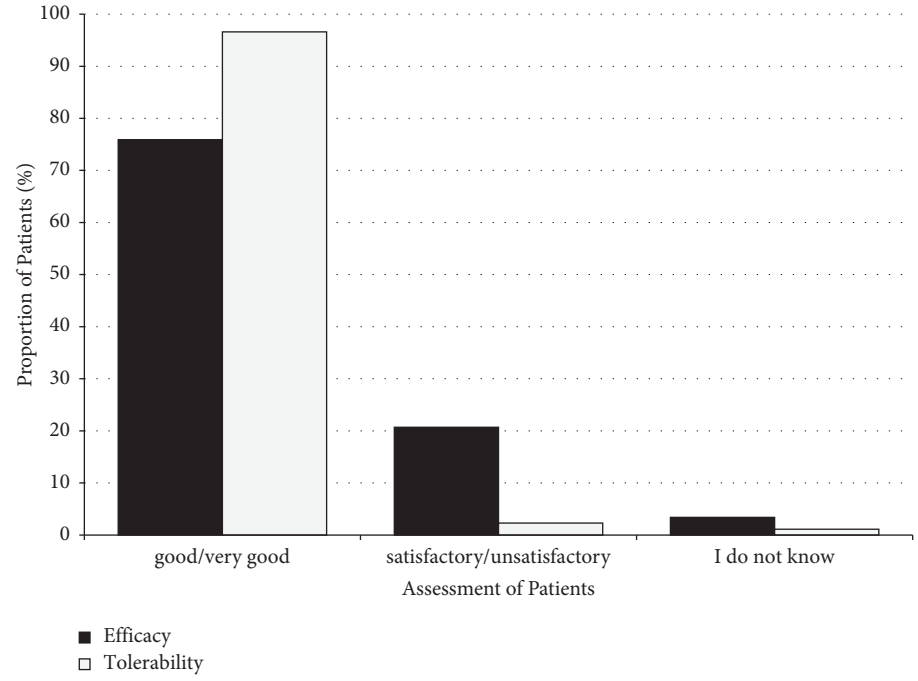

Figure 4: Subjective assessment of the efficacy and tolerability of Neurodoron® at study end ($N = 174$); assessment options: "very good," "good," "satisfactory," "unsatisfactory," and "I do not know."

also had a burnout diagnosis. 272 patients with stress-related nervous fatigue were analyzed in the present pharmacy-based NIS. The proportion of women was comparable, as was the mean age (78.0% and 50.3 years (physician-based NIS) vs. 73.9% and 44.8 years (pharmacy-based NIS)). As expected from the design of the studies, the mean intake duration of Neurodoron® of 42.0 days was longer in the physician-based NIS than in this NIS with 36.0 days (treatment duration was set at 6 weeks for the physician-based NIS compared to 21 days in this NIS.). For the present NIS, the documentation at the study end did not take place at a fixed date in the pharmacy but was completed by the

patient at home. Therefore, a deviation from the planned treatment duration of 21 days was to be expected. On average, the documentation was completed by the patients significantly later resulting in a longer treatment duration. One explanation for that fact could have been satisfaction with the preparation, both in terms of efficacy and safety; details are as follows.

Patients of the physician-based NIS showed a significant reduction of all 39 recorded symptoms such as irritability, headaches, and sleep disorder. The double-blind RCT that followed in 2011/2012 [41] to demonstrate the efficacy in patients with nervous fatigue following diagnostic criteria defined in ICD-10 [42] showed similar results. While there was no statistically significant difference to the placebo in the symptom sum score, 10 of the 12 symptoms tested in a post hoc analysis showed favourable trends in the Neurodoron® group compared to the control group. Statistically significant improvements were observed for the symptoms of nervousness and irritability. Consistent with the results of the first two studies conducted with Neurodoron® (physician-based NIS and RCT), this pharmacy-based NIS also showed that the MP can successfully reduce stress burden and stress-related symptoms such as fatigue, irritability, and sleep disorders in the OTC environment typical for Neurodoron®. Patients also reported a clear improvement in their perception of tension and worries and improved joy and better coping with the demands placed on them. When comparing the patients' subjective assessment of efficacy and safety, data from both the physician-based and the pharmacy-based NIS are very similar (efficacy/safety evaluation of Neurodoron® "good" or "very good": physician-based NIS 78.7%/95.7% [40], pharmacy-based NIS 75.9%/96.6%).

Regarding efficacy, in the present NIS, the positive patient assessment of the product was also reflected in the fact that 86.9% were "satisfied" or "very satisfied" with the treatment, 75.9% rated the efficacy as "good" or "very good," and 82.9% would recommend the treatment. The results of the two NISs provide consistent efficacy findings.

Regarding safety, the noteworthy good safety assessment by patients was confirmed by only one reported ADR within the entire study duration of one and a half years (with abdominal pain and nausea an uncritical ADR that was considered possibly related to the product). This shows, in summary, an exceptionally good safety profile of the product.

Real-life use observed in non-interventional studies brings out well the strengths of anthroposophic medicinal products. NISs are therefore a good way to complement a randomized controlled trial with its strict prerequisites. For example, patients in the RCT were not allowed to take any other medication for stress-related symptoms and were asked not to change their habits (daily activities, non-drug therapies, etc.). In contrast, the anthroposophic approach recommends a holistic therapy that also introduces lifestyle changes to improve the participant's quality of life. As the results of nervous exhaustion are manifold, individual therapy with several simultaneous measures is common practice. The individual therapeutic approach considers the patient within his/her entire life situation. The positive results of this and the previously conducted NIS reflect common treatment practice insofar more adequately. By this holistic approach, for instance, sleep and fatigue improve, which then indirectly facilitate regeneration of the activation systems, which is reflected in decreasing nervousness and irritability.

The goal of physicians and pharmacists is to offer individual treatment. A suitable target group would be patients who experience themselves as nervous, irritable, and inwardly restless and wish for more serenity and sovereignty in everyday life. It is conceivable that these individuals, in particular, will benefit from Neurodoron®, whereby the preparation could also be used as an adjunct to meditation and relaxation procedures.

There are limitations that should be considered for the interpretation of the data. The NIS was uncontrolled; therefore, confirmation of efficacy based on hypothesis-testing was out of scope. As Neurodoron® is a drug that emerges from AM, the mostly individualized and multimodal therapy concepts in the fields of AM make it more difficult to capture efficacy because of absent randomization and blinding possibilities. Controlled clinical trials provide important information that is complemented by non-interventional study results. The value of non-interventional studies lies in particular in their good external validity, as they allow insights into the reality of medical practice or, in this case, self-medication [47, 48].

Additionally, a certain selection bias for enrollment in the NIS was present due to the design of the study. Only patients who sought pharmacy advice, were open to CAM and were willing to participate in a clinical study were enrolled. These conditions may have introduced gender and social status bias with an unknown effect on NIS results. One might also speculate that patients are seeing a physician at a more advanced stage of the disease, which might also impact the results. However, there were good reasons for the chosen design. Neurodoron® is an OTC product and is mainly used for self-medication. Therefore, a pharmacy-based NIS may provide even better insight into the main patient population than a physician-based NIS. Overall, a certain selection bias cannot be excluded.

In general, stress impairments fluctuate in their intensity as they strongly depend on the increase or decrease of the stressors and the ability of the affected person to cope with the stressful situation. In the present NIS, patients with acute and/or chronic stress qualified for study participation. As the majority of patients (82.7%) reported to have a combination of both acute and chronic stress, it can be assumed that a rather stable and permanently ongoing stress level was present. Therefore, we consider it very unlikely that the improvement in stress symptoms can be exclusively explained by a sudden decrease or even disappearance of

stressors. Together with the results of previous studies with Neurodoron®, these results suggest a positive effect of the treatment. However, as this NIS was uncontrolled, it is not possible to quantify the influence of treatment with Neurodoron® vs. fluctuation of individual stressors or adaption of coping strategies with respect to the observed outcome.

Lastly, the effect of Neurodoron® treatment might have been even underestimated in the NIS because patients also qualified for the NIS if they already had taken Neurodoron® before the study started (33.5% of patients). It could be assumed that these patients had benefited from Neurodoron® treatment and therefore wanted to continue it. As there are no baseline data without Neurodoron® treatment available for these patients, it cannot be ruled out that the improvement that was observed during the NIS was underestimated. This circumstance was deliberately accepted in order to get the whole picture of self-medication with Neurodoron® in pharmacies.

5. Conclusion

The results of this study complement the picture that has emerged from the previous studies: Neurodoron® seems to stabilize the balance between activation and recovery systems and to strengthen stress resilience. Neurodoron® appears to be a beneficial option for the treatment of nervous exhaustion and other stress-related symptoms either as monotherapy or as a component of a holistic treatment approach. What remains to be done is to support the present results with data from interventional and non-interventional trials, also in selected patient populations.

Data Availability

The data that support the findings of this study are not publicly available due to containing information that could compromise the privacy of research participants. Disclosure of data would not be in accordance with the European General Data Protection Regulation.

Ethical Approval

The NIS was notified to the German Federal Institute for Drugs and Medical Devices (BfArM) according to the German legal requirements (§ 67 para. 6, sentence 1 AMG (German Arzneimittelgesetz (German Drug Law)). Ethics approval is generally not required for this type of pharmacy-based NIS.

Consent

All study participants gave their written informed consent to participate in the NIS.

Conflicts of Interest

RH and CS are employees of Weleda AG, Germany. JH and KS work for daacro GmbH & Co. KG, a clinical research organization, Germany. The authors declare that there are no conflicts of interest.

Authors' Contributions

RH was substantially involved in the conception of the study, study design, and analysis of the study and supported the conduct of the study. CS substantially contributed to data acquisition, data preparation, and analysis of data. JH and KS were substantially involved in the interpretation of data and drafted the manuscript. All authors participated in writing and reviewing the manuscript critically and have approved the final article.

Acknowledgments

This study was financed by the pharmaceutical company Weleda AG, Arlesheim, the employer of RH and CS. Weleda commissioned the CRO daacro for their contribution to the manuscript. The authors would like to thank Dr. Claudia Rother, Dr. Martin Schnelle, and Luitgard Spitznagel-Schminke from Weleda AG: Dr. Claudia Rother was responsible for the preparation and conduct of the NIS and managed the cooperation with the CRO; Dr. Martin Schnelle contributed to the study design; Luitgard Spitznagel-Schminke supported medical writing and gave valuable input for the finalization of the manuscript. The authors also thank Nicole Weber, Simone Beitzel, and Franziska Eckert ((former) employees of daacro GmbH & Co. KG) for their support in writing the manuscript and to all the participating pharmacies for their assistance in recruiting stressed individuals. Also, the authors are grateful to all the anonymous patients for their valuable contribution to this study.

References

[1] B. S. McEwen, "Neurobiological and systemic effects of chronic stress," *Chronic Stress*, vol. 1, Article ID 247054701769232, 2017.

[2] D. H. Hellhammer and J. Hellhammer, "Stress. The brain-body connection," *Key Issues in Mental Health*, vol. 174, pp. 1–10, Karger, Basel, Switzerland, 2008.

[3] S. Cohen, D. Janicki-Deverts, and G. E. Miller, "Psychological stress and disease," *JAMA*, vol. 298, no. 14, pp. 1685–1687, 2007.

[4] R. Dantzer, "Neuroimmune interactions: from the brain to the immune system and vice versa," *Physiological Reviews*, vol. 98, no. 1, pp. 477–504, 2018.

[5] E. R. de Kloet, M. Joëls, and F. Holsboer, "Stress and the brain: from adaptation to disease," *Nature Reviews Neuroscience*, vol. 6, no. 6, pp. 463–475, 2005.

[6] D. B. O'Connor, J. F. Thayer, and K. Vedhara, "Stress and health: a review of psychobiological processes," *Annual Review of Psychology*, vol. 72, no. 1, pp. 663–688, 2021.

[7] R. S. Bhagat, J. Segovis, and T. Nelson, *Work Stress and Coping in the Era of Globalization*, Routledge, New York, NY, USA, 2012.

[8] T. Fischer, M. Reuter, and R. Riedl, "The digital stressors scale: development and validation of a new survey instrument to measure digital stress perceptions in the workplace context," *Frontiers in Psychology*, vol. 12, Article ID 607598, 2021.

[9] P. Andlin-Sobocki, B. Jonsson, H.-U. Wittchen, and J. Olesen, "Cost of disorders of the brain in Europe," *European Journal of Neurology*, vol. 12, no. s1, pp. 1–27, 2005.

[10] L. Heuer, *Burnout und psychische Belastungen am Arbeitsplatz. Ursachen, Folgen und Maßnahmen zur Prävention*, GRIN Verlag, München, Germany, 2016.

[11] The Lancet Global Health, "Mental health matters," *Lancet Global Health*, vol. 8, no. 11, p. e1352, 2020.

[12] K. Wohlers and M. Hombrecher, *Entspann Dich, Deutschland: TK-Stressstudie*, Techniker Krankenkasse, Hamburg, Germany, 2016, https://www.tk.de/resource/blob/2026630/9154e4c71766c410dc859916aa798217/tk-stressstudie-2016-data.pdf.

[13] J. W. Mason, "A review of psychoendocrine research on the sympathetic-adrenal medullary system," *Psychosomatic Medicine*, vol. 30, no. 5, pp. 631–653, 1968.

[14] D. H. Hellhammer, A. A. Stone, J. Hellhammer, and J. Broderick, "Measuring stress," in *Encyclopedia of Behavioral Neuroscience*, G. F. Koob, M. Le Moal, and R. F. Thompson, Eds., vol. 2, pp. 186–191, Academic Press, Oxford, UK, 2010.

[15] A. L. Russell, J. G. Tasker, A. B. Lucion et al., "Factors promoting vulnerability to dysregulated stress reactivity and stress-related disease," *Journal of Neuroendocrinology*, vol. 30, no. 10, Article ID e12641, 2018.

[16] American Psychiatric Association, *Diagnostic and Statistical Manual of Mental Disorders*, American Psychiatric Association, Washington, DC, USA, 5th edition, 2018.

[17] M. A. Busch, U. E. Maske, L. Ryl, R. Schlack, and U. Hapke, "Prävalenz von depressiver Symptomatik und diagnostizierter Depression bei Erwachsenen in Deutschland," *Bundesgesundheitsblatt-Gesundheitsforschung-Gesundheitsschutz*, vol. 56, no. 5-6, pp. 733–739, 2013.

[18] M. Nakao, "Work-related stress and psychosomatic medicine," *BioPsychoSocial Medicine*, vol. 4, no. 1, p. 4, 2010.

[19] G. M. Slavich and M. R. Irwin, "From stress to inflammation and major depressive disorder: a social signal transduction theory of depression," *Psychological Bulletin*, vol. 140, no. 3, pp. 774–815, 2014.

[20] J. Alonso, M. C. Angermeyer, S. Bernert et al., "Prevalence of mental disorders in europe: results from the European study of the epidemiology of mental disorders (ESEMeD) project," *Acta Psychiatrica Scandinavica*, vol. 109, no. s420, pp. 21–27, 2004.

[21] Gesundheitsreport, *Gesundheit zwischen Beruf und Familie*Techniker Krankenkasse, Hamburg, Germany, 2016, https://www.tk.de/resource/blob/2034302/acfc2cb8154862732690440b578e3e9c/gesundheitsreport-2016-data.pdf.

[22] "Psychopharmaka gegen Stress," *Dtsch Aerztebl*, vol. 110, no. 3, p. 99, 2013.

[23] D. M. Eisenberg, R. B. Davis, S. L. Ettner et al., "Trends in alternative medicine use in the United States, 1990–1997," *JAMA*, vol. 280, no. 18, pp. 1569–1575, 1998.

[24] N. Gorji, R. Moeini, and S. Mozaffarpur, "On the therapeutic applications of music therapy in Persian medicine," *Traditional and Integrative Medicine*, vol. 6, no. 1, pp. 41–54, 2021.

[25] F. Afrasiabian, M. Mirabzadeh Ardakani, K. Rahmani et al., "Aloysia citriodora Palau (lemon verbena) for insomnia patients: a randomized, double-blind, placebo-controlled clinical trial of efficacy and safety," *Phytotherapy Research*, vol. 33, no. 2, pp. 350–359, 2019.

[26] R. E. Taylor-Piliae, H. W. Morrison, C.-H. Hsu, S. Whitman, and M. Grandner, "The feasibility of tai chi exercise as a beneficial mind-body intervention in a group of community-dwelling stroke survivors with symptoms of depression," *Evidence-based Complementary and Alternative Medicine*, vol. 2021, Article ID 8600443, 12 pages, 2021.

[27] K. Gopukumar, S. Thanawala, V. Somepalli, T. S. S. Rao, V. B. Thamatam, and S. Chauhan, "Efficacy and safety of ashwagandha root extract on cognitive functions in healthy, stressed adults: a randomized, double-blind, placebo-controlled study," *Evidence-based Complementary and Alternative Medicine*, vol. 2021, Article ID 8254344, 10 pages, 2021.

[28] R. Akrami, M. H. Hashempur, A. Tavakoli, M. Nimrouzi, M. Sayadi, and M. Roodaki, "Effects of fumaria parviflora L on uremic pruritus in hemodialysis patients: a randomized, double-blind, placebo-controlled trial," *Jundishapur Journal of Natural Pharmaceutical Products*, vol. 12, no. 3, pp. 1–8, 2016.

[29] M. Ghadimi, F. Foroughi, S. Hashemipour et al., "Randomized double-blind clinical trial examining the Ellagic acid effects on glycemic status, insulin resistance, antioxidant, and inflammatory factors in patients with type 2 diabetes," *Phytotherapy Research*, vol. 35, no. 2, pp. 1023–1032, 2021.

[30] H. J. Hamre, A. Glockmann, K. Heckenbach, and H. Matthes, "Use and safety of anthroposophic medicinal products: an analysis of 44,662 patients from the EvaMed pharmacovigilance network," *Drugs-Real World Outcomes*, vol. 4, no. 4, pp. 199–213, 2017.

[31] M. Schunk, L. Le, Z. Syunyaeva et al., "Effectiveness of a specialised breathlessness service for patients with advanced disease in Germany: a pragmatic fast-track randomised controlled trial (BreathEase)," *European Respiratory Journal*, vol. 58, no. 2, Article ID 2002139, 2021.

[32] T. Stub, A. E. Kristoffersen, G. Overvåg, M. C. Jong, F. Musial, and J. Liu, "Adverse effects in homeopathy: a systematic review and meta-analysis of observational studies," *Explore*, vol. 18, no. 1, pp. 114–128, 2022.

[33] P. J. Wagner, D. Jester, B. LeClair, A. T. Taylor, L. Woodward, and J. Lambert, "Taking the edge off: why patients choose St. John's Wort," *Journal of Family Practice*, vol. 48, no. 8, pp. 615–619, 1999.

[34] International Association of Anthroposophic Pharmacists IAAP, *Anthroposophic Pharmaceutical Codex APC*, International Association of Anthroposophic Pharmacists IAAP, Dornach, Switzerland, 2020, https://iaap-pharma.org/fileadmin/user_upload/pdf/apc/Anthroposophic_Pharmaceutical_Codex__APC__edition_4.2.pdf.

[35] U. Meyer and P. A. Pedersen, *Anthroposophische Pharmazie*, Salumed-Verlag, Berlin, Germany, 1st edition, 2017.

[36] L. Simon, "Relationship of the natural kingdoms to the four human entities," in *Medizinische Sektion der Freien Hochschule für Geisteswissenschaft, Dornach/Switzerland–Gesellschaft Anthroposophischer Ärzte in Deutschland*, Narayana Verlag, Vademecum Anthroposophic Medicines, Kandern, Germany, 4th edition, 2017.

[37] H. Schramm, "Chap. 3.2 Natursubstanzen und ihre Wirkungen," in *Schramm H. Heilmittel der anthroposophischen Medizin: Grundlage–Arzneimittelporträts–Anwendung*, pp. 102-103, Urban & Fischer in Elsevier, Munich, Germany, 2009.

[38] F. Husemann and O. Wolff, *Anthroposophical Approach to Medicine, Chap Mineral Remedies,* vol. 6, Anthroposophic Press Inc, New York, NY, USA, 1987.

[39] M. Glöckler and G. Soldner, "Anthroposophische Arzneimittel mit Blick auf die funktionelle Dreigliederung und die Wesensglieder des Menschen," in *Anthroposophische Medizin–Arzneitherapie für 350 Krankheitsbilder*, M. Girke, G. Glöckler, and Soldner, Eds., pp. 10-11, Wiss Verlag-Ges, Stuttgart, Germany, 2020.

[40] C. Rother and J. Oexle, "Einsatz von Neurodoron bei Patienten mit nervöser Erschöpfung aufgrund von Stress," *Der Merkurstab*, vol. 63, pp. 171–177, 2010.

[41] R. Hufnagel, B. Bergtholdt, J. Hellhammer, C. Semaca, and M. Schnelle, "Effects of Neurodoron in patients with nervous exhaustion-results from a randomized controlled clinical trial," *European Journal of Integrative Medicine*, vol. 8, no. Suppl 1, p. 43, 2016.

[42] World Health Organization, *The ICD-10 Classification of Mental and Behavioural Disorders–Diagnostic Criteria for Research*, World Health Organization, Geneva, Switzerland, 1993, http://www.who.int/classifications/icd/en/GRNBOOK.pdf.

[43] C. Kommission, "Anthroposophische Arzneimittel. Aufbereitungsmonographien. BfArM," in *Gesellschaft Anthroposophischer Ärzte (GAÄD) in Deutschland e.V. Filderstadt*Bundesanzeiger, Köln, Nordrhein-Westfalen, Germany, 1999.

[44] A. Bond and M. Lader, "The use of analogue scales in rating subjective feelings," *British Journal of Medical Psychology*, vol. 47, no. 3, pp. 211–218, 1974.

[45] H. Fliege, M. Rose, P. Arck, S. Levenstein, and B. F. Klapp, "Validierung des "Perceived Stress Questionnaire" (PSQ) an einer deutschen Stichprobe," *Diagnostica*, vol. 47, no. 3, pp. 142–152, 2001.

[46] M. Glöckler, *Anthroposophische Arzneitherapie für Ärzte und Apotheker*, Wiss Verlag-Ges, Stuttgart, Germany, 5th edition, 2014.

[47] A. Anglemyer, H. T. Horvath, and L. Bero, "Healthcare outcomes assessed with observational study designs compared with those assessed in randomized trials," *Cochrane Database of Systematic Reviews*, vol. 2014, no. 4, Article ID MR000034, 2014.

[48] D. Mishra and J. Vora, "Non interventional drug studies in oncology: why we need them?" *Perspectives in Clinical Research*, vol. 1, no. 4, pp. 128–133, 2010.

Hindawi
Evidence-Based Complementary and Alternative Medicine
Volume 2022, Article ID 7663212, 13 pages
https://doi.org/10.1155/2022/7663212

Research Article

Elucidation of Potential Targets of San-Miao-San in the Treatment of Osteoarthritis Based on Network Pharmacology and Molecular Docking Analysis

Man Chu,[1,2] Ting Gao,[3] Xu Zhang,[1] Wulin Kang,[2] Yu Feng,[4] Zhe Cai,[5,6] and Ping Wu[5]

[1]*Faulty of Medical Technology, Shaanxi University of Chinese Medicine, Xianyang, China*
[2]*The Affiliated Hospital of Shaanxi University of Chinese Medicine, Xianyang, China*
[3]*Department of Pharmaceutics, General Hospital of Ningxia Medical University, Yinchuan, Ningxia, China*
[4]*Department of Sports Medicine and Arthroscopy, General Hospital of Ningxia Medical University, Yinchuan, Ningxia, China*
[5]*Department of Allergy, Immunology and Rheumatology, Guangzhou Women and Children's Medical Center, Guangzhou, China*
[6]*Institute of Chinese Medicine and State Key Laboratory of Research on Bioactivities and Clinical Applications of Medicinal Plants, The Chinese University of Hong Kong, Hong Kong*

Correspondence should be addressed to Yu Feng; fengyu_7072@163.com, Zhe Cai; caifranklin@163.com, and Ping Wu; 13053560626@163.com

Received 7 August 2021; Revised 14 October 2021; Accepted 13 December 2021; Published 18 January 2022

Academic Editor: Jie Liu

Copyright © 2022 Man Chu et al. This is an open access article distributed under the Creative Commons Attribution License, which permits unrestricted use, distribution, and reproduction in any medium, provided the original work is properly cited.

Background. To examine the potential therapeutic targets of Chinese medicine formula San-Miao-San (SMS) in the treatment of osteoarthritis (OA), we analyzed the active compounds of SMS and key targets of OA and investigated the interacting pathways using network pharmacological approaches and molecular docking analysis. *Methods*. The active compounds of SMS and OA-related targets were searched and screened by TCMSP, DrugBank, Genecards, OMIM, DisGeNet, TTD, and PharmGKB databases. Venn analysis and PPI were performed for evaluating the interaction of the targets. The topological analysis and molecular docking were used to confirm the subnetworks and binding affinity between active compounds and key targets, respectively. The GO and KEGG functional enrichment analysis for all targets of each subnetwork were conducted. *Results*. A total of 57 active compounds and 203 targets of SMS were identified by the TCMSP and DrugBank database, while 1791 OA-related targets were collected from the Genecards, OMIM, DisGeNet, TTD, and PharmGKB databases. By Venn analysis, 108 intersection targets between SMS targets and OA targets were obtained. Most of these intersecting targets involve quercetin, kaempferol, and wogonin. Moreover, intersecting targets identified by PPI analysis were introduced into Cytoscape plug-in CytoNCA for topological analysis. Hence, nine key targets of SMS for OA treatment were obtained. Furthermore, the potential binding conformations between active compounds and key targets were found through molecular docking analysis. According to the DAVID enrichment analysis, the main biological processes of SMS in the treatment of OA include oxidative stress, response to reactive oxygen species, and apoptotic signaling pathways. Finally, we found wogonin, the key compound in SMS, might play a pivotal role on Toll-like receptor, IL-17, TNF, osteoclast differentiation, and apoptosis signaling pathways through interacting with four key targets. *Conclusions*. Therefore, this study elucidated the potential active compounds and key targets of SMS in the treatment of OA based on network pharmacology.

1. Introduction

Osteoarthritis (OA) is a common degenerative joint disease worldwide, especially affecting the health and quality of life of patients at the middle-age or older. OA is a heterogeneous disease with multiple phenotypes and triggers, such as age, cartilage damage, metabolic disorders, subchondral bone remodeling, and inflammation [1]. Obesity, sex, age, genetics, diet, traumatic injury, abnormal joint load, and joint alignment are the risk factors for OA [2]. OA is mainly

characterized by a low level of intra-articular inflammation and the degeneration or destruction of articular cartilage. These pathological features usually lead to pain of knee joint, a significant decline in patients' quality of life, sleeping disorders, and even a series of mental and psychological disorders [3–5].

At present, there are two main strategies in the treatment of OA. The first strategy is based on the western medicine theory, which focuses on eliminating osteophytes, promoting articular cartilage repair, and correcting imbalanced mechanical burden of joint. Western medicine currently used, such as nonsteroid anti-inflammatory drugs or selective COX-2 inhibitors, mainly aim at alleviating joint pain. However, they have little effect on the recovery of chondrogenic development and the improvement of OA progression. Besides, the side effects of western medicine limit their long-term application [6–8]. Biological inhibitors such as tumor necrosis factor (TNF) and interleukin- (IL-) 6 inhibitors can relieve the inflammatory symptoms in rheumatoid arthritis, but their efficacy is limited in OA [9]. The second strategy is based on the traditional Chinese medicine (TCM). OA can be treated through various approaches such as oral administration of herbal medicine, topical treatment, physiotherapy, and so on. TCM formula San-Miao-San (SMS) derived from the Chinese Medical History "Orthodox Medicine Science-Numbness" is a novel formula for treating OA. SMS has been used to treat arthralgia syndrome for hundreds of years. It is composed of Rhizoma Atractylodis/Cang Zhu (CZ), Cortex Phellodendri/Huang Bo (HB), and Achyranthis Bidentatae/Niu Xi (NX) [10]. HB with bitter nature is good at clearing dryness, dampness, and internal heat. CZ powder with bitter nature is good at invigorating spleen and clearing dryness and dampness. NX tonifies liver and kidney and strengthens muscles and bones. It is specially used to treat numb syndromes and weakness of feet [11]. Several studies have shown that SMS or modified SMS improves the efficacy of western medicine for treating rheumatoid arthritis and gouty arthritis [10, 12, 13]. Our previous study demonstrated that *Ganoderma lucidum*-SMS combined with hyaluronic acid gel can alleviate cartilage degeneration in traumatic OA [14].

Treatment using TCM often involves the synergistic action of multicomponents and multitargets. The principle theory of TCM for treating chronic disease is consistent with the basic theory of network pharmacology. Therefore, this study intends to use the approaches of network pharmacology and molecular docking to discover the mechanism of SMS for OA treatment, so as to provide a theoretical support for further investigation.

2. Materials and Methods

2.1. Screening Active Compounds and Targets of Compounds in SMS. Traditional Chinese Medicine Systems Pharmacology Database (Version:2.3, https://old.tcmsp-e.com/tcmsp.php) were used to search Chinese medicine composition of SMS with keywords "Cortex Phellodendri," "Radix Achyranthis Bidentatae," and "Rhizoma Atractylodis" [15]. Oral bioavailability (OB) and drug-likeness (DL) were used to screen each compound, and those compounds that met OB ≥ 30% and DL ≥ 0.18 were considered to be the potential active components. The active targets of components in SMS were screened out from the DrugBank database (https://www.drugbank.ca/) [16].

2.2. Screening OA-Related Disease Targets in Human. The five databases including Genecards (https://www.genecards.org/) [17], OMIM (https://omim.org/) [18], DisGeNet (https://www.disgenet.org/) [19], TTD (https://db.idrblab.net/ttd/) [20], and PharmGKB (https://www.pharmgkb.org/) [21] were screened to collect OA-related disease targets by searching the keyword "knee osteoarthritis (UMLS CUI: C0409959) or osteoarthritis."

2.3. Compound-Target Network Construction. The compound-target network of SMS was constructed by using Cytoscape software (version 3.7.2, Boston, MA, USA) [22]. After sorting and classifying the active components of SMS and its corresponding targets, the effective compounds of SMS and common target genes of compounds and OA were used to create network nodes. The relationship between the nodes was illustrated by connecting lines in the Cytoscape software. Therefore, a network between the active compounds of SMS and the target genes of OA could be established. After that, the compound-target network was exported with the degree centrality of targets.

2.4. Construction of Protein-Protein Interaction (PPI) Network. The PPI network of target was constructed through the Search Tool for the Retrieval of Interacting Genes/Proteins (STRING, https://string-db.org/) online database [23]. "Multiple proteins names" were selected and the screened genes were input. "*Homo sapiens*" was selected as the target species, and the PPI network with the minimum required interaction score ≥0.4 was constructed, without isolated proteins.

2.5. Topological Optimization of Interaction Network. The key targets of interaction network were analyzed in the topological analysis. The CytoNCA plug-in tool of Cytoscape was used to analyze the topological parameters of all nodes in PPI network in the way of being without weight, including degree centrality (DC), betweenness centrality (BC), closeness centrality (CC), eigenvector centrality (EC), information centrality (IC), and local average connectivity-based method (LAC). The median values of the topological parameters were considered as a standard rule to filter targets of compounds. The obtained nodes were the key nodes in the interaction network.

2.6. Bioinformatics Analysis. David Bioinformatics Resources 6.7 (https://david-d.ncifcrf.gov/) was used for gene ontology (GO) and Kyoto Encyclopedia of Genes and Genomes (KEGG) enrichment analysis [24]. In this study, the

Benjamini–Hochberg method was used to control the false discovery rate (FDR) of multiple hypothesis testing and corrected $p < 0.05$ was significant [25]. The analysis of GO functional enrichment and KEGG pathway enrichment was presented in the visual graphics and data tables.

2.7. Molecular Docking Analysis. AutoDock software (AutoDock 4.2, San Carlos, CA, USA) was used for protein-compound docking analysis [26]. In brief, the two-dimensional (2D) structure of the compound was obtained from the NCBI PubChem structure file, and the three-dimensional (3D) structure was constructed by ChemBio 3D Ultra software (Cambridgesoft, version 14.0) after energy minimization. The crystal structure of receptor protein was obtained from the PDB website (https://www.rcsb.org/) [27]. The crystal structure of ligand/compound was extracted by PyMoL software (San Carlos, CA, USA). Use AutoDock software to add polar hydrogen to the entire receptor, and the grid box was set to contain the entire receptor region. In all docking studies, 20 docking conformations were generated for each pair of ligand and receptor. The affinity energy was calculated using genetic algorithm. A binding energy less than 0 indicated that the ligand could spontaneously bind to the receptor. It was generally believed that if the ligand binds to the receptor stably, the lower the energy fraction, the greater the binding possibility [26].

3. Results

3.1. The Active Compounds and Potential Targets of Compounds in SMS. A total of 365 components were found through searching the Traditional Chinese Medicine Systems Pharmacology (TCMSP) database, including 49 components from Rhizoma Atractylodis/CZ, 176 components from Radix Achyranthis Bidentatae/NX, and 140 components from Cortex Phellodendri/HB. The active ingredients in SMS were screened according to the principle of pharmacokinetics. If their OB $\geq$ 30% and DL $\geq$ 0.18 [15], they were considered as the active compounds. A total of 57 potential active compounds were obtained after eliminating the duplication (Table 1), and a total of 203 targets corresponding with these active compounds were confirmed by searching the DrugBank database (Supplementary Table S1). After screening, there were 9, 20, and 37 active compounds in CZ, NX, and HB, respectively.

3.2. Compound-Target Network. Although we have found the potential active compounds and their corresponding targets in SMS, the therapeutic mechanism of SMS in OA has not been fully understood. In order to understand more intuitively how the potential active compounds of SMS play a therapeutic role on OA, a total of 2239 OA-related disease targets were obtained. They include 368 targets from DisGeNet database, 1835 targets from GeneCards database, 6 targets from Online Mendelian Inheritance in Man (OMIM) database, 9 targets from Pharmacogenetics Knowledge Base (PharmGKB) database, and 21 targets from Therapeutic Target Database (TTD) (Figure 1(a), Supplementary Table S2). After eliminating the duplicates by Venn analysis, we found that 1971 targets were related to OA disease, and 108 intersection targets between OA-related targets and targets of SMS active compounds (Figure 1(a)). These intersection targets were considered as the active targets of SMS in the treatment of OA (Figures 1(a) and 1(b)). Therefore, a component-target network containing 25 active compounds of SMS and 108 intersection targets was constructed using Cytoscape software (Figure 1(b)). After further analysis of the component-target network, the degree centrality of the active target was determined by its connection. Through the analysis of the degree centrality of 25 SMS active compounds and 108 intersection targets in each herb (Figure 1(c)), SMS active compounds with the highest degree centrality were quercetin (MOL000098, degree centrality = 85), kaempferol (MOL000422, degree centrality = 34), and wogonin (MOL000173, degree centrality = 29). Quercetin derived from NX and HB, kaempferol from NX, and wogonin (degree centrality = 29) from CZ and NX were flavonoid compounds and had the largest number of active targets (Figure 1(c)): quercetin (85 targets), kaempferol (34 targets), and wogonin (29 targets). Meanwhile, we found that the top four targets with the highest degree centrality among the 108 intersection targets were prostaglandin-endoperoxide synthase- (PTGS-) 2 (degree centrality = 25), PTGS1 (degree centrality = 18), androgen receptor (AR, degree centrality = 15), and beta-2 adrenergic receptor gene (ADRB2, degree centrality = 13) (Figure 1(c)). Two of them were coding enzymes (PTGS2 and PTGS1), and the other two were receptors (AR and ADRB2). Moreover, all of them could be found in the diagrams of degree centrality of quercetin, kaempferol, and wogonin (Figure 1(d)), and in the diagrams of degree centrality of 29 intersection targets, which were extracted by Venn analysis among CZ, HB, and NX (Figure 1(e)). Then, three clusters of these 29 intersection targets were formed by PPI network.

3.3. Analysis of Key Targets of SMS in the Treatment of OA. As we know, the physiological functions of proteins were usually regulated by protein interactions and their corresponding pathways. In order to uncover the functions and mechanism of SMS in the treatment of OA, a PPI network of the 108 intersection targets identified above was constructed by online String v11.0 (Figure 2). The key targets of SMS could be further identified by the topological analysis of the PPI network (Figure 2). As the median values of each intersection target in DC, BC, CC, EC, IC, and LAC were 42.344, 0.217, 6.000, 0.048, 3.107, and 2.800, respectively, the nodes that were greater than these median values were filtered. A total of 27 nodes that met the requirements were therefore selected. All of them were used to construct an interactive sub-network for further topological analysis (Figure 2). Through similar screening criteria, the median values of BC, CC, DC, EC, IC, and LAC were calculated, 9 refined key targets (estrogen receptor- (ESR-) 1, proto-oncogene c-Fos (FOS), mitogen-activated protein kinase- (MAPK-) 1, MAPK14, Rela (p65 NF-κB), TP53, TNF, transcription factor activator protein-1 (Jun), and Myc

Table 1: The potential active compounds in SMS.

	MOL ID	MOL Name	OB (%)	DL	CM
1	MOL000422	Kaempferol	41.88	0.24	NX
2	MOL001006	Poriferasta-7, 22E-dien-3β-ol	42.98	0.76	NX
3	MOL002714	Baicalein	33.52	0.21	NX
4	MOL002776	Baicalin	40.12	0.75	NX
5	MOL002897	Epiberberine	43.09	0.78	NX
6	MOL003847	Inophyllum E	38.81	0.85	NX
7	MOL004355	Spinasterol	42.98	0.76	NX
8	MOL012461	28-Norolean-17-en-3-ol	35.93	0.78	NX
9	MOL012505	Bidentatoside, ii_qt	31.76	0.59	NX
10	MOL012537	Spinoside A	41.75	0.4	NX
11	MOL012542	β-Ecdysterone	44.23	0.82	NX
12	MOL000622	Magnograndiolide	63.71	0.19	HB
13	MOL000762	Palmidin A	35.36	0.65	HB
14	MOL000787	Fumarine	59.26	0.83	HB
15	MOL000790	Isocorypalmine	35.77	0.59	HB
16	MOL001131	Phellamurin_qt	56.6	0.39	HB
17	MOL001455	(S)-canadine	53.83	0.77	HB
18	MOL001771	Poriferast-5-en-3beta-ol	36.91	0.75	HB
19	MOL002636	Kihadalactone A	34.21	0.82	HB
20	MOL002641	Phellavin_qt	35.86	0.44	HB
21	MOL002644	Phellopterin	40.19	0.28	HB
22	MOL002651	Dehydrotanshin one II A	43.76	0.4	HB
23	MOL002652	Delta7-dehydrosophoramine	54.45	0.25	HB
24	MOL002656	Dihydroniloticin	36.43	0.81	HB
25	MOL002659	Kihadanin A	31.6	0.7	HB
26	MOL002660	Niloticin	41.41	0.82	HB
27	MOL002662	Rutae carpine	40.3	0.6	HB
28	MOL002663	Skimmianin	40.14	0.2	HB
29	MOL002666	Chelerythrine	34.18	0.78	HB
30	MOL002668	Worenine	45.83	0.87	HB
31	MOL002670	Cavidine	35.64	0.81	HB
32	MOL002671	Candletoxin A	31.81	0.69	HB
33	MOL002672	Hericenone H	39	0.63	HB
34	MOL002673	Hispidone	36.18	0.83	HB
35	MOL002894	Berberrubine	35.17	0.73	HB
36	MOL005438	Campesterol	37.58	0.71	HB
37	MOL006392	Dihydroniloticin	36.43	0.82	HB
38	MOL006401	Melian one	40.53	0.78	HB
39	MOL006413	Phellochin	35.41	0.82	HB
40	MOL006422	Thalifendine	44.41	0.73	HB
41	MOL013352	Obacunone	43.29	0.77	HB
42	MOL000088	β-Sitosterol 3-O-glucoside_qt	36.91	0.75	CZ
43	MOL000092	Daucosterin_qt	36.91	0.76	CZ
44	MOL000094	Daucosterol_qt	36.91	0.76	CZ
45	MOL000179	2-Hydroxyisoxypropyl-3-hydroxy-7-isopentene-2, 3-dihydrobenzofuran-5-carboxylic	45.2	0.2	CZ
46	MOL000184	NSC63551	39.25	0.76	CZ
47	MOL000186	Stigmasterol 3-O-β-D-glucopyranoside_qt	43.83	0.76	CZ
48	MOL000188	3β-Acetoxyatractylone	40.57	0.22	CZ
49	MOL000085	β-Daucosterol_qt	36.91	0.75	CZ, NX
50	MOL000173	Wogonin	30.68	0.23	CZ, NX
51	MOL000098	Quercetin	46.43	0.28	NX, HB
52	MOL00358	β-Sitosterol	36.91	0.75	NX,HB
53	MOL000449	Stigmasterol	43.83	0.76	NX, HB
54	MOL000785	Palmatine	64.6	0.65	NX, HB
55	MOL001454	Berberine	36.86	0.78	NX, HB
56	MOL001458	Coptisine	30.67	0.86	NX, HB
57	MOL002643	Delta-7-stigmastenol	37.42	0.75	NX, HB

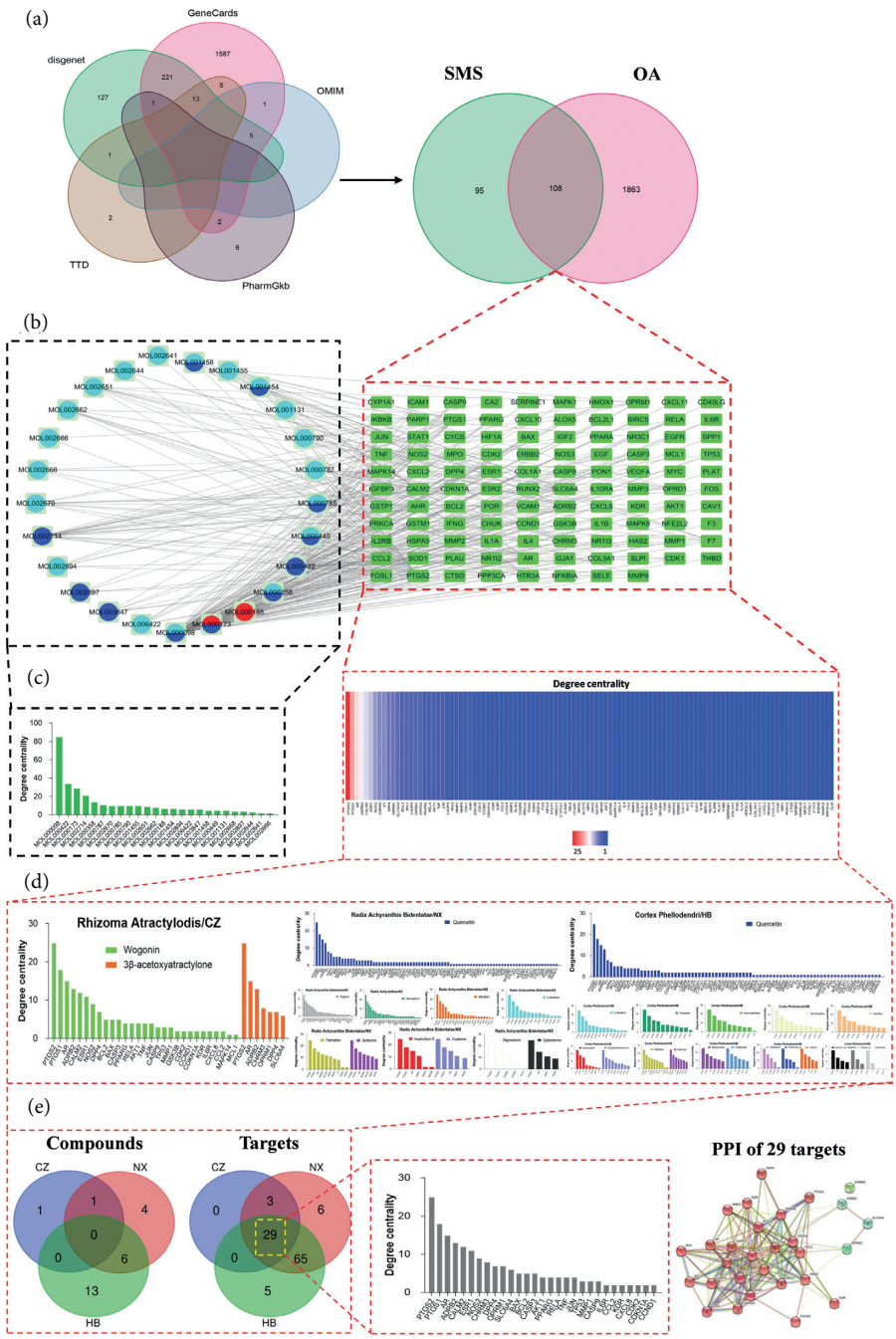

FIGURE 1: Analysis of active compound-target network of SMS for OA treatment. (a) Venn analysis of 5 databases for OA related disease targets, and intersection targets between OA-related targets and targets of SMS active compounds. (b) Analysis of active compound-target network of SMS. Red circle: compounds from Rhizoma Atractylodis. Blue circle: compounds from Radix Achyranthis Bidentatae. Indigo circle: compounds from Cortex Phellodendri. (c) The degree centrality of SMS active compounds and intersection targets. The reddish color indicates smaller degree centrality and vice versa. (d) The degree centrality of intersection targets of active compounds among CZ, HB, and NX. The bar charts with different colors represent the different active compounds corresponding intersection targets. (e) Venn diagram shows the intersection compounds and targets among CZ, HB, and NX. The bar chart shows the degree centrality of 29 intersection targets among CZ, HB, and NX. The 29 intersection targets show 3 clusters in protein-protein interaction network.

proto-oncogene protein (Myc)) were found because their median values of BC, CC, DC, EC, IC, and LAC were greater than 6.510, 0.591, 8.000, 0.156, 4.935, and 5.500, respectively (Figure 2). As the same compounds of SMS could interact with both 27 core nodes and 9 key targets in the compound-target network, they may play a key role in OA treatment. We then combined the degree centrality of targets and analyzed the key targets of active compounds in each herb. By Venn analysis of these targets among the three herbs (CZ, HB, and NX), it was found that 12 targets could correspond

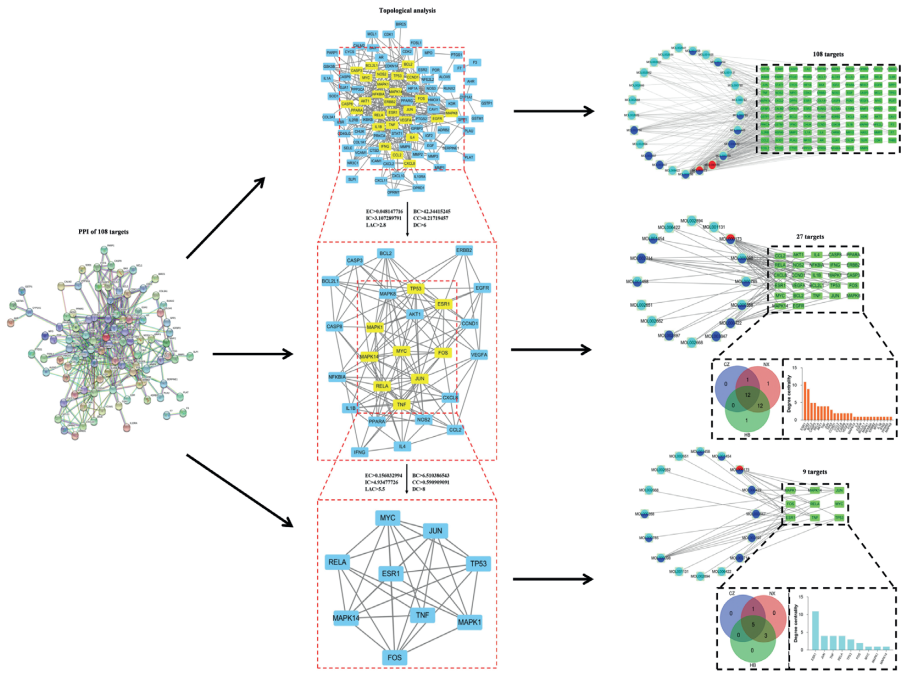

Figure 2: Topological analysis of intersection targets between OA-related targets and targets of SMS active compounds. The 108 intersection targets shown in protein-protein interaction network are performed for topology network analysis twice. The parameters such as BC, CC, DC, EC, IC, and LAC represent the filter conditions. The yellow rectangles represent the key targets in the subnetwork obtained from topology analysis. The active compounds-key targets network of each screening analysis is presented with the degree centrality of key targets and the intersection targets among CZ, HB, and NX.

with the active compounds of all herbs, and 5 of them were the key targets (Figure 2). We also found that three compounds (quercetin, kaempferol, and wogonin) could interact with these key targets (Supplementary Tables S3–S5), which also implied that these three compounds might be the key active compounds of SMS in OA treatment.

3.4. Bioinformatics Analysis. To have a more macroscopic and overall understanding of the physiological processes and biological function of the intersection targets, we performed the GO functional enrichment analysis and KEGG pathway enrichment analysis on all targets of each subnetwork. The most important biological processes (BP), cell compositions (CC), and molecular functions (MF) involved in these targets were shown in Figure 3 (corrected $p < 0.05$). They include 2 common BP (response to lipopolysaccharide, and response to molecule of bacterial origin), 4 common CC (membrane raft, membrane microdomain, transcription regulator complex, and RNA polymerase II transcription regulator complex), and 3 common MF (DNA-binding transcription factor binding; DNA-binding transcription activator activity, RNA polymerase II-specific; and RNA polymerase II-specific DNA-binding transcription factor binding). Through KEGG analysis, the most important signaling pathways were shown in Figure 3 (corrected $p < 0.05$), including 15 common KEGG pathways, such as Toll-like receptor (TLR), IL-17, and TNF signaling pathways, osteoclast differentiation, and apoptosis. The comprehensive results of GO and KEGG enrichment analysis were listed in Supplementary Tables S6–S11.

3.5. Comprehensive Analysis of Compound-Target Network with Molecular Docking. To have an in-depth understanding of the interactions between active compounds of SMS and their targets, a comprehensive analysis of molecular docking between the active compounds and targets was performed to explore and verify the potential key compounds of SMS in OA treatment (Figure 4). Therefore, the PPI network was further analyzed based on the compound-target network, which was composed of 25 active compounds of SMS and 29 intersection targets (Figure 4(b)). In addition, the topological analysis for the 29 intersection targets found above was performed, and 10 potential key targets (AKT1, CASP3, CCL2, CCND1, CXCL8, ESR1, JUN, PTGS2, TNF, and TP53) were obtained through previous screening criteria. Their median values of BC, CC, DC, EC, IC, and LAC were greater than 7.034, 0.659, 14.000, 0.192, 6.044, and 11.029, respectively (Figure 4(a)). When compared with the previous 9 key targets obtained from the Venn analysis, we found 4 common targets (ESR1, TNF, TP53, and JUN) which could form a PPI network. To further understand the biological function of these targets in OA, we carried out GO function enrichment and KEGG pathway enrichment analysis (Figure 4(c)). From the GO enrichment analysis, most of these targets were enriched for negative regulation on the transcription by RNA polymerase II (GO: 0000122), nuclear chromatin (GO: 0000790), and RNA polymerase II transcription factor binding (GO: 0001085), implicating that they might be the main functions of these targets. From the KEGG enrichment analysis, we found that the main pathways involved were MAPK signaling pathway (hsa04010) and Wnt signaling pathway (hsa04310), as the number of

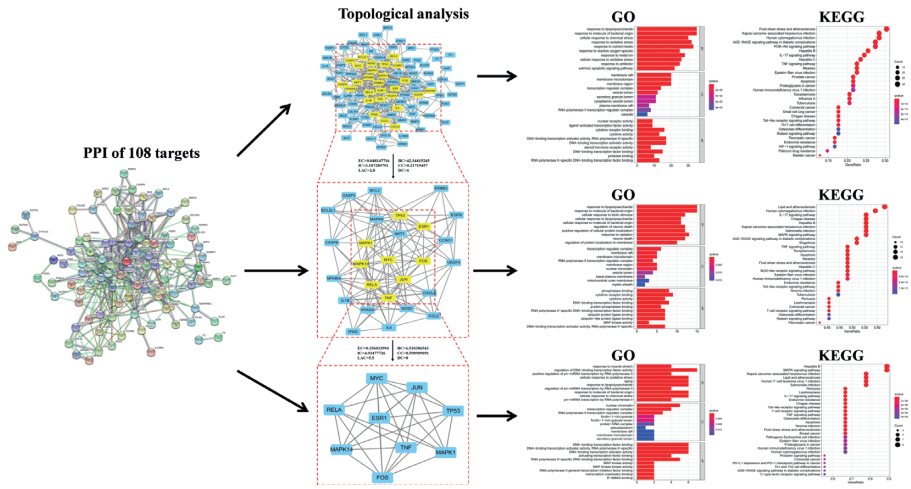

FIGURE 3: GO function enrichment and KEGG pathway enrichment analysis of PPI network. The important biological processes (BP), cell composition (CC), and molecular function (MF) of GO function enrichment analysis of intersection targets between OA-related targets and targets of SMS active compounds are followed by each topological analysis. The results of the GO function enrichment analysis present in bar chart. The length of the bar in the figure indicates the number of targets participating in each function. The results of the KEGG pathway enrichment analysis are plotted. The size of the circle in the picture indicates the number of targets participating in the path. The reddish color indicates smaller p value and vice versa.

genes involved in these pathways was high. It may imply that these signaling are the main pathway involved in these targets (Figure 4(c) and Supplementary Tables S12 and S13). Therefore, the common active compounds of these targets were obtained by Venn analysis. We found wogonin was the only compound that formed a central network with its corresponding targets and pathways. The binding affinity between wogonin and 4 common targets were evaluated by molecular docking (Figure 4(d)). The results of the minimum energy fraction from 20 docking schemes of each group were selected as the docking structure model. The lower energy fraction (less than −5 kcal/mol) indicated the better degree of a ligand binding to its receptor in the molecular docking analysis [26]. The identification symbols of each target protein in the Protein Data Bank (PDB) were shown as follows: ESR1 (3OS8), TP53 (1Sal), TNF (7Kp9), and JUN (5Fv8) [27]. Among them, most of the binding between wogonin and targets was through the formation of hydrogen bonds or pi bonds, and some interactions were produced by van der Waals force. As the docking score of ESR1 (−8.4 kcal/mol) was the highest, the combination of ESR1 and wogonin may play an important role in targeting the key process of OA.

4. Discussion

The syndrome of knee arthralgia described in the "Su Wen···Chang Ci Jie Lun" of TCM literature belongs to the category of OA. According to the theory of TCM, OA is the functional deficiency of liver and kidney, which involves vessel blocking and joint pain. Therefore, it is believed that the multidrugs and multitargets approach should be considered in the treatment of OA [28]. Different from the "one monomer compound for one disease treatment" methodology, network pharmacology can be used to study the potential mechanisms of various components of TCM formulas like SMS in OA treatment. In the previous study, we have found that *Ganoderma lucidum*-SMS can directly alleviate cartilage degeneration in the knee joint by activating the chondrogenic signaling pathway in a traumatic OA rat model [14]. Additionally, *Ganoderma lucidum*-SMS plays an indirect regulatory role on the integrity of subchondral bone microstructure that offers a stabilized physiological environment for the recovery of the damaged cartilage. Meanwhile, besides the synergistic anti-inflammatory effect of *Ganoderma lucidum* and SMS, a target-specific signaling pathway (MAPK pathway) has been found during OA progression. However, the active ingredients of *Ganoderma lucidum*-SMS and their targets in OA, as well as the interactive relationship and key genes of the signaling pathway involved, are not well illustrated. Therefore, through the approaches of network pharmacology and molecular docking, we discovered the potential active ingredients of SMS and the related targets to provide a potential mechanism of SMS in OA treatment.

In this study, the potential active compounds and targets of SMS and OA-related target proteins were obtained from TCMSP, DrugBank, GeneCards, OMIM, DisgenET, and PharmGKB databases. The main targets of SMS on OA were obtained by Venn analysis, and the sources of the intersection targets were further analyzed. Quercetin, kaempferol, and wogonin were found to be the key active components of SMS in the treatment of OA. Quercetin, a polyphenolic flavonoid, has been reported to possess anti-inflammatory, antioxidant, and antiallergic activities. It is reported that intra-articular injection of quercetin may inhibit the production of IL-1β and TNF-α by regulating TLR-4/NF-κB pathway and reduce the degradation of cartilage and the apoptosis of chondrocytes in an OA rat model [29]. It is confirmed that quercetin can significantly inhibit the expression of matrix metalloproteinases and inflammatory mediators and can promote the production of

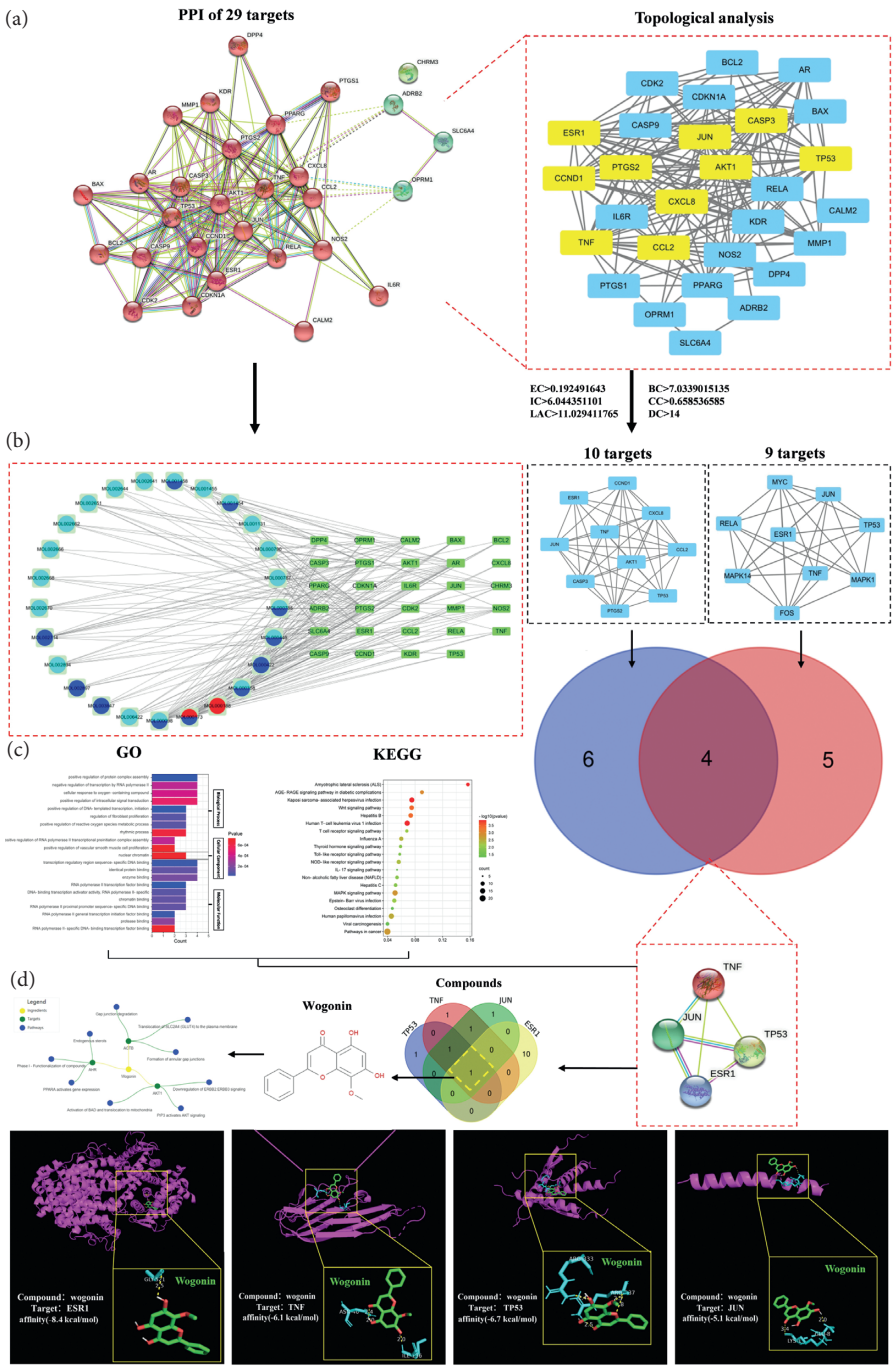

FIGURE 4: Comprehensive analysis of SMS active compounds-key targets network with molecular docking. (a) The protein-protein interaction network and topological analysis of 29 intersection targets. There are 10 yellow rectangles obtained from topology analysis that represent the key targets, compared with previous found 9 key targets for Venn analysis. (b) The interactive network of SMS active compounds and 29 intersection targets. The interaction of 10 and 9 key targets present in each subnetwork. (c) The KEGG pathway enrichment and GO function enrichment analysis of 4 intersection targets in PPI network. These intersection targets are derived from Venn analysis of subnetworks. The reddish color indicates smaller p value and vice versa. (d) The molecular structure presents the active compound wogonin, which is derived from Venn analysis of above 4 key targets' corresponding compounds. The targets and pathways of wogonin are present in central network diagram, which is output from a TCM database (Integrative Pharmacology-Based Research Platform of Traditional Chinese Medicine, TCMIP v2.0). Then, the three-dimensional conformations of wogonin and corresponding targets including the affinity energy present in the molecular docking diagram. The yellow rectangles present the spatial docking of wogonin in each target.

cartilage synthesis factors in chondrocytes [29]. In addition, quercetin plays an antiapoptotic role in chondrocytes by reducing intracellular reactive oxygen species (ROS), restoring mitochondrial membrane potential, and inhibiting the caspase 3 pathway [30]. Other studies have shown that quercetin treatment can reduce oxidative stress, endoplasmic reticulum stress, and chondrocytes apoptosis [31]. Kaempferol is also a flavonoid compound and has anti-apoptotic and anti-inflammatory pharmacological activities. It has been reported that kaempferol inhibits the production and release of inflammatory cytokines (TNF-α and IL-6), mediators (nitric oxide/NO and prostaglandin E2), and signaling molecules (SRC, SYK, and IRAK4), as well as the release of ROS [32]. It was found that kaempferol significantly reduced the production of proinflammatory mediators by inhibiting the NF-κB pathway, which suggests a prominent anti-inflammatory and antiarthritis effects of kaempferol in IL-1β-stimulated rat chondrocytes [33]. Wogonin is also a flavonoid that exhibits anti-inflammatory and antioxidant effects on chondrocytes and cartilage explants by activating ROS/extracellular regulated protein kinases (ERK)/nuclear factor erythroid 2-related factor 2 (NRF2) signaling pathway. These signaling pathways were involved in oxidative stress, inflammatory response, and matrix degradation in OA [34]. Matrix metalloproteinase-(MMP-) 3 plays an important role in the pathophysiology of OA through the degradation of extracellular matrix components like proteoglycan. One study reported that wogonin could downregulate the expression of MMP-3 in chondrocytes to protect cartilage degradation [35, 36]. In summary, all of the above key active components of SMS may play a synergistical role on OA-related targets to perform the antiapoptotic, antioxidant, and anti-inflammatory effects.

In this study, the key targets of SMS for the treatment of OA obtained by Venn analysis, PPI network, topological analysis, and molecular docking analysis include ESR1, FOS, MAPK1, MAPK14, Rela, TP53, TNF, Jun, and Myc. The association between the ESR gene polymorphisms and OA has been found in several studies [37, 38]. For example, ESR variants, which are the genetic markers of OA, are associated with the susceptibility of joint pain in women [38]. What we found is wogonin can bind to the glycine (Gly521) residue in the ligand-binding domain of ESR1 (shown in Figure 4(d)). In addition, the increased c-Jun protein in IL-1β-stimulated chondrocytes can form a heterodimer of activator protein-1 (AP-1) with FOS [39]. Meanwhile, the IL-1β-activated c-Jun N-terminal kinase (JNK), one of the important branches of MAPK family, can form a vital JNK-c-Jun pathway for chondrocyte apoptosis [39]. Thus, JNK and c-Jun are often indicated to be the important targets of anti-inflammatory therapy in chondrocyte apoptosis [40]. Therefore, the progression of OA can be effectively alleviated by regulating the JNK signaling pathway [41]. The mechanism of the MAPK signaling pathway in OA has been extensively studied. JNK and p38 MAPK signaling pathways are related to the apoptosis of chondrocytes in OA. The osteoblasts derived from subchondral bone may inhibit the anabolism and promote catabolism of chondrocytes in OA through the ERK1/2 signaling pathway [42, 43]. Hence, we believe that MAPK, as a mediator to regulate the expression of proinflammatory cytokines and the downstream MMPs, may be involved in the potential pathway for preventing OA progression [44]. Besides MAPK, the level of phosphorylated Rela is also significantly increased in OA. It also upregulates the expression of proinflammatory cytokines, chemokines, and matrix degrading enzymes [45]. In this study, several cell compositions like the transcription regulator complex and molecular function like DNA-binding transcription activator activity were identified (shown in Figure 3). Because the phosphorylated p53 accumulated induce chondrocytes apoptosis or senescence under the stimulation of nitric oxide (NO), IL-1β, and mechanical stress in OA, we believe TP53 may involve in the above cell compositions and molecular functions [46, 47]. Most importantly, we found the 4 major targets of wogonin (shown in Figure 4(d)). TNF-α is one of them, and it is considered to be an important factor in cartilage degeneration during the development of OA. The inhibitor of TNF-α also has an inhibitory effect on the progression of OA [48]. Interestingly, in this study, we found that wogonin could interact with TNF-α (7Kp9) through forming hydrogen bonds with its amino acid residues asparagine (Asn40) and isoleucine (Ile136). Meanwhile, we predicted the potential interactive sites and affinity energies between wogonin and amino acid residues of each target. Most of the potential bindings between wogonin and targets are through the hydrogen bonds (shown in Figure 4(d)). However, the real effect and mechanism of interaction between SMS active compounds and OA-related key targets require further experimental verifications.

Besides the key targets found in SMS-treated OA and their interactive network, the mechanism of the active compounds participated in the cellular function and signaling pathways is clarified in GO and KEGG enrichment analysis (shown in Figure 3). GO functional analysis of genes shows that these target genes play a potential role on a series of biological processes by affecting apoptotic signaling pathways, cellular responses to oxidative stress, responses to nutrient levels, ROS, and metal ions. Many studies have shown that the imbalanced coupling mechanism between chondrocyte proliferation and apoptosis are two of the reasons for OA progression [49, 50]. For instance, chondrocyte apoptosis is the main cause for OA progression, and excessive oxidative stress triggers the activation of apoptosis- or necrosis-related pathways in chondrocytes, thereby leading to cartilage degeneration in OA [51]. Oxidative stress can also promote the development of inflammation [52]. For example, ROS can directly or indirectly reduce the cartilage matrix by activating all of the potential MMPs to increase proinflammatory cytokines and chemokines, thereby resulting in cell apoptosis [53, 54].

From the results of KEGG enrichment analysis (shown in Figure 3), the main signaling pathways involved in SMS treated OA are TLR, IL-17, and TNF signaling pathways, osteoclast differentiation, and apoptosis. The differentiated osteoclasts from synovial membrane involve bone resorption in the progressive OA [55–57]. Nuclear factor- (NF-) κB ligand (RANKL), a member of the TNF cytokine ligand superfamily, is essential for osteoclast differentiation and can

also regulate bone resorption and prevent osteoclasts from death [58]. An upregulation of RANKL in chondrocytes is correlated with the cartilage degeneration and osteoclast density in the mineralized tissues [59]. It is implied that RANKL could be a key signaling molecule in the crosstalk between the cartilage and bone. The relationship between the cartilage RANKL score and osteoclast density strongly suggests that the chondrocytes could modulate osteoclast recruitment for subchondral bone remodeling in OA [60]. Moreover, the interaction of RANKL and RANK induces osteoclast progenitor to differentiate into osteoclast. Subsequently, the RANK-RANKL complex induces an activation of TNF receptor-associated factor 6 (TRAF6), which in turn involves the activation of NF-κB and MAPKs, including p38 and JNK [61]. In addition, TLR plays an important role in nonspecific immunity and acts as a bridge between specific immunity and nonspecific immunity. The signaling pathway involved in this receptor is closely related to immune or inflammatory diseases. Therefore, the activation of TLR4 can trigger the downstream NF-κB signaling and upregulate the expression of IL-1β and TNF-α to exacerbate inflammation in OA [62, 63].

5. Conclusions

The existing treatment of OA still cannot meet the current clinical demands, and the side effects of long-term use of western medicine should not be ignored. TCM has the "multicomponents and multitargets" characteristics and has been used to treat various chronic diseases in a systematic and holistic manner. This study explored the mechanism of SMS in the treatment of OA based on network pharmacology. We have found that wogonin is the key compound in SMS, which may play a therapeutic role through four key targets (ESR1, JUN, TP53, and TNF) and act on TLR, IL-17, and TNF, osteoclast differentiation, and apoptosis signaling pathways. The results of network pharmacological analysis provide a valuable reference for elucidating the anti-inflammatory mechanism of SMS and its compounds in the treatment of OA and discovering new drugs from TCM. However, the corresponding targets of specific active components of SMS and the synergistic effect between them require further study.

Abbreviations

SMS: San-Miao-San
OA: Osteoarthritis
TCMSP: Traditional Chinese Medicine Systems Pharmacology
OMIM: Online Mendelian Inheritance in Man
TTD: Therapeutic Target Database
PharmGKB: Pharmacogenetics Knowledge Base
PPI: Protein-protein interaction
DAVID: Database for Annotation, Visualization, and Integrated Discovery
TNF: Tumor necrosis factor
IL: Interleukin
TCM: Traditional Chinese medicine
CZ: Cang Zhu/Rhizoma Atractylodis
HB: Huang Bo/Cortex Phellodendri
NX: Niu Xi/Achyranthis Bidentatae
OB: Oral bioavailability
DL: Drug-likeness
PTGS: Prostaglandin-endoperoxide synthase
AR: Androgen receptor
ADRB2: Beta-2 adrenergic receptor gene
BC: Betweenness centrality
CC: Closeness centrality
DC: Degree centrality
EC: Eigenvector centrality
IC: Information centrality
LAC: Local average connectivity-based method
ERS: Estrogen receptor
FOS: Protooncogene c-Fos
Jun: Transcription factor AP-1
Myc: Myc protooncogene protein
GO: Gene ontology
KEGG: Kyoto Encyclopedia of Genes and Genomes
MAPK: Mitogen-activated protein kinase
BP: Biological processes
CC: Cell composition
MF: Molecular function
PDB: Protein Data Bank
ROS: Reactive oxygen species
ERK: Extracellular regulated protein kinases
NRF2: Nuclear factor erythroid 2-related factor 2
AP-1: Activator protein-1
MMP: Matrix metalloproteinase
AP-1: Activator protein-1
JNK: c-Jun N-terminal kinase
NF: Nuclear factor
NO: Nitric oxide
RANKL: Nuclear factor- (NF-) κB ligand
TRAF6: TNF receptor-associated factor 6
TLR: Toll-like receptor
STRING: Search Tool for the Retrieval of Interacting Genes/Proteins
FDR: False discovery rate
2D: Two-dimensional.

Data Availability

The datasets used and/or analyzed during the current study are available from the corresponding author on reasonable request.

Conflicts of Interest

The authors declare that they have no conflicts of interest.

Authors' Contributions

M. C. and X. Z. were responsible for data curation; T. G. and M. C. were responsible for formal analysis; M. C., P. W., Y. F., and Z. C. were responsible for funding acquisition; W. K. was responsible for investigation; W. K. and T. G. were responsible for methodology; M. C., X. Z., W. K., and Z. C.

were responsible for resources; M. C., T. G., and W. K. were responsible for software; Y. F., P. W., and Z. C. were responsible for supervision; M. C., X. Z., P. W., and Z. C. were responsible for validation; Z. C. was responsible for visualization; M. C. was responsible for the writing of the original draft; P. W. and Z. C. were responsible for review and editing. All authors have read and agreed to the published version of the manuscript.

Acknowledgments

The authors thank all funding supporters including the Project of Educational Commission of Shaanxi Province of China, the Natural Science Foundation of Guangdong Province, and the Guangzhou Science and Technology Plan Project of Guangdong Province. The authors thank all authors' contributions to this study. The authors thank Dr. Miranda Sin-Man Tsang contributions to polish the manuscript. This work was supported by the Project of Educational Commission of Shaanxi Province of China (ref. 20JK0608), the Project of Shaanxi University of Chinese Medicine (ref: 2020GP14), the Natural Science Foundation of Guangdong Province (no. 2020A1515110193), the Natural Science Foundation of Ningxia Hui Autonomous Region (no. 2021AAC05021), and the Guangzhou Science and Technology Plan Project of Guangdong Province (no. 202102010290).

Supplementary Materials

The data used to support the findings of this study are available in Supplementary Tables S1–S13. (*Supplementary Materials*)

References

[1] W. E. Van Spil, O. Kubassova, M. Boesen, A.-C. Bay-Jensen, and A. Mobasheri, "Osteoarthritis phenotypes and novel therapeutic targets," *Biochemical Pharmacology*, vol. 165, pp. 41–48, 2019.

[2] L. A. Mandl, "Osteoarthritis year in review 2018: clinical," *Osteoarthritis and Cartilage*, vol. 27, no. 3, pp. 359–364, 2019.

[3] G. A. Hawker, M. A. M. Gignac, E. Badley et al., "A longitudinal study to explain the pain-depression link in older adults with osteoarthritis," *Arthritis Care and Research*, vol. 63, no. 10, pp. 1382–1390, 2011.

[4] L. Wong, R. Yiu, C. Chiu et al., "Prevalence of psychiatric morbidity in Chinese subjects with knee osteoarthritis in a Hong Kong orthopedic clinic," *East Asian Arch Psychiatry*, vol. 25, pp. 150–158, 2015.

[5] J. C. Branco, A. M. Rodrigues, N. Gouveia et al., "Prevalence of rheumatic and musculoskeletal diseases and their impact on health-related quality of life, physical function and mental health in Portugal: results from EpiReumaPt- a national health survey," *RMD Open*, vol. 2, no. 1, Article ID e000166, 2016.

[6] B. S. Rafanan, B. F. Valdecañas, B. P. Lim et al., "Consensus recommendations for managing osteoarthritic pain with topical NSAIDs in Asia-Pacific," *Pain Management*, vol. 8, no. 2, pp. 115–128, 2017.

[7] S. R. Smith, B. R. Deshpande, J. E. Collins, J. N. Katz, and E. Losina, "Comparative pain reduction of oral non-steroidal anti-inflammatory drugs and opioids for knee osteoarthritis: systematic analytic review," *Osteoarthritis and Cartilage*, vol. 24, no. 6, pp. 962–972, 2016.

[8] F. Wattand and M. Gulati, "New drug treatments for osteoarthritis: what is on the horizon?" *European Journal of Rheumatology*, vol. 2, no. 1, pp. 50–58, 2017.

[9] P. R. Coryell, B. O. Diekman, and R. F. Loeser, "Mechanisms and therapeutic implications of cellular senescence in osteoarthritis," *Nature Reviews Rheumatology*, vol. 17, no. 1, pp. 47–57, 2021.

[10] Z. Cai, C. Wong, J. Dong et al., "Anti-inflammatory activities of Ganoderma lucidum (Lingzhi) and San-Miao-San supplements in MRL/lpr mice for the treatment of systemic lupus erythematosus," *Chinese Medicine*, vol. 4, no. 11, p. 23, 2016.

[11] T. Zhou, D. Sun, and P. Wu, "Clinical research on San miao powder combined fibrinogenase for injection in treatment of acute deep venous thrombosis of lower limbs," *Zhong guo Zhong Xi Yi Jie He Za Zhi*, vol. 32, no. 7, pp. 918–921, 2012.

[12] Y. Xi Bao, C. Kwok Wong, E. Shan Tam, P. Chung Leung, Y. Bing Yin, and C. Wai Kei Lam, "Immunomodulatory effects of lingzhi and san-miao-san supplementation on patients with rheumatoid arthritis," *Immunopharmacology and Immunotoxicology*, vol. 28, no. 2, pp. 197–200, 2006.

[13] E. K. Li, L.-S. Tam, C. K. Wong et al., "Safety and efficacy of Ganoderma lucidum (lingzhi) and San Miao San supplementation in patients with rheumatoid arthritis: a double-blind, randomized, placebo-controlled pilot trial," *Arthritis and Rheumatism*, vol. 57, no. 7, pp. 1143–1150, 2007.

[14] M. Chu, P. Wu, M. Hong et al., "Lingzhi and San-Miao-San with hyaluronic acid gel mitigate cartilage degeneration in anterior cruciate ligament transection induced osteoarthritis," *Journal of Orthopaedic Translation*, vol. 26, pp. 132–140, 2021.

[15] J. Ru, P. Li, J. Wang et al., "TCMSP: a database of systems pharmacology for drug discovery from herbal medicines," *Journal of Cheminformatics*, vol. 6, no. 1, pp. 13–18, 2014.

[16] D. S. Wishart, K. Craig, A. C. Guo et al., "DrugBank: a knowledgebase for drugs, drug actions and drug targets," *Nucleic Acids Research*, vol. 36, pp. 901–906, 2007.

[17] M. Safran, I. Dalah, J. Alexander et al., "GeneCards Version 3: the human gene integrator," *Database*, vol. 2010, Article ID baq020, 2010.

[18] A. Hamosh, A. F. Scott, J. S. Amberger, C. A. Bocchini, and V. A. McKusick, "Online Mendelian Inheritance in Man (OMIM), a knowledge base of human genes and genetic disorders," *Nucleic Acids Research*, vol. 33, pp. D514–D517, 2005.

[19] J. Piñero, À. Bravo, N. Queralt-Rosinach et al., "DisGeNET: a comprehensive platform integrating information on human disease-associated genes and variants," *Nucleic Acids Research*, vol. 45, pp. D833–D839, 2017.

[20] Y. Wang, S. Zhang, F. Li et al., "Therapeutic target database 2020: enriched resource for facilitating research and early development of targeted therapeutics," *Nucleic Acids Research*, vol. 48, pp. D1031–D1041, 2020.

[21] M. Hewett, "PharmGKB: the Pharmacogenetics Knowledge Base," *Nucleic Acids Research*, vol. 30, no. 1, pp. 163–165, 2002.

[22] C. T. Lopes, M. Franz, F. Kazi, S. L. Donaldson, Q. Morris, and G. D. Bader, "Cytoscape Web: an interactive web-based network browser," *Bioinformatics*, vol. 26, no. 18, pp. 2347-2348, 2010.

[23] C. v. Mering, M. Huynen, D. Jaeggi, S. Schmidt, P. Bork, and B. Snel, "STRING: a database of predicted functional associations between proteins," *Nucleic Acids Research*, vol. 31, no. 1, pp. 258–261, 2003.

[24] W. Da, B. Sherman, and R. Lempicki, "Systematic and integrative analysis of large gene lists using DAVID bioinformatics resources," *Nature Protocol*, vol. 4, pp. 44–57, 2008.

[25] M. Shen, S. Tian, Y. Li et al., "Drug-likeness analysis of traditional Chinese medicines: 1. property distributions of drug-like compounds, non-drug-like compounds and natural compounds from traditional Chinese medicines," *Journal of Cheminformatics*, vol. 4, no. 1, pp. 31–36, 2012.

[26] O. Trott and A. J. Olson, "AutoDock Vina: improving the speed and accuracy of docking with a new scoring function, efficient optimization, and multithreading," *Journal of Computational Chemistry*, vol. 31, pp. 455–461, 2010.

[27] H. M. Berman, T. Battistuz, T. N. Bhat et al., "The protein data bank," *Acta Crystallographica Section D Biological Crystallography*, vol. 58, no. 6, pp. 899–907, 2002.

[28] Z. Wu, W. Li, G. Liu, and Y. Tang, "Network-based methods for prediction of drug-target interactions," *Frontiers in Pharmacology*, vol. 9, p. 1134, 2018.

[29] J. Zhang, J. Yin, D. Zhao et al., "Therapeutic effect and mechanism of action of quercetin in a rat model of osteoarthritis," *Journal of International Medical Research*, vol. 48, no. 3, Article ID 300060519873461, 2020.

[30] Y. Hu, Z. Gui, Y. Zhou, L. Xia, K. Lin, and Y. Xu, "Quercetin alleviates rat osteoarthritis by inhibiting inflammation and apoptosis of chondrocytes, modulating synovial macrophages polarization to M2 macrophages," *Free Radical Biology and Medicine*, vol. 145, pp. 146–160, 2019.

[31] K. Feng, Z. Chen, L. Pengcheng, S. Zhang, and X. Wang, "Quercetin attenuates oxidative stress-induced apoptosis via SIRT1/AMPK-mediated inhibition of ER stress in rat chondrocytes and prevents the progression of osteoarthritis in a rat model," *Journal of Cellular Physiology*, vol. 234, no. 10, pp. 18192–18205, 2019.

[32] S. H. Kim, J. G. Park, G.-H. Sung et al., "Kaempferol, a dietary flavonoid, ameliorates acute inflammatory and nociceptive symptoms in gastritis, pancreatitis, and abdominal pain," *Molecular Nutrition and Food Research*, vol. 59, no. 7, pp. 1400–1405, 2015.

[33] Z. Zhuang, G. Ye, and B. Huang, "Kaempferol alleviates the interleukin-1β-induced inflammation in rat osteoarthritis chondrocytes via suppression of NF-κB," *Medical Science Monitor*, vol. 23, pp. 3925–3931, 2017.

[34] N. M. Khan, A. Haseeb, M. Y. Ansari, P. Devarapalli, S. Haynie, and T. M. Haqqi, "Wogonin, a plant derived small molecule, exerts potent anti-inflammatory and chondroprotective effects through the activation of ROS/ERK/Nrf2 signaling pathways in human Osteoarthritis chondrocytes," *Free Radical Biology and Medicine*, vol. 106, pp. 288–301, 2017.

[35] H. R. Lijnen, "Matrix metalloproteinases and cellular fibrinolytic activity," *Biochemistry*, vol. 67, no. 1, pp. 92–98, 2002.

[36] J. S. Park, H. J. Lee, D. Y. Lee et al., "Chondroprotective effects of wogonin in experimental models of osteoarthritis in vitro and in vivo," *Biomolecules and Therapeutics*, vol. 23, no. 5, pp. 442–448, 2015.

[37] A. Bergink, J. Meurs, J. Loughlin et al., "Estrogen receptor alpha gene haplotype is associated with radiographic osteoarthritis of the knee in elderly men and women," *Arthritis and Rheumatology*, vol. 48, pp. 1913–1922, 2014.

[38] S.-C. Kang, D.-G. Lee, J.-H. Choi, S. T. Kim, Y.-K. Kim, and H.-J. Ahn, "Association between estrogen receptor polymorphism and pain susceptibility in female temporomandibular joint osteoarthritis patients," *International Journal of Oral and Maxillofacial Surgery*, vol. 36, no. 5, pp. 391–394, 2007.

[39] G. Martin, P. Bogdanowicz, F. Domagala, H. Ficheux, and J.-P. Pujol, "Rhein inhibits interleukin-1 beta-induced activation of MEK/ERK pathway and DNA binding of NF-kappa B and AP-1 in chondrocytes cultured in hypoxia: a potential mechanism for its disease-modifying effect in osteoarthritis," *Inflammation*, vol. 27, no. 4, pp. 233–246, 2003.

[40] Z. Ye, Y. Chen, R. Zhang et al., "C-Jun N-terminal kinase - c-Jun pathway transactivates Bim to promote osteoarthritis," *Canadian Journal of Physiology and Pharmacology*, vol. 92, no. 2, pp. 132–139, 2014.

[41] Z. Li, D. Meng, G. Li, J. Xu, K. Tian, and Y. Li, "Celecoxib combined with diacerein effectively alleviates osteoarthritis in rats via regulating JNK and p38MAPK signaling pathways," *Inflammation*, vol. 38, no. 4, pp. 1563–1572, 2015.

[42] M. Zhong, D. H. Carney, H. Jo, B. D. Boyan, and Z. Schwartz, "Inorganic phosphate induces mammalian growth plate chondrocyte apoptosis in a mitochondrial pathway involving nitric oxide and JNK MAP kinase," *Calcified Tissue International*, vol. 88, no. 2, pp. 96–108, 2011.

[43] I. Prasadam, S. Gennip, T. Friis, W. Shi, R. Crawford, and Y. Xiao, "ERK-1/2 and p38 in the regulation of hypertrophic changes of normal articular cartilage chondrocytes induced by osteoarthritic subchondral osteoblasts," *Arthritis and Rheumatism*, vol. 62, pp. 1349–1360, 2010.

[44] R. F. Loeser, E. A. Erickson, and D. L. Long, "Mitogen-activated protein kinases as therapeutic targets in osteoarthritis," *Current Opinion in Rheumatology*, vol. 20, no. 5, pp. 581–586, 2008.

[45] L. Xu, C. Sun, S. Zhang et al., "Sam68 promotes NF-κB activation and apoptosis signaling in articular chondrocytes during osteoarthritis," *Inflammation Research*, vol. 64, no. 11, pp. 895–902, 2015.

[46] P. F. Zan, J. Yao, Z. Wu, Y. Yang, S. Hu, and G. D. Li, "Retracted: cyclin D1 gene silencing promotes IL-1β-induced apoptosis in rat chondrocytes," *Journal of Cellular Biochemistry*, vol. 119, no. 1, pp. 290–299, 2018.

[47] R. Qu, X. Chen, W. Wang et al., "Ghrelin protects against osteoarthritis through interplay with Akt and NF-κB signaling pathways," *The FASEB Journal*, vol. 32, pp. 1044–1058, 2018.

[48] M. Loef, F. P. B. Kroon, S. A. Bergstra et al., "TNF inhibitor treatment is associated with a lower risk of hand osteoarthritis progression in rheumatoid arthritis patients after 10 years," *Rheumatology*, vol. 57, no. 11, pp. 1917–1924, 2018.

[49] X. Zhou, L. Jiang, G. Fan et al., "Role of the ciRS-7/miR-7 axis in the regulation of proliferation, apoptosis and inflammation of chondrocytes induced by IL-1β," *International Immunopharmacology*, vol. 71, pp. 233–240, 2019.

[50] H. Yang, D. Wu, H. Li, N. Chen, and Y. Shang, "Down-regulation of microRNA-448 inhibits IL-1β-induced cartilage degradation in human chondrocytes via upregulation of matrilin-3," *Cellular and Molecular Biology Letters*, vol. 23, no. 1, pp. 7–11, 2018.

[51] P. Lepetsos and A. G. Papavassiliou, "ROS/oxidative stress signaling in osteoarthritis," *Biochimica et Biophysica Acta - Molecular Basis of Disease*, vol. 1862, no. 4, pp. 576–591, 2016.

[52] P. Jolbäck, O. Rolfson, M. Mohaddes et al., "Does surgeon experience affect patient-reported outcomes 1 year after primary total hip arthroplasty?" *Acta Orthopaedica*, vol. 89, pp. 265–271, 2018.

[53] Y. E. Henrotin, P. Bruckner, and J.-P. L. Pujol, "The role of reactive oxygen species in homeostasis and degradation of

cartilage," *Osteoarthritis and Cartilage*, vol. 11, no. 10, pp. 747–755, 2003.

[54] D. Li, W. Wang, and G. Xie, "Reactive oxygen species: the 2-edged sword of osteoarthritis," *The American Journal of the Medical Sciences*, vol. 344, no. 6, pp. 486–490, 2012.

[55] P. Bettica, G. Cline, D. J. Hart, J. Meyer, and T. D. Spector, "Evidence for increased bone resorption in patients with progressive knee osteoarthritis: longitudinal results from the Chingford study," *Arthritis & Rheumatism*, vol. 46, no. 12, pp. 3178–3184, 2002.

[56] L. Danks, A. Sabokbar, R. Gundle, and N. A. Athanasou, "Synovial macrophage-osteoclast differentiation in inflammatory arthritis," *Annals of the Rheumatic Diseases*, vol. 61, no. 10, pp. 916–921, 2002.

[57] Y. Suzuki, Y. Tsutsumi, M. Nakagawa et al., "Osteoclast-like cells in an in vitro model of bone destruction by rheumatoid synovium," *Rheumatology*, vol. 40, no. 6, pp. 673–682, 2001.

[58] T. Nakashima, M. Hayashi, and H. Takayanagi, "New insights into osteoclastogenic signaling mechanisms," *Trends in Endocrinology and Metabolism*, vol. 23, no. 11, pp. 582–590, 2012.

[59] A. R. Upton, C. A. Holding, A. A. S. S. K. Dharmapatni, and D. R. Haynes, "The expression of RANKL and OPG in the various grades of osteoarthritic cartilage," *Rheumatology International*, vol. 32, no. 2, pp. 535–540, 2012.

[60] A. Bertuglia, M. Lacourt, C. Girard, G. Beauchamp, H. Richard, and S. Laverty, "Osteoclasts are recruited to the subchondral bone in naturally occurring post-traumatic equine carpal osteoarthritis and may contribute to cartilage degradation," *Osteoarthritis and Cartilage*, vol. 24, no. 3, pp. 555–566, 2016.

[61] N. Maruotti, A. Corrado, and F. P. Cantatore, "Osteoblast role in osteoarthritis pathogenesis," *Journal of Cellular Physiology*, vol. 232, no. 11, pp. 2957–2963, 2017.

[62] L. P. Pisani, D. Estadella, and D. A. Ribeiro, "The role of Toll like receptors (TLRs) in oral carcinogenesis," *Anticancer Research*, vol. 37, pp. 5389–5394, 2017.

[63] S. Rakoff-Nahoum and R. Medzhitov, "Regulation of spontaneous intestinal tumorigenesis through the adaptor protein MyD88," *Science*, vol. 317, no. 5834, pp. 124–127, 2007.

Hindawi
Evidence-Based Complementary and Alternative Medicine
Volume 2022, Article ID 8548378, 10 pages
https://doi.org/10.1155/2022/8548378

Research Article

Determination of 18 Trace Elements in 10 Batches of the Tibetan Medicine Qishiwei Zhenzhu Pills by Direct Inductively Coupled Plasma-Mass Spectrometry

Ke Fu,[1] Yinglian Song,[1] Dewei Zhang,[2] Min Xu,[1] Ruixia Wu,[1] Xueqing Xiong,[2] Xianwu Liu,[1] Lei Wu,[1] Ya Guo,[2] You Zhou,[1] Xiaoli Li,[1] and Zhang Wang[3]

[1]*College of Pharmacy, Chengdu University of Traditional Chinese Medicine, Chengdu 611137, China*
[2]*Wanzhou Institute for Drug and Food Control, Chongqing 404000, China*
[3]*College of Ethnomedicine, Chengdu University of Traditional Chinese Medicine, Chengdu 611137, China*

Correspondence should be addressed to Dewei Zhang; 23616980@qq.com and Zhang Wang; wangzhangcqcd@cdutcm.edu.cn

Received 1 December 2021; Accepted 27 December 2021; Published 13 January 2022

Academic Editor: Jie Liu

Copyright © 2022 Ke Fu et al. This is an open access article distributed under the Creative Commons Attribution License, which permits unrestricted use, distribution, and reproduction in any medium, provided the original work is properly cited.

Qishiwei Zhenzhu pills (QSW) was first recorded in the Tibetan medicine classic *Si Bu Yi Dian* and has been used to treat "Baimai" disease, stroke, paralysis, hemiplegia, cerebral hemorrhage, and other diseases till today. This prescription contains more than 70 medicines including myrobalan, pearl, agate, opal, bezoar, coral, musk, gold, silver, and a mineral mixture Zuotai. As a result, QSW contains a large amount of mercury, copper, lead, and other trace elements. The aim of this study was to determine the 18 trace elements (lithium, beryllium, scandium, vanadium, chromium, manganese, cobalt, nickel, copper, arsenic, strontium, argentum, cadmium, cesium, barium, lead, aurum, and mercury) in 10 batches of QSW produced by 5 pharmaceutical companies (Ganlu Tibetan Medicine Co., Ltd. has 6 different batches) by direct inductively coupled plasma-mass spectrometry (ICP-MS). ICP-MS is a rapid, sensitive, accurate methodology allowing the determination of 18 elements simultaneously. The results showed that each element had an excellent linear relationship in the corresponding mass concentration range. The results showed that the rank order of the elements in QSW was copper > mercury > lead from high to low, with the mass fraction higher than 6000 μg/kg; the mass fractions of argentum, arsenic, manganese, aurum, strontium, barium, chromium, and nickel were in the range of 33–1034 μg/kg; and the mass fractions of vanadium, cobalt, lithium, beryllium, cadmium, scandium, and cesium were lower than 10 μg/kg. The reproducibility from the same manufacturer (Tibet Ganlu Tibetan Medicine Co., Ltd.) was relatively high; however, the element amounts among 5 manufacturers were different, which could affect the efficacy and toxicity of QSW. All in all, ICP-MS can be used as an effective tool for the analysis of trace elements in QSW and standard quality control needs to be enforced across different manufactures.

1. Introduction

Qishiwei Zhenzhu pills (QSW), a Tibetan medicine རྩྭ་བདགས་འཛེགས།, is also known as Ranna Sangpei. It was first recorded in the great classical work of Tibetan medicine, *Si Bu Yi Dian*. QSW has the functions of tranquilizing mind, activating "meridians and collaterals", and harmonizing "Qi and blood." It is mainly used to treat "Baimai" disease and "Longxue" disorder, stroke, paralysis, hemiplegia, epilepsy, cerebral hemorrhage, and other diseases and is listed in *the 2020 edition of Pharmacopoeia of China* [1]. QSW contains more than 70 medicines including herbs, animal products, and minerals [2]. QSW is effective experimentally against vascular dementia in rats [3] and protects against lipopolysaccharide plus 1-methyl-4-phenyl-1,2,3,6-tetrahydropyridine-induced chronic neuroinflammation and dopaminergic neuron loss in mice [4]. We have demonstrated that QSW is effective against cerebral ischemia/reperfusion injury in rats [5, 6]. Furthermore, QSW can increase the ratio of Bcl-2/Bax, increase the levels of superoxide dismutase and catalase, reduce the levels of malondialdehyde, neurogenic specific olefinol enzyme and S-100β protein, alleviate lipid peroxidation injury, and

downregulate the expression of caspase-3 protein to achieve the protective effect on brain tissue [7–9]. Besides, QSW at therapeutic doses appears to be safe in acute toxicity studies in rats [10] and does not affect hepatic cytochrome P450 in mice [11].

In the preliminary work, we used high-performance liquid chromatography to simultaneously determine the six components in QSW, including gallic acid, corilagin, agarwood, ellagic acid, crocin I, and crocin II, in order to reveal the plant-based active components in QSW [12]. We have also used gas chromatography-mass spectrometry to profile the fat-soluble and volatile components in QSW and found that the fat-soluble and volatile components are the active components in QSW [5, 13]. Besides, we have recently used liquid chromatography-mass spectrometry to identify 42 chemical components in QSW, including 11 triterpenoids, 10 flavonoids, 8 organic acids and their derivatives, 4 diterpenoids, 4 tannins, 2 steroids, and 3 other components. It is worth mentioning that chlorogenic acid, ellagic acid, luteolin, cholic acid, and glycyrrhizin are detected in QSW for the first time [14]. A large number of trace elements contained in QSW, as its potential active components, are mainly derived from minerals. Therefore, in addition to botanical components, the mineral (such as pearl, agate, opal, gold, silver, and a mineral mixture Zuotai; Table 1) contained in QSW cannot be ignored. For example, Zuotai (made mainly by processing mercury) is the main ingredient of many precious Tibetan medicine preparations including QSW. Therefore, the determination of the content of mercury and other trace elements in QSW has become an urgent task at present as mercury is a concerned toxic heavy metal.

Inductively coupled plasma-mass spectrometry (ICP-MS) is an advanced technology to analyze more than 70 elements in a solution, and the linear dynamic range can reach 9 orders of magnitude [15]. It has been widely used in the analysis of trace and ultra-trace inorganic elements in medicine, food, and other industries due to its high sensitivity, simultaneous determination of multiple elements, and strong anti-interference ability [16–18]. Therefore, ICP-MS is undoubtedly a very effective method for in vitro quantitative analysis of heavy metals in QSW and traditional drugs. Besides, when QSW or traditional drugs are absorbed by the human body, a series of changes will occur, such as changes in the valence of heavy metals. ICP-MS in conjunction with other instruments for detecting element valence is its better advantage. For examples, Chen et al. established a method for the determination of soluble arsenic and its forms in realgar Chinese patent medicines by biomimetic extraction high-performance liquid chromatography (HPLC)-ICP-MS [19]. Jin et al. used HPLC-ICP-MS to determine the morphological changes of five arsenic species in *Niuhuang Jiedu* tablets, such as betaine, dimethyl arsine, trivalent arsenic, monomethyl arsine, and pentavalent arsenic, so as to make the study of heavy metal elements in *Niuhuang Jiedu* tablets more in-depth and detailed [20].

We have used ICP-MS to determine the absorption, distribution, and excretion of 18 elements in cerebral ischemia-reperfusion rats treated with QSW [21], highlighting the retention of minerals in the gut as a basis of gut-microbiota-brain axis for QSW-induced neuroprotection [5]. But it is worth noting that QSW is granted in the treatment of various diseases [1] and produced by at least 5 pharmaceuticals. Batch-to-batch variation, especially elements/minerals variations, could affect the pharmacological efficacy and toxicity potential of QSW in the treatment of diseases. Quality control in complementary and alternative medicines is needed [22, 23]. Therefore, the aim of the current study was to determine the 18 elements in 10 batches of QSW produced by 5 pharmaceuticals via ICP-MS. The research results can provide a scientific basis for the quality control and pharmacology as well as toxicology of Tibetan medicine.

Table 1: Minerals in QSW.

The type of components	Pinyin (Chinese name)	English name
Mineral and gemstone medicine	Zhenzhu	Pearl
	Jiuyanshi	Nine's eye
	Shanhu	Coral
	Songshi	Tophus
	Maoyanshi	Cat's eye
	Manao	Agate
	Qingjinshi	Lapis lazuli
	Lanbaoshi	Sapphire
Metal medicine	Jin	Gold
	Yin	Silver
	Tong	Copper
	Tie	Iron
Mixture	Zuotai	——

The above components are most likely to be the main source of trace elements in QSW.

2. Materials and Methods

2.1. Reagents and Chemicals. All solutions were prepared with deionized water provided by a water purification system (18 MΩ; Shengdeli Ultra-Pure Water System, Chongqing, China). Nitric acid (HNO_3, 65%, Suprapur) and hydrogen peroxide (H_2O_2, 50%, Suprapur) were obtained from Chongqing Chuandong Chemical Industry Group Co., Ltd. (Chongqing, China). Tuning solutions (1.0 μg/L of barium (Ba), cerium, cobalt (Co), indium (In), lithium (Li), uranium) were purchased from Thermo Fisher Scientific (USA). Internal standards stock solution (1000 μg/mL of rhodium (Rh), In, rhenium (Re), bismuth (Bi)) and gold standards stock solution (1000 μg/mL) were purchased from National Nonferrous Metals and Electronic Materials Analysis and Testing Center (Beijing, China). 1000 μg/mL of reference standard solutions for Li (GSB04-1734-2004), beryllium (Be, GSB04-1718-2004), scandium (Sc, GSB 04-1750-2004), vanadium (V, GSB04-1759-2004), chromium (Cr, GSB04-1723-2004a), manganese (Mn, GSB04-1736-2004), Co (GSB04-1722-2004), nickel (Ni, GSB04-1740-2004), copper (Cu, GSB04-1725-2004), arsenic (As, GSB04-1714-2004), strontium (Sr, GSB 04-1754-2004), argentum (Ag, GSB04-1712-2004), cadmium (Cd, GSB04-1721-2004),

cesium (Cs, GSB04-1724-2004), Ba (GSB04-1717-2004), aurum (Au, GSB04-1715-2004), mercury (Hg, GSB04-1729-2004), and lead (Pb, GSB04-1742-2004) were purchased from National Nonferrous Metals and Electronic Materials Analysis and Testing Center (Beijing, China).

QSW from 5 manufacturers in 10 batches were collected (Table 2), which were the most popular brands in the Chinese market.

2.2. Preparation of Reference Standard Solutions and Internal Standards Stock Solution. The reference standard solutions containing 18 kinds of metal elements to be measured, such as Li, Be, Sc, V, Cr, Mn, and Co, are precisely measured, and when it is used, it is diluted with 10% nitric acid into a mixed reference standard solution of various element series mass concentration: Li, Be, Sc, V, Co, Cd, Cs (0, 0.5, 2.0, 10, 25, 50 μg/L); Cr, Mn, Ni, Cu, As, Sr, Ag, Ba, Au, Pb (0, 0.5, 2.0, 10, 25, 50 mg/L); Hg (0, 20, 50, 100, 150, 200 μg/L). The reference standard solution of mercury is separately configured, and the other 17 elements are configured as a mixed reference standard solution. All reference standard solutions are in a constant volume of 50 ml.

The internal standards stock solution containing Rh, Re, In, and Bi was diluted with 10% nitric acid to form a mixed internal standards stock solution with a concentration of 10 μg/mL, which was used to correct the interference caused by the matrix effect and ensure the accuracy of the determination results.

2.3. Preparation of Gold Standards Stock Solution. A suitable amount of gold standards stock solution is diluted with 10% nitric acid to 10 μg/mL and stored in a refrigerator. (When Hg is added, it is easy to produce the memory effect and adsorption effect, which affect the accuracy of the determination results. Hence, 20 μL of gold standard solution was added to stabilize.)

2.4. Sample Preparation. QSW samples were digested by the microwave digestion system (Matching PTFE Tank, Milestone ETHOS A; Shenzhen Huashengda Instrument Equipment Co., Ltd., Shenzhen, China). 10 batches of QSW were wrapped and crushed with filter paper (no grinding with mortar to prevent the introduction of heavy metals); then 0.0500 g of the above-mentioned tablets powder was accurately weighed in a microwave digestion tube, into which 10 mL of Suprapur® concentrated nitric acid (65%) solution and 0.2 mL of hydrogen peroxide solution (50%) were added; after gently shaking, tighten the cover of the digestion tube, place the digestion tube evenly on the turntable in the microwave oven, close the door of the oven, and input the microwave heating program (Table 3). The digestion time is 60 minutes. After digestion, the volume was adjusted to 50 mL with ultra-pure water, Hg is easy to be adsorbed, and then 0.1 mL of the mixture was added into a 50 mL volumetric bottle with gold standard solution to stabilize.

2.5. Operating Conditions of ICP-MS. Multielement detection was carried out using an ICP-MS system (ICAP-Q Series; Thermo Fisher Scientific, USA). The parameters of ICP-MS system are shown in Table 4.

2.6. Linearity and Limit of Quantitation (LOQ). The multielement mixed standard solution under "Section 2.2" was injected into the instrument at the same time with the internal standard solution and determined in turn; the average measured values of the three readings of each mass concentration are ordinate (Y), and the corresponding mass concentration of the standard solution of the corresponding elements is abscissa (X). In addition, the blank solution was prepared and determined for 11 consecutive times, and the LOQ of different trace elements were determined by dividing the standard deviation of the response value by the slope of the standard curve of the corresponding elements.

2.7. Precision and Repeatability. The contents of 18 trace elements Li, Be, Sc, V, Cr, Mn, Co, Ni, Cu, As, Sr, Ag, Cd, Cs, Ba, Pb, Au, and Hg were determined for 6 consecutive injections, and the response values of each element were calculated. Besides, QSW (batch number 17156A) was selected as the sample to prepare six sample solutions in parallel, and the response values of each element were calculated.

2.8. Accuracy. QSW (batch number 17156A) was selected as the samples for investigation; about 0.0250 g sample was precisely weighed, precision addition of appropriate standard element solution (about 100% level of known content). According to the preparation method of sample solution under "Section 2.4" and ICP-MS working parameters under "Section 2.5", the recovery rate of 18 elements was calculated.

2.9. Statistical Analysis. The experimental data were processed by SPSS 21.0 software, and the measurement data were expressed as mean ± SD.

3. Results

3.1. Linearity and Limit of Quantitation (LOQ). The standard curve was drawn, linear regression was carried out, and the regression equations of 18 trace elements were obtained. In addition, the LOQ of the 18 trace elements all met the analysis requirements (Table 5).

3.2. Precision and Repeatability. The precision of 18 elements was good, which can meet the requirements of analysis. Besides, %RSD values of the 18 elements were less than 5%, indicating good repeatability (Table 5).

3.3. Accuracy. The recovery rate of 18 elements was calculated (Table 5). The average recovery of 18 elements was 95.10%–111.13% (%RSD was 2.13%–4.24%).

Table 2: Production enterprise, batch number, and approval number of QSW.

No.	Manufacturing enterprise	Batch number	Approval number
1	Ganlu Tibetan Medicine Co., Ltd.	17156A	SFDA approval number: Z54020062
2		18055A	
3		17027A	
4		17001A	
5		17102A	
6		17103A	
7	Jinhe Tibetan Medicine Co., Ltd.	20171115	SFDA approval number: Z63020062
8	Sichuan Aba Tibetan Medical Hospital	1703013	Z20060418
9	Sichuan Ganzi Tibetan Medical Hospital	17070501	Z20060302
10	Sichuan Baiyu Tibetan Medical Research Institute	20181012	Z20061067

Table 3: Microwave digestion steps.

No.	Steps
Step 1	Temperature rises to 120°C within 15 min and maintains for 5 min at 1600 W power.
Step 2	Temperature rises to 150°C within 7 min and maintains for 7 min at 1600 W power.
Step 3	Temperature rises to 190°C within 7 min and maintains for 15 min at 1600 W power.

Table 4: ICP-MS parameters.

ICP-MS system	Working parameters
RF power	1.3 kW
Carrier gas velocity	1.14 L/min
Sampling depth	6.8 mm
Auxiliary gas flow rate	0.9 L/min
Residence time per point	20 ms
Vertical position of rectangular tube	1.8 mm
Horizontal position of rectangular tube	0.6 mm
Atomizer	Babington
Atomization chamber flow rate	0.98 L/min
Atomization chamber pressure	2.85×10^5 Pa

3.4. Results of 18 Trace Elements in 10 Batches of QSW. The contents of 18 trace elements in 10 batches of QSW are shown in Table 6 and Figure 1. The heat map of the determination results of trace elements in 10 batches of QSW is shown in Figure 2. Overall, the average element contents of 10 batches of QSW were in the order of Cu > Hg > Pb from high to low, with the mass fraction higher than 6000 μg/kg; the mass fractions of Ag, As, Mn, Au Sr, Ba, Cr, and Ni were in the range of 33–1034 μg/kg; and the mass fractions of V, Co, Li, Be, Cd, Sc, and Cs were lower than 10 μg/kg.

3.5. Visual Analysis. According to the test results of trace elements, 18 trace elements were screened out and mass distribution curves were made according to their atomic number. In order to facilitate comparison, some trace elements with great difference in quantity are enlarged or reduced to the same order of magnitude at the same time of measurement (expansion 10 times: Li, Be, V, Co; expansion 100 times: Sc, Cd, Cs; reduction 10 times: As, Sr; reduction 100 times: Mn, Ag, Au; reduction 1000 times: Cu, Hg, Pb). QSW samples from Ganlu Pharmaceuticals have similar peak shapes. Among them, only the contents of V and Ba in batch 18055A were slightly different from other batches (Figure 3). However, different manufacturers have different peak shapes, with QSW from Baiyu had higher Sc, V, Cr, As, Cd, and Ba and QSW from Aba had As and Ba. Besides, the contents of trace elements in QSW produced by Jinhe and Ganzi were similar to that produced by Ganlu (Figure 4). The results imply that the contents of trace elements in QSW could be different from different manufacturers.

4. Discussion and Conclusion

In this article, we have established a sensitive, fast, and efficient ICP-MS method for the determination of trace elements in QSW. The contents of 18 trace elements (Li, Be, Sc, V, Cr, Mn, Co, Ni, Cu, As, Sr, Ag, Cd, Cs, Ba, Pb, Au, Hg) in 10 batches of QSW from 5 pharmaceuticals were determined, and batch-to-batch variations were revealed. The results point to the importance of quality control in the production of QSW and provide an element reference for the quality control of QSW, a famous Tibetan medicine listed in *the 2020 edition of Pharmacopoeia of China* [1].

Traditional Tibetan medicine preparations have added minerals and heavy metal elements as active components. Many valuable Tibetan medicines contain Zuotai as the main ingredient. For example, QSW, *Ershiwuwei Zhenzhu Pills, Renqing Changjue* pills, and *Renqing Mangjue* pills all contain Zuotai and have been included in the Chinese Pharmacopoeia [1]. Zuotai is mainly made of mercury [24]. Its main components are beta-HgS and sulfur [25], and it is insoluble in acid [26]. It is not used alone but as an addition to Tibetan medicine formulae in clinic to increase the curative effect, reduce side effects, invigorate the "spleen," and nourish and strengthen the body [27]. The results of this study show that the average content of Hg in QSW of various manufacturers is extremely high, among which the highest can reach 15940 μg/kg, with the average amount of 7598 μg/kg, the 2nd highest element in QSW. Mercury is a toxic heavy metal of public safety concern, but mercury sulfides are

Table 5: Linearity, LOQ, repeatability, precision, and recovery values for the elements.

Elements	Linear equation	R^2	BEC ($ng \cdot mL^{-1}$)	Linear range ($\mu g \cdot L^{-1}$)	LOQ ($ng \cdot mL^{-1}$)	Repeatability (%)	Precision (%)	Average recovery	Recovery (%)
Li	$Y = 183.452X + 30.010$	0.9997	0.164	0~50	0.0111	3.24	3.92	95.97	3.77
Be	$Y = 120.419X + 1.646$	0.9997	0.014	0~50	0.0710	3.45	4.40	100.82	4.24
Sc	$Y = 3568.724X + 38.237$	0.9999	0.011	0~50	0.0058	3.64	2.03	105.03	2.57
V	$Y = 11335.341X + 785.694$	0.9999	0.069	0~50	0.0186	1.43	2.72	102.21	4.17
Cr	$Y = 18508.555X + 9806.206$	0.9998	0.530	0~50000	0.0445	4.33	1.56	99.50	3.40
Mn	$Y = 8186.298X + 5839.477$	0.9999	0.713	0~50000	0.0631	4.44	1.26	99.60	3.60
Co	$Y = 33478.709X + 423.562$	0.9998	0.013	0~50	0.0030	4.05	2.35	96.56	3.81
Ni	$Y = 8849.339X + 2884.817$	0.9999	0.326	0~50000	0.0611	1.66	2.52	104.69	2.13
Cu	$Y = 23141.640X + 27031.196$	0.9992	1.168	0~50000	0.0769	4.32	1.39	99.31	3.73
As	$Y = 1441.687X + 193.154$	0.9999	0.134	0~50000	0.0709	1.97	1.54	106.64	3.03
Sr	$Y = 10750.883X + 18797.632$	0.9990	1.748	0~50000	0.0825	4.19	2.52	111.09	2.95
Ag	$Y = 56823.927X + 172271.407$	0.9882	3.032	0~50000	0.2512	1.60	1.68	111.13	3.58
Cd	$Y = 8600.838X + 114.995$	0.9998	0.013	0~50	0.0108	3.65	3.27	98.93	4.31
Cs	$Y = 42739.545X + 791.782$	0.9995	0.019	0~50	0.0026	3.09	2.58	97.47	3.92
Ba	$Y = 8843.577X + 38308.402$	0.9993	4.332	0~50000	0.1084	4.10	2.03	95.10	3.43
Au	$Y = 66686.274X + 38970.881$	0.9999	0.584	0~50000	0.0517	4.31	3.82	99.96	3.22
Hg	$Y = 20700.587X + 1037.767$	0.9989	0.050	0~200	0.0101	2.72	1.95	101.97	3.86
Pb	$Y = 169100.063X + 223195.948$	0.9996	1.320	0~50000	0.1003	4.33	4.18	96.45	3.39

The elements are arranged in the order of their molecular weight.

Table 6: Results of 18 trace elements in 10 batches of QSW ($\mu g \cdot kg^{-1}$).

Elements	Content ($\mu g \cdot kg^{-1}$)										
	Ganlu						Jinhe	Aba	Ganzi	Baiyu	Mean ± SD
	17156A	18055A	17027A	17001A	17102A	17103A	20171115	1703013	17070501	20181012	
Li	3.472	2.635	2.633	1.603	2.431	2.893	5.067	3.210	2.633	3.613	3.019 ± 0.919
Be	1.472	1.715	1.627	0.9080	1.118	1.504	——	——	0.07500	0.2260	0.8650 ± 0.7210
Sc	0.8980	0.8280	0.7690	0.5140	0.7070	0.7110	0.3920	0.3230	0.6340	1.680	0.7460 ± 0.3770
V	8.566	17.26	6.766	4.742	6.819	7.025	7.748	2.665	6.751	15.92	8.426 ± 4.613
Cr	109.7	47.45	49.89	34.39	67.48	78.20	68.33	23.55	17.64	401.65	89.83 ± 112.9
Mn	1512	1267	737.4	571.4	1174	1293	227.5	141.4	214.1	629.1	776.7 ± 504.7
Co	6.367	4.573	6.857	3.326	5.044	4.941	1.771	7.249	5.622	5.733	5.148 ± 1.650
Ni	48.87	28.30	22.77	18.18	35.49	35.64	32.55	17.31	10.60	80.26	33.00 ± 19.98
Cu	12160	10506	9875	8162	10119	10240	1807	12897	6396	19436	10160 ± 4541
As	417.3	342.4	1163	945.7	770.6	601.9	573.9	1460	773.9	1305	835.4 ± 377.0
Sr	287.3	255.6	235.3	183.7	231.6	242.6	219.7	201.5	131.8	188.1	217.7 ± 43.57
Ag	1293	1169	944.1	810.2	955.0	1025	647.3	960.4	480.0	2062	1034 ± 430.6
Cd	0.2610	0.3060	0.1660	0.2100	0.2110	0.2470	0.2090	0.3360	0.4590	1.595	0.4000 ± 0.4280
Cs	0.5050	0.4310	0.3680	0.3150	0.3980	0.3870	0.4660	0.7810	0.3450	0.4290	0.4430 ± 0.1320
Ba	57.96	279.2	42.44	36.19	48.28	53.62	62.67	383.4	41.55	331.8	133.7 ± 138.9
Pb	11690	10976	7595	6416	8875	10184	727.2	1767	1571	8341	6814 ± 4080
Au	1252	1209	496.8	768.3	899.2	1099	174.8	163.3	155.0	155.0	637.3 ± 462.7
Hg	6118	5601	6267	4397	5682	5200	12024	7944	15937	4811	7398 ± 3715

The data are means of 3 determinations. The symbol "——" means undetected or below the limit of detection.

frequently included in Indian Ayurvedic medicine [28], Tibetan medicines [29], and Chinese medicines [30]. The chemical form of Hg (HgS vs $HgCl_2$) makes a big difference. Another important factor is "dose differentiates a poison from a remedy." The amount of Hg contained in QSW varies 3.6-fold (4397–15940 μg/kg) from batch to batch; a low amount of HgS could compromise it therapeutic effects, but a high amount of Hg could increase its risk. Thus, quality control in evaluating different batch products of QSW for Hg content is important.

Another toxic heavy metal of concern is lead (Pb). Pb-based traditional herbometallic preparations are also widely used in Ayurveda [31], Tibetan medicines, and Chinese medicines [29], but with increasing public alert [32, 33]. Although the chemical forms of Pb used in traditional medicines (PbS, PbO) are different from environmental Pb compounds (lead acetate, etc.) [29], the amount of lead contained in traditional medicines still alarms the public. For example, overdose of *Mahayograj Guggulu* is the most common cause responsible for Pb intoxication cases from

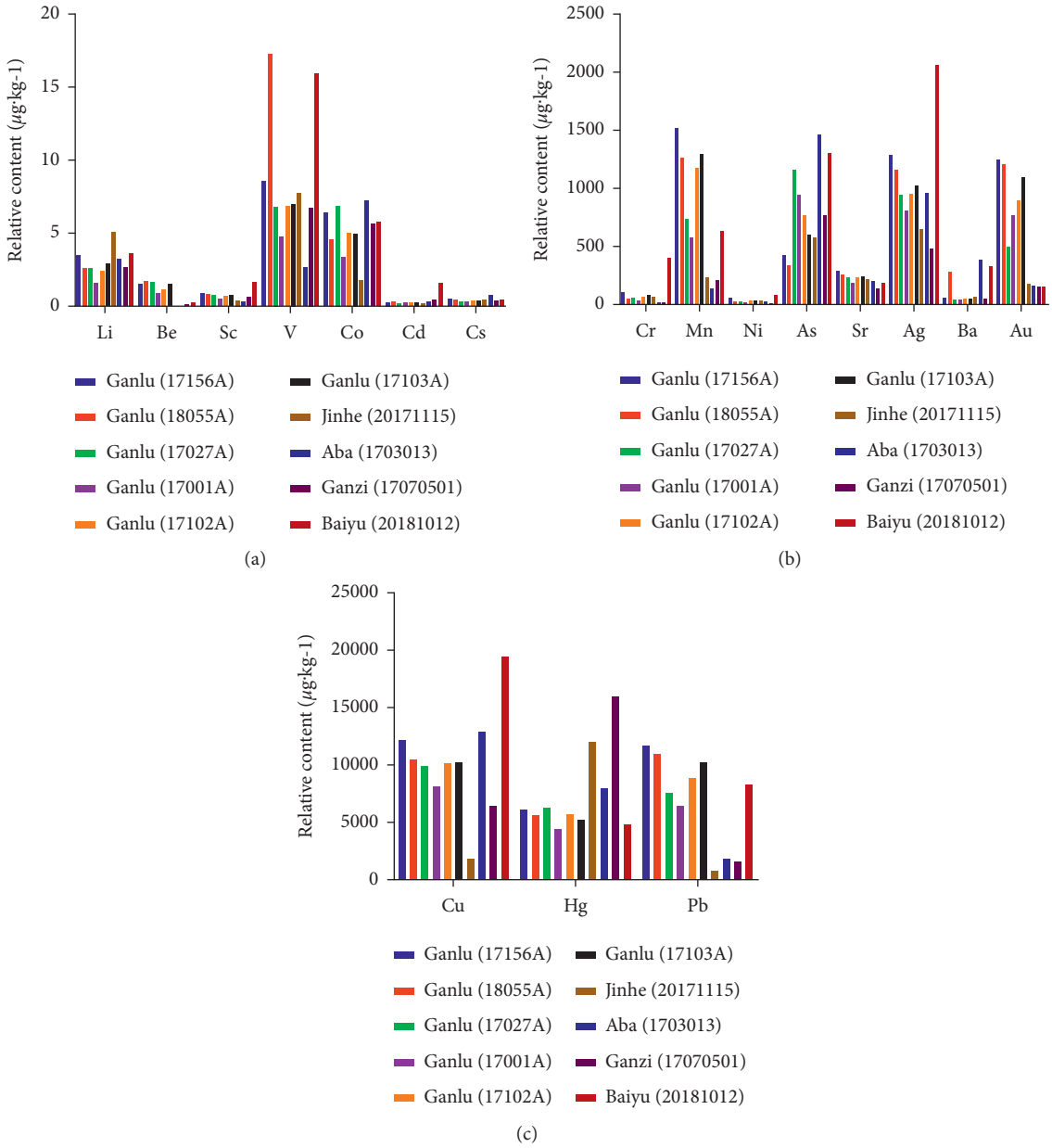

Figure 1: The content of 18 elements in 10 batches of QSW.

traditional Indian medicines [32]. The amount of Pb contained in QSW varies 16-fold (727–11690 μg/kg); a low amount of PbS may reduce efficacy of QSW, but a high amount of Pb definitely represents a risk to human health [34]. Considering 16-fold variations in Pb content in QSW, the quality control of QSW for Pb content is very important.

Copper (Cu) is an essential element for human body; however, excess Cu is also toxic [35]. In the Tibetan medicine "*Renqing Changjue*", changes in element concentrations, including Cu, in biofluids and tissues were examined, and the precautions with long-term administration are pointed out [36]. The amount of Cu was the highest among 18 elements in QSW and varied 10-fold (1807–19430 μg/kg), similar to the copper content variation (10-fold) in other traditional medicines [37]. A low amount of CuS could compromise its therapeutic effects, but a high amount of Cu could be toxic, especially for long-term administration. Thus, quality control in products of QSW for Cu content is also important.

Manganese (Mn) is an essential metal that is required as a cofactor for many enzymes and is necessary for optimal biological function; however, Mn overexposure is associated with neurotoxicity [38]. Many Tibetan medicines contain Mn and other trace elements to exert anti-anoxic effects [39]; on the other hand, inappropriate overexposure to Mn from traditional medicine practice caused neurotoxicity [40, 41]. The amount of Mn in QSW ranged from 141 to 1512 μg/kg, with a 10-fold variation in different batches of QSW. Insufficient Mn may reduce QSW therapeutic effects, but a high amount of Mn could be toxic, especially to the brain

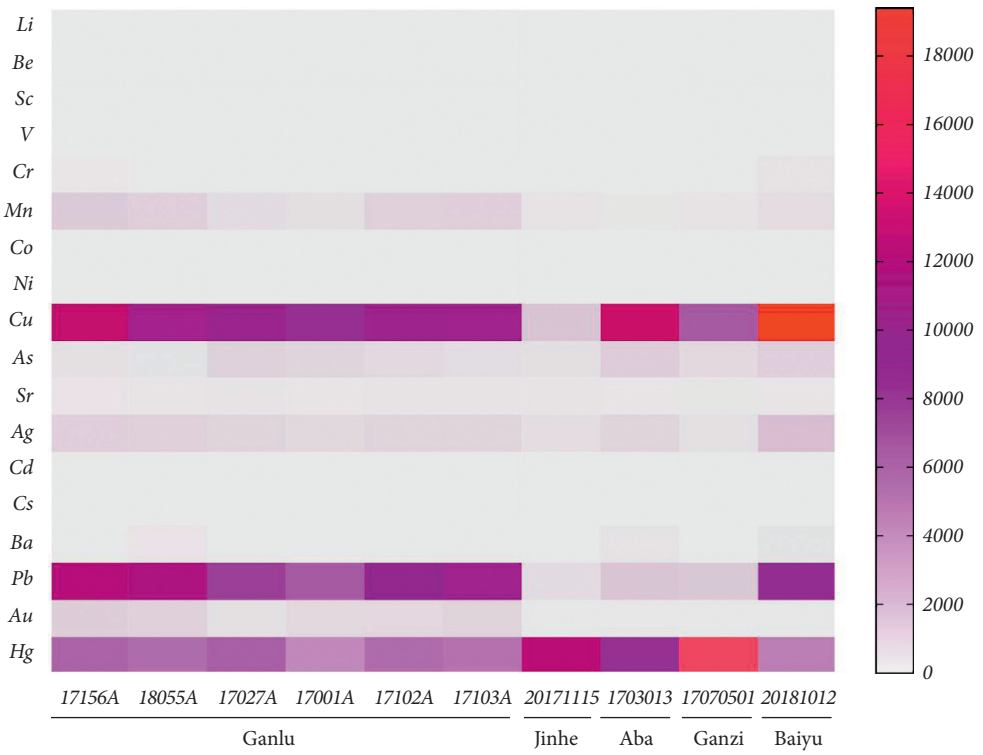

Figure 2: The heat map of determination results of trace elements in 10 batches of QSW. (Note: the redder the color, the higher the content; the grayer the color, the lower the content. For example, the figure shows that the content of Hg in Ganzi (17070501) and Cu in Baiyu (20181012) is very high.)

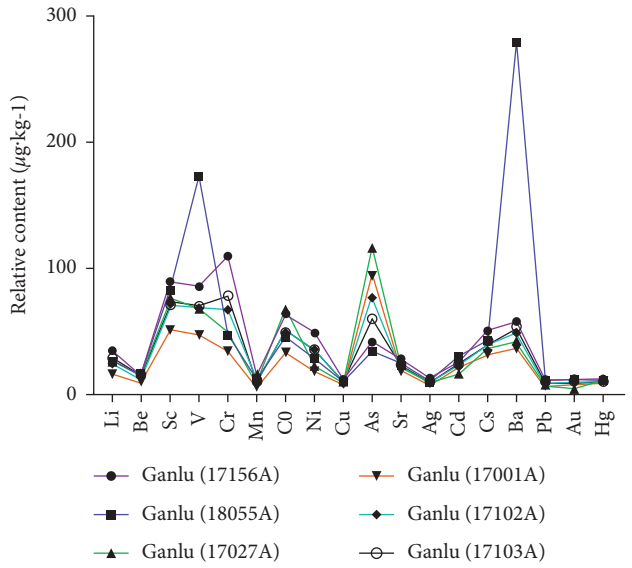

Figure 3: Intuitive analysis of the determination of trace elements in the samples of QSW. (The same manufacturers have similar peak shapes. Among them, only the contents of V and Ba in batch 18055A are slightly different from other batches.) Expansion 10 times: Li, Be, V Co. Expansion 100 times: Sc, Cd, Cs. Reduction 10 times: As, Sr. Reduction 100 times: Mn, Ag, Au. Reduction 1000 times: Cu, Hg, Pb.

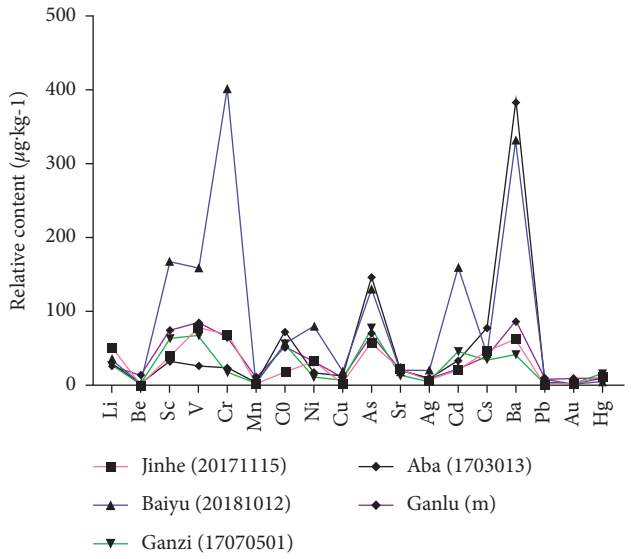

Figure 4: Intuitive analysis of the determination of trace elements in samples of QSW. (The peak shapes of different manufacturers are different, indicating that the content of trace elements in QSW of different manufacturers is quite different.) Ganlu (m) represents the average value of Ganlu's 6 batches of QSW. Expansion 10 times: Li, Be, V Co. Expansion 100 times: Sc, Cd, Cs. Reduction 10 times: As, Sr. Reduction 100 times: Mn, Ag, Au. Reduction 1000 times: Cu, Hg, Pb.

[38]. Thus, quality control of QSW for Mn content is important.

The rank orders of the 18 elements contained in QSW (mean values in μg/kg) were Cu (10160), Hg (7398), Pb (6814), followed by Ag (1034), As (835), Mn (776), Au (637), Sr (217), Ba (133), Cr (90), and Ni (33). The elements with trace amounts were V (8.426), Co (5.148), Li (3.019), Be (0.856), Sc (0.746), Cs (0.443), and Cd (0.400). Due to different manufacturers of QSW, some of the trace elements fluctuate greatly. In addition to the above discussed major metals with toxicological significance (Hg, Pb, Cu, and Mn), batch-to-batch variations of other elements with appreciable amounts were Ag (2.7-fold), As (3.9-fold), Au (8.1-fold), Ba (6.7-fold), Sr (2.2-fold), Cr (12-fold), and Ni (5-fold). Arsenic is a major metalloid of toxicological significance affecting human health and can be derived from traditional medicines [30, 42], and its content from Aba (1461 μg/kg) was 4 times higher than that from Ganlu 18055A (342 μg/kg). Even for elements with trace amount, such variations could not be ignored. For example, Cd is an accumulative, highly toxic heavy metal, which can also be derived from traditional medicines [33]. In QSW, it had a smallest content but varied 9.6-fold across batches, and Cd from Baiyu (1.595 μg/kg) was 4–10 times higher than that from other batches; such variations should not be ignored. Thus, the contents of these elements in QSW and their batch-to-batch variations could influence their biological functions and also affect their toxicity.

It should be noted that the 6 batches of QSW from Ganlu Tibetan Pharmaceuticals were relatively stable with less batch-to-batch variations compared with other 4 batches from Jinhe, Aba, Ganzi, and Baiyu pharmaceuticals. For example, Cu contents from 6 Ganlu batches ranged from 8616 to 12155 μg/kg, only a 1.4-fold variation, but Cu from Baiyu (19440 μg/kg) was 11.7-fold higher than that of Jinhe (1807 μg/kg); Hg contents from 6 Ganlu batches ranged from 4398 to 6267 μg/kg, only a 1.4-fold variation, but Hg from Ganzi (15734 μg/kg) was 2.8 times higher than that from Ganlu (5545 μg/kg). Pb from 6 Ganlu batches ranged from 6416 to 11690 μg/kg, only a 1.8-fold variation, but Pb from Jinhe (727 μg/kg) was 12.8 times lower than that from Ganlu (9289 μg/kg). Mn from 6 Ganlu batches ranged from 571 to 1512 μg/kg, with 2.6-fold variation, but Mn from Aba (141 μg/kg) was 7.7 times lower than that from Ganlu (1092 μg/kg). Thus, to enforce the same quality control among different pharmaceuticals are necessary.

In conclusion, the present study used ICP-MS to simultaneously determine 18 elements in QSW from 10 batches and analyzed batch-to-batch variations from 5 pharmaceuticals, and the biological and toxicological significance of such batch-to-batch variations were discussed, highlighting the importance for quality control of producing traditional medicines such as QSW.

Data Availability

The data supporting the conclusions are included in the manuscript. The data sets used and/or analyzed during the current study are available from the corresponding author on reasonable request.

Conflicts of Interest

The authors declare that there are no conflicts of interest regarding the publication of this paper.

Authors' Contributions

Ke Fu, Yinglian Song, and Deiwei Zhang are responsible for assisting in the experiment and participating in the writing of articles; Min Xu, Ruixia Wu, Xueqing Xiong, Xianwu Liu, Lei Wu, Ya Guo, You Zhou, and Xiaoli Li are responsible for assisting in the experiment; and Deiwei Zhang and Zhang Wang function as corresponding authors. Ke Fu and Yinglian Song contributed equally to this work.

Acknowledgments

The authors thank the Chengdu University of Traditional Chinese Medicine and the Wanzhou Institute for Drug and Food Control for providing us with a research platform. This study was supported by China Postdoctoral Science Foundation (2012M511916); the Project of Sichuan Provincial Administration of Traditional Chinese Medicine (2012-E-040); and the Science and Technology Development Fund of Chengdu University of Traditional Chinese Medicine (ZRQN1544).

References

[1] Chinese Pharmacopoeia Commission, *Pharmacopoeia of the People's republic of China*China Medical Science and Technology Press, Beijing, China, 2020.

[2] E. J. An and Y. R. Suo, "Advances in modern pharmacology of QSW of Tibetan medicine," *Journal of Medicine&Pharmacy of Chinese Minorities*, vol. 10, no. 2, pp. 33–35, 2004.

[3] P. Wu, Y. Luo, L. Zhen et al., "Rannasangpei is a therapeutic agent in the treatment of vascular dementia," *Evidence-based Complementary and Alternative Medicine: eCAM*, vol. 2016, Article ID 2530105, 23 pages, 2016.

[4] A.-L. Hu, S. Song, Y. Li et al., "Mercury sulfide-containing Hua-Feng-Dan and 70W (Rannasangpei) protect against LPS plus MPTP-induced neurotoxicity and disturbance of gut microbiota in mice," *Journal of Ethnopharmacology*, vol. 254, Article ID 112674, 2020.

[5] M. Xu, R. Wu, Y. Liang et al., "Protective effect and mechanism of Qishiwei Zhenzhu pills on cerebral ischemia-reperfusion injury via blood-brain barrier and metabonomics," *Biomedicine & Pharmacotherapy*, vol. 131, Article ID 110723, 2020.

[6] K. Fu, D. Zhang, Y. Song et al., "Tibetan medicine Qishiwei Zhenzhu pills can reduce cerebral ischemia-reperfusion injury by regulating gut microbiota and inhibiting inflammation," *Evidence-based Complementary and Alternative Medicine: eCAM*, vol. 2021, Article ID 2251679, 13 pages, 2021.

[7] M. Zhu, X. Liu, H. Rong et al., "Anti-apoptotic effect of Qishiwei Zhenzhu pills on cerebral ischemia-reperfusion injury in rats," *Tianjin Medical Journal*, vol. 43, no. 2, pp. 150–153, 2015.

[8] L. Zeng, Y. Luo, F. Huang et al., "Effects of Qishiwei Zhenzhu pills on SOD, CAT and MDA in the brain tissue of rats with focal cerebral ischemia," *World Chinese Medicine*, vol. 9, no. 3, pp. 347–349+354, 2014.

[9] L. Zeng, Y. Luo, F. Huang et al., "Neuroprotective effect of Qishiwei Zhenzhu pills on focal cerebral ischemia rats," *Pharmacology and Clinics of Chinese Materia Medica*, vol. 30, no. 1, pp. 90–92, 2014.

[10] W. L. Xu, W. J. Sun, Z. Wang, G. L. Liu, Y. M. Xu, and Y. Liang, "Experimental study on acute toxicity of Tibetan medicine Qishiwei Zhenzhu pill in rats," *China Medical Herald*, vol. 13, no. 35, pp. 4–7, 2020.

[11] Y. Nie, S.-F. Xu, Y.-L. Lu et al., "Zuotai (β-HgS)-containing 70 Wei Zhen-Zhu-Wan differs from mercury chloride and methylmercury on hepatic cytochrome P450 in mice," *F1000Research*, vol. 10, p. 203, 2021.

[12] W. Xu, Y. Liang, Z. Wang, G. Liu, and W. Sun, "Simultaneous determination of six components in QSW by HPLC Chinese," *Traditional Patent Medicine*, vol. 39, no. 10, pp. 2072–2076, 2017.

[13] K. Fu, Y. Liang, M. Xu et al., "Analysis of volatile oil and fat-soluble components in QSW by GC-MS," *Chinese Traditional Patent Medicine*, vol. 41, no. 12, pp. 3006–3012, 2019.

[14] M. Xu, *Qualitative and Quantitative Analysis of Chemical Components in Qishiwei Zhenzhu Pills and its Mechanism of Effect Based on LC-MS and Network Pharmacology*Chengdu University of Traditional Chinese Medicine, Chengdu, China, 2021.

[15] J. W. Olesik, "Inductively coupled plasma mass spectrometers," *Treatise on Geochemistry*, vol. 15, pp. 309–336, 2014.

[16] D. Beauchemin, "Environmental analysis by inductively coupled plasma mass spectrometry," *Mass Spectrometry Reviews*, vol. 29, no. 4, pp. 560–592, 2010.

[17] B.-H. Chen, S.-J. Jiang, and A. C. Sahayam, "Determination of Cr(VI) in rice using ion chromatography inductively coupled plasma mass spectrometry," *Food Chemistry*, vol. 324, Article ID 126698, 2020.

[18] J. Huang, X. Hu, J. Zhang, K. Li, Y. Yan, and X. Xu, "The application of inductively coupled plasma mass spectrometry in pharmaceutical and biomedical analysis," *Journal of Pharmaceutical and Biomedical Analysis*, vol. 40, no. 2, pp. 227–234, 2006.

[19] Q. S. Chen, Y. Cheng, and Z. F. Meng, "Bionic extraction-HPLC-ICP-MS determination of soluble arsenic in Chinese traditional patent medicine containing realgar," *Chinese Journal of Pharmaceutical Analysis*, vol. 485, pp. 323–332, 2018.

[20] P. Jin, X. Liang, L. Xia et al., "Determination of 20 trace elements and arsenic species for a realgar-containing traditional Chinese medicine Niuhuang Jiedu tablets by direct inductively coupled plasma-mass spectrometry and high performance liquid chromatography-inductively coupled plasma-mass spectrometry," *Journal of Trace Elements in Medicine and Biology*, vol. 33, pp. 73–80, 2016.

[21] Y. L. Song, K. Fu, D. W. Zhang et al., "The absorption, distribution, and excretion of 18 elements of Tibetan medicine Qishiwei Zhenzhu pills in rats with cerebral ischemia," *Evidence-based Complementary and Alternative Medicine*, vol. 2021, Article ID 4508533, 11 pages, 2021.

[22] Y. Zheng, C. Fan, M. Liu et al., "Overall quality control of the chemical and bioactive consistency of ShengMai Formula," *Journal of Pharmaceutical and Biomedical Analysis*, vol. 189, Article ID 113411, 2020.

[23] R. Rosecrans and J. C. Dohnal, "The effect of complimentary and alternative medicine products on laboratory testing," *Seminars in Diagnostic Pathology*, vol. 26, no. 1, pp. 38–48, 2009.

[24] C. Duojie and X. Niu, "Master of traditional Chinese medicine NiMa and Tibetan medicine "zuo tai" processing," *Journal of Medicine&Pharmacy of Chinese Minorities*, vol. 24, no. 11, pp. 31-32, 2018.

[25] C. Li, D. Zhan, C. Lengben et al., "Analysis of chemical composition, mercury coordination structure and microstructure of Tibetan medicine Zuotai," *Spectroscopy and Spectral Analysis*, vol. 35, no. 4, pp. 1072–1078, 2015.

[26] W. Haynes, R. David, and J. Thomas, *CRC Handbook of Chemistry and Physics*, pp. 201-202, CRC Press, Boca Raton, FL, USA, 2014.

[27] B. Yang, J. Jiang, Y. Jiang et al., "Study on the functional characteristics and safety of mercury in Tibetan medicine," *Zuotai*, vol. 1, pp. 74–80, 2004.

[28] S. U. Kamath, B. Pemiah, R. K. Sekar, S. Krishnaswamy, S. Sethuraman, and U. M. Krishnan, "Mercury-based traditional herbo-metallic preparations: a toxicological perspective," *Archives of Toxicology*, vol. 86, no. 6, pp. 831–838, 2012.

[29] J. Liu, F. Zhang, V. Ravikanth, O. A. Olajide, C. Li, and L. X. Wei, "Chemical compositions of metals in bhasmas and Tibetan Zuotai are a major determinant of their therapeutic effects and toxicity," *Evidence-based Complementary and Alternative Medicine: eCAM*, vol. 2019, Article ID 1697804, 23 pages, 2019.

[30] J. Liu, L.-X. Wei, Q. Wang et al., "A review of cinnabar (HgS) and/or realgar (As 4 S 4)-containing traditional medicines," *Journal of Ethnopharmacology*, vol. 210, pp. 340–350, 2018.

[31] S. Nagarajan, K. Sivaji, S. Krishnaswamy et al., "Safety and toxicity issues associated with lead-based traditional herbo-metallic preparations," *Journal of Ethnopharmacology*, vol. 151, no. 1, pp. 1–11, 2014.

[32] I. Koch, M. Moriarty, K. House et al., "Bioaccessibility of lead and arsenic in traditional Indian medicines," *The Science of the Total Environment*, vol. 409, no. 21, pp. 4545–4552, 2011.

[33] S. Bolan, A. Kunhikrishnan, B. Seshadri et al., "Sources, distribution, bioavailability, toxicity, and risk assessment of heavy metal(loid)s in complementary medicines," *Environment International*, vol. 108, pp. 103–118, 2017.

[34] J. L. Thompson, H. V. Schaff, J. A. Dearani et al., "Risk of recurrent gastrointestinal bleeding after aortic valve replacement in patients with Heyde syndrome," *The Journal of Thoracic and Cardiovascular Surgery*, vol. 144, no. 1, pp. 112–116, 2012.

[35] A. Alhusaini, I. H. Hasan, N. Aldowsari, and N. Alsaadan, "Prophylactic administration of nanocurcumin abates the incidence of liver toxicity induced by an overdose of copper sulfate: role of CYP4502E1, NF-κB and bax expressions," *Dose-response: A Publication of International Hormesis Society*, vol. 16, no. 4, Article ID 1559325818816284, 2018.

[36] L. Zhang, C. Rezeng, Y. Wang, and Z. Li, "Changes in copper, zinc, arsenic, mercury, and lead concentrations in rat biofluids and tissues induced by the "renqing Changjue" pill, a traditional Tibetan medicine," *Biological Trace Element Research*, vol. 199, no. 12, pp. 4646–4656, 2021.

[37] E. T. Gyamfi, "Assessment of essential and non-essential elements in selected traditional medicines from India, Ghana and China," *Environmental Science and Pollution Research*, vol. 28, no. 2, pp. 1812–1822, 2021.

[38] M. R. Miah, O. M. Ijomone, C. O. A. Okoh et al., "The effects of manganese overexposure on brain health," *Neurochemistry International*, vol. 135, Article ID 104688, 2020.

[39] Q. X. Wu, L. Ji, J. L. Ku, and P. Song, "Analysis of trace elements and macro elements in 13 anti-anoxic traditional

Tibetan medicine," *Guang Pu Xue Yu Guang Pu Fen Xi*, vol. 28, no. 8, pp. 1938–1941, 2008.

[40] R. A. Street, G. M. Kabera, and C. Connolly, "Ethnopharmacological use of potassium permanganate in South African traditional medicine," *South African Medical Journal*, vol. 108, no. 3, pp. 187–189, 2018.

[41] E. Roos, S. K. T. S. Wärmländer, J. Meyer et al., "Amyotrophic lateral sclerosis after exposure to manganese from traditional medicine procedures in Kenya," *Biological Trace Element Research*, vol. 199, no. 10, pp. 3618–3624, 2021.

[42] R. Liu, X. Li, N. Huang, M. Fan, and R. Sun, "Toxicity of traditional Chinese medicine herbal and mineral products," *Pharmacological Advances in Natural Product Drug Discovery*, vol. 87, pp. 301–346, 2020.

Hindawi
Evidence-Based Complementary and Alternative Medicine
Volume 2021, Article ID 4508533, 11 pages
https://doi.org/10.1155/2021/4508533

Research Article

The Absorption, Distribution, and Excretion of 18 Elements of Tibetan Medicine Qishiwei Zhenzhu Pills in Rats with Cerebral Ischemia

Yinglian Song,[1] Ke Fu,[1] Dewei Zhang,[2] Min Xu,[1] Ruixia Wu,[1] Xueqing Xiong,[2] Xianwu Liu,[1] Lei Wu,[1] Ya Guo,[2] You Zhou,[1] Xiaoli Li,[1] and Zhang Wang[3]

[1]*College of Pharmacy, Chengdu University of Traditional Chinese Medicine, Chengdu 611137, China*
[2]*Wanzhou Institute for Drug and Food Control, Chongqing 404000, China*
[3]*College of Ethnomedicine, Chengdu University of Traditional Chinese Medicine, Chengdu, 611137, China*

Correspondence should be addressed to Zhang Wang; wangzhangcqcd@cdutcm.edu.cn

Received 4 October 2021; Revised 12 December 2021; Accepted 13 December 2021; Published 28 December 2021

Academic Editor: Lixin Wei

Copyright © 2021 Yinglian Song et al. This is an open access article distributed under the Creative Commons Attribution License, which permits unrestricted use, distribution, and reproduction in any medium, provided the original work is properly cited.

The aim of this study is to determine 18 elements in Tibetan medicine Qishiwei Zhenzhu pills (QSW) and their absorption, distribution, and excretion in rats with cerebral ischemia. Microwave digestion and inductively coupled plasma mass spectrometry (ICP-MS) were used to determine 18 elements of QSW in simulated gastrointestinal (GI) juice. Rats were given QSW (66.68 mg/kg) followed by middle cerebral artery occlusion (MCAO). Sham rats received saline and were not subjected to MCAO. ICP-MS was applied to determine the content of 18 elements in hepatic venous blood, abdominal aortic blood, brain, liver, kidney, hair, urine, and feces 24 h after MCAO. In vitro results showed that the extraction rate of Mn, Cu, Sr, Pb, Au, and Hg of QSW in gastric juice (1 h) was higher than that in water, and the contents of Cu, Au, Sr, and As were higher in intestinal juice (4 h) than in water. In vivo results showed that the contents of elements in the blood were quite low, and QSW increased Ni, Cr, Sr, Co, and V in artery blood and decreased V in venous blood. Elements in the tissues were also low, and QSW increased brain Li but decreased Cr and Cd; QSW increased kidney Ag and Cs and liver Mn but decreased liver Ni. QSW increased urinary excretion of Li, Sr, Hg, Cs, and V; QSW increased Hg content in hair but decreased Ni. Stool is the main excretion pathway of the elements in QSW, with Ba, Mn, Sr, Cd, V, Cu, Cs, Li, Pb, Ag, Hg, Cr, As, and Co the highest. In summary, this study examined the distribution of 18 elements in QSW-treated MCAO rats. The accumulation of these elements in blood and tissues was extremely low, and the majority was excreted in feces within 24 h, highlighting the importance of the gut-microbiota-brain axis in QSW-mediated brain protection.

1. Introduction

Cerebral ischemia is the commonest type of cerebral infarction [1]. On the basis of vascular wall lesions caused by cerebral atherosclerosis, vascular stenosis, occlusion, or thrombosis may result in ischemia and hypoxic necrosis of local brain tissues due to interruption of the blood supply, which result in corresponding symptoms and signs in the nervous system [2]. Cerebral ischemia is equivalent to ischemic stroke in traditional Chinese medicine, "Baimai" disease in Tibetan medicine, and "Sa" disease in Mongolian medicine. The usual symptoms of "Baimai" disease are skewed mouth and eyes, numbness in limbs, rigidity, angular arch reflex, paralysis, hemiplegia, unconsciousness, and head tremors [3].

Qishiwei Zhenzhu pills (QSW), of which the Tibetan name is, are also known as Ranna Sangpei and was first recorded in the great classical work of Tibetan medicine *Si Bu Yi Dian*. QSW have the functions of tranquilizing the mind, activating meridians and collaterals, and harmonizing qi and blood. They are mainly used to treat "Baimai" disease, "Longxue" disorder, stroke, paralysis, hemiplegia, epilepsy,

cerebral hemorrhage, and other diseases [4]. According to the published literature, there should be 32 kinds of plant medicine, 8 kinds of animal medicine, more than 20 kinds of mineral and gem medicine, and a mineral mixture (Zuotai) in QSW. QSW are a confidential prescription, only the names of some medicines are disclosed, and the specific prescription proportion is unknown. Only 12 plant medicines, 8 animal medicines, 8 mineral and gemstone medicines, 4 metal medicines, and Zuotai are known and are listed in Supplementary Table 1 [5]. QSW consist of more than 10 metallic elements, such as gold, silver, and copper, more than 20 minerals and gemstones, such as sapphire and agate, and a mineral mixture Zuotai [6]. In particular, in accordance with the theories of Tibetan medicine, Zuotai is the main ingredient of many important Tibetan medicinal preparations. Zuotai is obtained from mercury and other minerals by a complex processing procedure, and hence QSW contain a large amount of mercury. The high mercury content in QSW results in serious health problems [7–9]. Therefore, the determination of the contents of mercury and other mineral components in QSW is very important for safety in clinical use.

The choice of detection method is important for the determination of trace elements, and a variety of different methods are used to detect elements. For example, Yang et al. [10] used synchrotron radiation X-ray fluorescence (SR-XRF) technology to quantify and semiquantify nine and fifteen elements in Tibetan herbal medicines and Tibetan medicine preparations, respectively. Flame atomic absorption (FAAS) with wet digestion method has also been used to quantitatively analyze various trace elements in Tibetan medicine Nan Hanshuishi [11]. In addition, the total mercury in the Tibetan medicine Dangzuo and the free mercury in the artificial gastric juice are also measured using the gold amalgam enrichment-atomic fluorescence (GAE-AFS) method [12]. Among a variety of detection methods, compared with traditional inorganic analysis technology, ICP-MS technology has the advantages such as lower detection limit, wider dynamic linear range, less interference, higher analysis precision, and analysis speed, and it can provide accurate isotope information and has a wide range of applications [13]. In medicine, it can be applied to the analysis of hair, blood samples, urine samples, biological tissues, biological mechanism research of proteins, enzymes, etc., drug quality control, etc. [14]. This research uses ICP-MS technology for experiment; the results will provide new ideas for the establishment of determination methods as well as the quality control and clinical rational application of QSW in the future [15].

As for the determination of trace elements in QSW, the following studies have been conducted: Suo et al. used inductively coupled plasma-atomic emission spectrometry (ICP-AES) to analyze and test more than 20 trace element components of QSW [16]. Li et al. used ICP-AES to determine the contents of 9 trace elements (Cu, Fe, Co, Mn, V, Zn, Mg, P, and K) in QSW and provided a theoretical basis for explaining their clinical effects on the basis of synergistic and antagonistic elements [17]. Li and Suo analyzed the long-term accumulation and toxic effects of trace elements present in QSW in animal tissues and organs. The results showed that most of the trace elements present in QSW did not accumulate in the heart, liver, kidneys, or other tissues and organs. Excessive amounts of heavy metals such as arsenic and cadmium were ingested after the administration of QSW and were mainly excreted through feces and urine [18]. Du et al. quantitatively analyzed the contents and distribution of toxic heavy metals (As, Hg, and Pb) in QSW on the basis of the findings of Li et al. [19]; but, at present, there have been no studies of the accumulation of trace elements in the body during the treatment of cerebral ischemia with QSW. In this study, we established a new, sensitive, selective, and accurate method for simultaneous quantitative analysis of the contents in the simulated GI juice and water of 18 elements in the QSW and their absorption, distribution, and excretion in rats with cerebral ischemia. By comparing the contents in the simulated GI juice and water of each element and their changes in the blood, distribution in the brain, liver, and kidney tissues, and excretion in hair, urine, and feces, the pharmacodynamic medicinal substance basis and toxicity of the QSW and its metabolism in the body can be found.

We have shown that QSW are effective in the treatment of cerebral ischemia injury [20]. The disposition of 18 elements during the treatment of MCAO by QSW could add our understanding of the protection mechanisms of QSW against cerebral ischemia injury. The results clearly demonstrated that 24 h after QSW administration to MCAO rats, these elements' accumulation in the blood and tissues were extremely low, and the amount found in feces were extremely high, implying these elements in the GI tract could modulate gut microbiota [21] to produce neuroprotection through the gut-microbiota-brain axis.

2. Materials and Methods

2.1. Drugs. QSW (batch number: 17103A, Guoyao Zhunzi: Z54020062) was purchased from Tibet Ganlu Tibetan Medicine Co., Ltd.

2.2. Reagents. Rh (internal standard stock solution [ISS]), In (ISS), Re (ISS), Bi (ISS), Li (standard solution [SS]), Be (SS), Sc (SS), V (SS), Cr (SS), Mn (SS), Co (SS), Ni (SS), Cu (SS), As (SS), Sr (SS), Ag (SS), Cd (SS), Cs (SS), Ba (SS), Pb (SS), Au (SS), and Hg (SS) all 22 reagents were produced by the National Nonferrous Metals and Electronic Materials Analysis and Testing Center. Pepsin and pancreatin were manufactured by Xinxiangsheng Biopharmaceutical Co., Ltd.

2.3. Instruments and Working Parameters. An inductively coupled plasma mass spectrometer (ICP-MS) (mode: ICAP-Q Series; Thermo Fisher Scientific, USA) was used with the following parameters: RF power 1.3 kW, carrier gas flow rate 1.14 L/min, sampling depth 6.8 mm, rectangular tube horizontal position 0.6 mm, auxiliary gas flow rate 0.9 L/min, spray chamber flow rate 0.98 L/min, and spray chamber pressure 2.85×105 Pa.

A microwave digestion apparatus (model: Milestone ETHOS A; Huashengda Instrument Equipment Co., Ltd.) was employed with the following parameters: (1) increase the temperature from room temperature to 120°C within 15 min and maintain for 5 min (1600 W); (2) increase the temperature to 150°C within 7 min and maintain for another 7 min (1600 W); and (3) within 7 min, increase the temperature to 190°C and maintain for 15 min (1600 W).

The following instruments were also used: an electronic analytical balance (model: XP204; Mettler-Toledo) and a constant temperature oscillator (model: SHZ-82; Guowang Instrument Manufacturing Co., Ltd.).

2.4. Preparation of Standard Solution. Gold working solutions with a mass concentration of 10 μg/mL were formulated (The Hg element easily produces memory effect as well as adsorption effect.). Precision stock solutions containing 18 tested metal elements, including Li, Be, Sc, V, Cr, Mn, Co, Ni, Cu, As, Sr, Ag, Cd, Cs, Ba, Pb, Au, and Hg, were used at appropriate amounts and diluted clinically with 10% HNO_3 to form mixed standard solutions with serial mass concentrations of each element: Li, Be, Sc, V, Co, Cd, Cs (0, 0.5, 2.0, 10, 25, 50 μg/L); Cr, Mn, Ni, Cu, As, Sr, Ag, Ba, Au, Pb (0, 0.5, 2.0, 10, 25, 50) $\times 10^3$ μg/L; Hg (0, 0.2, 0.5, 1.0, 1.5, 2.0) $\times 10^2$ μg/L; the standard solutions of mercury were configured individually; and the other 17 elements were configured into mixed standard solutions. Precision stock solutions of internal standards containing Rh, Re, In, and Bi diluted with 10% HNO_3 to a mixed internal standard solution at a concentration of 10 μg/mL and used.

2.5. Preparation of Test Samples of QSW. The QSW were wrapped with filter paper and crushed (not with a mortar to prevent the introduction of heavy metals). Exactly 0.0500 g of the sample was poured slowly into a polytetrafluoroethylene (PTEF) digestion tank, which was soaked in HNO_3 overnight, washed, and dried. Afterward, 10 mL of HNO_3 and 2 mL of H_2O_2 (both of premium grade) were added, shaken slowly, fixed, placed under the microwave heating program, and digested for 60 min. After the digestion was completed, the microwave digestion apparatus was turned off and cooled for a while. The digestion tank was removed and cooled to room temperature. The test solution was transferred to a 50 mL volumetric flask and washed three to four times. A constant volume was achieved. Given that Hg is easy to be adsorbed, 0.1 mL of the sample was placed in a 50 mL volumetric flask and added with gold standard solution to stabilize for testing (equivalent to 500-fold dilution).

2.6. Sample Preparation of QSW after the Digestion of Simulated GI Juice. Artificial GI juice was prepared in accordance with the *Pharmacopoeia of the People's Republic of China* (2015 edition, Vol. IV) [22]. For the preparation of artificial gastric juice, 16.4 mL of diluted hydrochloric acid was added with 800 mL of water and 10 g of pepsin, shaken well, and diluted to 1000 mL with water. For the preparation of artificial intestinal juice, phosphate buffer (containing pancreatin) and 6–8 g of potassium dihydrogen phosphate were dissolved in 500 mL of water, and the pH was adjusted to 6.8 with 0.1 mol/L sodium hydroxide solution. In addition, 10 g of pancreatin was dissolved in an appropriate amount of water. The two liquids were then mixed, added with water, and diluted to 1000 mL.

Simulated GI juice digestion and water samples were prepared using the method of Jin's research group [23]: 0.5000 g of finely ground QSW (approximately equivalent to the amount taken by a patient with mild to moderate diseases) was placed in a 200 mL conical flask with 100 mL of artificial gastric juice. The solution was vortexed at 37°C for 1 h and filtered, and the residual liquid was washed three times with artificial gastric juice. The filtrate was diluted with water to 200 mL to obtain an extract of artificial gastric juice. Another portion of the same sample powder was placed in a 200 mL conical flask filled with 100 mL of artificial intestinal juice, vortexed at 37°C for 4 h, and filtered. The residue was washed three times with artificial intestinal juice, and the filtrate was diluted with water to 200 mL to obtain an extract of artificial intestinal juice. Another part of the same sample powder was placed in a 200 mL conical flask with 100 mL of water, and then two copies were made and vortexed at 37°C for 1 h and 4 h, respectively, filtered, and rinsed with clean water three times. The filtrate was diluted to 200 mL with water to obtain the water extract. Approximately 1 mL was obtained for each of these four extracts, placed into the PTEF digestion tank, and added 4 mL of HNO_3 (premium grade). The remaining steps were similar to "Preparation of Test Samples of QSW" to prepare the test solution for testing.

2.7. Experimental Animals. Twelve male SD rats of SPF grade weighing 250–280 g were purchased from Chengdu Dashuo Experimental Animal Co., Ltd. (license number: SCXK [Sichuan] 2015-030, experimental animal quality certificate number: No. 51203500008744). The experiment was conducted in the National Medicine Resource Evaluation Laboratory of the Chengdu University of Traditional Chinese Medicine (the third-level scientific research laboratory of the State Administration of Traditional Chinese Medicine, NO.TCM-2009-320).

2.8. Animal Grouping and Test Drug Dosage. All male SD rats were divided into the following two large groups, each group with 6 animals: Sham operation group (abbreviated as Sham) and Qishiwei Zhenzhu pills group (abbreviated as QSW + MCAO) (66.68 mg/kg) [24, 25]. Based on the group, the rats were administered saline or QSW once through intragastric administration, and the administration volume was 10 mL/kg. The dosage of 66.68 mg/kg QSW is 4 times the daily dose for clinical adults, which is the optimal dose [26, 27].

2.9. Preparation of the MCAO Model. Performing animal modeling immediately after intragastric administration, refer to the predecessor model preparation method [26–29],

separate the right common carotid artery (CCA), external carotid artery (ECA), and internal carotid artery (ICA) and ligate the ECA. Separate the pterygopalatine artery inward along the ICA and ligate at the bifurcation. Cut an incision between the distal and proximal ends of the ECA, insert the tie wire into the ICA about 20 mm, and suture the wound and sterilize it. The animal was kept warm until awoke after modeling. The middle cerebral artery was occluded for 2 hours and then reperfused. In the Sham group, only the wound was sutured and a model was not made.

2.10. Collection and Determination of Animal Samples. At 24 h after intragastric administration of saline in the Sham group and after successful modeling for 24 h in the QSW + MCAO group, 20% urethane solution was injected intraperitoneally (0.6 mL/100 g) to anesthetize the rats, and then the rats in each group were treated with heparin sodium anticoagulation tube to collect blood from the hepatic portal vein and abdominal aorta. After taking blood from the hepatic vein and abdominal aorta, the liver, brain, kidney, as well as feces, urine, and hair were quickly collected, and then the rats were killed with cervical dislocation. When taking urine, gently squeeze the abdomen of the rat's bladder to speed up the collection of urine. Abdominal aortic blood, hepatic portal vein blood, and urine samples were measured to 0.50 mL using a pipette. The feces were obtained from the colon, and the back hairs of rats were collected. The feces and hair samples were weighed at 0.5000 g. And the brain, liver, and kidney were taken, weighed 0.5000 g, and then were homogenized. Transfer each of the above samples into the PTEF digestion tank, and add 8 mL HNO_3 (premium grade), same as "Preparation of Test Samples of QSW"; finally, transfer the digested test solution to a 25 mL volumetric flask to constant volume to be tested.

2.11. Statistical Analysis. SPSS 21.0 software was used for data analysis, and the data were expressed as mean ± SD. The independent sample t-test was performed for the comparison between two groups. When the test result is $p < 0.05$, the difference between groups is considered to be significant.

3. Results

3.1. In Vitro Quantitative Analysis of Minerals and Heavy Metals in QSW by ICP-MS

3.1.1. Methodological Investigation. Referring to the preparation of standard curves by subject group of Guo et al. [30], the multiple mixed standard solution under "Preparation of Standard Solution" was injected into the instrument at the same time as the internal standard solution, and the determinations were performed sequentially; taking the average measurement value of 3 readings measured for each mass concentration as the ordinate (y) and the mass concentration of the standard solution corresponding elements as the abscissa (x), the standard curve was plotted; then linear regression was performed to obtain the regression equations of 18 metal elements, and the results are shown in Supplementary Table 2. The results showed that each element had a good linear relationship in the corresponding mass concentration range. The mixed standard solution was taken for six consecutive injections, the contents of 18 minerals and heavy metals were determined, and the RSD value of the response value of each element was calculated; see Supplementary Table 2 for details. The measurement precision of the 18 elements is good and meets the analysis requirements.

Referring to the repeatability experiment of Guo Hong Li's research group [30], and using the same way, 6 sample solutions were prepared in parallel, and the sample solutions and the internal standard solutions were injected into the instrument at the same time; then sequential determination was performed, and the RSD value of each element is shown in Supplementary Table 2. The RSD values of the 18 elements were all less than 5%, indicating good repeatability. In addition, accurately weighed 6 samples (QSW), each 0.0250g, referring to "Preparation of Test Samples of QSW" to prepare sample solutions and internal standard solutions were prepared according to "Preparation of Standard Solution," then the sample solutions and internal standard solutions were injected into the instrument at the same time, and the recovery rates of 18 elements were calculated. The results are shown in Supplementary Table 2. The average sample recovery rate of 18 elements is 95.10%–111.13% (RSD, 2.13%–4.24%).

Referring to "Preparation of Test Samples of QSW," the blank solution was prepared by the same method, injected into the instrument, and measured 11 times continuously, and the detection limit of each element was obtained. See Supplementary Table 2 for details.

3.1.2. Content of Minerals and Heavy Metal Elements in QSW. After detection by ICP-MS, the contents of 18 elements in QSW are obtained: Li 2.893 μg/kg, Be 1.504 μg/kg, Sc 0.711 μg/kg, V 7.025 μg/kg, Cr 78.201 μg/kg, Mn 1292.577 μg/kg, Co 4.941 μg/kg, Ni 35.643 μg/kg, Cu 10240.028 μg/kg, As 601.874 μg/kg, Sr 242.575 μg/kg, Ag 1025.272 μg/kg, Cd 0.247 μg/kg, Cs 0.387 μg/kg, Ba 53.618 μg/kg, Pb 10184.186 μg/kg, Au 1098.911 μg/kg, and Hg 5200.500 μg/kg. The element content of QSW samples from high to low is Cu > Pb > Hg, which are all higher than 5000 μg/kg; the contents of Mn, As, Ag, and Au are all higher than 600 μg/kg; and the contents of Li, Be, Sc, V, Cr, Co, Ni, Sr, Cd, Cs, and Ba are all less than 300 μg/kg.

3.1.3. Content of Minerals and Heavy Metals in QSW after Digestion with Simulated GI Juice. The content of each element after GI digestion was determined. The contents of Mn, Cu, Sr, Pb, Au, and Hg in gastric juice (1 h) are significantly higher than those in water, which may be related to the easier dissolution of these trace elements under acidic conditions. The contents of Cu, Au, Sr, and As were higher in intestinal juice (4 h) than in water. In the simulated digestion experiment of artificial gastric juice and intestinal juice, the release changes of Cu and Pb are obvious: in gastric juice, the release of Cu and Pb was 17.65 and 30.56 μg/kg, respectively;

while in intestinal juice, the release of Cu and Pb was 4.406 and 0.764 μg/kg, respectively, and the change of Pb is the most significant. Therefore, after the clinically used QSW are digested by artificial GI juice, the released heavy metal elements were very low and many elements have fallen below the detection limit. See Table 1 for details.

3.2. In Vivo Analysis of Minerals and Heavy Metals in QSW by ICP-MS

3.2.1. In Vivo Processes of Minerals and Heavy Metals. As with previous experiments [20], the model was successful. Table 2 shows that the absorption of Li into the blood is not obvious, which is mainly excreted through feces and urine, and almost no excretion through hair; there is a certain distribution in the brain, suggesting that it may have a certain relationship with the efficacy or toxicity of QSW. The absorption of Be into the blood is not obvious, and the Be absorbed into blood is almost not excreted through urine and hair, and feces are the main excretion route. The absorption of Sc into the blood is not obvious, and the Sc absorbed into the blood is almost not excreted through urine and hair, and feces are its main excretion route. V is obviously absorbed into the blood, which is mainly excreted through feces and urine but hardly through hair. Cr is absorbed into the blood obviously; the Cr absorbed into the blood is hardly excreted through urine and hair, mainly through feces; it is mainly distributed in the brain, suggesting that it may have a certain relationship with the efficacy or toxicity of QSW. The absorption of Mn into the blood is not obvious, and the Mn absorbed into the blood is almost not excreted through urine and hair but mainly through feces; it is mainly distributed in the liver. Co is absorbed into the blood obviously, the Co absorbed into the blood is hardly excreted through urine and hair, and feces are its main excretion route. Ni is absorbed into the blood obviously, the Ni absorbed into the blood is hardly excreted through urine and hair, and feces are its main excretion route. The absorption of Cu into the blood is not obvious, and the Cu absorbed into the blood is hardly excreted through urine and hair, and feces are its main excretion route. The absorption of As into the blood is not obvious, and the As absorbed into the blood is finally excreted through feces and urine, of which feces are the main route, and it is almost not excreted through hair. Sr is absorbed into the blood obviously, the more it is absorbed over time; the Sr absorbed into the blood is finally excreted through feces and urine, of which feces is the main route, and it is hardly excreted through hair. Ag is not obviously absorbed into the blood, mainly excreted through feces and urine but almost not through hair; there is a distribution in the kidney at 24 h; there is no obvious distribution in the brain. The absorption of Cd into the blood is not obvious, and it is mainly excreted through feces and urine, but almost not through hair; it is mainly distributed in the brain, suggesting that it may have a certain relationship with efficacy or toxicity of QSW. The absorption of Cs into the blood is not obvious, and it is mainly excreted through feces and urine, but almost not through hair; it is mainly distributed in the kidney. Ba is not obviously absorbed into the blood, and it is mainly excreted through feces, but almost not through urine and hair; it has no obvious distribution in the brain, liver, and kidney. The absorption of Pb into the blood is obvious, the Pb absorbed into the blood is finally excreted through feces and urine, of which feces are the main route, and it is almost not excreted through hair; it is mainly distributed in the liver and kidney. The absorption of Au into the blood is not obvious, and the Au absorbed into the blood is hardly excreted through urine and hair, and feces are its main excretion route. The absorption of Hg into the blood is not obvious, and the Hg absorbed into the blood is excreted through feces, urine, and hair, of which feces is the main path.

3.2.2. Analysis of the Content of Minerals and Heavy Metals in Blood and Different Tissues. Changes in the content of minerals and heavy metals in the blood are shown in Table 2 and Figure 1. In hepatic venous blood, the V content in the QSW + MCAO was significantly reduced compared with the Sham group ($p < 0.05$). In abdominal aortic blood, the contents of V, Cr, Co, Ni, and Sr were increased by QSW + MCAO ($p < 0.05$). However, as far as the content of each trace element in Table 2 is concerned, the trace element content between the Sham and QSW + MCAO groups is not different and the content is extremely low. Taking into account the trace elements in the blood itself, the differences between experimental animals, and the measurement sensitivity of ICP-MS itself, it can be considered that the content of trace elements and even heavy metals in the QSW + MCAO remained in the blood 24 h after successful modeling is extremely low.

The brain, kidney, and liver were used to analyze the distribution and accumulation of minerals and heavy metals in the tissues, and the results are shown in Table 2 and Figure 2. In brain tissues, the content of Li increased by QSW + MCAO ($p < 0.05$), while the content of Cr and Cd decreased significantly ($p < 0.05$). In kidney tissues, Ag and Cs contents increased by QSW + MCAO at 24 h of MCAO ($p < 0.05$). In liver tissues, the content of Mn increased by QSW + MCAO at 24 h of MCAO, while the content of Ni decreased ($p < 0.05$). The results showed that at 24 h of QSW + MCAO, the content of Mn in the liver was higher than that of the Sham group and was statistically significant (Table 2). Therefore, we speculate that the liver of QSW + MCAO rats is the site of Mn metabolism.

Urine, hair, and feces are main excretion routes for minerals, and the results are shown in Table 2 and Figure 3. In urine, at 24 h of QSW + MCAO, the contents of Li, V, Sr, Ag, Cd, Cs, and Hg increased significantly ($p < 0.05$). In the hair, the content of Ni decreased, while the content of Hg increased by QSW + MCAO ($p < 0.05$). In feces, at 24 h of MCAO, the contents of Li, V, Cr, Mn, Co, Cu, As, Sr, Ag, Cd, Cs, Ba, Pb, and Hg increased significantly ($p < 0.05$). Therefore, we speculate that the hair of QSW + MCAO rats could be the site of Hg metabolism. Although other elements are not statistically significant, their content is still increasing sharply (Be, Sc, Ni, Au). It can be seen that feces is the main excretion pathway of trace elements and heavy metals in QSW.

Table 1: Determination results of contents of 18 elements in GI juice (μg/kg).

Element	Water extraction (1 h)/(μg/kg)	Stomach digestion (1 h)/(μg/kg)	Water extraction (4 h)/(μg/kg)	Intestinal digestion (4 h)/(μg/kg)
Li	**0.044**	—	0.094	0.049
Be	—	—	—	—
Sc	—	—	—	—
V	—	—	—	—
Cr	—	—	—	—
Mn	0.518	6.179	—	—
Co	0.040	0.081	0.011	0.019
Ni	2.653	—	—	—
Cu	2.292	17.651	0.853	4.406
As	3.663	4.228	0.581	0.845
Sr	0.446	8.598	0.080	0.928
Ag	72.985	51.974	45.854	41.845
Cd	—	—	—	—
Cs	0.004	0.013	—	0.006
Ba	—	—	—	—
Pb	1.686	30.558	1.269	0.764
Au	1.790	4.846	0.903	2.959
Hg	1.170	4.518	3.406	1.102

The symbol "—" means not detected or lower than the detection limit. Bold indicates that the data are consistent with other data.

Compared with the content of minerals and heavy metals in QSW itself, it can be seen that the content of 18 elements in the abdominal aortic blood, hepatic venous blood, brain, liver, and kidney of QSW + MCAO rats is extremely low, the absorption is not high, and most of them are excreted through feces, and a few are excreted through urine and hair, which further proves taking QSW is relatively safe.

4. Discussion

This study concludes that the contents of Hg, Cu, Pb, Ag, As, Mn, and Au in QSW are relatively high. Under normal conditions, intake of such high levels of trace elements and even heavy metals is toxic to the human body when in excess amounts. However, after QSW were digested by artificial GI juice, the release of these heavy metals is very low, and many elements have fallen below the detection limit. These minerals and heavy metals must also be absorbed into the blood to exert their physiological effects in the human body. Hence, the low release of heavy metals may be acceptable. Finally, one QSW pill usually takes 3 to 7 days to be absorbed. At this time, the body's normal metabolism will also metabolize most of the trace elements. Therefore, the high content of trace elements and even heavy metals in QSW is not a sound basis to declare this Tibetan medicine as unsafe. The *Pharmacopoeia of the People's Republic of China* only conducts the microscopic identification of pearl, nine eye stone, and *Dalbergia odoratum* and the thin-layer identification of cholic acid, saffron, agarwood, benzoin, and safflower [4]. This process does not involve the quality control of trace elements or even heavy metals. However, heavy metals should have strict limits whether they are being used as toxic ingredients or as the basis of medicinal substances. At present, the research on minerals and heavy metals in QSW at home and abroad is still in infancy. No work has focused on the in vivo and in vitro aspects to systematically and quantitatively analyze the content of minerals and heavy metals in QSW. According to the in vitro simulated gastric digestion experiment in this work, the dissolution rate of other elements is higher than that of water extraction, except for the undetected and Ag elements. Two explanations for this phenomenon are presented. One is that hydrochloric acid destroys the internal structure of these minerals and heavy metals, thus allowing them to be dissolved in gastric juice. Another is the precipitation reaction of free silver dissolved in gastric juice and hydrochloric acid, thereby lowering the total silver content in gastric juice compared with that in water. In the simulated intestinal digestion experiment, the content of almost all detected minerals and heavy metals was far lower than that in the gastric juice.

Zuotai, an important component in QSW, is mainly made of mercury. It is not used alone in clinical practice but plays an important role in Tibetan medicine preparations, such as improving curative effects, reducing side effects, strengthening the spleen, and nourishing the body. [31]. Because Zuotai contains mercury, which is a toxic heavy metal element, its safety has received extensive attention. Previous studies [32] have conducted experiments on the dissolution of Zuotai in simulated GI, and the results showed that the dissolution of mercury in the simulated intestinal juice of Zuotai was significantly lower than that in the simulated gastric juice. Our study on QSW also showed the same result. Therefore, gastric juice digestion plays a key role in the absorption and metabolism of minerals and heavy metals in QSW.

The content of minerals and heavy metals in cerebral ischemia rats treated with QSW was determined. In our experiment, we also studied the QSW with a dose of 5 g/kg and executed them at 0.5 h after making the model. The results showed that there was no significant difference from the Sham group. The reason may be that the time is too

Table 2: Changes in the contents of 18 elements in rats with cerebral ischemia ($n = 6$, μg/kg).

Element	Group	Absorption		Distribution			Excretion		
		Hepatic venous blood	Abdominal aortic blood	Brain	Kidney	Liver	Urine	Hair	Feces
Li	Sham	1.799 ± 1.469	0.573 ± 0.240	0.021 ± 0.027	0.025 ± 0.035	—	0.298 ± 0.082	0.603 ± 0.128	0.9705 ± 0.03541
	QSW + MCAO	0.846 ± 0.119	0.827 ± 0.227	0.121 ± 0.053*	0.261 ± 0.148	0.112 ± 0.113	2.921 ± 1.687*	1.658 ± 0.417	22.74 ± 2.601*
Be	Sham	0.041 ± 0.070	0.007 ± 0.008	0.021 ± 0.028	0.006 ± 0.008	0.006 ± 0.008	0.006 ± 0.007	0.002 ± 0.031	0.0447 ± 0.0216
	QSW + MCAO	0.015 ± 0.018	0.002 ± 0.006	—	0.002 ± 0.004	0.026 ± 0.058	0.005 ± 0.007	105.5 ± 211.1	87.93 ± 0.660
Sc	Sham	0.018 ± 0.024	0.002 ± 0.002	0.016 ± 0.013	0.002 ± 0.002	0.021 ± 0.028	0.001 ± 0.002	0.019 ± 0.007	0.0434 ± 0.0171
	QSW + MCAO	0.001 ± 0.001	0.001 ± 0.001	0.006 ± 0.005	0.008 ± 0.006	0.012 ± 0.007	0.004 ± 0.004	40.63 ± 81.18	95.76 ± 14.48
V	Sham	0.430 ± 0.328	0.029 ± 0.005	0.441 ± 0.072	0.736 ± 0.486	0.845 ± 0.664	0.023 ± 0.004	0.319 ± 0.033	11.28 ± 0.532
	QSW + MCAO	0.070 ± 0.087*	0.045 ± 0.011*	0.132 ± 0.015	1.057 ± 0.341	0.524 ± 0.199	0.068 ± 0.033*	11.16 ± 21.32	35.49 ± 23.53*
Cr	Sham	9.508 ± 6.316	7.412 ± 1.188	192.2 ± 26.37	9.153 ± 0.409	25.71 ± 18.07	6.913 ± 0.679	21.61 ± 1.308	0.912 ± 0.6191
	QSW + MCAO	11.09 ± 0.701	9.344 ± 0.713*	9.889 ± 1.242*	17.99 ± 16.83	36.01 ± 19.77	7.268 ± 0.506	25.31 ± 21.61	12.740 ± 8.081*
Mn	Sham	1.166 ± 1.643	0.027 ± 0.055	12.38 ± 3.375	30.41 ± 12.66	29.13 ± 0.699	0.038 ± 0.075	7.336 ± 0.793	330.8 ± 167.5
	QSW + MCAO	2.246 ± 5.481	0.009 ± 0.022	10.08 ± 1.656	262.3 ± 52.30	80.75 ± 10.24*	0.241 ± 0.248	40.16 ± 30.79	50480 ± 27940*
Co	Sham	0.044 ± 0.023	0.013 ± 0.006	0.493 ± 0.272	1.481 ± 1.650	1.395 ± 1.362	0.135 ± 0.177	0.115 ± 0.016	0.2862 ± 0.1663
	QSW + MCAO	0.047 ± 0.053	0.026 ± 0.004*	0.089 ± 0.011	1.783 ± 0.303	0.589 ± 0.116	0.139 ± 0.074	0.656 ± 0.748	42.86 ± 9.576*
Ni	Sham	41.84 ± 21.08	31.91 ± 4.188	977.7 ± 616.2	36.22 ± 0.577	38.97 ± 0.064	28.98 ± 2.942	77.52 ± 12.03	30.60 ± 13.27
	QSW + MCAO	46.04 ± 2.302	37.96 ± 3.100*	37.06 ± 4.362	36.94 ± 1.428	36.74 ± 1.222*	28.79 ± 2.422	38.78 ± 0.989*	1460 ± 1977
Cu	Sham	66.99 ± 47.98	54.53 ± 48.46	147.2 ± 17.60	196.4 ± 2.363	206.3 ± 24.72	59.11 ± 39.59	147.6 ± 5.267	12.68 ± 62.45
	QSW + MCAO	41.11 ± 41.22	46.93 ± 44.93	140.3 ± 9.885	255.4 ± 48.35	220.1 ± 13.79	30.79 ± 44.10	269.9 ± 105.1	2325 ± 191.3*
As	Sham	368.9 ± 269.3	209.02 ± 74.28	3.215 ± 1.613	19.27 ± 6.584	19.73 ± 4.745	1.541 ± 0.038	1.792 ± 0.352	0.2964 ± 0.1596
	QSW + MCAO	101.2 ± 3.592	157.4 ± 25.59	2.042 ± 0.275	19.59 ± 4.862	23.95 ± 5.165	4.224 ± 0.464	55.86 ± 104.4	81.92 ± 9.358*
Sr	Sham	3.028 ± 4.483	0.026 ± 0.052	0.658 ± 0.299	0.262 ± 0.371	0.598 ± 0.042	0.581 ± 0.082	2.085 ± 0.1211	18.63 ± 7.826
	QSW + MCAO	1.156 ± 2.427	0.451 ± 0.132*	0.516 ± 0.144	1.055 ± 0.492	0.265 ± 0.494	5.612 ± 3.481*	6.876 ± 5.843	3091 ± 1423*
Ag	Sham	0.116 ± 0.053	0.011 ± 0.014	0.854 ± 1.242	0.016 ± 0.001	0.091 ± 0.079	—	0.632 ± 0.979	0.1119 ± 0.01198
	QSW + MCAO	0.130 ± 0.150	0.020 ± 0.023	0.142 ± 0.079	0.195 ± 0.097*	0.147 ± 0.091	0.058 ± 0.036	5.781 ± 10.01	151.30 ± 69.56*
Cd	Sham	0.030 ± 0.034	—	0.064 ± 0.031	0.229 ± 0.086	0.232 ± 0.095	—	0.025 ± 0.008	0.0107 ± 0.0559
	QSW + MCAO	0.022 ± 0.038	0.001 ± 0.002	0.003 ± 0.004*	0.153 ± 0.088	0.152 ± 0.076	0.005 ± 0.004	18.79 ± 37.49	2063 ± 203.9*
Cs	Sham	0.119 ± 0.076	0.051 ± 0.019	0.269 ± 0.047	0.435 ± 0.007	0.509 ± 0.105	0.069 ± 0.001	0.056 ± 0.005	0.0156 ± 0.0056
	QSW + MCAO	0.054 ± 0.010	0.078 ± 0.009	0.296 ± 0.068	0.908 ± 0.167*	0.782 ± 0.097	0.233 ± 0.114*	15.02 ± 29.69	242.5 ± 113.5*
Ba	Sham	3.597 ± 3.848	1.477 ± 1.124	0.512 ± 0.465	0.235 ± 0.332	0.453 ± 0.634	—	2.103 ± 0.291	4.731 ± 1.736
	QSW + MCAO	2.816 ± 5.429	0.352 ± 0.233	0.580 ± 1.037	0.662 ± 0.559	0.257 ± 0.500	—	6.439 ± 6.517	10360 ± 8227*
Pb	Sham	0.925 ± 1.059	—	—	—	0.161 ± 0.028	—	0.830 ± 0.362	0.2564 ± 0.1205
	QSW + MCAO	0.477 ± 1.168	—	0.122 ± 0.176	1.216 ± 0.951	2.672 ± 2.554	0.204 ± 0.378	6.747 ± 3.947	198.40 ± 154.50*
Au	Sham	0.024 ± 0.027	—	0.003 ± 0.006	0.013 ± 0.018	0.007 ± 0.009	—	—	0.0131 ± 0.0204
	QSW + MCAO	0.010 ± 0.017	0.004 ± 0.006	0.020 ± 0.029	0.351 ± 0.372	0.179 ± 0.207	0.022 ± 0.043	3.171 ± 3.106	12.01 ± 23.46
Hg	Sham	0.630 ± 0.394	0.429 ± 0.174	0.283 ± 0.099	0.468 ± 0.423	0.592 ± 0.445	0.050 ± 0.012	0.624 ± 0.103	0.0117 ± 0.005
	QSW + MCAO	0.460 ± 0.226	0.359 ± 0.032	0.358 ± 0.112	2.998 ± 1.231	0.606 ± 0.083	0.794 ± 0.446*	9.332 ± 2.793*	118.50 ± 84.31*

The symbol "—" means not detected or lower than the detection limit; compared with the Sham group, $^*p < 0.05$.

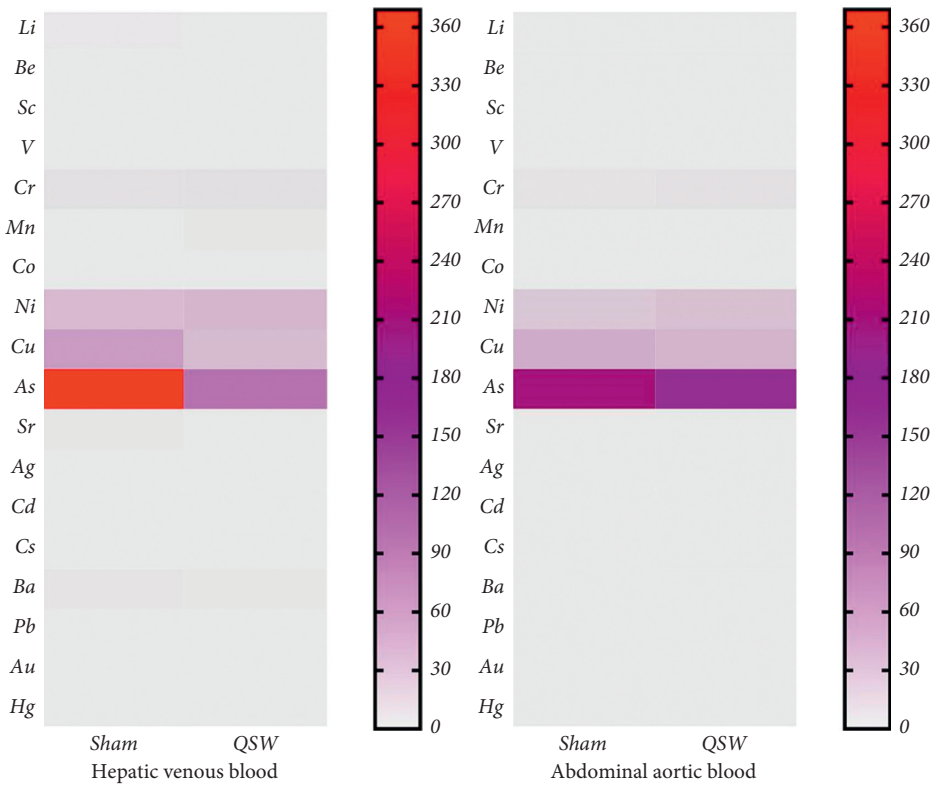

Figure 1: Heatmap of 18 elements in the artery and vein ($n = 6$). (*Note.* The redder the color, the higher the content; the grayer the color, the lower the content.)

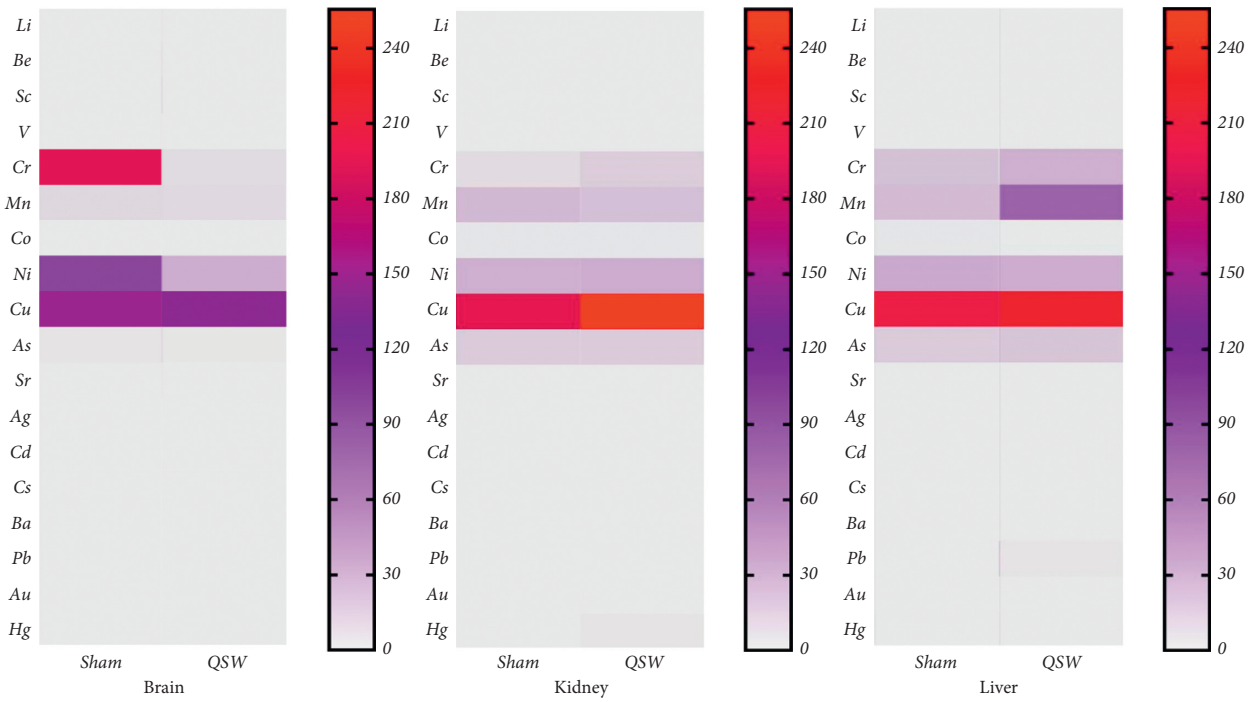

Figure 2: Heatmap of 18 elements in the brain, kidney, and liver ($n = 6$). (*Note.* The redder the color, the higher the content; the grayer the color, the lower the content.)

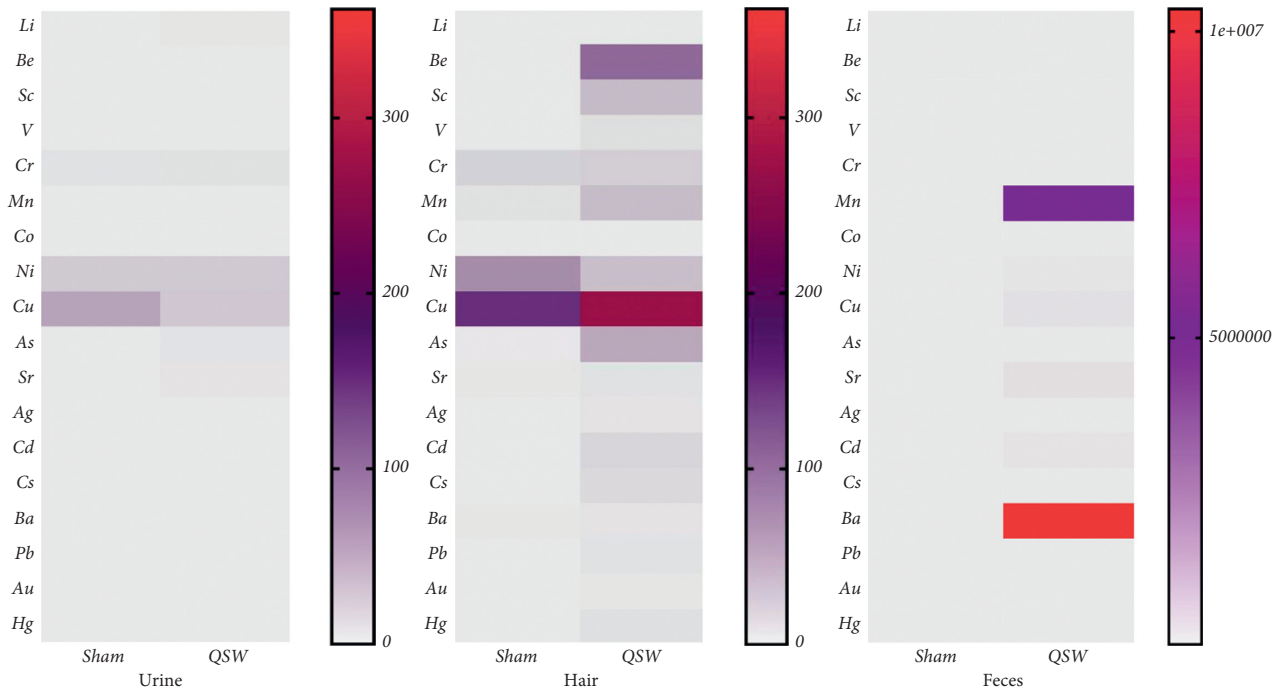

Figure 3: Heatmap of 18 elements in urine, hair, and feces ($n = 6$). (*Note.* The redder the color, the higher the content; the grayer the color, the lower the content.)

short; the elements of QSW cannot be absorbed and distributed, even if its dose is large enough. These pilot results showed that it takes a certain period of time to produce effect after taking QSW.

When the rats were treated with QSW (66.68 mg/kg) first, then at 24 h of successful modeling, the Hg, Pb, Cu, As, and other heavy metal elements are mainly excreted in feces, and the heavy metals that are absorbed into the blood or accumulated in the brain, liver, kidney, and other tissues are extremely low. Nonetheless, in the measurement of elements accumulated in brain tissues, it was found that the content of Li increased, and the content of Cd and Cr decreased, and both were significant; Li was absorbed into the body and mainly distributed in the brain, indicating that its main target site to exert its pharmacological or toxic effects is the brain. Hence, Li is possibly to be the material basis of QSW for the treatment of cerebral ischemia. According to reports in the literature, Li can improve the integrity of the blood-brain barrier, sensorimotor deficits, and cerebral edema in animals with cerebral hemorrhage [33]. The excretion of minerals in the feces is the main route of disposition of these elements, including the above three. Considering their long-term stay in the GI tract, the gut-microbiota-brain axis in QSW-mediated brain protection is evident [21].

QSW is rich in minerals and heavy metals than other Chinese patent medicines. These toxic elements cause strong toxic reactions only when in their free form and in excess; if minerals and heavy metals are combined with other macromolecular compounds, then their toxic reactions are greatly weakened or directly converted into nontoxic chemical compounds [34]. Heavy metals are generally viewed as toxic to the human body. From the perspective of traditional medicine, toxicity can be reduced by processing or strict dosage control; "both poison and medicine" is a relevant saying. Main ingredients, such as Zuotai of QSW, must undergo "mercury refining method" [35] to ensure that the toxicity of Hg and other metal elements is greatly reduced or even removed. When metals enter the body, complex physiological changes may cause them to combine with certain macromolecular substances to reduce their toxicity or exert pharmacological effects. For example, when Cd and Cr are absorbed into the blood and are distributed in the brain, they may combine with some macromolecular substances to exhibit a therapeutic effect. Whether decreased Cd and Cr in the brain by QSW could contribute to its neuroprotection is unknown and worth investigating. QSW increased Ag and Cs in the kidney and increased Mn but decreased Ni in the liver; the biological significance of such changes also requires further investigation. In addition, the human body's absorption of mercury and other minerals is low mainly because most of them are excreted in feces, which indicates the importance of the gut-microbiota-brain axis in QSW-mediated brain protection; secondly, the content of trace elements of the human body required is not high, although the absorption is low, it may just meet the needs of the human body. Moreover, the Li, Cr, Cd, and other elements detected in brain tissues are likely to be the material basis for QSW to treat cerebral ischemia.

However, what about the accumulation of QSW in the body after long-term use? The dosage of QSW in the instructions is 1 g (1 pill) per day for critically ill patients, and general patients take 1 g every 3 to7 days. In this study, rats were given the clinically equivalent dose of QSW, that is, the optimal dose (66.68 mg/kg), and within 24 h after the

successful modeling, most of the minerals and heavy metals have been excreted through urine or feces, and then after 3 to 7 days, the minerals and heavy metals in the body may be less. Therefore, whether it is for critically ill patients or general patients, the accumulation of minerals and heavy metals in the body after long-term use of QSW is very small and basically does not accumulate; it is safe to take QSW.

In our experiment, the results showed that these elements can be detected in the Sham group. These trace elements could be essential components in the body. This study is the first to use ICP-MS to examine the in vivo absorption, distribution, and excretion of minerals and heavy metals from QSW and further objectively prove its safety. However, there is also one deficiency, that is, we did not set up the model control group (MCAO group), and we do not know whether it will affect the content of these elements in the body after modeling. Nonetheless, Sham rats without receiving QSW provided a basal control for absorption, distribution, and excretion of elements following QSW administration.

5. Conclusions

Quantifying the minerals and heavy metals in QSW in vivo and in vitro will help improve its quality standards. The abundant minerals and heavy metals in this medicine may either be the basis of its main medicinal substances or promote the therapeutic effects of its effective ingredients. The absorption, distribution, and excretion of minerals and heavy metals from QSW in MCAO rats add to our understanding of neuroprotective effects of QSW. The accumulation of the elements in blood and tissues was extremely low, and the majority was excreted in feces within 24 h, highlighting the importance of the gut-microbiota-brain axis in QSW-mediated brain protection.

Abbreviations

QSW: Qishiwei Zhenzhu pills
ICP-MS: Inductively coupled plasma mass spectrometry
GI: Gastrointestinal
MCAO: Middle cerebral artery occlusion
ICP-AES: Inductively coupled plasma-atomic emission spectrometry
SR-XRF: Synchrotron radiation X-ray fluorescence
FAAS: Flame atomic absorption
GAE-AFS: Gold amalgam enrichment-atomic fluorescence
ISS: Internal standard stock solution
SS: Standard solution
PTEF: Polytetrafluoroethylene
CCA: Common carotid artery
ECA: External carotid artery
ICA: Internal carotid artery.

Data Availability

Data supporting the conclusions are included in the manuscript. The data sets used and/or analyzed during the current study are also available from the corresponding author on reasonable request.

Ethical Approval

The use of animals was approved by the Sichuan Provincial Committee for the Control of Experimental Animals, Chengdu University of Traditional Chinese Medicine, and conformed to the Guide for the Care and Use of Laboratory (approval number: SYXK (Chuan) 2020-124).

Conflicts of Interest

All authors declare no conflicts of interest.

Authors' Contributions

Yinglian Song, Ke Fu, and Dewei Zhang contributed equally to this work. Yinglian Song and Ke Fu are responsible for assisting in the experiment and participating in the writing of articles; Dewei Zhang is mainly responsible for the research; Min Xu, Ruixia Wu, Xueqing Xiong, Xianwu Liu, Lei Wu, Ya Guo, You Zhou, and Xiaoli Li are responsible for assisting in the experiment.

Acknowledgments

This study was supported by China Postdoctoral Science Foundation (2012M511916); the Project of Sichuan Provincial Administration of Traditional Chinese Medicine (2012-E-040); and the Science and Technology Development Fund of Chengdu University of Traditional Chinese Medicine (ZRQN1544). The authors thank the Chengdu University of Traditional Chinese Medicine and Wenzhou Institute for Drug and Food Control for providing with a research platform in this article; and Zhang Wang directs the writing of the article and functions as our corresponding author.

Supplementary Materials

Supplementary Table 1. Composition of QSW. *Supplementary Table 2.* Results of linear equations and correlation coefficients of 18 elements. (*Supplementary Materials*)

References

[1] J. Wu, *Neurology*, pp. 150–192, People's Medical Publishing House, Beijing, China, 2005.
[2] C. J. Liu, *Study on the Relationship between Middle Cerebral Artery Stenosis and Progressive Ischemic Stroke*, Nangchang University, Nanchang, China, 2019.
[3] L. J. Zheng, X. Q. Ren, M. Q. Wang et al., "Exploring the rule of the diagnosis and treatment of stroke based on the Tibetan medical theory of white meridian," *Modernization of Traditional Chinese Medicine and Materia Medica-World Science and Technology*, vol. 19, no. 2, pp. 370–374, 2017.
[4] National Pharmacopoeia Committee, *Pharmacopoeia of the People's Republic of China. Vol. I*, China Medical Science and Technology Press, Beijing, China, 2015.

[5] W. L. Xu, W. J. Sun, and Z. Wang, "Comparison with the modern research progress of the Rannasangpei and twenty five pearl pill based on prescription data mining," *Chinese Journal of Ethnomedicine and Ethnopharmacy*, vol. 26, no. 4, pp. 59–63+71, 2017.

[6] E. J. An and Y. R. Suo, "Advances in modern pharmacology of Qishiwei Zhenzhu pills of Tibetan medicine," *Journal of Medicine & Pharmacy of Chinese Minorities*, vol. 10, no. 2, pp. 33–35, 2004.

[7] L.-L. Zhou, H.-J. Chen, Q.-Q. He, C. Li, L.-X. Wei, and J. Shang, "Evaluation of hepatotoxicity potential of a potent traditional Tibetan medicine Zuotai," *Journal of Ethnopharmacology*, vol. 234, pp. 112–118, 2019.

[8] C. Li, W. Xu, S. Chu et al., "The chemical speciation, spatial distribution and toxicity of mercury from Tibetan medicine Zuotai, β-HgS and HgCl2 in mouse kidney," *Journal of Trace Elements in Medicine & Biology*, vol. 45, pp. 104–113, 2018.

[9] Q. Wu, W.-K. Li, Z.-P. Zhou et al., "The Tibetan medicine Zuotai differs from HgCl2 and MeHg in producing liver injury in mice," *Regulatory Toxicology and Pharmacology*, vol. 78, pp. 1–7, 2016.

[10] H. X. Yang, C. Li, Y. Z. Du, and L.-X. Wei, "Metallic elemental analysis of Tibetan herbal medicines and Tibetan medicine preparations by synchrotron radiation X-ray fluorescence," *Spectroscopy and Spectral Analysis*, vol. 35, no. 6, pp. 1730–1734, 2015.

[11] J. F. Jiang, L. X. Wei, and Y. Z. Du, "Determination of calcium and other five trace elements in calcium from four provinces by FAAS with wet digestion," *Chinese Journal of Spectroscopy Laboratory*, vol. 28, no. 6, pp. 2862–2865, 2011.

[12] C. Li, H. X. Yang, and L. X. Wei, "Determination of total mercury and ionic mercury in artificial gastric juice of Tibetan medicine Dangzuo by GAE-AFS," *Spectroscopy and Spectral Analysis*, vol. 31, no. 7, pp. 1950–1953, 2011.

[13] D. Y. Chen and T. Christopher, "ICP-MS and its application," *Modern Instruments & Medical Treatment*, no. 4, pp. 8–11+38, 2001.

[14] J. Q. Huang, X. Hu, and J. R. Zhang, "Application of ICP-MS technology in pharmaceutical analysis," *China Pharmacy*, vol. 17, no. 8, pp. 624–626, 2006.

[15] L.-Y. Du, T. Jiang, K. Wei et al., "Simultaneous quantification of four ginsenosides in rat plasma and its application to a comparative pharmacokinetic study in normal and depression rats using UHPLC-MS/MS," *Journal of Analytical Methods in Chemistry*, vol. 2021, Article ID 4488822, 11 pages, 2021.

[16] Y. R. Suo, T. C. Li, and C. Q. Ai, "Study on mineral elements of Tibetan medicine Qishiwei zhenzhu pills," *Qinghai Science and Technology*, vol. 10, no. 5, pp. 26–29, 2003.

[17] Y. Li, F. S. Yi, and T. C. Li, "Determination of trace elements in Tibetan medicine Qishiwei zhenzhu pills," *Guangdong Trace Elements Science*, vol. 8, no. 11, pp. 51-52, 2001.

[18] T. C. Li and Y. R. Suo, "Study on the accumulation level of mineral elements in Tibetan medicine Qishiwei zhenzhu pills," *Journal of the Graduate School of the Chinese Academy of Sciences*, vol. 20, no. 3, pp. 348–352, 2003.

[19] Z. Du, B. Z. Ciren, and B. Gong, "Distribution and excretion of toxic heavy metals in Qishiwei zhenzhu pills in beagle dogs," *Pharmaceutical Journal of Chinese People's Liberation Army*, vol. 27, no. 6, pp. 487–489, 2011.

[20] M. Xu, R. X. Wu, Y. Liang et al., "Protective effect and mechanism of Qishiwei Zhenzhu pills on cerebral ischemia-reperfusion injury via blood-brain barrier and metabonomics," *Biomedicine & Pharmacotherapy*, vol. 131, 2020.

[21] K. Fu, D. W. Zhang, Y. L. Song et al., "Tibetan medicine Qishiwei Zhenzhu pills can reduce cerebral ischemia-reperfusion injury by regulating gut microbiota and inhibiting inflammation," *Evidence-Based Complementary and Alternative Medicine*, vol. 2021, Article ID 2251679, 13 pages, 2021.

[22] National Pharmacopoeia Committee, *Pharmacopoeia of the People's Republic of China. Vol. IV*, Vol. 130, China Medical Science and Technology Press, ,Beijing,China, 2015.

[23] P. Jin, X. Liang, L. Xia et al., "Determination of 20 trace elements and arsenic species for a realgar-containing traditional Chinese medicine Niuhuang Jiedu tablets by direct inductively coupled plasma-mass spectrometry and high performance liquid chromatography-inductively coupled plasma-mass spectrometry," *Journal of Trace Elements in Medicine & Biology*, vol. 33, pp. 73–80, 2016.

[24] W. W. Liang, C. J. Huang, and Z. Wang, "Preliminary study of time-effect relationship of Tibetan Rannasangpei Pills for the treatment of cerebral ischemia-reperfusion injury," *Pharmacology and Clinics of Chinese Materia Medica*, vol. 31, no. 1, pp. 182–187, 2015.

[25] W. L. Xu, W. J. Sun, and Z. Wang, "Dose-effect relationship of Qishiwei Zhenzhu Pills against cerebral ischemicreperfusion injury in rats," *Drugs & Clinic*, vol. 32, no. 1, pp. 10–15, 2017.

[26] Y. Liang, *Study on the Blood Absorption Components and the Mechanism of Rannasangpei for Blood-Brain Barrier Injury after Cerebral Ischemia Based on GC-MS Metabonomics*, Chengdu University of Traditional Chinese Medicine, Chengdu, China, 2019.

[27] G. Liu, G. Tang, W. Liang et al., "PK-PD correlation of Erigeron breviscapus injection in the treatment of cerebral ischemia-reperfusion injury model rats," *Journal of Molecular Neuroscience*, vol. 71, no. 2, pp. 302–324, 2020.

[28] Y. Liang, K. Fu, and Z. Wang, "Study on the dose-time-effect relationship of Tibetan medicine rannasangpei in cerebral ischemiareperfusion injury model rats with intragastric administration," *China Pharmacy*, vol. 30, no. 1, pp. 94–98, 2019.

[29] Y. Liang, W. J. Sun, and Z. Wang, "Protective effects of Qishiwei Zhenzhu Pills on blood-brain barrier in cerebral ischemia-reperfusion injury rats," *Chinese Traditional Patent Medicine*, vol. 41, no. 4, pp. 767–773, 2019.

[30] H. L. Guo, S. Zhang, and L. Y. Liu, "Determination of 13 kinds of metal elements in 10 common Chinese materia medica injections by ICP-MS," *Chinese Traditional and Herbal Drugs*, vol. 46, no. 17, pp. 2568–2572, 2015.

[31] B. S. Yang, J. C. Jiang, and Y. Jiang, "Study on the features and safety of mercury in the Tibetan medicine "Zuotai"," *Tibetan Studies*, no. 1, pp. 74–80, 2004.

[32] M. Zhang, H. T. Bi, and C. Li, "The difference of mercury dissolution of Tibetan medicine Zuotai in simulated gastric juice and intestinal juice," *Chinese Traditional Patent Medicine*, vol. 40, no. 10, pp. 2302–2304, 2018.

[33] W. Li, R. Li, S. Zhao, C. Jiang, Z. Liu, and X. Tang, "Lithium posttreatment alleviates blood-brain barrier injury after intracerebral hemorrhage in rats," *Neuroscience*, vol. 383, pp. 129–137, 2018.

[34] Y. F. Shi, M. Y. Xie, and S. P. Nie, "Study on elemental speciation analysis and transference characteristics of Arnebia euthroma (Royle) Johnst by ICP-MS," *Spectroscopy and Spectral Analysis*, vol. 27, no. 2, p. 378, 2007.

[35] M. M. Wang, Y. Z. Lv, and L. Suo, "The current situation and countermeasures of the development of Tibetan medicine with mercury refining method and Tibetan medicine," *Journal of Medicine & Pharmacy of Chinese Minorities*, vol. 24, no. 12, pp. 26–28, 2018.

Hindawi
Evidence-Based Complementary and Alternative Medicine
Volume 2021, Article ID 5773802, 9 pages
https://doi.org/10.1155/2021/5773802

Research Article

Exploring the Mechanisms of Arsenic Trioxide (*Pishuang*) in Hepatocellular Carcinoma Based on Network Pharmacology

Xinmiao Wang,[1] **Luchang Cao**,[1] **Jingyuan Wu**,[1,2] **Guanghui Zhu**,[1,2] **Xiaoyu Zhu**,[1] **Xiaoxiao Zhang**,[1] **Duoduo Han**,[1] **Ning Shui**,[1] **Baoyi Ni**,[1] **and Jie Li**[1]

[1]*Guang'anmen Hospital, China Academy of Chinese Medical Sciences, Beijing 100053, China*
[2]*Beijing University of Traditional Chinese Medicine, Beijing 100029, China*

Correspondence should be addressed to Jie Li; qfm2020jieli@yeah.net

Received 14 October 2021; Accepted 15 November 2021; Published 29 November 2021

Academic Editor: Jie Liu

Copyright © 2021 Xinmiao Wang et al. This is an open access article distributed under the Creative Commons Attribution License, which permits unrestricted use, distribution, and reproduction in any medium, provided the original work is properly cited.

Objective. Arsenic trioxide (*Pishuang*, Pishi, arsenolite, As_2O_3, and CAS 1327-53-3), a naturally occurring and toxic mineral as a drug for more than 2000 years in China, has been found to have a valuable function in hepatocellular carcinoma (HCC) in recent years. However, its exact mechanism remains to be elucidated. Therefore, this study was intended to explore the potential anti-HCC mechanism of arsenic trioxide through network pharmacology. *Methods*. The potential targets of arsenic trioxide were collected from PubChem and TargetNet. HCC targets were obtained from the GeneCards database. Then, a protein-protein interaction (PPI) network of arsenic trioxide and HCC common targets was established using STRING. GO and KEGG pathway enrichment analyses were performed by the Database for Annotation, Visualization, and Integrated Discovery (DAVID). Finally, an arsenic trioxide-target-pathway-HCC network was built by Cytoscape 3.2.1, and network topological analysis was carried out to screen the key candidate targets. *Results*. A total of 346 corresponding targets of arsenic trioxide and 521 HCC-related targets were collected. After target mapping, a total of 52 common targets were obtained. GO analysis showed that the biological process was mainly involved in the negative regulation of cellular senescence, response to tumor necrosis factor, and cellular response to hypoxia. Molecular functions included NF-kappa B binding, enzyme binding, p53 binding, and transcription factor binding. Cellular components mainly were replication fork, ESC/E(Z) complex, RNA polymerase II transcription factor complex, and organelle membrane. KEGG pathways were mainly enriched in the PI3K-Akt signaling pathway, VEGF signaling pathway, p53 signaling pathway, HIF-1 signaling pathway, TNF signaling pathway, AMPK signaling pathway, NF-kappa B signaling pathway, FoxO signaling pathway, ErbB signaling pathway, and MAPK signaling pathway. In the arsenic trioxide-target-pathway-HCC network, targets such as AKT1, RAF1, RELA, TP53, and PTEN had a higher degree. *Conclusions*. Our study showed that key targets of arsenic trioxide were mainly involved in multiple biological processes and pathways. It provided a theoretical basis for the screening of drug targets.

1. Introduction

Hepatocellular carcinoma (HCC) is a common malignant tumor with poor prognosis, characterized by strong invasion and rapid growth [1]. According to the latest data released by the International Agency for Research on Cancer (IARC), the incidence and mortality of HCC ranked 6th and 3rd among all cancers, respectively. The total number of new HCC cases worldwide was 905,677, accounting for 4.7% of all new cancer cases, while the number of HCC deaths was 830,180, accounting for 8.3% of all cancer deaths. The current therapies mainly include hepatic resection, liver transplantation, transarterial chemoembolization (TACE), and ablation. Meanwhile, the small-molecule targeted drugs such as sorafenib and lenvatinib and monoclonal antibodies such as nivolumab are also used for the systematic treatment of advanced HCC [2]. In spite of the development of modern medicine, the present therapeutic options of HCC are still limited. For example, all the registered studies including sorafenib failed to find any treatment to improve recurrence-free survival. In addition, tumor recurrence rate after surgery or ablation of HCC is as high as 70% [3]. Therefore, new

anti-HCC therapies are urgently needed to improve the poor prognosis.

Nature is a rich source of natural products, among which minerals have attracted widespread attention in drug research and development because of their multitargeted activities and potential effect of anticancer. Arsenic trioxide (*Pishuang*, in Chinese Pinyin, As_2O_3, and CAS 1327-53-3), a natural and toxic substance be applied as a drug for more than 2000 years in China, has been found to have a valuable function in acute promyelocytic leukemia in recent years [4, 5]. Interestingly, studies have reported that arsenic trioxide has antineoplastic effects on HCC *in vitro* and *in vivo*. For instance, Bian et al. reported that the HCC patients who used arsenic trioxide transcatheter hepatic artery chemoembolization interventional therapy have a higher total effective rate and 1-year and 2-year survival rates than the control group ($P < 0.05$) [6]. Wang demonstrated that arsenic trioxide can inhibit proliferation and induce apoptosis of HCC cells through the ROS-mediated mitochondrial pathway [7]. Deng showed that arsenic trioxide could inhibit the growth of HCC subcutaneous transplanted tumors of nude mice and induce the apoptosis of hepatoma HepG2 cells [8]. Cai et al. proved that arsenic trioxide could induce upregulation of miR-1294 and suppress tumor growth in HCC cells by targeting TEAD1 and PIM1 [9]. Hu et al. reported that As_2O_3 nanoparticles could inhibit HCC tumor growth in the mice model, likely through downregulating PCNA- and DNMT-related proteins and upregulating GSDME-N [10]. Zhang et al. found that arsenic trioxide combined with canstatin could significantly inhibit HCC cell proliferation, migration, and adhesion abilities, promoted cell apoptosis, and inhibited tumor growth *in vitro* and *in vivo* [11]. It is observed that arsenic trioxide has a considerable prospect in the treatment of HCC. However, the exact mechanism underlying the therapeutic action of arsenic trioxide against HCC remains to be elucidated due to its character of multitarget and multipathway.

Network pharmacology is a new discipline to explore the mechanism of drug efficacy [12]. It is a research method for designing multitarget drug molecules by selecting the key nodes in the network based on the theory of systems biology and network analysis. Not only does it benefit to the success rate of drug screening in clinical trials but also contribute to seeking for the most effective treatment for patients [13]. Therefore, this study was intended to explore the potential anti-HCC mechanism of arsenic trioxide through network pharmacology (Figure 1).

2. Materials and Methods

2.1. Collecting Targets of Arsenic Trioxide. We collected targets of arsenic trioxide by the following 3 ways: (1) by importing "CAS 1327-53-3" in PubChem [14] (https://pubchem.ncbi.nlm.nih.gov/), we collected targets' information (full name and gene symbol) of arsenic trioxide in "Chemical-Gene Co-Occurrences in Literature" and then applied UniProt [15] (https://www.uniprot.org/) to supplement their UniProt ID. (2) By inputting "CAS 1327-53-3" in PubChem, we obtained arsenic trioxide-related targets' information in "BioAssay Results" and used UniProt to collect their UniProt ID. (3) The arsenic trioxide-related targets' information was collected by inputting SMILES "O1[As]2O[As]3O[As]1O[As](O2)O3" in TargetNet [16] (http://targetnet.scbdd.com/). Targets in which prediction probability was 0 should be removed.

2.2. Collection of HCC-Related Targets. HCC-related targets were collected by retrieving "hepatocellular carcinoma" and "liver cancer" in GeneCards [17] (https://www.genecards.org/, version: 5.3). Only targets with "relevance score ≥20" could be included. The collected information included gene full name, gene symbol, and UniProt ID.

2.3. Construction of the Protein-Protein Interaction (PPI) Network. By mapping arsenic trioxide targets and HCC targets, we obtained arsenic trioxide and HCC common targets. Then, PPI network was constructed (combined score ≥0.9) through STRING [18] (http://string-db.org, version 11.0). The OmicShare tools (https://www.Omicshare.com/) were used to draw Venn diagrams.

2.4. GO and KEGG Analyses. Gene ontology (GO) and Kyoto Encyclopedia of Genes and Genomes (KEGG) analyses were performed by the Database for Annotation, Visualization, and Integrated Discovery [19] (DAVID, http://david.ncifcrf.Gov, version: 6.8). GO mainly included molecular function (MF), biological process (BP), and cellular component (CC). KEGG was used to identify the main anti-HCC signaling pathways of arsenic trioxide. In this study, we selected 20 GO terms and 10 KEGG pathways to be visualized by OmicShare tools.

2.5. Construction of the Arsenic Trioxide-Target-Pathway-HCC Network and Screening of Candidate Targets. The arsenic trioxide-target-pathway-HCC network was built by Cytoscape 3.2.1 [20] (http://www.cytoscape.org/). Network topological analysis was carried out to screen the key candidate targets. The topological parameters (degree, average shortest path length, closeness centrality, neighborhood connectivity, and radiality) of every node in the network were analysed, and all the results were ranked by "degree."

3. Results

3.1. Collection of Arsenic Trioxide Targets. We obtained 34 targets in PubChem "Chemical-Gene Co-Occurrences in Literature," 17 targets in PubChem "BioAssay Results," and 310 targets collected from TargetNet. Finally, a total of 346 targets of arsenic trioxide were obtained after removing repeated targets (Supplementary Table S1).

3.2. Collection of HCC Targets. With the filtering criteria of "relevance score ≥20," a total of 521 HCC-related targets were collected (Supplementary Table S2).

3.3. Construction of the PPI Network. After mapping arsenic trioxide targets and HCC targets, a total of 52 common targets were obtained (Figure 2). To better understand the

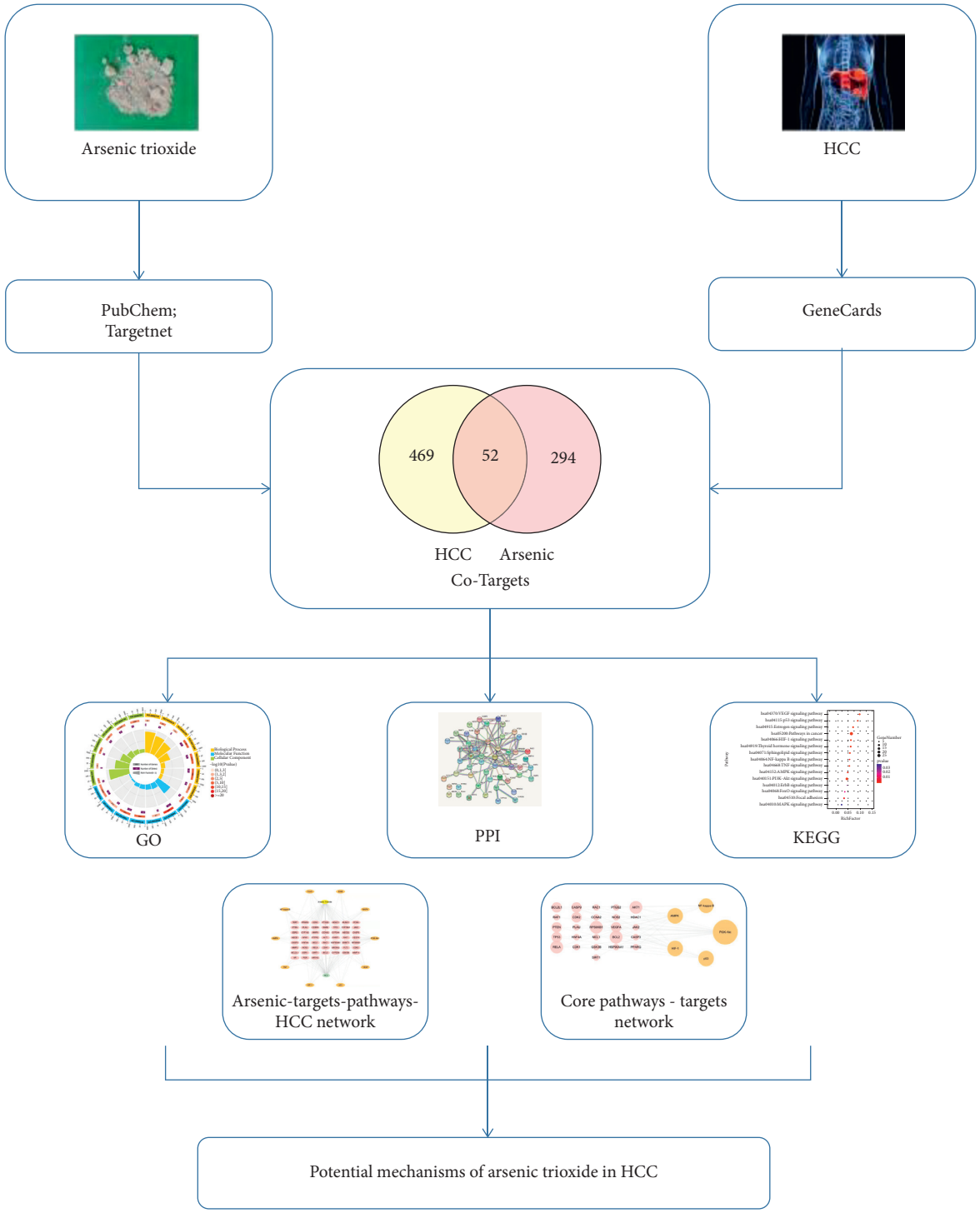

Figure 1: Workflow for arsenic trioxide against HCC.

interactive relationships between the common targets, a PPI network (combined score ≥0.9) was built by STRING (Figure 3).

3.4. GO and KEGG Analyses. GO analysis showed that the biological process was mainly involved in the negative regulation of cellular senescence, response to tumor necrosis factor, cellular response to hepatocyte growth factor stimulus, and cellular response to hypoxia. Molecular functions included NF-kappa B binding, enzyme binding, p53 binding, and transcription factor binding. Cellular components mainly were replication fork, ESC/E(Z) complex, RNA polymerase II transcription factor complex, and organelle membrane (Figure 4).

There were 70 KEGG pathways obtained by DAVID, among which 59 pathways' P values were less than 0.05 (Supplementary Table S3). As shown in Figure 5, pathways

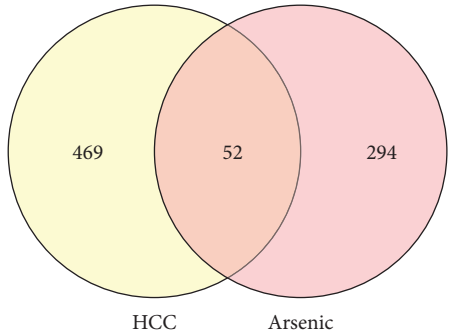

Figure 2: Venn diagram of arsenic trioxide (*Pishuang*) targets and HCC targets.

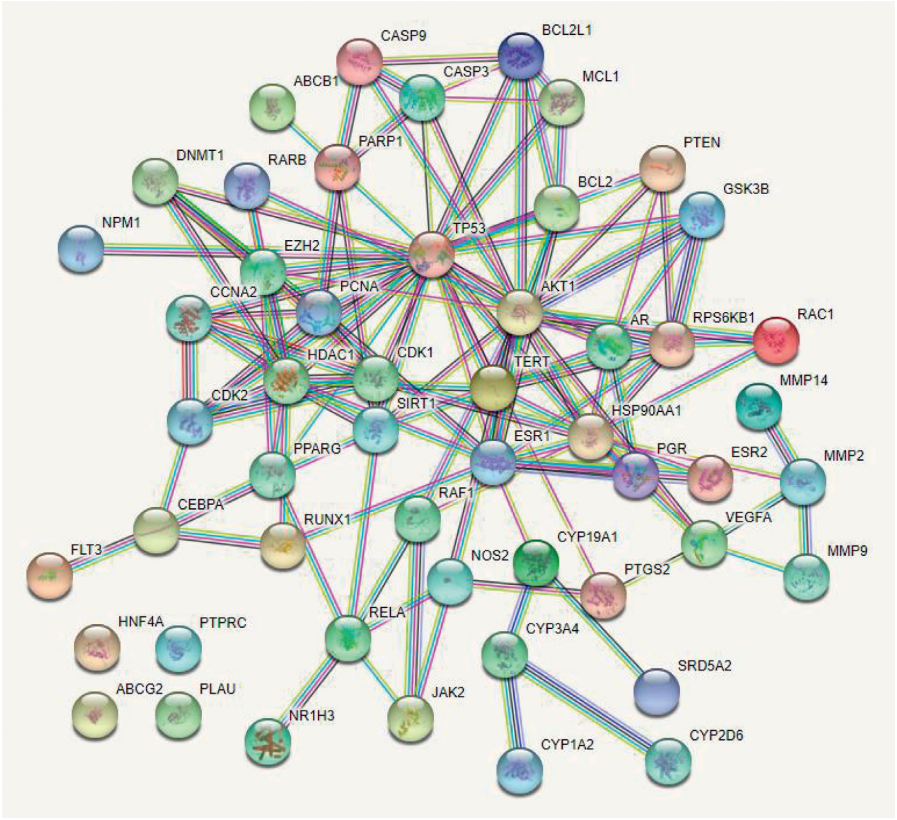

Figure 3: PPI network of common targets. Network nodes represent proteins. Edges represent protein-protein associations.

closely associated with HCC included the VEGF signaling pathway, p53 signaling pathway, HIF-1 signaling pathway, NF-kappa B signaling pathway, TNF signaling pathway, AMPK signaling pathway, PI3K-Akt signaling pathway, ErbB signaling pathway, FoxO signaling pathway, MAPK signaling pathway, estrogen signaling pathway, pathways in cancer, thyroid hormone signaling pathway, focal adhesion, and sphingolipid signaling pathway.

3.5. Construction of the Arsenic Trioxide-Target-Pathway-HCC Network and Screening of Candidate Targets. Based on the common targets' and pathways' information, an arsenic trioxide-target-pathway-HCC network was constructed by Cytoscape 3.2.1 (Figure 6). The network topology analysis showed that targets such as AKT1, RAF1, RELA, RPS6KB1, TP53, and PTEN and pathways such as the PI3K-Akt signaling pathway, VEGF signaling pathway, p53 signaling pathway, and HIF-1 signaling pathway had a higher degree (Tables 1 and 2).

Combining the research hotpots of HCC, we screened five pathways as the core pathways, and the relationships between each pathway and genes are shown in Figure 7.

4. Discussion

In this study, we obtained 346 targets of arsenic trioxide and 52 arsenic trioxide and HCC targets in common, which suggested that arsenic trioxide might be effective on HCC suppression by multitargets. As shown in the networks of

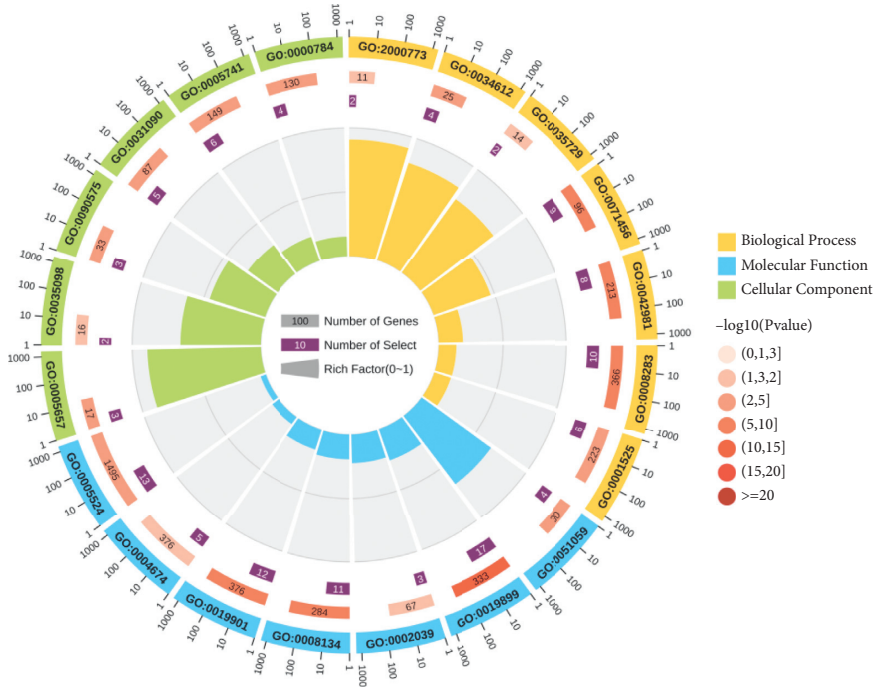

Figure 4: GO analysis. There are four circles in the figure. From outside to inside, the first circle is the classification of enrichment. Different colors represent different classifications. The second circle shows the number of background genes and *P* value. The more the genes, the longer the bars; the smaller the *P* value, redder the color. The third circle is the total number of prospective genes. The fourth circle represents rich factor, which indicates the ratio of genes in the current study versus the total genes in the term. GO:0071456: cellular response to hypoxia; GO:0008283: cell proliferation; GO:0042981: regulation of apoptotic process; GO:0034612: response to tumor necrosis factor; GO:0001525: angiogenesis; GO:2000773: negative regulation of cellular senescence; GO:0035729: cellular response to hepatocyte growth factor stimulus; GO:0005741: mitochondrial outer membrane; GO:0031090: organelle membrane; GO:0005657: replication fork; GO:0090575: RNA polymerase II transcription factor complex; GO:0000784: nuclear chromosome, telomeric region; GO:0035098: ESC/E(Z) complex; GO:0019899: enzyme binding; GO:0008134: transcription factor binding; GO:0019901: protein kinase binding; GO:0051059: NF-kappa B binding; GO:0005524: ATP binding; GO:0002039: p53 binding; GO:0004674: protein serine/threonine kinase activity.

arsenic trioxide-target-pathway-HCC and core pathway-target, nodes of AKT1, RAF1, TP53, and PTEN have a higher degree, indicating that they might be the key targets of arsenic trioxide for HCC therapy. Interestingly, AKT1 could regulate GSK-3β phosphorylation, another important target in the network and an isoform of GSK-3 which ubiquitously expressed serine/threonine kinase. Studies showed that regulating the Akt1/GSK-3β pathway could change HCC cell viability and migration [21]. Furthermore, it was reported that activation of GSK-3β contributed to arsenic trioxide-induced apoptosis in cancer cells [22]. As the significant marker in cancer treatment, RAF1 was found to overexpress in various cancers [23–25]. Accordingly, RAF-targeted small-molecule inhibitors have been applied in HCC and demonstrated high efficacy [26]. It was observed that the expression of RAF1 decreased following treatment with selective arsenic trioxide doses (1 μM) [27]. The tumor suppressor PTEN is also a phosphoinositide phosphatase regulating the PI3K/Akt signaling pathway. Recent studies showed that PTEN mutations/deletions or low PTEN expression are closely related to HCC [28]. Goussetis and Platanias demonstrated that arsenic trioxide can induce upregulation of PTEN [29]. In the situation of TP53 mutation, cells with DNA damage can escape apoptosis and transform into cancer cells [30], which existed in at least 25% of HCC patients [31]. The high mutation rate of TP53 makes it to be a very promising potential therapeutic target. What is more exciting is that mutant p53 protein can be targeted by arsenic trioxide for degradation and plays a role in arsenic trioxide-mediated growth suppression [32].

GO analysis showed that the targets were mainly enriched in the regulation of cellular senescence, response to tumor necrosis factor, and hypoxia. Senescence is a cellular state in which cells lose their ability to proliferate [33]. A study showed that senescent cells could regulate immune cell activity and clear away atypical proliferative hepatocytes by secreting senescence-associated secretory phenotype factors [34]. Interestingly, Cheng et al. found that arsenic trioxide could induce a significant dose-related increase in the incidence of cellular senescence [35]. In addition, due to the imbalance between the rate of tumor cell proliferation and nutrient supply of vascular [36], hypoxia is a characteristic of solid tumors. Studies have shown that hypoxia occurred in the metastasis, poor prognosis, and radiation resistance of HCC [37, 38]. Arsenic trioxide could promote the apoptosis of cancer cells via hypoxia-inducible factor (HIF)-1α [39]. Most factors that regulate the progression of HCC are closely associated with inflammation. TNF-α, an important inflammatory mediator in immune responses, was demonstrated to induce tumor cell lysis [40, 41]. Furthermore,

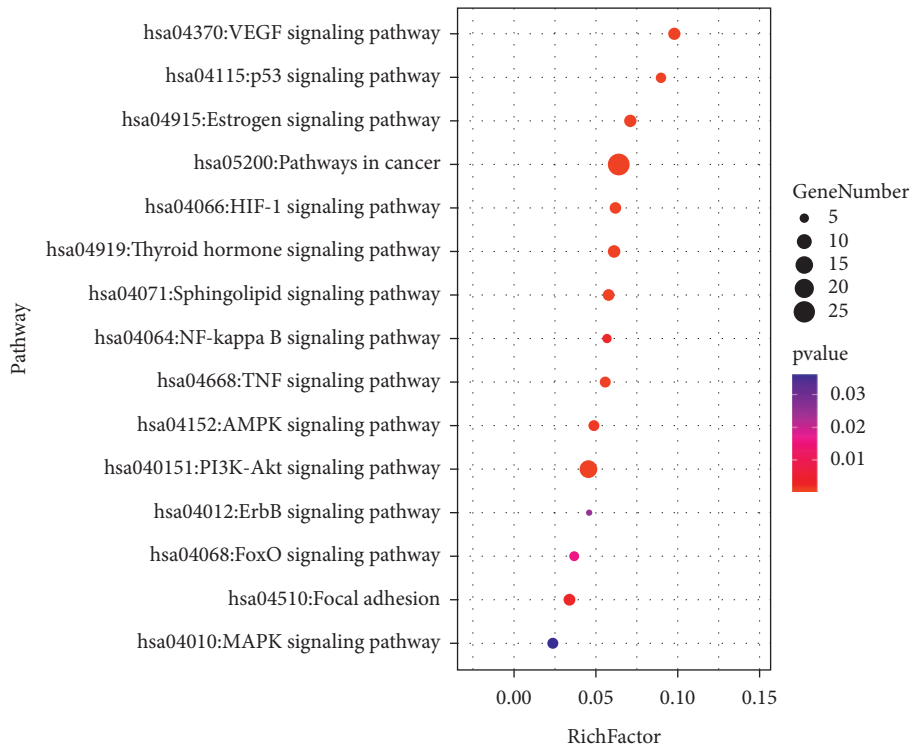

Figure 5: KEGG analysis. Node color is displayed in a gradient from red to green in the descending order of the *P* value. The size of the nodes is arranged in the ascending order according to the number of genes. Rich factor is the ratio of genes in the current study versus the total genes in the term.

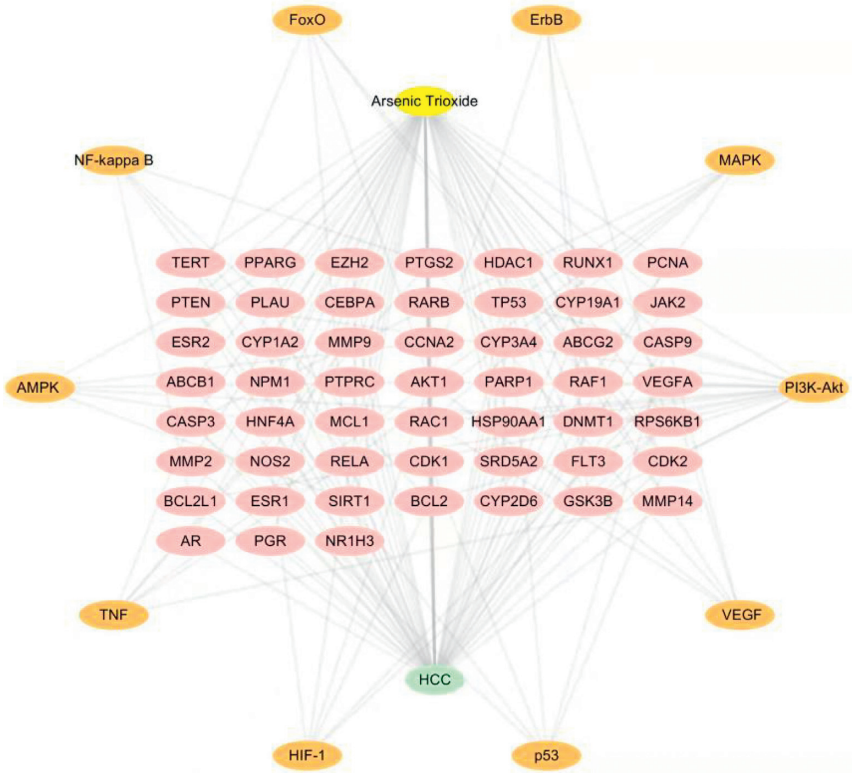

Figure 6: Arsenic trioxide-target-pathway-HCC network. Yellow node represents arsenic trioxide, green node represents HCC, pink nodes represent common targets, and orange nodes represent pathways.

Table 1: Network topology analysis of targets (top 20 of degree).

No.	Targets	Degree	Average shortest path length	Closeness centrality	Neighborhood connectivity	Radiality
1	AKT1	10	1.873	0.534	15.900	0.782
2	RAF1	7	1.968	0.508	20.143	0.758
3	RELA	7	1.968	0.508	20.429	0.758
4	RPS6KB1	6	2.000	0.500	22.667	0.750
5	TP53	5	2.032	0.492	26.400	0.742
6	PTEN	5	2.032	0.492	26.200	0.742
7	VEGFA	5	2.032	0.492	26.400	0.742
8	CASP3	5	2.032	0.492	24.400	0.742
9	PTGS2	5	2.032	0.492	24.200	0.742
10	BCL2	5	2.032	0.492	26.200	0.742
11	CASP9	5	2.032	0.492	26.400	0.742
12	CDK2	5	2.032	0.492	26.200	0.742
13	RAC1	5	2.032	0.492	26.400	0.742
14	BCL2L1	4	2.063	0.485	31.250	0.734
15	GSK-3B	4	2.063	0.485	31.000	0.7341
16	SIRT1	4	2.063	0.485	28.750	0.7341
17	PPARG	3	2.095	0.477	36.667	0.726
18	JAK2	3	2.095	0.477	40.000	0.726
19	MMP9	3	2.095	0.477	36.667	0.726
20	HNF4A	3	2.095	0.477	36.667	0.726

Table 2: Network topology analysis of pathways.

No.	Entry ID	Pathway	Degree	Average shortest path length	Closeness centrality	Neighborhood connectivity	Radiality
1	hsa04151	PI3K-Akt signaling pathway	16	2.317	0.432	5.125	0.671
2	hsa04370	VEGF signaling pathway	6	2.635	0.380	6.167	0.591
3	hsa04115	p53 signaling pathway	6	2.762	0.362	4.667	0.560
4	hsa04066	HIF-1 signaling pathway	6	2.667	0.375	6.000	0.583
5	hsa04668	TNF signaling pathway	6	2.635	0.380	5.500	0.591
6	hsa04152	AMPK signaling pathway	6	2.698	0.371	4.833	0.575
7	hsa04010	MAPK signaling pathway	6	2.635	0.380	6.500	0.591
8	hsa04064	NF-kappa B signaling pathway	5	2.794	0.358	4.800	0.552
9	hsa04068	FoxO signaling pathway	5	2.698	0.371	6.200	0.575
10	hsa04012	ErbB signaling pathway	4	2.762	0.362	6.750	0.560

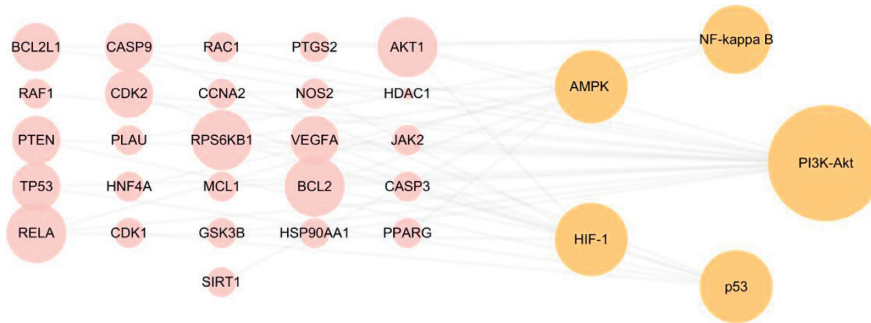

Figure 7: Core pathway-target network. Pink nodes represent targets, and orange nodes represent pathways. The nodes' size was determined by degree. The larger the node, the higher the degree.

TNF-α expression was upregulated during the apoptosis of tumor cells by arsenic trioxide [42]. Notably, the results of KEGG pathway analysis were highly coincident with GO analysis. For example, HIFs are the "master" transcription factors responsible for gene expression in hypoxia [43]. Regulating the PI3K/Akt pathway and HIF-1α protein synthesis can inhibit hypoxia-induced angiogenesis and metastasis [44]. Mutant p53 induces a hypoxia transcriptional program in the tumor [45]. AMPK and NF-kappa B pathways were also found to participate in the inflammatory

response during hypoxia and reoxygenation [46]. Accordingly, we speculate that arsenic trioxide may play an anti-HCC role through the regulation of cellular senescence, tumor necrosis factor, and hypoxia and is closely related to HIF, PI3K/Akt, p53, AMPK, and NF-kappa B pathways. In addition, although there is a lack of direct evidence that arsenic trioxide exerts anti-HCC effect by the estrogen signaling pathway, thyroid hormone signaling pathway, focal adhesion, and sphingolipid signaling pathway, studies have reported that these pathways are extremely related with HCC [47–50] and have higher rich factor in KEGG analysis, which indicates that these pathways might be the potential anti-HCC pathways of arsenic trioxide and points out the way for our future research.

In conclusion, we undertake a network pharmacology approach to explore the underlying anti-HCC molecular mechanisms of arsenic trioxide, which could provide a theoretical basis for the screening of drug targets. Our study showed that key targets of arsenic trioxide were mainly involved in multiple biological processes and pathways. In the near future, the series of promising results need to be verified by additional research, including *in vitro* and *in vivo* experiments.

Data Availability

The data used to support the results of this study can be obtained from the corresponding author upon reasonable request.

Conflicts of Interest

The authors declare that there are no conflicts of interest.

Authors' Contributions

Xinmiao Wang, Luchang Cao, and Jingyuan Wu contributed equally to this work.

Supplementary Materials

Supplementary Table S1: arsenic trioxide targets. Supplementary Table S2: hepatocellular carcinoma targets. Supplementary Table S3: KEGG pathways ($P < 0.05$). (*Supplementary Materials*)

References

[1] W. Wang and C. Wei, "Advances in the early diagnosis of hepatocellular carcinoma," *Genes & Diseases*, vol. 7, no. 3, pp. 308–319, 2020.

[2] Z. Chen, H. Xie, M. Hu et al., "Recent progress in treatment of hepatocellular carcinoma," *American Journal of Cancer Research*, vol. 10, no. 9, pp. 2993–3036, 2020.

[3] X.-D. Zhu, K.-S. Li, and H.-C. Sun, "Adjuvant therapies after curative treatments for hepatocellular carcinoma: current status and prospects," *Genes & Diseases*, vol. 7, no. 3, pp. 359–369, 2020.

[4] H.-H. Zhu, J. Hu, F. Lo-Coco, and J. Jin, "The simpler, the better: oral arsenic for acute promyelocytic leukemia," *Blood*, vol. 134, no. 7, pp. 597–605, 2019.

[5] E. Lengfelder, W.-K. Hofmann, and D. Nowak, "Treatment of acute promyelocytic leukemia with arsenic trioxide: clinical results and open questions," *Expert Review of Anticancer Therapy*, vol. 13, no. 9, pp. 1035–1043, 2013.

[6] X. Bian, Z. Wang, and Z. Song, "Clinical efficacy and safety of arsenic trioxide in interventional treatment of advanced primary liver cancer with transcatheter hepatic arterial chemoembolization," *Journal of Clinical and Experimental Medicine*, vol. 20, no. 7, pp. 705–708, 2021.

[7] L. Wang, *The Mechanism of Arsenic Trioxide Induces Apoptosis in Human Hepatocellular Carcinoma Cells and ROS-Related Mitochondrial Pathway*, The Fourth Military Medical University, Xi'an, China, 2014.

[8] Z. T. Deng, *Research on the Mechanism of Autophagy and Apoptosis Induced by Arsenic Trioxide in Hepatic Carcinoma Cell*, Nanjing University of Chinese Medicine, Nanjing, China, 2015.

[9] X. Cai, L. Yu, Z. Chen, F. Ye, Z. Ren, and P. Jin, "Arsenic trioxide-induced upregulation of miR-1294 suppresses tumor growth in hepatocellular carcinoma by targeting TEAD1 and PIM1," *Cancer Biomarkers*, vol. 28, no. 2, pp. 221–230, 2020.

[10] J. Hu, Y. Dong, L. Ding et al., "Local delivery of arsenic trioxide nanoparticles for hepatocellular carcinoma treatment," *Signal Transduction and Targeted Therapy*, vol. 4, no. 1, p. 28, 2019.

[11] F. Zhang, J. Duan, H. Song, L. Yang, M. Zhou, and X. Wang, "Combination of canstatin and arsenic trioxide suppresses the development of hepatocellular carcinoma," *Drug Development Research*, vol. 82, no. 3, pp. 430–439, 2021.

[12] A. L. Hopkins, "Network pharmacology: the next paradigm in drug discovery," *Nature Chemical Biology*, vol. 4, no. 11, pp. 682–690, 2008.

[13] W. Zhou, Y. Wang, A. Lu, and G. Zhang, "Systems pharmacology in small molecular drug discovery," *International Journal of Molecular Sciences*, vol. 17, no. 2, p. 246, 2016.

[14] S. Kim, J. Chen, T. Cheng et al., "PubChem in 2021: new data content and improved web interfaces," *Nucleic Acids Research*, vol. 49, pp. D1388–D1395, 2021.

[15] UniProt, "UniProt: a worldwide hub of protein knowledge," *Nucleic Acids Research*, vol. 47, pp. D506–D515, 2019.

[16] Z.-J. Yao, J. Dong, Y.-J. Che et al., "TargetNet: a web service for predicting potential drug-target interaction profiling via multi-target SAR models," *Journal of Computer-Aided Molecular Design*, vol. 30, no. 5, pp. 413–424, 2016.

[17] G. Stelzer, N. Rosen, I. Plaschkes et al., "The GeneCards suite: from gene data mining to disease genome sequence analyses," *Current Protocols in Bioinformatics*, vol. 54, no. 1, pp. 1–30, 2016.

[18] C. v. Mering, M. Huynen, D. Jaeggi, S. Schmidt, P. Bork, and B. Snel, "STRING: a database of predicted functional associations between proteins," *Nucleic Acids Research*, vol. 31, no. 1, pp. 258–261, 2003.

[19] G. J. Dennis, B. T. Sherman, D. A. Hosack, J. Yang, W. Gao, and H. C. Lane, "DAVID: database for annotation, visualization, and integrated discovery," *Genome Biology*, vol. 4, no. 5, 2003.

[20] P. Shannon, A. Markiel, O. Ozier et al., "Cytoscape: a software environment for integrated models of biomolecular interaction networks," *Genome Research*, vol. 13, no. 11, pp. 2498–2504, 2003.

[21] Z.-W. Zhong, W.-C. Zhou, X.-F. Sun, Q.-C. Wu, W.-K. Chen, and C.-H. Miao, "Dezocine regulates the malignant potential and aerobic glycolysis of liver cancer targeting Akt1/GSK-3β pathway," *Annals of Translational Medicine*, vol. 8, no. 7, p. 480, 2020.

[22] R. Wang, L. Xia, J. Gabrilove, S. Waxman, and Y. Jing, "Downregulation of Mcl-1 through GSK-3β activation contributes to arsenic trioxide-induced apoptosis in acute myeloid leukemia cells," *Leukemia*, vol. 27, no. 2, pp. 315–324, 2013.

[23] W. J. Tan, J. C. Lai, A. A. Thike et al., "Novel genetic aberrations in breast phyllodes tumours: comparison between prognostically distinct groups," *Breast Cancer Research and Treatment*, vol. 145, no. 3, pp. 635–645, 2014.

[24] Z. H. Xu, J. B. Hang, J. A. Hu, and B. L. Gao, "RAF1-MEK1-ERK/AKT axis may confer NSCLC cell lines resistance to erlotinib," *International Journal of Clinical and Experimental Pathology*, vol. 6, no. 8, pp. 1493–1504, 2013.

[25] F. Wang, C. Jiang, Q. Sun et al., "miR-195 is a key regulator of Raf1 in thyroid cancer," *OncoTargets and Therapy*, vol. 8, pp. 3021–3028, 2015.

[26] A. Gauthier and M. Ho, "Role of sorafenib in the treatment of advanced hepatocellular carcinoma: an update," *Hepatology Research*, vol. 43, no. 2, pp. 147–154, 2013.

[27] K. M. Mohammadi, A. Haghi, M. Salami, B. Chahardouli, S. H. Rostami, and K. Malekzadeh, "Arsenic trioxide and thalidomide combination induces autophagy along with apoptosis in acute myeloid cell lines," *Cell Journal*, vol. 22, no. 2, pp. 193–202, 2020.

[28] M. Vinciguerra and M. Foti, "PTEN at the crossroad of metabolic diseases and cancer in the liver," *Annals of Hepatology*, vol. 7, no. 3, pp. 192–199, 2008.

[29] D. J. Goussetis and L. C. Platanias, "Arsenic trioxide and the phosphoinositide 3-kinase/akt pathway in chronic lymphocytic leukemia: fig. 1," *Clinical Cancer Research*, vol. 16, no. 17, pp. 4311-4312, 2010.

[30] J. Long, A. Wang, Y. Bai et al., "Development and validation of a TP53-associated immune prognostic model for hepatocellular carcinoma," *EBioMedicine*, vol. 42, pp. 363–374, 2019.

[31] J.-S. Lee, "The mutational landscape of hepatocellular carcinoma," *Clinical and Molecular Hepatology*, vol. 21, no. 3, pp. 220–229, 2015.

[32] W. Yan, Y. Zhang, J. Zhang, S. Liu, S. J. Cho, and X. Chen, "Mutant p53 protein is targeted by arsenic for degradation and plays a role in arsenic-mediated growth suppression," *Journal of Biological Chemistry*, vol. 286, no. 20, pp. 17478–17486, 2011.

[33] N. D. Karakousis, A. Papatheodoridi, A. Chatzigeorgiou, and G. Papatheodoridis, "Cellular senescence and hepatitis B-related hepatocellular carcinoma: an intriguing link," *Liver International*, vol. 40, no. 12, pp. 2917–2927, 2020.

[34] C. Wang, W.-J. Chen, Y.-F. Wu et al., "The extent of liver injury determines hepatocyte fate toward senescence or cancer," *Cell Death & Disease*, vol. 9, no. 5, p. 575, 2018.

[35] Y. Cheng, Y. Li, C. Ma et al., "Arsenic trioxide inhibits glioma cell growth through induction of telomerase displacement and telomere dysfunction," *Oncotarget*, vol. 7, no. 11, pp. 12682–12692, 2016.

[36] L. H. Gray, A. D. Conger, M. Ebert, S. Hornsey, and O. C. A. Scott, "The concentration of oxygen dissolved in tissues at the time of irradiation as a factor in radiotherapy," *British Journal of Radiology*, vol. 26, no. 312, pp. 638–648, 1953.

[37] J. T. Erler and A. J. Giaccia, "Lysyl oxidase mediates hypoxic control of metastasis: figure 1," *Cancer Research*, vol. 66, no. 21, pp. 10238–10241, 2006.

[38] K. Graham and E. Unger, "Overcoming tumor hypoxia as a barrier to radiotherapy, chemotherapy and immunotherapy in cancer treatment," *International Journal of Nanomedicine*, vol. 13, pp. 6049–6058, 2018.

[39] L. Zhang, Y. Zhou, J. Kong et al., "Effect of arsenic trioxide on cervical cancer and its mechanisms," *Experimental and Therapeutic Medicine*, vol. 20, no. 6, p. 1, 2020.

[40] H. Wang, J. Liu, X. Hu, S. Liu, and B. He, "Prognostic and therapeutic values of tumor necrosis factor-alpha in hepatocellular carcinoma," *Medical Science Monitor*, vol. 22, pp. 3694–3704, 2016.

[41] F. Balkwill, "TNF-α in promotion and progression of cancer," *Cancer and Metastasis Reviews*, vol. 25, no. 3, pp. 409–416, 2006.

[42] Y. Z. Chen, Y. Wu, M. J. Huang, and L. H. Lv, "Effect of endogenous TGF-β1 and TNF-α on the As2O3 inducing apoptosis of HL-60 cells," *Chinese Journal of Hematology*, vol. 5, pp. 10–13, 2003.

[43] S. Shu, Y. Wang, M. Zheng et al., "Hypoxia and hypoxia-inducible factors in kidney injury and repair," *Cells*, vol. 8, no. 3, pp. 207–3, 2019.

[44] K. Patra, S. Jana, A. Sarkar, D. P. Mandal, and S. Bhattacharjee, "The inhibition of hypoxia-induced angiogenesis and metastasis by cinnamaldehyde is mediated by decreasing HIF-1α protein synthesis via PI3K/Akt pathway," *BioFactors*, vol. 45, no. 3, pp. 401–415, 2019.

[45] N. Sethi, O. Kikuchi, J. McFarland et al., "Mutant p53 induces a hypoxia transcriptional program in gastric and esophageal adenocarcinoma," *JCI Insight*, vol. 4, no. 15, 2019.

[46] X. Chen, X. Li, W. Zhang et al., "Activation of AMPK inhibits inflammatory response during hypoxia and reoxygenation through modulating JNK-mediated NF-κB pathway," *Metabolism*, vol. 83, pp. 256–270, 2018.

[47] O. A. Sukocheva, "Estrogen, estrogen receptors, and hepatocellular carcinoma: are we there yet?" *World Journal of Gastroenterology*, vol. 24, no. 1, pp. 1–4, 2018.

[48] P. Manka, J. D. Coombes, R. Boosman, K. Gauthier, S. Papa, and W. K. Syn, "Thyroid hormone in the regulation of hepatocellular carcinoma and its microenvironment," *Cancer Letters*, vol. 419, pp. 175–186, 2018.

[49] N. Shang, H. Wang, T. Bank et al., "Focal adhesion kinase and β-catenin cooperate to induce hepatocellular carcinoma," *Hepatology*, vol. 70, no. 5, pp. 1631–1645, 2019.

[50] J. Simon, A. Ouro, L. Ala-Ibanibo, N. Presa, T. C. Delgado, and M. L. Martínez-Chantar, "Sphingolipids in non-alcoholic fatty liver disease and hepatocellular carcinoma: ceramide turnover," *International Journal of Molecular Sciences*, vol. 21, no. 1, p. 40, 2019.

Hindawi
Evidence-Based Complementary and Alternative Medicine
Volume 2021, Article ID 2251679, 13 pages
https://doi.org/10.1155/2021/2251679

Research Article

Tibetan Medicine Qishiwei Zhenzhu Pills Can Reduce Cerebral Ischemia-Reperfusion Injury by Regulating Gut Microbiota and Inhibiting Inflammation

Ke Fu,[1] Dewei Zhang,[2] Yinglian Song,[1] Min Xu,[1] Ruixia Wu,[1] Xueqing Xiong,[2] Xianwu Liu,[1] Lei Wu,[1] Ya Guo,[2] You Zhou,[1] Xiaoli Li,[1] and Zhang Wang[3]

[1]*College of Pharmacy, Chengdu University of Traditional Chinese Medicine, Chengdu 611137, China*
[2]*Wanzhou Institute for Drug and Food Control, Chongqing 404000, China*
[3]*College of Ethnomedicine, Chengdu University of Traditional Chinese Medicine, Chengdu 611137, China*

Correspondence should be addressed to Zhang Wang; wangzhangcqcd@cdutcm.edu.cn

Received 4 October 2021; Revised 19 October 2021; Accepted 27 October 2021; Published 11 November 2021

Academic Editor: Jie Liu

Copyright © 2021 Ke Fu et al. This is an open access article distributed under the Creative Commons Attribution License, which permits unrestricted use, distribution, and reproduction in any medium, provided the original work is properly cited.

Cerebral ischemia is a series of harmful reactions, such as acute necrosis of tissue, inflammation, apoptosis, autophagy, and blood-brain barrier injury, due to the insufficient blood supply to the brain. Inflammatory response and gut microbiota imbalance are important concomitant factors of cerebral ischemia and may increase the severity of cerebral ischemia through the gut-brain axis. Qishiwei Zhenzhu pills (QSW) contain more than 70 kinds of medicinal materials, which have the effects of anti-cerebral infarction, anti-convulsion, anti-dementia, and so on. It is a treasure of Tibetan medicine commonly used in the treatment of cerebral ischemia in Tibetan areas. In this study, we gave rats QSW (66.68 mg/kg) once by gavage in advance and then immediately established the rat middle cerebral artery occlusion (MCAO) model. After 24 hours of treatment, the neuroprotection, intestinal pathology, and gut microbiota were examined. The results showed that QSW could significantly reduce the neurobehavioral abnormalities and cerebral infarction rate in MCAO rats. Furthermore, qPCR, western blot, and immunohistochemistry results showed that QSW could effectively inhibit IL-6, IL-1β, and other inflammatory factors so as to effectively reduce the inflammatory response of MCAO rats. Furthermore, QSW could improve intestinal integrity and reduce intestinal injury. 16S rRNA sequencing showed that QSW could significantly improve the gut microbiota disorder of MCAO rats. Specifically, at the phylum level, it can regulate the abundance of *Firmicutes* and *Proteobacteria* in the gut microbiota of rats with MCAO. At the genus level, it can adjust the abundance of *Escherichia* and *Shigella*. At the species level, it can adjust the abundance of *Lactobacillus johnsonii* and *Lactobacillus reuteri*. All in all, this study is the first to show that QSW can reduce the severity of cerebral ischemia-reperfusion injury by regulating gut microbiota and inhibiting the inflammatory response.

1. Introduction

Cerebral ischemia (CI) or ischemic stroke is due to insufficient blood supply to the brain, which causes hypoxia or ischemia in some areas [1]. Cerebral ischemia-reperfusion injury (I/R) refers to the damage of brain cells caused by CI. The brain is extremely sensitive to hypoxia or ischemia because it receives approximately 750–1,000 mL of blood flow every minute, and its oxygen consumption accounts for approximately 20% of the total for the entire human body. In China, the number of CI cases accounts for approximately 17% to 55% of stroke cases [2], a common clinical cardiovascular and cerebrovascular disease with a fatality rate of more than 40% within 1 month; however, effective treatments are still lacking [3]. Studies have shown that peripheral white blood cells, including T cells, B cells, and neutrophils, can also aggravate the symptoms of CI in the early stage of stroke and release proinflammatory mediators [4]. These immune cells and cytokines can interact not only with each other but also with brain cells. In addition, some clinical studies have found that metabolic syndrome patients with ischemic stroke have higher levels of inflammatory

markers and arterial stiffness index than healthy people [5]. All of these studies suggest that inflammation plays a key role in tissue damage after CI.

Gut microbiota are trillions of microorganisms that exist in the human gastrointestinal tract and are inextricably linked to the human body [6]. The microorganisms in the gut microbiota contain genes that are more than 100 times that of the human nuclear genome [7]. These species live in the intestine and perform physiological functions that are essential to humans. Symbiotic physiology occurs between the host and the gut microbiome [8, 9]. The gut microbiota regulates the immune and metabolic balance in the human intestine [6] and can be roughly divided into three categories according to their functions: beneficial, harmful, and conditional pathogenic bacteria. Beneficial bacteria (30%), which include *Lactobacillus*, *Eubacteria*, *Bacillus vulvae*, *Peptococcus*, *Clostridium lecani*, *Cocci*, *Clostridium butyricum*, and *Rossella*, mainly promote gastrointestinal peristalsis and absorption and vitamin synthesis. These organisms can also promote the excretion of harmful substances to the body and protect the body from pathogens. Harmful bacteria (10%), including *Escherichia coli*, *Staphylococcus*, *Streptococcus*, *Clostridium*, *Tetanus*, and *Bacteroides*, can produce harmful substances, increase the intestinal reabsorption of harmful substances, and lead to intestinal abnormal peristalsis, which makes the body vulnerable to pathogen invasion. Conditional pathogenic bacteria (60%), including *E. coli*, *Bacteroides*, *Desulfovibrio*, *Candida albicans*, *Pseudomonas aeruginosa*, and *Proteus*, live in harmony with the human body under normal conditions and will cause harm only under certain conditions [10]. The microbiota-gut-brain axis is a two-way communication network [11]. Several signal molecules (such as catecholamines, serotonin, dynorphin, and cytokines) used by the host for nerve and neuroendocrine signal transduction may also be secreted into the intestinal lumen by neurons, immune cells, and enterochromaffin cells for the gut-brain bidirectional communication [12].

Qishiwei Zhenzhu pills (QSW) are a commonly used traditional Tibetan medicine for treating "bai mai" disease in Tibetan areas, are included in the Pharmacopoeia of the People's Republic of China (2015 edition, Vol. I), and have anti-cerebral infarction [13], anti-convulsant [14], anti-dementia [15], and other effects. This medicine was first published in the Tibetan medicine classic Si Bu Yi Dian and is mainly used for the treatment of "bai mai" disease, stroke, paralysis, hemiplegia, cerebral hemorrhage, and other diseases [16, 17]. This recipe contains more than 70 kinds of medicinal materials, such as myrobalan, pearl, agate, opal, bezoar, coral, musk, gold, silver, and Zuotai [18]. Given its broad range of ingredients, the research on the material basis of its medicinal effects is relatively complicated. The Tibetan medicine Zuotai is the main component of many precious Tibetan medicine preparations (including QSW) and is mainly composed of mercury and other metal elements.

Our recent analysis of 18 elements in QSW revealed the majority of minerals are not absorbed and excreted in the feces, implying the importance of gut-brain axis in QSW-mediated neuroprotection [19]. Therefore, QSW, one of the most effective drugs for the treatment of CI/stroke in Tibetan medicine, could affect microbiota as a mechanism of action. An in-depth study of its action toward CI, inflammation, and microbiota will help provide a clear and deep understanding of QSW in the prevention and treatment of CI. A rat middle cerebral artery occlusion (MCAO) model was used to verify neuroprotective effects of QSW, and a panel of inflammatory mediators were examined via qPCR, western blot, and immunohistochemistry. 16S rRNA sequencing was used to analyze the effects of QSW on the gut microbiota of MCAO rats. The results clearly demonstrated the protective effects of QSW are related to its anti-inflammatory properties and importantly to its effects on gut microbiota regulation.

2. Materials and Methods

2.1. Drugs and Reagents. QSW (18055A) was purchased from Tibet Ganlu Tibetan Medicine Co. Ltd. Nimodiping (Nmdp, BJ45200) was purchased from Bayer medical and health care Co. Ltd. MN Nucleo Spin 96 Soil Kit, KOD FX Neo, and KOD FX Neo Buf (2X) were bought from TOYOBO. Animal Total RNA Isolation Kit was acquired from FOREGENE Company. Anti-IL-6 and IL-1β rabbit antibodies were purchased from Britain Abcam (Shanghai) Trading Co. Ltd. Anti-β-actin rabbit antibody was bought from Wuhan Aibotech Biotechnology Co. Ltd. Other chemicals, solvents, and reagents are of analytical grade.

2.2. Experimental Animal Model and Design. All Sprague–Dawley (SD) rats of SPF grade were obtained from Chengdu Dashuo Experimental Animal Co. Ltd. (license number: SCXK (Sichuan) 2015-030, experimental animal quality certificate number: 51203500008742). The SD rats were bred in an environment with a 12:12 h light/dark cycle, a room temperature of $25 \pm 2^{\circ}$C, and $50 \pm 5\%$ humidity. SD rats weighing 250 to 280 g were randomly divided into four groups as follows ($n = 6$/group; Figure 1): Sham, I/R, Nmdp (30 mg/kg, po) + I/R group, and QSW (66.68 mg/kg, po) + I/R group. The selected dose refers to the dose used in the previous experiment of the research group [20–22]. The experiment was conducted in the National Medicine Resource Evaluation Laboratory of Chengdu University of Traditional Chinese Medicine (the third-level scientific research laboratory of the State Administration of Traditional Chinese Medicine, NO. TCM-2009-320). The animal study was reviewed and approved by the Animal Care and Use Committee of Chengdu University of Traditional Chinese Medicine.

2.3. Middle Cerebral Artery Occlusion (MCAO) Modeling. Anesthetized rats were cut along the midline of the rat neck, and the myofascial membranes were isolated obtuse along the sternocleidomastoid muscle. The right common carotid artery (CCA), external carotid artery (ECA), and internal carotid artery (ICA) were separated, and ECA was litigated. The pterygopalatine artery inward along the ICA were separated and ligated at the bifurcation. An incision between

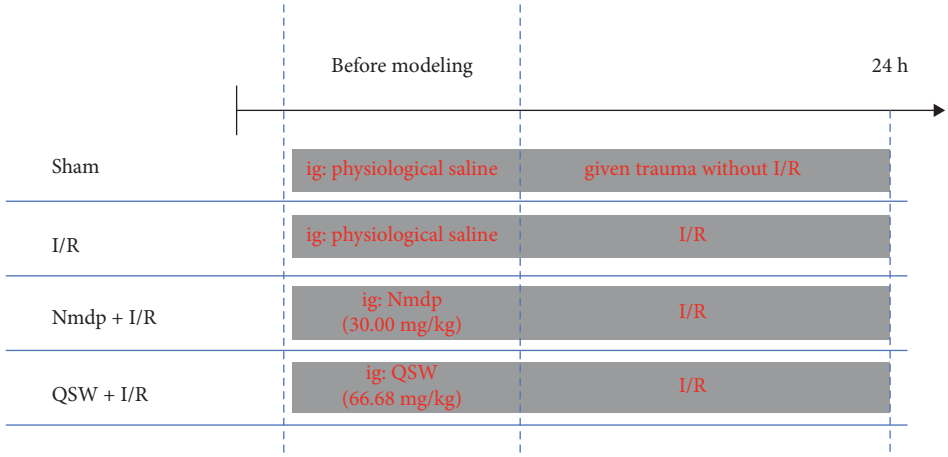

Figure 1: Experimental design.

the distal and proximal ends of the ECA was cut; the tie wire was inserted into the ICA about 20 mm; and the wound was sutured and sterilized. The Sham group only prepared sutures and did not make a model [23]. Following 2 h of CI in rats, the suture was slowly removed to achieve reperfusion. The neck wound was subsequently sutured, and iodophor disinfection was performed. Thereafter, rats were returned to the cage.

2.4. Neurological Deficit Score. Reflecting the neurological deficits, the neurobehavioral scores of the experimental rats were measured at 24 hours after CI; the five-level method was used [24, 25]: the first level (−) is no symptoms of nerve injury, the second level (+) is the inability to fully extend the left front paw, the third level (++) is turning to the left, the fourth level (+++) is dumping to the left, and the fifth level (++++) is unable to walk spontaneously and loss of consciousness.

2.5. Cerebral Infarction Ratio. Twenty-four hours after CI, rats were anesthetized, and blood was taken from the abdominal aorta and sacrificed. The process is as follows: Take out the whole brain, absorb the moisture on the surface and weigh it, freeze it in the refrigerator at −20°C for 20–30 min, cut it into five evenly with a blade, dye it with the prepared 1% TTC dye solution at 30°C for 30 min, then separate the infracted part (the pale part), use filter paper to absorb the surface moisture, and weigh again. Cerebral infarction ratio = weight of cerebral infarction part (g)/brain tissue weight (g) × 100%.

2.6. Histological Analysis. After the brain was taken, the ileum, cecum, and colon tissues were taken, washed with running water, rinsed with normal saline, and fixed in 10% neutral formaldehyde for intestinal pathological examination. Three indicators were measured in the ileum, including the height of the villi, the width of the villi, and the depth of the crypts. The measurement indicators of the cecum and colon tissue were the thickness of the mucosa.

2.7. Gut Microbiota Analysis. While taking the colon, the contents of the colon were collected in a 10 mL dry sterilized centrifuge tube, stored them in an ultralow temperature refrigerator at −80°C, and then sent to Biomarker Technologies (BMK) for 16S rRNA sequencing. Species taxonomy analysis, α diversity analysis [26], and species microbial composition structure analysis were performed using BMKCloud (http://www.biocloud.net).

2.8. Quantitative Real-Time Polymerase Chain Reaction Analysis. The rats were sacrificed by anesthesia after 24 h of CI, and the brain tissues from the ischemic side were placed in an ultralow temperature refrigerator at −80°C for testing. The RT fluorescent PCR system (total = 20 μL) consists of 2 × Real PCR EasyTM Mix-SYBR (10 μL), forward primer (10 μM, 0.8 μL), reverse primer (10 μM, 0.8 μL), template (DNA) (2 μL), and ddH2O (6.4 μL). Semiquantitative RT-PCR was performed using the following temperature scheme to determine the internal control (β-actin): 45 cycles of predenaturation at 95°C for 30 s, denaturation at 95°C for 5 s, annealing at 55°C for 30 s, extension at 72°C for 30 s, and fluorescence collection. The samples were analyzed by RT-PCR amplification curve and melting curve. $F = 2^{-\triangle\triangle CT}$ was used to calculate the relative amount of mRNA, $\triangle\triangle$CT = (average CT value of target gene in drug group- – average CT value of internal reference gene in the drug group) – (average CT value of target gene in the blank group – average of reference gene in blank group CT value). The gene primer sequence is listed in Table 1.

2.9. Western Blot Analysis. Brain samples were collected from the hippocampus of rats; RIPA lysis solution (brain tissue: lysis solution = 1:10) was added to the brain tissue; the brain samples were cut and placed on ice for 10 min lysis; the lysis solution (12,000 rpm; 4°C) was centrifuged for 10 min; and the supernatant was taken. The further process is as follows: dilute the stock solution, prepare a 1 mg/mL working solution, add 200 μL of BCA working solution, and place it at 37°C for 30 min. Take 50 μg from each experimental group, and add 5× loding buffer at a ratio of 4:1, heat

Table 1: Primers for real-time PCR.

Gene	Forward primer (5′-3′)	Reverse primer (5′-3′)
IL-6	ACAGAGGATACCACCCACAACAGACC	CGGAACTCCAGAAGACCAGAGCAGAT
IL-1β	ATCCTCTCCAGTCAGGCTTCCTTGTG	AGCTCTTGTCGAGATGCTGCTGTGA
p38-MAPK	GACGAATGGAAGAGCCTGACCTACGA	TGGACAAACGGACAGACAGACAGACA
TNF-α	CCAGCCAGGAGGGAGAACAGCAACT	CCGCCACGAGCAGGAATGAGAAGAG

cycle at 95°C for 15 min with a thermal cycler, and store the prepared working solution at −80°C. After sample loading and electrophoresis, membrane transfer, blocking, and antibody culture (primary antibody concentration: Occludin 1: 20,000; Claudin-5 1:1,000; MMP-9 1:1,000; β-actin 1:5,000), incubate overnight at 4°C. Adding appropriately fluorescently labeled secondary antibodies (dilution concentration 1:5,000), incubate at room temperature for 2-3 h, develop, and fix. Then use the gel imaging system to scan and analyze and express it in terms of the relative expression of the target protein. According to the formula, the relative expression of the target protein = the integral optical density (IOD) of the target protein/IOD of the internal reference for determination.

2.10. Immunofluorescence. The fixed tissue was dehydrated, embedded, and sliced by an automatic dehydrator. The dewaxed slices were immersed in 0.01 M citrate buffer (pH 6.0), heated in the microwave oven with high fire until boiling, and then cut off the power. After an interval of 5 min, the chips were repeatedly cooled. The chips were washed 3 times with PBS, 5 minutes each time, 10% serum blocking solution was added, and they were placed in room temperature for 30 minutes. The first antibody was dripped at 4°C overnight; the second antibody was dripped at 37°C for 30 minutes; DAPI was dripped and incubated at room temperature for 10 minutes; and the slices were sealed. The image of the slices was collected by fluorescence scanning microscope camera system, and the fluorescence intensity and area of all the images were measured by the ImageJ analysis system.

2.11. Statistical Analysis. The SPSS 21.0 software was applied for data analysis. The data we measured were exhibited by means ± SD. The Student's *t*-test and one-way ANOVA were performed for the comparison between two groups and difference among numerous groups, respectively. Tukey's post hoc tests were applied, for more than two groups. A value of $P < 0.05$ was considered significant statistically.

3. Results

3.1. QSW Alleviates the Brain Injury Caused by CI in Rats. To evaluate the protective effect of QSW on MACO, rats were given QSW in advance, and then a MACO model was established. Compared with those in the Sham group, the rats in the I/R group had neurobehavioral abnormalities at 24 h after MACO ($P < 0.01$). The neurobehavioral abnormalities were significantly improved in the QSW group (66.68 mg/kg) 24 hours after MACO ($P < 0.05$ vs. I/R; Table 2). The results of TTC staining showed that the area of cerebral infarction in rats with MACO could be significantly reduced by QSW (Figure 2(a)). Compared with that of the Sham group, the cerebral infarction rate of rats in the I/R group increased significantly ($P < 0.01$), and the cerebral infarction rate of rats in the QSW group (66.68 mg/kg) was significantly reduced ($P < 0.05$; Figure 2(b)).

Table 2: QSW on behavioral scores.

Group	Dose (mg·kg^{-1})	Neurobehavioral at 24 h					
		−	+	++	+++	++++	P value
Sham	—	6	0	0	0	0	0.0017**
I/R	—	0	0	2	4	0	—
Nmdp + IR	30.00	0	0	5	1	0	0.0419*
QSW + IR	66.68	0	0	6	0	0	0.0017**

Compared with the I/R group, *$P < 0.05$ and **$P < 0.01$.

3.2. QSW Improves Intestinal Integrity in MCAO Rats. The H&E staining results showed that the intestinal mucosal structure of MACO rats in the QSW group had a significant change in morphology (Figures 3(a)–3(c)). In three different intestinal regions (ileum, cecum, and colon), compared with the Sham group, the villus height and crypt depth of the ileum in the I/R group were significantly reduced ($P < 0.05$), and the villus width also tended to decrease ($P > 0.05$). The thickness of the mucosa of the cecum did not change significantly ($P > 0.05$), whereas that of the colon was significantly reduced ($P < 0.05$). These results showed that MACO modeling would cause intestinal mucosal damage. Compared with the I/R group, the QSW group showed an increase in the villus height, villus width, crypt depth of ileum, and the mucosal thickness of the cecum and colon ($P > 0.05$). This finding shows that QSW has a certain repairing effect on the intestinal mucosa injury caused by MCAO rats (Figures 3(d)–3(h)).

3.3. QSW Changes the Overall Composition of Gut Microbiota. In order to evaluate the effect of QSW on the gut microbiota community, we used 16S rRNA gene amplification and sequence analysis. The result indicated that 146618 sequencing numbers and 518 OTUs were obtained from 24 samples. Compared with the Sham group, the number of OTUs increased ($P > 0.05$) in the I/R group. After QSW pretreatment, the number of OTUs decreased ($P > 0.05$ vs. I/R; Figure 4(a)). Venn diagrams show that there were 393 OTUs in all four groups (Figure 4(b)). According to different alpha diversity indices, as shown in Figures 4(c) and 4(d), compared with the Sham group, the species richness (Ace index) of the I/R group was significantly increased ($P < 0.05$), while the species diversity (Shannon index) was

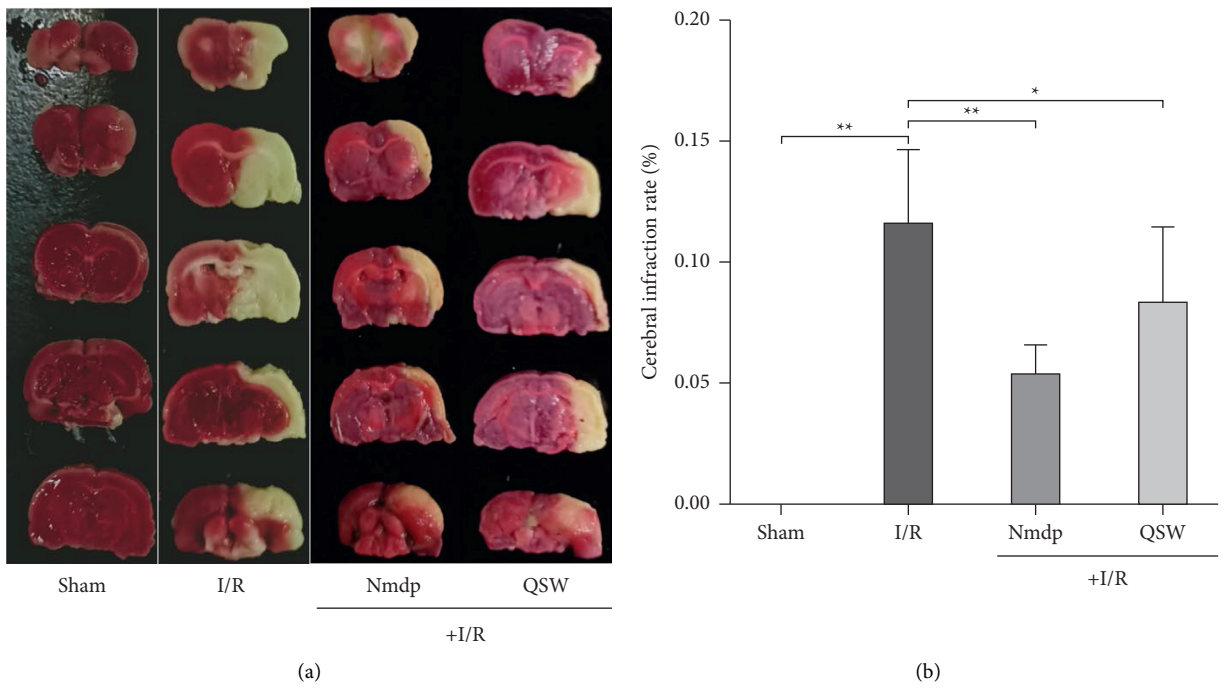

Figure 2: TTC. (a) Representative TTC staining of rat brain slices. Unstained areas indicate tissue damage. (b) QSW alleviates cerebral infarction. The data were presented as means ± SD; $n = 6$ rats per group. Compared with the I/R group, $^{*}P < 0.05$ and $^{**}P < 0.01$.

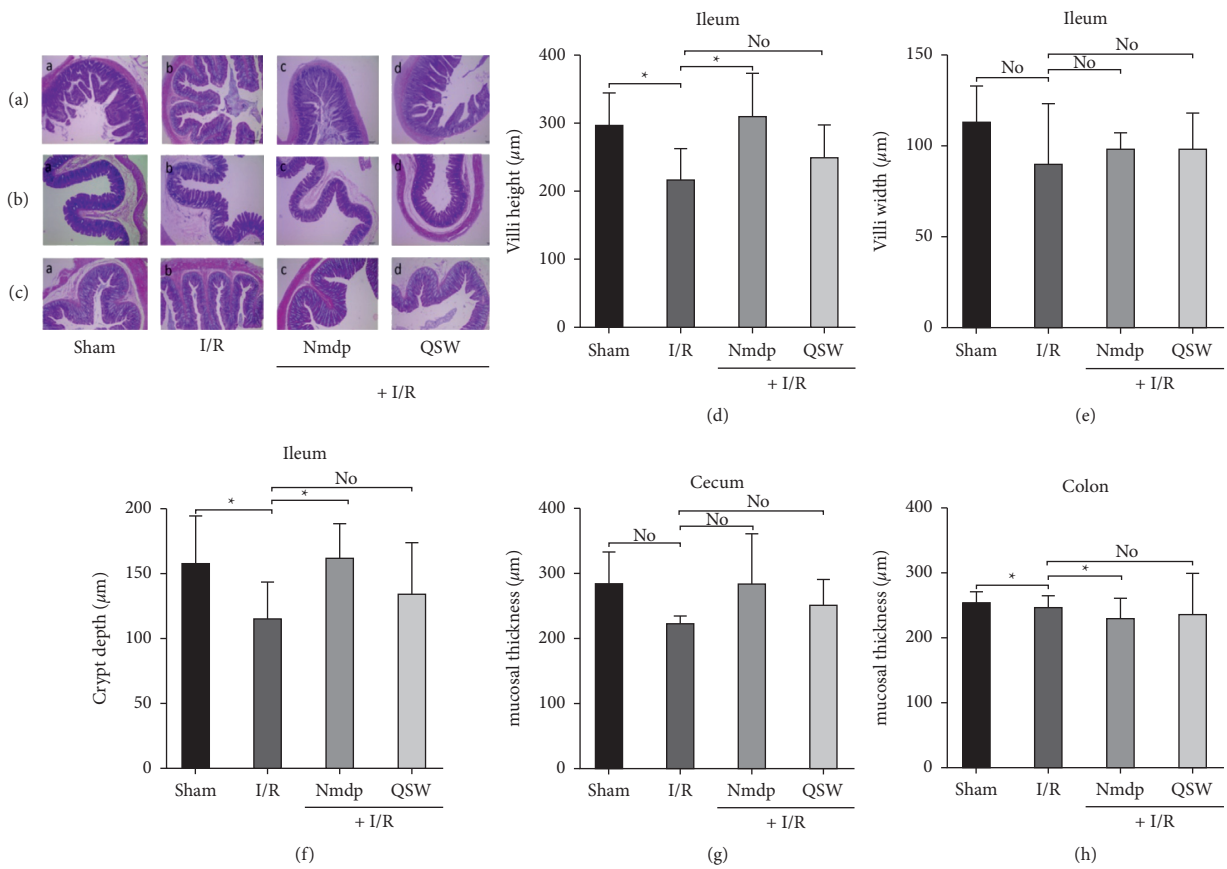

Figure 3: Intestinal damage: (a) H&E staining of the ileum (100× magnification); (b) HE staining of the cecum (100× magnification); (c) HE staining of the the colon (100× magnification); and (d–h) the villi height, villi width, crypt depth, and mucosal layer thickness of the cecum and colon were measured using the BA200 Digital trinocular camera system. The data were presented as means ± SD; $n = 6$ rats per group. Compared with the I/R group, $^{*}P < 0.05$ and $^{**}P < 0.01$. "No" means no significant difference.

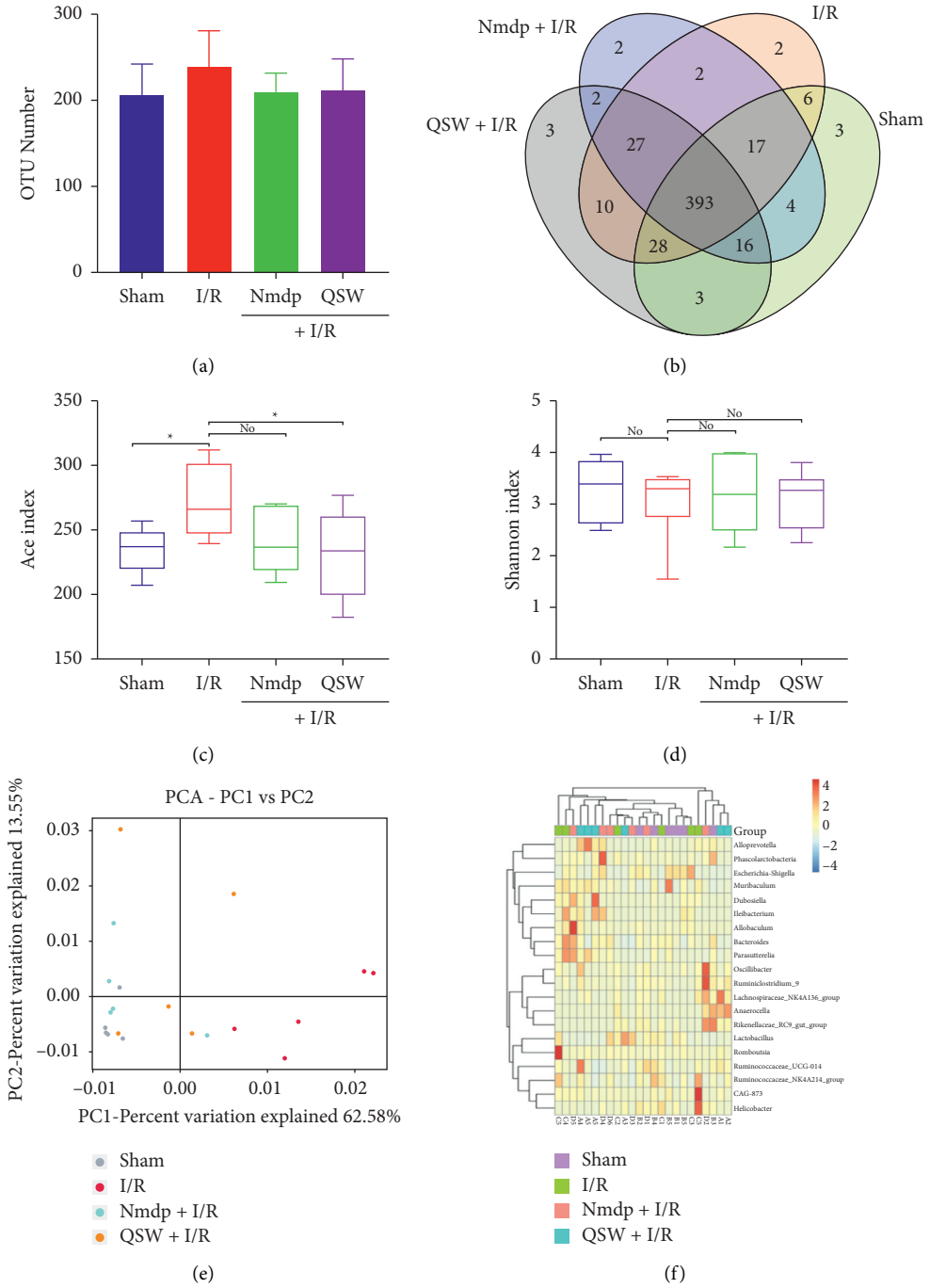

Figure 4: Composition of microbiota: (a) OTU numbers, (b) OTU Venn analysis, (c) Ace index ($^{*}P < 0.05$ and $^{**}P < 0.01$), (d) Shannon index ($^{*}P < 0.05$ and $^{**}P < 0.01$), (e) principal component analysis (PCA) for the weighted UniFrac distance of the gut microbiota, and (f) heat map analysis of intestinal flora 16S rRNA detection genus level. The data were presented as means ± SD; $n = 6$ rats per group.

decreased ($P > 0.05$). After pretreatment with QSW, Ace index decreased significantly ($P < 0.05$ vs. I/R), and Shannon index decreased ($P > 0.05$ vs. I/R).

As shown in Figure 4(e), PCA analysis showed that the microbial populations of four groups had different clusters. Compared with the Sham group, the gut microbiota of I/R showed significant structural changes. The total gut microbiota of the QSW group was more similar to that of the Sham group. Additionally, heat map analysis at the genus classification level showed that the composition of gut microbiota in the QSW group was closer to that in the Sham group (Figure 4(f)).

3.4. QSW Regulates Gut Microbiota Composition in MCAO Rats. Next, at the level of phylum classification, *Firmicutes*, *Proteobacteria*, and *Bacteroidetes* are the dominant phyla in the gut microbiota of the four groups of rats. The remaining phyla are *Verrucomicrobia*, *Epsilonbacteraeota*, *Spirochaetes*,

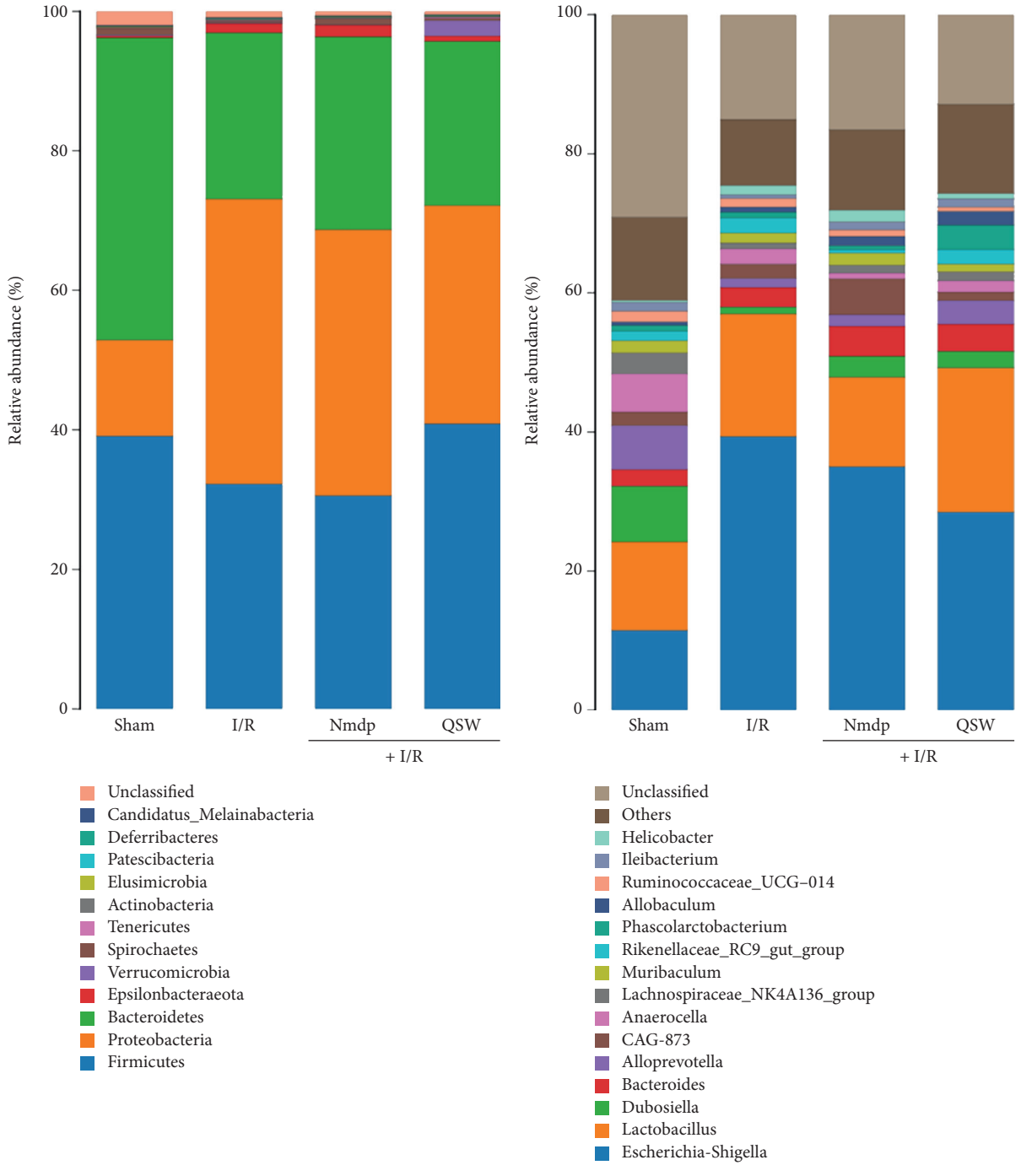

(a) (b)

Figure 5: Continued.

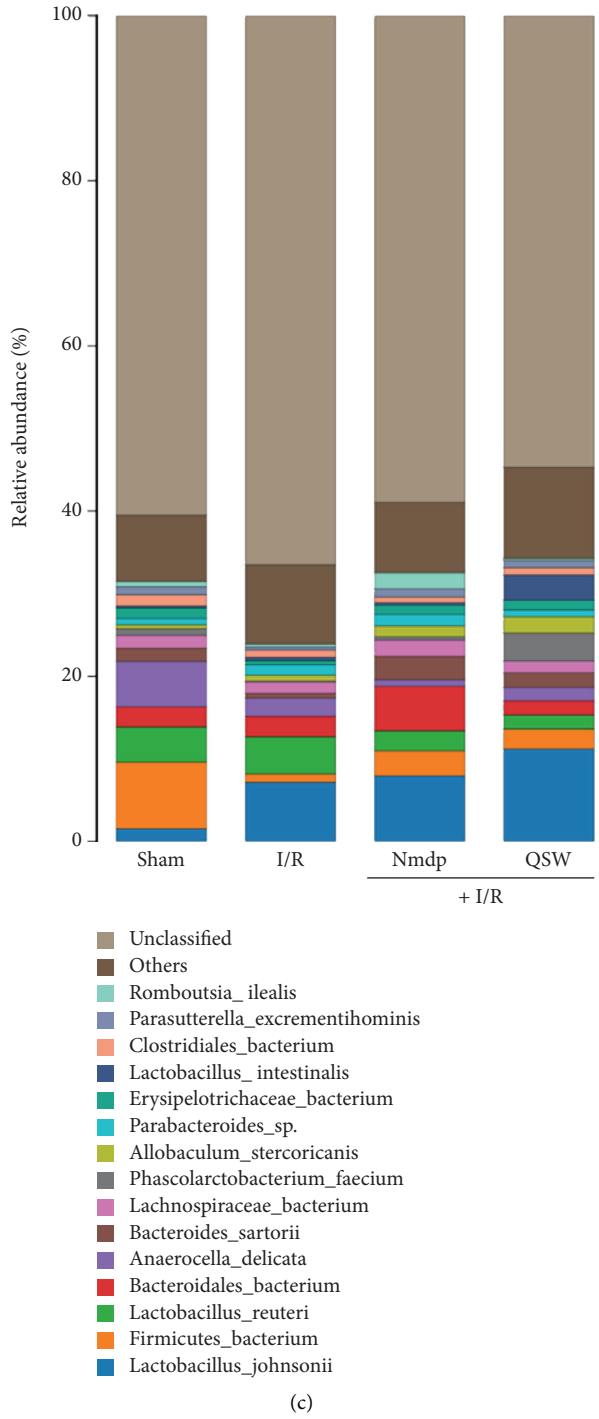

(c)

Figure 5: The relative abundance of gut microbiota: (a) phylum level, (b) genus level, and (c) species level.

Tenericutes, *Actinobacteria*, *Patescibacteria*, and *Elusimicrobia*. Compared with the Sham group, after successful MCAO, the abundance of *Firmicutes* and *Bacteroidetes* in the gut microbiota of rats decreased, while the abundance of *Proteobacteria* increased. When MCAO model rats were treated with QSW, the abundance of *Firmicutes* in the gut microbiota of rats increased, while the abundance of *Proteobacteria* is reduced (Figure 5(a)). At the taxonomic level of genus, *Escherichia Shigella* and *Lactobacillus* are the dominant bacterial genera in the gut microbiota of the four groups of rats. Meanwhile, the remaining genera are *Bacteroides*, *Alloprevotella*, *Phascolarctobacterium*, *Rikenellaceae-RC9-gut-group*, *Anaerocella*, *Dubosiella*, *CAG-873*, and *Allobaculum*. Compared with the Sham group, after successful MCAO, the abundance of *Escherichia Shigella* in the gut microbiota of rats increased significantly. When MCAO model rats were given QSW, the abundance of *Escherichia Shigella* in the gut microbiota of rats is reduced (Figure 5(b)).

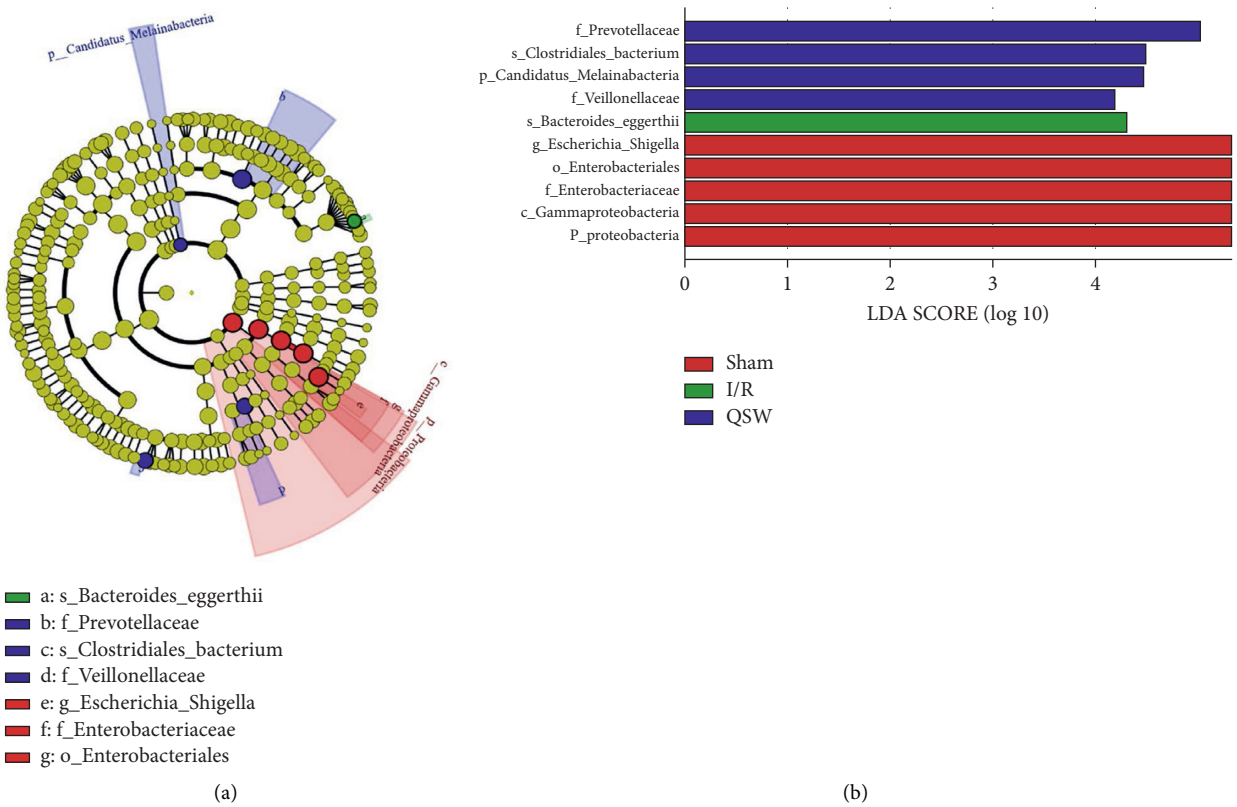

Figure 6: LEfSe analysis comparing differences in the gut microbiota among groups. Species with no significant difference are uniformly yellow, and other colored dots indicate different species in the group.

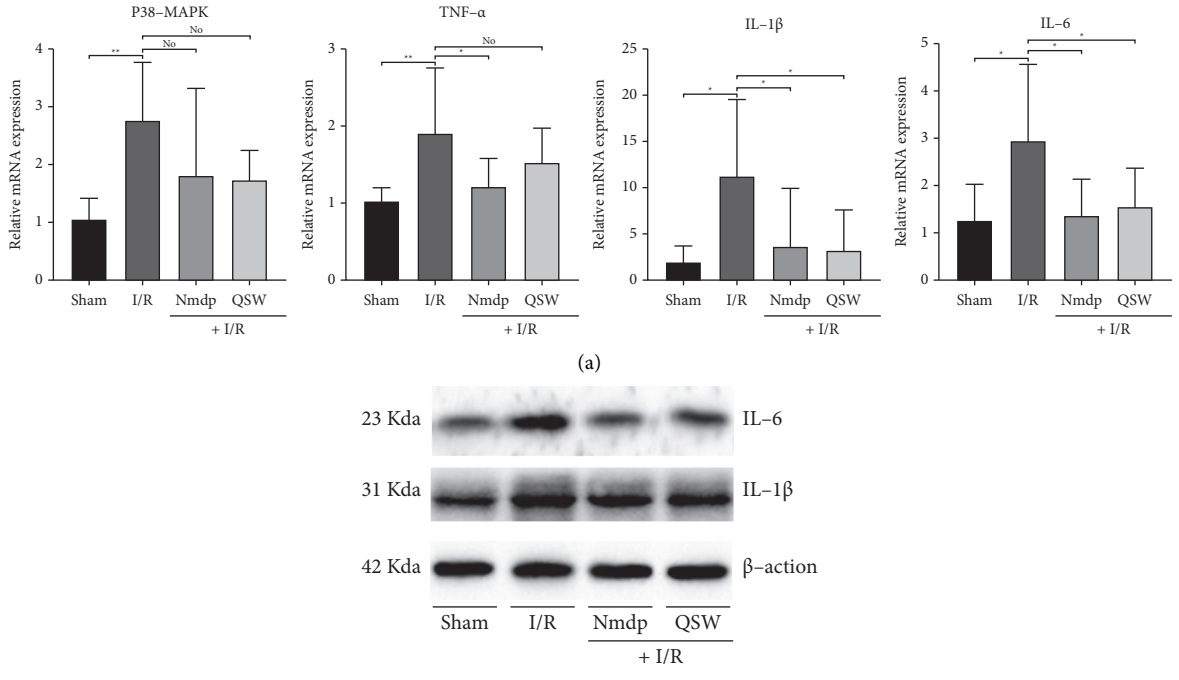

Figure 7: Continued.

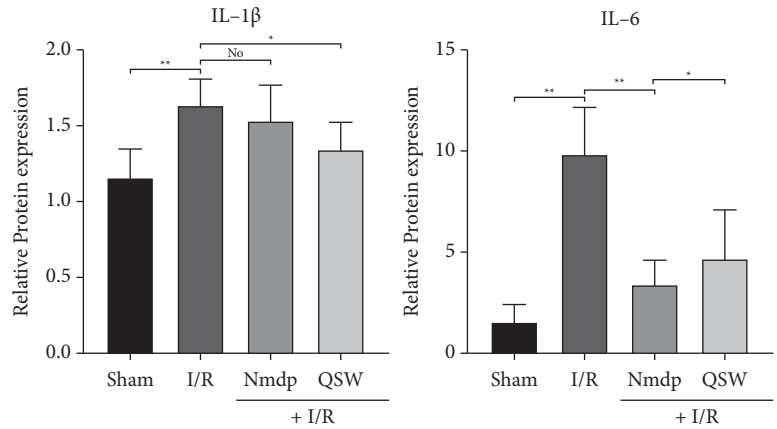

Figure 7: Inflammation: (a) the mRNA levels of p38-MAKP, TNF-α, IL-1β, and IL-6 in the hippocampus of the ischemic side were measured by RT-PCR; (b) the protein levels of IL-1β and IL-6 in the hippocampus of the ischemic side were measured by western blot; and (c) histogram analysis of the levels of IL-1β and IL-6. The data were presented as means ± SD; $n = 6$ rats per group. Compared with the I/R group, $^{*}P < 0.05$ and $^{**}P < 0.01$. "No" means no significant difference.

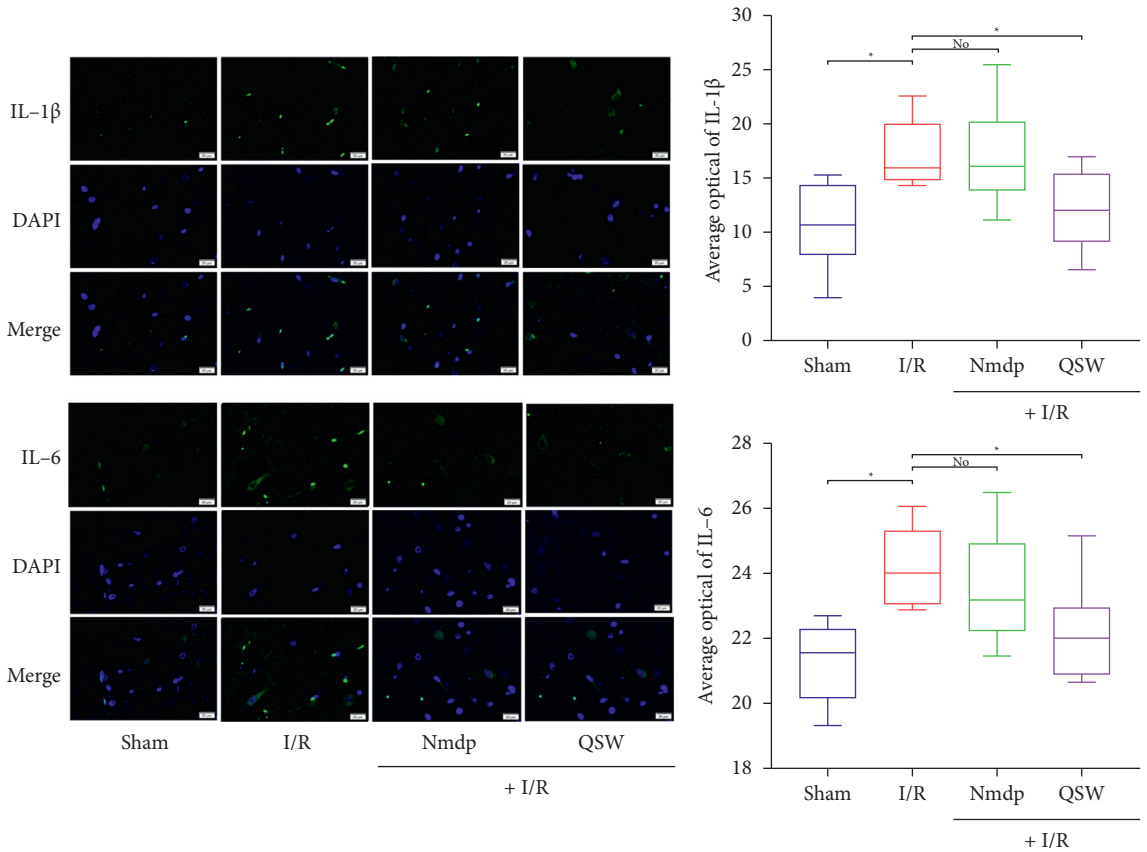

Figure 8: IL-1β and IL-6 IHC. Representative microphotographs of immunofluorescence staining (400×) for identification of IL-1β and IL-6. The data were presented as means ± SD; $n = 6$ rats per group. Compared with the I/R group, $^{*}P < 0.05$ and $^{**}P < 0.01$. "No" means no significant difference.

What's more, at the level of species classification, the four groups of rat gut microbiota with relative abundance greater than 0.1% are exemplified, so *Lactobacillus johnsonii*, *Firmicutes bacterium*, *Lactobacillus reuteri*, and *Bacteroidales bacterium* are the dominant strain in the gut microbiota of the four groups of rats. Compared with the Sham group, after successful MCAO modeling, the abundance of *F. bacterium* in the gut microbiota of rats was significantly

reduced, and the abundance of *L. johnsonii* was significantly increased. When MCAO model rats were given QSW, the abundance of *L. johnsonii* in the gut microbiota of rats increased, and *L. reuteri* abundance decreased (Figure 5(c)). In addition, the LEfSe analysis showed the species with significant differences among the groups (Figure 6).

3.5. QSW Attenuates Inflammatory Response in Rats with CI. We measured the expression of inflammatory factors in the tissue of the hippocampus on the ischemic side of the brain. The results showed that QSW could downregulate the expression of p38-MAPK, TNF-α ($P > 0.05$) and IL-1β and IL-6 ($P < 0.05$) mRNA compared with the I/R group (Figure 7(a)). In addition, we selected IL-1β and IL-6 for western blot and immunofluorescence experiment and found that QSW could downregulate the protein expression of IL-1β and IL-6 ($P < 0.05$) compared with the I/R group (Figures 7(b), 7(c), and 8). Therefore, we speculate that the QSW may inhibit inflammation and inflammation-related pathways to alleviate the inflammation of MCAO in rats.

4. Discussion and Conclusion

The present study confirmed and extended our prior study of the protective effect of QSW on I/R through the blood-brain barrier and metabolomics in the early stage [20]. QSW can protect against lipopolysaccharide plus 1-methyl-4-phenyl-1,2,3,6-tetrahydropyridine-induced neurotoxicity and disturbance of gut microbiota in mice [27]. But so far, there are few reports on the changes of microbiota and the effect of microbiota changes on neuroinflammation during the treatment of I/R with QSW.

In this study, we established the MCAO model and treated it with QSW by gavage. It was found that QSW reduced the neurobehavioral abnormalities and the ratio of cerebral infarction caused by I/R. This may be related to the improvement of microbiota imbalance and intestinal barrier damage by QSW. Our data also showed that QSW reduced IL-6 and IL-1β mRNA and protein expression levels, thereby inhibiting inflammation. This study can provide an important theoretical basis for the in-depth study of the anti-CI and central inflammation effects of QSW through the gut-brain axis and its reasonable clinical application.

It is reported that focal and transient MCAO in rodents has been reported to lead to neuropathological results similar to clinical CI. At present, there are methods to prevent cerebral infarction, but there is no way to improve the anatomical, neurochemical, and behavioral defects after CI [28]. Therefore, we established a rat MACO model to evaluate the effects of QSW on cerebral infarction and neuropathology. TTC results showed that QSW could significantly reduce the area of cerebral infarction. At the same time, the TTC experiment can also prove that our rat MACO model is successful. In addition, QSW can significantly improve neurological behavior. In conclusion, QSW can effectively protect the neurobehavioral abnormalities and the increase of cerebral infarction ratio caused by CI.

Gut microbiota is an important part of the intestinal barrier. It is very important for the physiological processes related to the functional maturity of the host intestinal mucosal barrier, nutrient absorption, immune system development, and energy metabolism [29, 30]. Recent evidence shows that the occurrence of CI is closely related to the changes of gut microbiota [31–33]. Therefore, more and more attention has been focused on the regulation of gut microbiota as a therapeutic strategy against CI and related diseases. In this study, we found that QSW can alleviate CI by regulating the composition of gut microbiota. At the phylum level, it can regulate the abundance of *Firmicutes* and *Proteobacteria* in the gut microbiota of rats with MCAO. At the genus level, it can adjust the abundance of *Escherichia and Shigella*. At the species level, it can adjust the abundance of *L. johnsonii* and *L. reuteri*. Cluster classification results also showed that the composition of the gut microbiota of rats in the QSW group was closer to that of the Sham group, suggesting that QSW could improve the environment of the gut microbiota in rats with CI. Besides, evidence suggests that *Helicobacter pylori* is the pathogenic mechanism of CI through its interference with lipid and lipoprotein metabolism and atherosclerosis promotion [34]. Meanwhile, *L. johnsonii* can inhibit *Helicobacter* in vitro and in vivo, and the combined anti-H. *pylori* urease IgY administration suppresses *H. pylori* to a greater extent than the monotherapy against *L. johnsonii* [35]. Therefore, QSW regulating the abundance of *Lactobacillus yoelii and L. reuteri* is possibly one of the mechanisms of treatment for CI and is probably related to *L. yoelii* control.

Inflammation is closely related to central nervous system diseases. Evidence indicates that the physiological basis of the inflammatory response in the central nervous system is the activation of microglia and astrocytes and the exudation of leukocytes [36]. Under the pathological conditions of CI and stroke, microglia and astrocytes secrete a large number of inflammatory factors, such as IL-1, TNF-α, NF-κB p65, ICAM-1, and other inflammatory factors that play a huge role in the inflammatory cascade [37, 38]. What's more, inhibition of the activation of p38MAPK signal pathway not only can reduce the neuronal damage by blocking the proapoptotic pathway but also can block the inflammatory signal-mediated effect [39]. In addition, a recent report showed that the imbalance of gut microbiota caused by antibiotic treatment affects the prognosis of poststroke neuroinflammation in experimental stroke models [32]. In another report, acute brain injury can cause gut microbiota imbalance, and gut microbiota is a key regulator of neuroinflammatory response after brain injury [40]. These findings highlight the key role of the microbiota as a potential therapeutic target to protect the normal function of the brain after injury. In this study, we found QSW can adjust the disordered gut microbiota to a balanced state. Besides, the expression of IL-6 and IL-1β mRNA in the ischemic lateral brain tissue of the QSW group decreased significantly, while the expression of p38-MAPK and TNF-α mRNA decreased. In addition, we further studied IL-6 and IL-1β western blot, and immunofluorescence experiments confirmed our PCR results.

In conclusion, the present study demonstrated that QSW can reduce the severity of I/R in rats by regulating gut microbiota and inhibiting the inflammatory response.

Data Availability

The data supporting the conclusions are included in the manuscript. The data sets used and/or analyzed during the current study are available from the corresponding author on reasonable request.

Conflicts of Interest

The authors declare that there are no conflicts of interest regarding the publication of this paper.

Authors' Contributions

Ke Fu, Dewei Zhang, and Yinglian Song contributed equally to this work. Ke Fu, Deiwei Zhang, and Yinglian Song were responsible for assisting in the experiment and participating in the writing of articles; Min Xu, Ruixia Wu, Xueqing Xiong, Xianwu Liu, Lei Wu, Ya Guo, You Zhou, and Xiaoli Li were responsible for assisting in the experiment; and Zhang Wang functioned as the corresponding author.

Acknowledgments

This study was supported by China Postdoctoral Science Foundation (2012M511916); Project of Sichuan Provincial Administration of Traditional Chinese Medicine (2012-E-040); and Science and Technology Development Fund of Chengdu University of Traditional Chinese Medicine (ZRQN1544). The authors thank the Chengdu University of Traditional Chinese Medicine and Wanzhou Institute for Drug and Food Control for providing us with a research platform. The authors are grateful for the technical support from Biomarker Technologies (BMC).

References

[1] H. Amani, E. Mostafavi, M. R. Alebouyeh et al., "Would colloidal gold nanocarriers present an effective diagnosis or treatment for ischemic stroke?" *International Journal of Nanomedicine*, vol. 14, pp. 8013–8031, 2019.

[2] B. Jiang, W.-Z. Wang, H. Chen et al., "Incidence and trends of stroke and its subtypes in China," *Stroke*, vol. 37, no. 1, pp. 63–65, 2006.

[3] B. Y. Hwang, G. Appelboom, A. Ayer et al., "Advances in neuroprotective strategies: potential therapies for intracerebral hemorrhage," *Cerebrovascular Diseases*, vol. 31, no. 3, pp. 211–222, 2011.

[4] J. Anrather and C. Iadecola, "Inflammation and stroke: an overview," *Neurotherapeutics*, vol. 13, no. 4, pp. 661–670, 2016.

[5] A. Tuttolomondo, R. Pecoraro, D. Di Raimondo et al., "Immune-inflammatory markers and arterial stiffness indexes in subjects with acute ischemic stroke with and without metabolic syndrome," *Diabetology & Metabolic Syndrome*, vol. 6, no. 1, p. 28, 2014.

[6] S. R. Gill, M. Pop, R. T. Deboy et al., "Metagenomic analysis of the human distal gut microbiome," *Science (New York, NY)*, vol. 312, no. 5778, pp. 1355–1359, 2006.

[7] J. A. Gilbert, M. J. Blaser, J. G. Caporaso, J. K. Jansson, S. V. Lynch, and R. Knight, "Current understanding of the human microbiome," *Nature Medicine*, vol. 24, no. 4, pp. 392–400, 2018.

[8] E. A. Franzosa, X. C. Morgan, N. Segata et al., "Relating the metatranscriptome and metagenome of the human gut," *Proceedings of the National Academy of Sciences*, vol. 111, no. 22, pp. E2329–E2338, 2014.

[9] R. E. Ley, C. A. Lozupone, M. Hamady, R. Knight, and J. I. Gordon, "Worlds within worlds: evolution of the vertebrate gut microbiota," *Nature Reviews Microbiology*, vol. 6, no. 10, pp. 776–788, 2008.

[10] Q. Ma, Y. Li, P. Li et al., "Research progress in the relationship between type 2 diabetes mellitus and intestinal flora," *Biomedicine & Pharmacotherapy*, vol. 117, Article ID 109138, 2019.

[11] J. F. Cryan and T. G. Dinan, "Mind-altering microorganisms: the impact of the gut microbiota on brain and behaviour," *Nature Reviews Neuroscience*, vol. 13, no. 10, pp. 701–712, 2012.

[12] S. H. Rhee, C. Pothoulakis, and E. A. Mayer, "Principles and clinical implications of the brain-gut-enteric microbiota axis," *Nature Reviews Gastroenterology & Hepatology*, vol. 6, no. 5, pp. 306–314, 2009.

[13] Y. Z. P. Jia and Y. H. Du, "Effect of Tibetan medicine Qishiwei Zhenzhu pills on cerebral ischemia infarct area in rats," *Tibetan Medicine*, vol. 33, no. 3, pp. 56-57, 2012.

[14] P. Hai, "Effects of Rannasangpei on level of amino acid in brain of mice with eclampsia," *Chinese Journal of Modern Applied Pharmacy*, vol. 20, no. 1, pp. 3–5, 2003.

[15] Z. Z. Bai, G. E. Jin, and D. X. Lu, "Effects of Tibetan medicine Rannasangpei on learning memory functions and superoxid dismutase and maleic dialdehyde in alzheimer disease model rats," *Chinese High Altitude Medicine and Biology*, vol. 32, no. 1, pp. 29–31+43, 2011.

[16] K. Fu, M. Xu, Y. Zhou et al., "The status quo and way forwards on the development of Tibetan medicine and the pharmacological research of Tibetan materia Medica," *Pharmacological Research*, vol. 155, Article ID 104688, 2020.

[17] China Medical Science and Technology Press, *Pharmacopoeia of the People's Republic of China*, pp. 450-451, China Medical Science and Technology Press, Beijing, China, 2015.

[18] E. J. An and Y. R. Suo, "Research progress in modern pharmacology of Tibetan medicine Qishiwei Zhenzhu pills," *Journal of Medicine & Pharmacy of Chinese Minorities*, vol. 10, no. 2, pp. 33–35, 2004.

[19] Y. Song, K. Fu, and D. Zhang, "The absorption, distribution, and excretion of 18 elements of Tibetan medicine Qishiwei Zhenzhu pills in rats with cerebral ischemia," *Evidence-Based Complementary and Alternative Medicine*, 2021.

[20] M. Xu, R. Wu, Y. Liang et al., "Protective effect and mechanism of Qishiwei Zhenzhu pills on cerebral ischemia-reperfusion injury via blood-brain barrier and metabonomics," *Biomedicine & Pharmacotherapy*, vol. 131, Article ID 110723, 2020.

[21] W. W. Liang, X. J. Huang, Z. Wang, N. N. Liu, Y. Tian, and T. Li, "Preliminary study on the time effect relationship of Tibetan medicine Qishiwei Zhenzhu pills on focal cerebral ischemia-reperfusion injury induced by thread suppository in rats," *Pharmacology and Clinics of Chinese Materia Medica*, vol. 31, no. 1, pp. 182–187, 2015.

[22] W. L. Xu, W. J. Sun, Z. Wang, G. L. Liu, Y. M. Xu, and Y. Liang, "Study on the dose effect relationship of Qishiwei

Zhenzhu pills on cerebral ischemia reperfusion injury in rats," *Drugs & Clinic*, vol. 32, no. 1, pp. 10–15, 2017.

[23] Z. Wang, Y. Zhang, and Q. P. Zhao, "Preliminary study on the time-effect relationship of erigeron breviscapus in the treatment of cerebral ischemia-reperfusion injury," *Pharmacology and Clinics of Chinese Materia Medica*, vol. 28, pp. 62–64, 2012.

[24] J. B. Bederson, L. H. Pitts, M. Tsuji, M. C. Nishimura, R. L. Davis, and H. Bartkowski, "Rat middle cerebral artery occlusion: evaluation of the model and development of a neurologic examination," *Stroke*, vol. 17, no. 3, pp. 472–476, 1986.

[25] E. Z. Longa, P. R. Weinstein, S. Carlson, and R. Cummins, "Reversible middle cerebral artery occlusion without craniectomy in rats," *Stroke*, vol. 20, no. 1, pp. 84–91, 1989.

[26] E. A. Grice, H. H. Kong, S. Conlan et al., "Topographical and temporal diversity of the human skin microbiome," *Science (New York, NY)*, vol. 324, no. 5931, pp. 1190–1192, 2009.

[27] A.-L. Hu, S. Song, Y. Li et al., "Mercury sulfide-containing Hua-Feng-Dan and 70W (Rannasangpei) protect against LPS plus MPTP-induced neurotoxicity and disturbance of gut microbiota in mice," *Journal of Ethnopharmacology*, vol. 254, Article ID 112674, 2020.

[28] C. V. Borlongan, T. K. Koutouzis, J. R. Jorden et al., "Neural transplantation as an experimental treatment modality for cerebral ischemia," *Neuroscience & Biobehavioral Reviews*, vol. 21, no. 1, pp. 79–90, 1997.

[29] F. Sánchez de Medina, I. Romero-Calvo, C. Mascaraque, and O. Martínez-Augustin, "Intestinal inflammation and mucosal barrier function," *Inflammatory Bowel Diseases*, vol. 20, no. 12, pp. 2394–2404, 2014.

[30] S. M. Jandhyala, R. Talukdar, C. Subramanyam, H. Vuyyuru, M. Sasikala, and D. Nageshwar Reddy, "Role of the normal gut microbiota," *World Journal of Gastroenterology*, vol. 21, no. 29, pp. 8787–8803, 2015.

[31] R. Chen, Y. Xu, P. Wu et al., "Transplantation of fecal microbiota rich in short chain fatty acids and butyric acid treat cerebral ischemic stroke by regulating gut microbiota," *Pharmacological Research*, vol. 148, Article ID 104403, 2019.

[32] C. Benakis, D. Brea, S. Caballero et al., "Commensal microbiota affects ischemic stroke outcome by regulating intestinal $\gamma\delta$ T cells," *Nature Medicine*, vol. 22, no. 5, pp. 516–523, 2016.

[33] M. S. Spychala, V. R. Venna, M. Jandzinski et al., "Age-related changes in the gut microbiota influence systemic inflammation and stroke outcome," *Annals of Neurology*, vol. 84, no. 1, pp. 23–36, 2018.

[34] P. U. Heuschmann, D. Neureiter, M. Gesslein et al., "Association between infection with *Helicobacter pylori* and Chlamydia pneumoniae and risk of ischemic stroke subtypes," *Stroke*, vol. 32, no. 10, pp. 2253–2258, 2001.

[35] Y. Aiba, K. Umeda, S. Rahman, S. V. Nguyen, and Y. Komatsu, "Synergistic effect of anti-*Helicobacter pylori* urease immunoglobulin Y from egg yolk of immunized hens and Lactobacillus johnsonii No. 1088 to inhibit the growth of *Helicobacter pylori* in vitro and in vivo," *Vaccine*, vol. 37, no. 23, pp. 3106–3112, 2019.

[36] M. Campanella, C. Sciorati, G. Tarozzo, and M. Beltramo, "Flow cytometric analysis of inflammatory cells in ischemic rat brain," *Stroke*, vol. 33, no. 2, pp. 586–592, 2002.

[37] J. B. Moon, C. H. Lee, C. W. Park et al., "Neuronal degeneration and microglial activation in the ischemic dentate gyrus of the gerbil," *Journal of Veterinary Medical Science*, vol. 71, no. 10, pp. 1381–1386, 2009.

[38] Y. Yan, *Reactive Astrocytes and Expression of Inflammatory Factor in Astrocytes after Focal Cerebral Ischemia/Reperfusion in Adult Rat*, Chongqing Medical University, Chongqing, China, 2007.

[39] J. Zhang and W. B. Du, "Effects of duhuo on p38MAPK signal transduction pathway in the brain of dementia rats," *Chinese Journal of Gerontology*, vol. 30, no. 11, pp. 1514-1515, 2010.

[40] V. Singh, S. Roth, G. Llovera et al., "Microbiota dysbiosis controls the neuroinflammatory response after stroke," *Journal of Neuroscience*, vol. 36, no. 28, pp. 7428–7440, 2016.